# Characterization of extracellular vesicles from red blood cells infected with asexual stages of *Plasmodium falciparum*

## Veronica Oluwatosin Opadokun

Institute of Parasitology

McGill University

December 2023



A thesis submitted to McGill University in partial fulfillment of the requirements of the degree of Doctor of Philosophy.

© Veronica O. Opadokun 2023

## Contents

Abstract		5
Résumé		6
Acknowled	dgments	8
Contribution	on to Original Knowledge	10
Contribution	on of Authors	11
List of Fig	ures and Tables	12
List of Abl	previations	15
Chapter 1:	Introduction	17
Chapter 2:	Literature Review	22
2.1.	Plasmodium falciparum: The parasite	23
2.1.1.	The life cycle of <i>P. falciparum</i>	23
2.1.2.	The ring stage (~ 0-24 h PI)	25
2.1.3.	The trophozoite stage (~22-38 h PI)	27
2.1.4.	The schizont stage (~38-48 h PI)	27
2.2.	Falciparum malaria: The disease	28
2.3.	Extracellular vesicles: A paradigm of intercellular communication	30
2.3.1.	A brief history of EVs	30
2.3.2.	EV types and terminologies	32
2.3.3.	EV biogenesis	34
2.3.3.1.	The biogenesis of exosomes	34
2.3.3.2.	The biogenesis of microvesicles	36
2.3.4.	The biomolecular composition of EVs	36
2.3.4.1.	EV proteins	38
2.3.4.2.	EV nucleic acids	38
2.3.4.3.	EV lipids	39
2.3.5.	Fate, biological functions, and applications of EVs	39
2.3.6.	EV isolation techniques and methodologies	41
2.4.	EVs in falciparum malaria	44
2.4.1.	Biogenesis of Pf-iRBC-EVs	45
2.4.2.	Composition of Pf-iRBC-EVs	47
2.4.3.	Pf-iRBC-EVs and P. falciparum biology: Parasite-parasite communication	49
2.4.4.	Pf-iRBC-EVs in malaria immunopathogenesis: Parasite-host interaction I	50
2.4.5.	Pf-iRBC-EVs and their therapeutic application: Parasite-host interaction II	52
Chapter 3:	Methods	55
3.1.	Cells: Red blood cells and parasite strain	56
3.2.	In vitro cell cultures: Parasite infected and uninfected cultures	56
3.2.1.	Sorbitol synchronization	57
3.2.2.	Percoll synchronization	57
3.3.	Harvesting EV-containing CM	58

3.3.1.	Mixed stage cultures (Objective 1)	58
3.3.2.	Synchronized cultures (Objectives 2 and 3)	58
3.4.	EV isolation by differential centrifugation	59
3.5.	Transmission electron microscopy (TEM)	61
3.6.	Nanoparticle tracking analysis (NTA)	
3.7.	Flow cytometry (FC)	62
3.8.	Protein analysis: Gel electrophoresis and WBA	62
3.8.1.	Preparation of controls	62
3.8.2.	Protein extraction and assay	63
3.8.3.	Gel electrophoresis and staining	63
3.8.4.	Western blot analysis (WBA)	64
3.9.	Protein analysis: Liquid chromatography-mass spectrometry analysis	64
3.10.	EV purification for RNA analysis	65
3.11.	RNA extraction	67
3.12.	RNA detection and validation.	67
3.13.	RNA sequencing	67
Chapter 4	: Results	69
4.1.	Preface to developing a malaria EV isolation protocol (Objective 1)	70
4.1.1.	Optimizing P. falciparum culture parameters for EV isolation	72
4.1.2.	Imaging mixed stage EVs	75
4.1.3.	Protein detection of mixed stage EVs	76
4.1.4.	Protein composition of mixed stage EVs	78
4.2.	Preface to EV proteomics (Objective 2)	80
4.2.1.	Physical characteristics of malaria EVs	82
4.2.2.	Total protein assay and in-gel protein detection of malaria EVs	85
4.2.3.	Protein composition of malaria EVs: Western blot analysis	86
4.2.4.	Protein composition of malaria EVs: Mass spectrometry	88
4.2.4.1.	Quantitative analysis of proteins in P1 and P2 EVs	88
4.2.4.2.	Known EV markers in P1 and P2 EVs	91
4.2.4.3.	Comparison of iRBC EV proteomics dataset with published proteomes	94
4.2.4.4.	Secreted and non-secreted parasite proteins in malaria EVs	96
4.2.4.5.	Gene ontology enrichment analysis of <i>P. falciparum</i> proteins	99
4.2.4.6.	Gene ontology enrichment analysis of human proteins	104
4.3.	Preface to EV transcriptomics (Objective 3)	107
4.3.1.	RNA detection in untreated EVs	108
4.3.2.	RNA detection and analysis in treated EVs	109
4.3.2.1.	Small RNA, microRNA Sequencing	112
4.3.2.2.	RNA-Seq/ transcriptome	113
4.3.2.3.	Transcript analysis: Top 50 genes	113
4.3.2.4.	Transcript analysis: Specific gene searches	117

Chapter 5: Discussion		120
5.1.	Important considerations for malaria EV isolation	
5.2.	P. falciparum alters the nature of RBC-derived EVs	124
5.3.	P. falciparum-iRBCs release multiple EV subtypes	125
5.4.	Specific markers can be defined for malaria EV subtypes	127
5.4.1.	Human proteins	127
5.4.2.	Parasite proteins	129
5.4.3.	Parasite RNA	
5.5.	Correlating malaria EV composition and function	
5.6.	Investigating EV biogenesis in <i>P. falciparum</i>	
Chapte	r 6: Conclusion and summary	
Referen	ces	
Append	ix	

#### **Abstract**

Plasmodium falciparum is an obligate parasite that causes the most severe form of malaria in humans and several aspects of the immunopathology of this deadly disease remain unknown. As such, malaria prevention, control and elimination strategies are impeded. A new aspect of the parasites biology has come to light in recent research which involves the release of extracellular vesicles (EVs) from *P. falciparum*-infected red blood cells (RBCs).

EVs are small membrane bound particles that contain functional biomolecular cargo and serve as a means of communication between and within cell populations. This biomolecular cargo is heterogenous, and largely depends on the parent cell from which the EVs are released, however, it generally includes proteins, nucleic acids (RNA and DNA), and lipids. Several roles which are crucial for the survival of malaria parasites and disease pathogenesis have been suggested for EVs. Despite the importance of these suggested functions, EVs released from *P. falciparum*-infected RBCs have not been fully characterized and the biomolecules in these EVs that may be responsible for their suggested functions are unknown.

Within the infected RBC, there are three developmental stages of *P. falciparum* namely the ring, trophozoite, and schizont. The distinct phenotype of each RBC stage defines its virulence and contribution to the pathogenesis of malaria. Therefore, these distinct phenotypes may induce the release of characteristically different EVs that may be implicated in different aspects of the biology of *P. falciparum* and pathophysiology of malaria. This study investigated the biomolecular cargo of EV subpopulations released from RBCs infected with the different stages of the parasite to delineate their shared and unique properties and biomolecular profiles, as well as gain insights into the potential relevance of the biomolecular components to EV biology, biogenesis, and functions.

Using a combination of techniques including nanoparticle tracking analysis, flow cytometry, Western blot analysis, transmission electron microscopy, mass spectrometry and RNA sequencing to study malaria derived EVs isolated by differential centrifugation, EVs derived from RBCs infected with the ring, trophozoite and schizont stages of *P. falciparum* were found to comprise at least 2 EV subtypes that are quantitatively and qualitatively distinct, with implications for their specific roles in malaria pathogenesis and parasite survival. Proteins and transcripts that are crucial for parasite survival and pathology in the human host, propagation of the parasite to its mosquito vector, as well as for understanding EV biogenesis in the parasite were identified.

#### Résumé

Plasmodium falciparum est un parasite obligatoire qui provoque la forme la plus sévère du paludisme chez les humains, et plusieurs aspects de l'immunopathologie de cette maladie mortelle demeurent inconnus. En tant que tel, les stratégies de prévention, de contrôle et d'élimination du paludisme sont entravées. Un nouvel aspect de la biologie des parasites a été mis en lumière dans des recherches récentes, impliquant la libération de vésicules extracellulaires (VE) à partir des globules rouges infectés par *P. falciparum* (GR).

Les VE sont de petites particules membranaires renfermant une cargaison biomoléculaire fonctionnelle et servant de moyen de communication entre et au sein des populations cellulaires. Cette cargaison biomoléculaire est hétérogène et dépend largement de la cellule parente à partir de laquelle les VE sont libérées, mais elle inclut généralement des protéines, des acides nucléiques (ARN et ADN) et des lipides. Plusieurs rôles cruciaux pour la survie des parasites du paludisme et la pathogenèse de la maladie ont été suggérés pour les VE. Malgré l'importance de ces fonctions suggérées, les VE libérées par les GR infectés par *P. falciparum* n'ont pas été entièrement caractérisées, et les biomolécules dans ces VE qui pourraient être responsables de leurs fonctions suggérées restent inconnues.

À l'intérieur des GR infectés, il existe trois stades de développement de *P. falciparum*, à savoir le stade anneau, le stade trophozoïte et le stade schizonte. Le phénotype distinct de chaque stade de GR définit sa virulence et sa contribution à la pathogenèse du paludisme. Par conséquent, ces phénotypes distincts peuvent induire la libération de VE caractéristiquement différentes, pouvant être impliquées dans différents aspects de la biologie de *P. falciparum* et de la physiopathologie du paludisme. Cette étude a examiné la cargaison biomoléculaire des sous-populations de VE libérées à partir de GR infectés par les différents stades du parasite afin de délimiter leurs propriétés et profils biomoléculaires communs et uniques, ainsi que pour obtenir des informations sur la pertinence potentielle des composants biomoléculaires pour la biologie, la biogenèse et les fonctions des VE.

En utilisant une combinaison de techniques, notamment l'analyse de suivi des nanoparticules, la cytométrie en flux, l'analyse par Western blot, la microscopie électronique en transmission, la spectrométrie de masse et le séquençage d'ARN pour étudier les VE dérivées du paludisme isolées par centrifugation différentielle, il a été constaté que les VE dérivées de GR infectés par les stades

anneau, trophozoïte et schizonte de *P. falciparum* comprenaient au moins 2 sous-types de VE qui étaient quantitativement et qualitativement distincts, avec des implications pour leurs rôles spécifiques dans la pathogenèse du paludisme et la survie du parasite. Des protéines et des transcriptions cruciaux pour la survie et la pathologie du parasite chez l'hôte humain, la propagation du parasite vers son vecteur moustique, ainsi que pour la compréhension de la biogenèse des VE chez le parasite, ont été identifiés.

#### Acknowledgments

To my beloved parents, Adebayo and Modupe Kolade. It would have brought you both so much joy to witness the completion of my thesis. I thank you for equipping me with the resilience I needed to see this phase through. Thank you for your undying love and support during your lifetime. May you continue to rest in peace. Oluwatobiloba and Oluwatamilore Opadokun, you showed up for me during my PhD in a way a mother should only be able to imagine. You have both been my biggest fans and greatest support and I thank you deeply. Without a doubt, you are more relieved than I am to have completed this amazing journey. And what a journey it has been! I am glad I had my family and friends to support me through it. I say thank you to my brothers and sisters, Femi Kolade, Kayode Kolade, Toyin Idowu, Sade Ayekun and Seun Kolade. To the best friends anyone could ask for, Kessiena Babalola, Yemisi Babafunso, Mary Adesoga, Blessing Adesina, and Peter Orisadare; thank you for jeering me on and for your constant words of encouragement. I wish I had the space to include the name of every member of the Opadokun family. You have all provided me with support and encouragement in one way or the other during my PhD, but please permit me to especially thank Bridget Abiola. Thank you all.

Dr. Petra Rohrbach, thank you for welcoming me into your research lab. Thank you for having such a high level of confidence and faith in me. You have given me a great opportunity to evolve as a scientist and independent learner and for this, I am grateful. To the members of my Advisory Committee, Dr. Elias Georges, and Dr. Igor Cestari, I say thank you for your constant words of advice and well thought out suggestions that helped me achieve the objectives of my thesis. I always looked forward to our committee meetings because I knew you would listen carefully to my progress and challenges and provide stimulating ideas and solutions. Thank you, Dr. Reza Salavati, for the insights you brought to my work. Your collaboration was such a privilege and I hope to be able to work with you again in the future.

I would like to sincerely thank my friend and colleague Jeffrey Agyapong. Thank you for tirelessly and selflessly helping me through my lab struggles. It has been a pleasure learning so much from such a meticulous researcher like you. I thank you for enjoying my music with me while working in the lab, for the constant banter, and for collaborating with me on my very first research paper. Thank you Poorya Mirzavand and Abdoulie Touray for patiently teaching me all I needed to know about working with RNA. Thank you, Dr. Peter Lee, for being so good at what

you do at the Institute, thank you for all our nice chats, and all the tips and tricks you shared with me for getting things done! I am grateful to several members of the Institute of Parasitology, past and present – Kathy Keller, Dr. Norma Bautista-Lopez, Dr. Charles Viau, Serghei Dernovici, Rishi Rajesh, Nisha Ramamurthy, Dr. Emily Curry, Dr. Jenn Noonan, Dr. Fadi Baakdah, Stephanie Kucykowicz, Dr. Maude Dagenais, Sarah Contreras-Wolfe, and Amanda Johnston. Thank you all for the special ways you have impacted me and for making the Institute such a pleasurable place to be.

To all the interns and students that I have had the pleasure of training over the years, especially – Vuyiswa Lukhele, Gabriel Ferrante, Megan Sawatzky, Valeria Munoz, Sophie Chauvin-Bosse, Paulo Otavio and Laura Gonzalez-Sanchez. Because of you all, I have grown as a confident teacher and mentor. I thank you all.

I would like to show my gratitude to Laura Montermini, Dr. Nadim Tawil and Hélène Pagé-Veillette for all the training you gave me with the NTA and FC and for our brainstorming sessions at the CAN. I thoroughly enjoyed working with you all. Thank you, Jeannie Mui, for patiently training me on the use of the transmission electron microscope. Lorne Taylor and Amy Wong, you showed keen interest in my thesis from the moment I approached you, and I thank you for working on the mass spectrometry and for never hesitating to answer any questions I had or provide me with guidance during the data analysis.

I am grateful to McGill University and the Faculty of Agricultural and Environmental Sciences for the Graduate Excellence Awards and Pilarczyk Fellowship I received.

And to the future readers of this thesis, thank you for taking the time. I hope you enjoy it.

### **Contribution to Original Knowledge**

This is the first study to perform a comprehensive analysis of multiple EV subtypes from all 3 intraerythrocytic stages of *Plasmodium falciparum*. The analyzed EVs were isolated using an original protocol that was developed as part of this study, and specifically tailored to malaria EV research. This protocol is the first known advance towards standardizing the isolation of malaria EVs and will be shared with the malaria EV community in intricate detail in an already completed methods manuscript. For the first time, recommendations for the proper isolation of malaria EVs have been detailed, to ensure the reproducibility, comparability, and validity of malaria EV studies.

Several biomolecules and biological processes have been identified in different malaria EV subpopulations and subtypes that will direct strategic future research of malaria EVs. The large volume of biomolecular data collected in this study will form the foundation of a malaria EV database that is currently lacking and will be invaluable for future studies of malaria EV biology, function, and biogenesis.

#### **Contribution of Authors**

All experimental work presented in this doctoral thesis was designed and executed by the author under the supervision of Dr. Petra Rohrbach. All EV isolations, experiments, EV preparations and data analyses in this thesis were also performed by the author with the exceptions of mass spectrometry and RNA sequencing.

NTA and FC were performed with the help of Laura Montermini, Dr. Nadim Tawil and Hélène Pagé-Veillette at the Centre for Applied Nanomedicine (CAN). Mass spectrometry of EVs was performed by Lorne Taylor and Amy Wong at the Proteomics and Molecular Analysis Platform of the McGill University Health Centre Research Institute. All proteomics data was analyzed and presented by the author.

RNA sequencing was performed by Raphaëlle Lambert at the Institut de recherche en immunologie et en cancérologie (IRIC), Université de Montréal. RNA bioinformatics analysis was done with the expert help of Patrick Gendron, the director of Information Technology and bioinformatics also at the IRIC, Université de Montréal. Further guidance on EV RNA data analysis was provided by Dr. Reza Salavati of the Institute of Parasitology, McGill University, and his PhD student Poorya Mirzavand.

The literature review on EVs in *P. falciparum* was garnered from my published literature review: Opadokun, T. and P. Rohrbach, Extracellular vesicles in malaria: an agglomeration of two decades of research. Malaria Journal, 2021. **20**(1): p. 442. Preliminary findings of the EV proteomics were published as a research article: Opadokun, T., J. Agyapong, and P. Rohrbach, Protein Profiling of Malaria-Derived Extracellular Vesicles Reveals Distinct Subtypes. Membranes, 2022. **12**(4): p. 397. Jeffrey Agyapong, my friend, and colleague at the Institute of Parasitology contributed to the data analysis published in this article.

This thesis and articles published during my doctorate program were written and edited by the author and reviewed by Dr. Petra Rohrbach.

# **List of Figures and Tables**

Figure 1. Global distribution of malaria transmission	23
Figure 2. Life cycle of <i>P. falciparum</i>	24
Figure 3. Asexual intraerythrocytic blood stages of <i>P. falciparum</i>	26
Figure 4. Pathology of falciparum malaria	29
Figure 5. Milestones in EV research history	31
Figure 6. Biogenesis of EVs	35
Figure 7. General biomolecular composition of EVs	37
Figure 8. EV interaction with recipient cells	40
Figure 9. Proposed mechanisms of EV biogenesis in Plasmodium falciparum-infected RBCs	46
Figure 10. Synchronization techniques for <i>P. falciparum</i> cultures	58
Figure 11. CM harvest from synchronized cultures	59
Figure 12. Optimized isolation protocol for <i>P. falciparum</i> infected RBC derived EVs	60
Figure 13. Workflow of EV-RNA extraction and analysis	66
Figure 14. Optimizing malaria EV isolation protocol: Parasitemia	73
Figure 15. Optimizing malaria EV isolation protocol: Age of RBCs	74
Figure 16. Optimizing malaria EV isolation protocol: RBC preparation	75
Figure 17. Visualizing EVs by TEM	76
Figure 18. Protein separation and detection by SDS-PAGE and silver staining	77
Figure 19. Protein composition of <i>Pf</i> -iRBC EVs	78
Figure 20. TEM micrographs of uRBC EVs and P. falciparum stage specific iRBC EVs	82
Figure 21. NTA of uRBC EVs and <i>P. falciparum</i> stage-specific iRBC EVs	83
Figure 22. Flow cytometry of <i>P. falciparum</i> stage-specific RBC EVs with anti-glycophorin A	84
Figure 23. Protein assay and detection of <i>P. falciparum</i> stage-specific iRBC EVs	85
Figure 24. Protein composition of <i>P. falciparum</i> stage-specific iRBC EVs	87
Figure 25. Relative abundance of human proteins in P1 and P2 EVs	89
Figure 26. Relative abundance of <i>P. falciparum</i> proteins in P1 and P2 EVs	90
Figure 27. Known markers present in P1 and P2 EVs	92
Figure 28. Comparison of 3 different <i>P. falciparum</i> proteomes of malaria EVs	95
Figure 29. A comparison of 2 different human proteomes of malaria EVs	97
Figure 30. Protein interactions of significantly abundant proteins in P1 iRBC EVs	. 100

Figure 31. GO analysis of significantly enriched shared P. falciparum proteins in P1 iR	BC EVs
	101
Figure 32. GO analysis of significantly enriched <i>P. falciparum</i> proteins in P1 iRBC EVs.	103
Figure 33. GO analysis of human proteins significantly enriched in P1 EVs	105
Figure 34. GO analysis of human proteins similarly enriched in P1 and P2 EVs	106
Figure 35. RNA profiles of iRBC and uRBC EVs	108
Figure 36. EV RNA detection with Nanodrop	109
Figure 37. RNA profiles of pre-treated iRBC P2 EVs	111
Figure 38. STAR alignment scores for small RNA sequencing	112
Figure 39. RNA sequencing analysis	114
Figure 40. Transcript analysis	115
Figure 41. Enriched biological processes of the 50 most expressed genes in iRBC P2 EV	s116
Figure 42. Normalized read counts of selected genes encoding potential malaria EV mark	cers118
Figure 43. Normalized read counts for genes encoding parasite ESCRT III machinery	proteins
	119
Table 1. Types and characteristics of EVs	33
Table 2. EV isolation techniques	43
Table 3. Biomolecular composition of <i>Pf</i> -iRBC-EVs	48
Table 4. EV isolation techniques and Pf-iRBC EV populations characterized in omics stu	dies 54
Table 5. List of antibodies used in Western blot analysis.	65
Table 6: Modified <i>P. falciparum</i> culture conditions to increase EV yield	72
Table 7. Distribution of significantly abundant known EV markers in P1 and P2 EVs	93
Table 8. Non-secretory <i>P. falciparum</i> iRBC EV proteins associated with membranes	98
Table 9. Absorbance ratios to assess RNA purity	110
Table 10. Mapping results for small RNA/microRNA sequencing	112
Table 11. Mapping results for RNA sequencing	113
Table 12. Reportable parameters in malaria EV studies	122

Appendix Figure 1. EV isolation at low parasitemia	155
Appendix Figure 2. Optimizing EV isolation with HEK293 cells	156
Appendix Figure 3. False C63+ malaria EVs isolated from cultures using non-leukoreduced F	RBCs
	157
Appendix Figure 4. Immunofluorescence imaging of infected and uninfected RBCs	157
Appendix Figure 5. Uncropped images	158
Appendix Figure 6. WBA of band 3	158
Appendix Figure 8. Expression of Calpain 5 in iRBC EVs	159
Appendix Figure 7. Bos taurus contaminants detected in EVs by mass spectrometry	159
Appendix Table 1. Full list of proteins from GO analysis of iRBC EVs	160

#### **List of Abbreviations**

**BCA:** Bicinchoninic acid

CPDA-1: Citric acid, sodium citrate, monobasic sodium phosphate, dextrose, and adenine

CM: Conditioned media

**DC:** Differential centrifugation

**DGC:** Density gradient centrifugation

**DV:** Digestive vacuole

**ESCRT:** Endosomal sorting complex required for transport

EVs: Extracellular vesicles

**FC:** Flow cytometry

**GYPA:** Glycophorin A

**HAP:** Histoaspartic protease

**ILVs:** Intraluminal vesicles

iRBCs: Infected red blood cells

**ISEV:** International Society for Extracellular Vesicles

LC-MS: Liquid chromatography-mass spectrometry

MISEV: Minimal Information for Studies of Extracellular Vesicles

MVB: Multivesicular body

**NTA:** Nanoparticle tracking analysis

**PBS:** Phosphate buffered saline

**PfEMP1:** *P. falciparum* erythrocyte membrane protein 1

**Pf-iRBC EVs:** P. falciparum-iRBC derived EVs

**PI:** Post invasion

**PVM:** Parasitophorous vacuole membrane

**RBCs:** Red blood cells

**R-iRBCs:** Ring-infected red blood cells

**RIFIN:** Repetitive interspersed family

S-iRBCs: Schizont-infected red blood cells

**SEC:** Size exclusion chromatography

STEVOR: Subtelomeric open reading frame

**TEM:** Transmission electron microscopy

**T-iRBCs:** Trophozoite-infected red blood cells

uRBC-EVs: Uninfected red blood cell-derived extracellular vesicles

**uRBCs:** Uninfected red blood cells

**VSAs:** Variable surface antigens

WBA: Western blot analysis

**Chapter 1: Introduction** 

"A 'small solution' to a 'big problem'". This expression almost perfectly describes the association between the two core themes of this thesis – extracellular vesicles (EVs) and *Plasmodium falciparum*. EVs are small particles that act as intercellular communicators, and *P. falciparum* is the causative agent of the deadliest form of malaria. Research has implicated malaria derived EVs in disease pathogenesis and parasite survival. However, an in-depth investigation of the biology of malaria derived EVs and their component biomolecule(s) that confer on them these important contributory roles is lacking. This research aimed to extensively characterize the biomolecular composition of malaria derived EVs, with a focus on *P. falciparum*, to determine the potential involvement of these biomolecules in the specific functions that have been described for malaria EVs by early studies. The research aim was achieved by strategically optimizing a differential centrifugation EV isolation protocol and extensively analyzing the isolated malaria EVs with a combination of techniques. This introductory chapter provides a brief background about *P. falciparum* and EVs as well as the context of the research, followed by the research problem and question, aims and objectives, relevance, and finally, the limitations.

Merozoites of *P. falciparum* infect red blood cells (RBCs), and the parasite subsequently develops through 3 intraerythrocytic asexual blood stages namely the rings, trophozoites and schizonts. Each life stage contributes to the immunopathology of falciparum malaria which is a consequence of the 'direct' interaction of parasite infected RBCs (iRBCs) with one another, uninfected RBCs (uRBCs) and endothelial cells lining blood vessels, accompanied by an intense inflammatory response. However, recent research has shown that malaria immunopathology may be aggravated by EVs that mediate 'indirect' communication between these cells and immune cells. EVs are released from, and taken up by, all living cells; they are small lipid bound particles that contain different functional proteins and nucleic acids and are consequently heterogenous in their composition and function.

EV research encompasses EV isolation methodologies, biology, biogenesis, function, and application. The field is represented by the International Society for Extracellular Vesicles (ISEV) that publishes guidelines with the goal of standardizing EV research protocols as well as advancing the reproducibility of key findings and interstudy comparisons in specialized fields of investigation [1, 2]. Nevertheless, despite advances in our understanding of the roles of EVs in physiological and pathological processes, EV research remains poorly standardized, and much is still unknown

about the biogenesis of EVs or the nature of these EVs in different cells [3]. This is the case for the nascent field of malaria EV research.

Three important functions have been described for malaria EVs. These include gametocytogenesis, drug resistance, and immunomodulation. Several studies of malaria EV biology have investigated the nature and cargo of malaria EVs, demonstrating that they contain both human and parasite biomolecules that may be involved in one or more of these biological processes [4]. Most of these studies, however, have focused on EVs released from RBCs infected with the ring stages of *P. falciparum*. The ring stage is a phenotypically distinct cell from the mature trophozoite and schizont stages [5, 6] that differentially alters the host RBC and, therefore, potentially releases, or induces the release of a characteristically distinct population of EVs from RBCs. EVs derived from RBCs infected with P. falciparum rings, trophozoites or schizonts have not been comprehensively and comparatively analyzed in a single study. In the absence of an encyclopedic characterization of malaria derived EVs, this research aimed to answer the following question: What are the physical and biomolecular characteristics of EVs released from RBCs infected with the 3 asexual blood stages of *P. falciparum*? The importance of this research question derives from the fact that the characteristic nature of any EV population largely determines their biodistribution, biological function and biomedical potential, and consequently, how these can be explored.

In this study, EVs were isolated from the conditioned media (CM) of *P. falciparum* cell cultures using differential centrifugation (DC). DC is the most used EV isolation technique across all fields of EV research [7, 8]. The caveat of this technique is that it is unstandardized, and different researchers use a variety of DC parameters and centrifugation steps to isolate malaria EVs. EVs isolated by different methodologies (and techniques), even from the same starting material, are often quantitatively, qualitatively, and more importantly, functionally diverse [9-11]. In view of this, ISEV, through the Minimal Information for Studies of Extracellular Vesicles (MISEV), advocates for standardization [1] and reproducibility [12] of EV isolation protocols. A crucial aim of this research, therefore, was to isolate a reasonably consistent population(s) of EVs from cultures of RBCs infected with each asexual stage of *P. falciparum*. To achieve this, an optimized and reproducible protocol for the isolation of EVs from cultures of *P. falciparum* by DC was developed. This was the first objective of this thesis.

The second and third objectives of the research work profoundly address the research question. Respectively, these were to analyze and compare the (1) protein and (2) RNA cargo in EVs released from RBCs infected with the asexual blood stages of *P. falciparum*. Proteomics of the EVs served a dual purpose. Firstly, a preliminary protein analysis of malaria EVs was important to validate the optimized protocol developed in objective 1. Secondly, a comprehensive protein analysis was essential to identify potential markers for malaria EV subpopulations and subtypes, as well as proteins that define EV biogenesis, biology, and functionality. Transcriptomics of malaria EVs was aimed at discovering unique or common RNA species, particularly those with regulatory functions.

This study pioneers the standardization of malaria EV isolation. For the first time, and by employing an optimized and reproducible EV isolation protocol, subpopulations, and subtypes of asexual malaria EVs have been comprehensively characterized in a single study. For the field of malaria EV research, which is still in its infancy, the thorough EV characterization performed in this study is invaluable for the accurate interpretation, validation, and application of published and future findings. Important biomolecules that may be implicated in the biogenesis of malaria EV and key functions have been identified and the data from this study will expectantly form the foundation of a malaria EV database which is currently unavailable. Such a database is critical for future compositional analyses, functional malaria EV studies and investigating malaria EV biogenesis.

Despite the significance of this study, it is subject to a few limitations. (1) The study focused on the 3D7 strain of *P. falciparum*. Therefore, the applicability of the EV isolation protocol and overall study findings to other laboratory strains or clinical isolates of *P. falciparum* cannot be fully determined. (2) The demographics of the blood donors for the malaria cultures were unknown, as such, the extent to which these may have influenced the study findings are also unknown; and (3) Two biological replicates were used for proteomics and 1 biological replicate for RNA sequencing and transcriptomics which limits the precision of the data. To address these limitations, I propose a replicated future study using another strain of *P. falciparum*, such as Dd2, obtaining the blood donor demographics with ethical approval, and performing the proteomics and transcriptomics on at least 1 more sample set.

Having introduced this thesis in chapter one, details of the theoretical framework for this research are provided in a comprehensive literature review on *P. falciparum* and malaria, EVs in

general, and EVs in malaria in chapter 2. Chapter 3 details the methods used in this study, while the results are explicitly described in Chapter 4. The collective findings of this study are discussed in detail in Chapter 5, and a conclusion/summary of this thesis is presented in Chapter 6.

**Chapter 2: Literature Review** 

#### 2.1. Plasmodium falciparum: The parasite

Belonging to the phylum Apicomplexa, *Plasmodium spp* are obligate unicellular protozoan parasites. These parasites are the causative agents of malaria, and humans are known to be infected by 5 members of the genus through the bite of infected mosquitoes. These include the 4 human parasites – *P. falciparum*, *P. vivax*, *P. ovale* and *P. malarie* and the simian parasite – *P. knowlesi*. Of these, *P. falciparum* is the most virulent, causing the severest forms of malaria and in some cases, death. In this regard, it is the most medically important *Plasmodium spp*, and therefore, the most widely researched. Although *P. falciparum* poses a global threat, it is mainly prevalent in Sub-Saharan Africa (Figure 1) [13]. In 2021, over 95% of the global 247 million cases of malaria and 619,000 malaria deaths occurred in Africa [14]. The high endemicity of falciparum malaria in this region is mainly due to the co-prevalence of *P. falciparum* and extremely efficient mosquito vectors, thereby sustaining the parasites' life cycle with continuous transmission of infection.

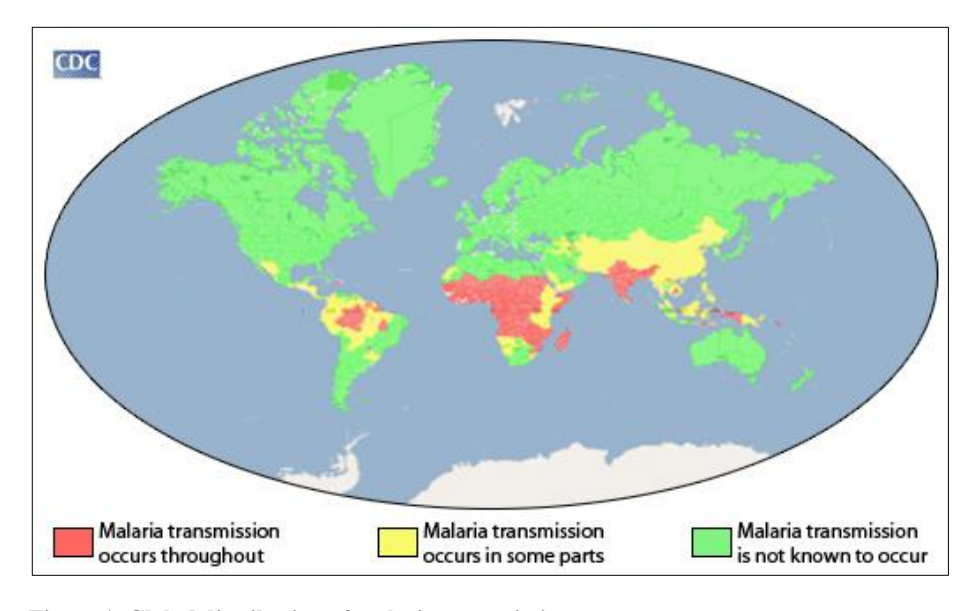


Figure 1. Global distribution of malaria transmission CDC, 2021 [13]

#### 2.1.1. The life cycle of *P. falciparum*

During the complex life cycle of *P. falciparum*, the parasite alternates between invertebrate and vertebrate hosts. The invertebrate hosts are female *Anopheles* mosquitos in which sexual development occurs, while asexual development occurs in the vertebrate human hosts (Figure 2). The life cycle of *P. falciparum* begins when a female anopheline mosquito ingests RBCs carrying

male and female gametocytes of the parasite during a blood meal from a malaria-infected human host. Within the mosquito midgut, the gametocytes emerge from the RBCs and form male and female gametes that fuse to form a zygote. The zygote transforms into a motile ookinete, which migrates across the midgut epithelium and differentiates into an oocyst. Within an oocyst, hundreds of sporozoites form in a process termed sporogony. Mature oocysts rupture, releasing the sporozoites into the mosquito's salivary gland. These sporozoites are infectious to the human host.

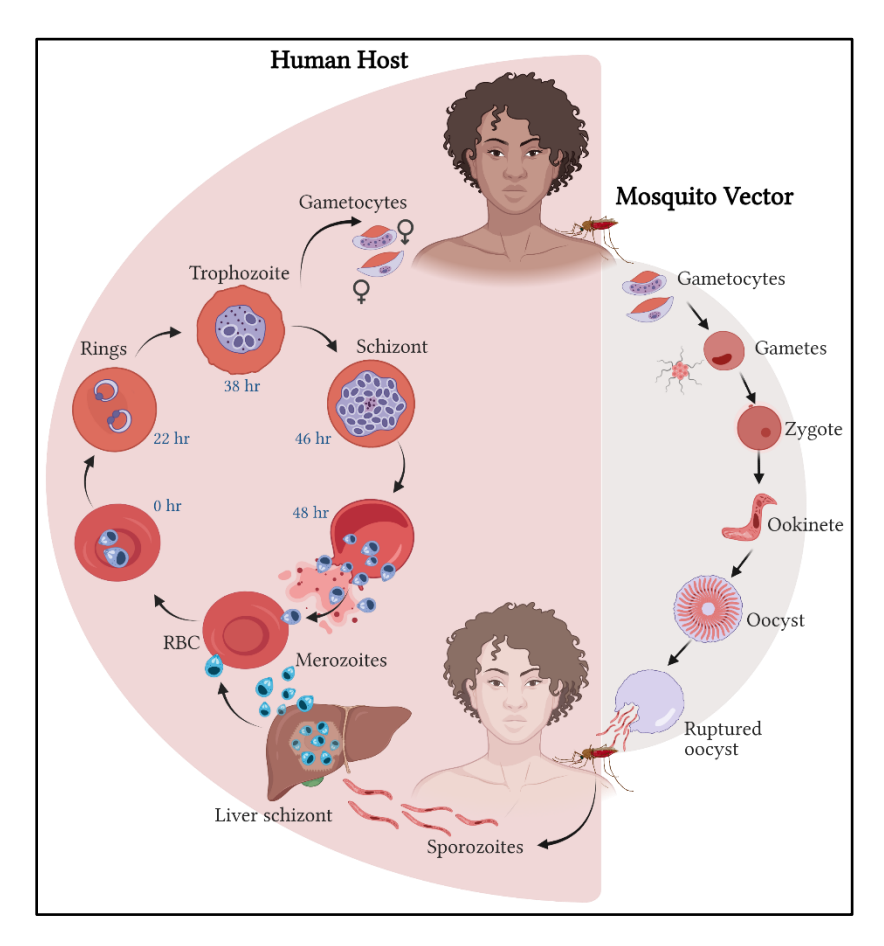


Figure 2. Life cycle of *P. falciparum*The parasite has a complex life cycle that spans between human and mosquito hosts. In humans, the developmental stages in the RBCs cause malaria. This intraerythrocytic phase lasts for ~48 hours. Created with BioRender.com

During the subsequent blood meal of the female anopheline mosquito, sporozoites are injected into the dermis of the human host. This marks the start of malaria infection. From the dermis, sporozoites enter the blood vessels, and quickly invade hepatocytes. Inside the hepatocytes, sporozoites undergo a single replication called pre-erythrocytic schizogony. The ensuing schizonts

rupture releasing thousands of motile merozoites into the vasculature. Merozoites then rapidly invade RBCs to begin the stage of cyclic replication called erythrocytic schizogony.

Following RBC invasion, merozoites begin differentiation into the first asexual intraerythrocytic life stage called the ring forms. The ring stage lasts for 22-24 hours post invasion (PI), during which time the parasite develops into the trophozoite stage. After a further 14-16 hours of growth, the trophozoites mature into schizonts. A fully mature schizont, termed a segmenter, ruptures the iRBC after 8-10 hours, destroying the RBC and releasing 16-32 merozoites alongside immunostimulatory malaria toxins. Each merozoite infects a new RBC and the cycle of asexual erythrocytic schizogony continues. Essentially, a cycle of erythrocytic schizogony is completed over ~48 hours. A small proportion of merozoites do not continue in this replicative cycle and instead, are committed to gametocytogenesis. They differentiate through 4 stages over a period of 11-15 days into male and female gametocytes. Mature gametocytes circulating in the bloodstream are taken up by a feeding female *Anopheles* mosquito, and the life cycle resumes.

Clearly, *P. falciparum* has a complex life cycle that involves multiple developmental sexual and asexual stages. However, it is the asexual erythrocytic phase involving the merozoites, rings, trophozoites and schizonts that is solely responsible for the clinical manifestations seen in malaria. Each of these blood stages has a distinct morphology and general biology, an understanding of which is crucial for the development of intervention strategies for malaria. The next 3 subsections describe the biology of the asexual intraerythrocytic blood stages: the rings, trophozoites and schizonts.

#### 2.1.2. The ring stage (~ 0-24 h PI)

The earliest form of the malaria parasite blood stages is commonly found in the peripheral circulation. These young parasites have a flat or cup-shaped, ring-like appearance, hence the name, 'ring stages' (Figure 2 and Figure 3A). It comprises a cytoplasm with a thin center and a thick rim with 1 or 2 visible chromatin dots. Within the rim of the cytoplasm are the major organelles such as the nucleus, apicoplast, mitochondrion, endoplasmic reticulum, and ribosomes; the center of the cytoplasm houses fewer organelles and is flattened [5, 15]. The parasite is enclosed in a plasma membrane which is in turn, surrounded by the parasitophorous vacuole and parasitophorous vacuolar membrane (PVM) (Figure 3D). Ring forms are typically very small, but vary in size throughout their development, occupying on average one-fifth of the diameter of an RBC [15, 16].

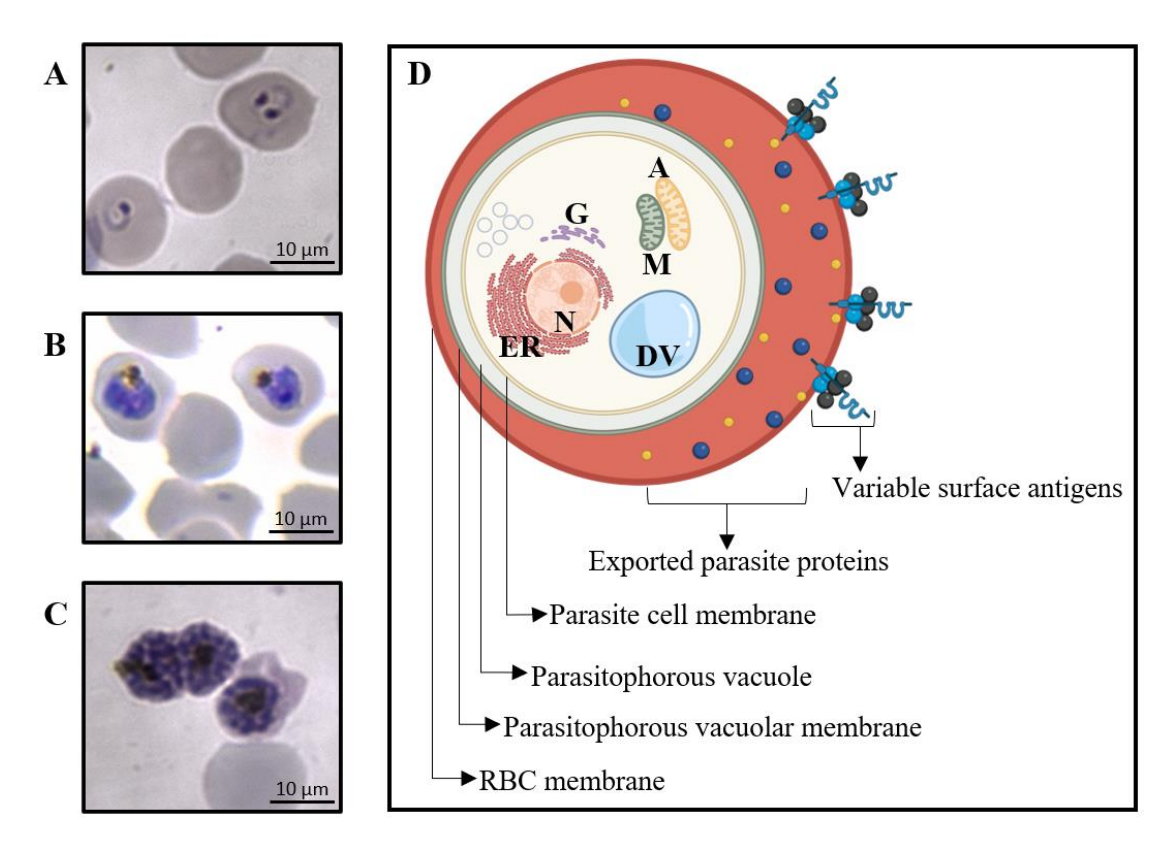


Figure 3. Asexual intraerythrocytic blood stages of P. falciparum

The ring (A), trophozoite (B), and schizont (C) stages are phenotypically distinct cells. Parasites are stained bluish-purple, red blood cells (RBCs) are stained greyish pink. (A) Ring forms with cytoplasmic ring and chromatin dot(s) prepare the RBC for mature stages. (B) Trophozoites are irregularly shaped with hemozoin pigment accumulating in the DV (stained yellowish purple) and are the most metabolically active. (C) Schizonts are the replicative stage and contain 16-32 daughter merozoites. (D) schematic representation of a parasite infected RBC. The parasite contains various organelles and exports proteins to the RBC cytosol (blue & yellow) and membrane (e.g., variable surface antigens). Within the RBC, the parasite is enveloped by the parasites cell membrane, parasitophorous vacuole and parasitophorous vacuolar membrane. N- nucleus, ER- endoplasmic reticulum, DV- digestive vacuole, G- Golgi complex, M- mitochondrion, A- apicoplast. Scale bar of light microscopy images scale bar -10 µm. Illustration created with BioRender.com.

At 10-15 hours PI, ingestion of the RBC cytosol (i.e., mainly hemoglobin) begins and feeding continues throughout intraerythrocytic development. Hemoglobin digestion is essential for amino acid supply and making space for the growing parasite [5, 16]. The parasite converts toxic heme from hemoglobin catabolism to hemozoin (malaria pigment) which is stored in numerous small vacuoles. The ring stage of *P. falciparum* has the least metabolic activity [17], but, during this stage, transcription of many parasite proteins begins [18, 19]. The morphology and function of the iRBC is not largely altered at this stage, and ring forms preserve the viability and survivability of the host RBC for the mature parasite stages [20, 21].

#### 2.1.3. The trophozoite stage (~22-38 h PI)

Rings differentiate into larger, more rounded, or irregularly shaped trophozoites (Figure 2 and Figure 3B). Trophozoites are the most metabolically active blood stage [16, 17]. They have a larger endoplasmic reticulum and more abundant ribosomes to accommodate the increased level of protein synthesis; a Golgi apparatus is present but is atypical and inconspicuous, and the parasitophorous vacuole and PVM expand with the growing parasite [5]. Trophozoites induce major modifications to the host RBCs and many proteins that are transcribed in the ring forms are expressed on the surface of trophozoite iRBCs [6, 16]. Many of these proteins form 'knobs' on the RBC membrane that present variable surface antigens (VSAs) [5]. Trophozoite stages sequester or 'hide' in the deep blood vessels of different organs and are not readily found in the peripheral circulation [19, 22]. Consumption of hemoglobin from the RBC cytosol is the greatest [17] but, unlike the ring stages, the trophozoites have a single, well-defined digestive vacuole that accumulates hemozoin [5].

#### 2.1.4. The schizont stage (~38-48 h PI)

The final intraerythrocytic stage is the replicating schizont. The parasite undergoes multiple rounds of nuclear and organellar division and reorganization. A nucleolus becomes apparent and merozoite organelles that had degenerated during the early ring stage are formed [5, 23]. Two-thirds or more of the RBC volume is occupied and individual merozoites surrounding the dark hemozoin pigment in the residual dense digestive vacuole can be observed under a light microscope (Figure 2 and Figure 3C). As with trophozoites, consumption of hemoglobin and export of parasite proteins continues [5, 6, 16]. There is maximal modification and distortion of the RBC membrane, with many more knobs forming on the RBC membrane surface [5, 20]. Schizont stages also sequester in deep blood vessels and are rarely seen in the peripheral blood [19, 22].

*P. falciparum* rings, trophozoites, and schizonts play a contiguous role in the pathology of falciparum malaria despite their distinct morphological, metabolic, and biochemical phenotypes [5, 6, 24, 25]. The reputation of *P. falciparum* as the most virulent *Plasmodium* species derives from several unique pathogenic features that are characterized by the direct interaction of parasite-iRBCs with various host cells, provoking the severe pathologies seen in malaria [26-28].

#### 2.2. Falciparum malaria: The disease

Clinical falciparum malaria may be asymptomatic, uncomplicated, severe, or fatal. The outcome of infection is largely dependent on the host's immune response and access to timely and efficient anti-malarial treatment. The most vulnerable are children under the age of five, pregnant women, immunocompromised individuals, and non-immune travelers to malaria endemic regions [29, 30]. The general symptoms of malaria are non-specific and include headache, fever, nausea, and muscle pains. In severe malaria, pathology results in organ specific syndromes which include cerebral malaria (coma), severe anemia, acidosis, respiratory distress, renal failure, and severe jaundice [26, 27, 30].

A fundamental pathogenic mechanism in falciparum malaria is "cytoadherence". This is the attachment of trophozoite- and schizont-stage iRBCs to different host cells in vital organs. This complex process is mediated by 3 major VSA families expressed by the parasite on the iRBC membrane (Figure 3D) that recognize and interact with specific host cell receptors. These VSA families are the major virulence factors of *P. falciparum*, namely *P. falciparum* erythrocyte membrane protein 1 (PfEMP1), subtelomeric open reading frame (STEVOR) and repetitive interspersed family (RIFIN) [19, 31]. Cytoadherence-associated phenomena include sequestration, rosetting, and autoagglutination (Figure 4).

Sequestration occurs when mature stage iRBCs adhere to the endothelial lining of the microvasculature in vital organs and by so doing, can 'hide' from the peripheral circulation, avoid splenic clearance, and evade immune cell detection [19, 32, 33]. Sequestration is at the core of malaria pathology and commonly occurs in the brain and placenta, resulting in cerebral and placental malaria respectively [30]. When a mature stage iRBC adheres to clusters of uRBCs with a resultant flower-like organization, the cytoadherence phenomenon is called rosette formation or rosetting [34-36]. Rosetting is believed to contribute to sequestration and to be important for merozoite invasion of uRBCs and immune evasion of iRBCs [35]. iRBCs are also able to adhere to each other, forming 'clumps' of iRBCs or autoagglutinates [37]. Autoagglutination of iRBCs is mediated by platelets [38-40], and, like rosetting, may contribute to sequestration [39].

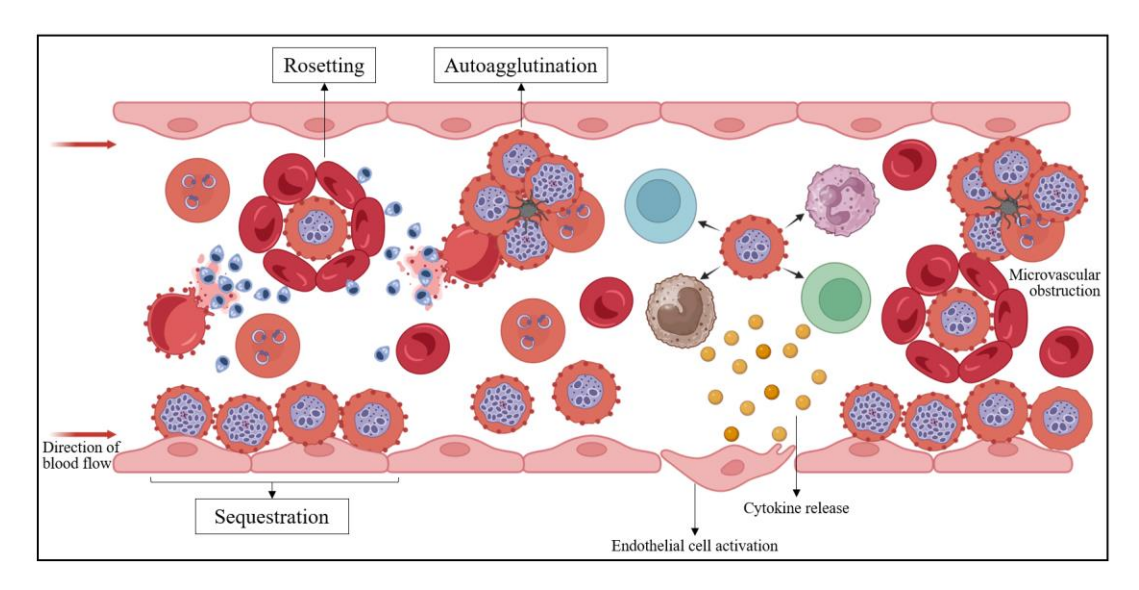


Figure 4. Pathology of falciparum malaria

iRBCs interact directly with host endothelial cells, uRBCs and other iRBCs via the cytoadherence-associated phenomena of sequestration, rosetting and autoagglutination respectively. *P. falciparum* iRBCs also activate immune cells causing cytokine release. Microvascular obstruction, exaggerated immune response, excessive endothelial cell activation, and disruption in vital organs results in the organ specific immunopathologies seen in falciparum malaria. Created with BioRender.com.

The complete picture of falciparum malaria pathology encompasses exponential parasite growth in the asexual erythrocytic phase, release of immunostimulatory parasite products, induction of a proinflammatory host immune response, endothelial cell activation, and biomechanical microvascular obstruction (Figure 4). [22, 28, 30]. The most well described aspects of falciparum malaria pathology are cytoadherence-mediated sequestration and the concomitant exaggerated host inflammatory response [19, 41]. Nevertheless, over a century after the discovery of malaria and decades of intensive research efforts, the intricate biomolecular mechanisms by which *P. falciparum* initiates and potentiates the pathophysiological processes occurring in the severe forms of falciparum malaria remain poorly understood.

For a complex disease such as falciparum malaria, the pathogenic basis is multi-factorial and new aspects of this pathological process continue to emerge [42, 43]. Common to the cytoadherence-associated phenomena of sequestration, rosetting, and autoagglutination is the direct contact and interaction between iRBCs and host cells. More recently, indirect intercellular communication mediated by extracellular vesicles (EVs) has been described as a contributory phenomenon that aggravates the immunopathology of falciparum malaria [4, 41, 44].

#### 2.3. Extracellular vesicles: A paradigm of intercellular communication

Communication between living cells is essential for their physiology and is integral to pathological processes. The most well-known and extensively researched mechanisms of cell communication are contact-dependent which relies on cell membrane receptor-ligand interaction, and chemical signaling that involves the secretion and uptake of signal molecules by cells [45]. In the case of *P. falciparum* infection, for example, parasitized RBCs express VSAs on the iRBC surface that recognize and interact with host cell receptors, and ruptured iRBCs release the toxic malaria pigment, hemozoin, that activates host immune cells.

Another paradigm of intercellular communication, also involving the release of signal molecules, but packaged into a delivery system, is now widely recognized. These delivery systems are known as extracellular vesicles (EVs). EVs are small, membrane-bound, cargo-carrying particles released by all viable cells into the extracellular space and taken up by recipient cells within which the released biomolecular cargo is processed and a biological response is produced [46, 47]. Although EVs are a relatively recent discovery in malaria, this mechanism of cell communication probably evolved thousands of years ago, alongside direct cell-to-cell contact and chemical signaling.

#### 2.3.1. A brief history of EVs

Erwin Chargaff and Randolph West, a duo of blood clotting researchers, unwittingly isolated EVs for the first time in 1946 (Figure 5). After subjecting plasma to high-speed centrifugation at 31,000 x g, Chargaff and West established that the resulting pellet had clotting properties [48]. This finding piqued the curiosity of the British physician Peter Wolf, who, in addition to plasma, isolated "coagulant material in particulate form" from serum and other blood fractions, by ultracentrifugation over 130,000 x g, as opposed to high-speed centrifugation [49]. Through a series of experiments on the coagulant material, Wolf was able to validate the findings of Chargaff and West, and for the first time, image the coagulant particles by electron microscopy. He concluded that these particles originated from platelets and referred to them as 'platelet dust' in 1967 [49].

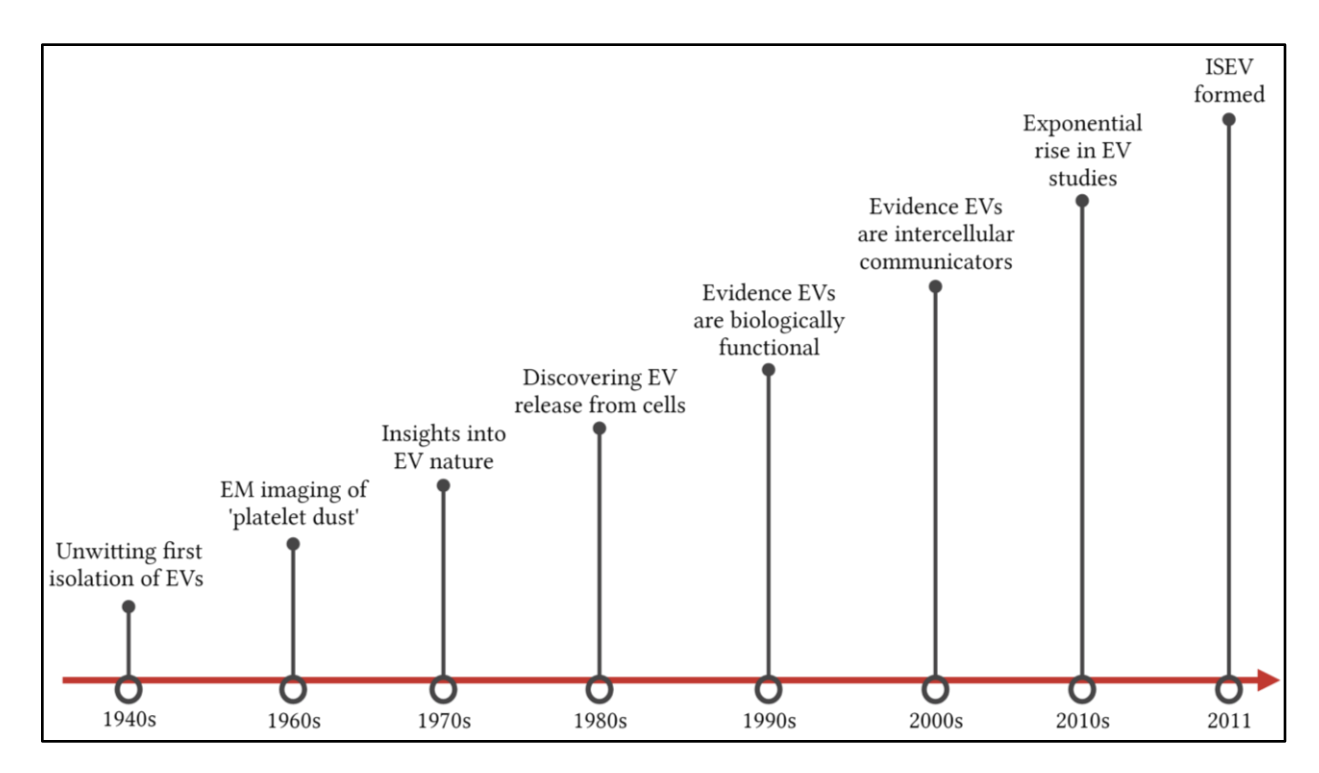


**Figure 5. Milestones in EV research history** Adapted from [3]. Created with BioRender.com.

In the decade that followed, the term 'microparticles' replaced 'platelet dust'. In these years, revolutionary work by Neville Crawford provided the first insights into the morphology, composition, and biological function of platelet microparticles [50]. Between the 1970's and 1980's, several studies suggested the release of EVs from non-mammalian cells and the earliest postulations about the mechanisms of their release were made [3, 51]. In 1983, seminal work by Rose Johnstone, a biochemist at McGill University's Faculty of Medicine, and Philip Stahl of the Washington University School of Medicine, provided evidence for the nature of EV release from cells. Johnstone and Stahl demonstrated that, during reticulocyte maturation, the transferrin receptor was contained in endocytic vesicles that were released from multivesicular bodies (MVBs) following their fusion with the cell membrane [52, 53]. Johnstone referred to this population of EVs as 'exosomes' [54]. Over the next 10-15 years, the field of EV research across various disciplines gradually became more cohesive, with increasing research into the biology of EVs [3]. The discovery in the mid 1990's that EVs had antigen presenting properties generated explosive interest for research into their functions, composition, and applications [3, 55].

The communicative role for EVs in cell biology was widely demonstrated in the 2000s and from 2010 onward, an exponential rise in EV research was seen across different fields of study, where EVs were shown to play key roles in physiological and pathological processes and acclaimed as biomarkers for several diseases [3, 51]. In a bid to amalgamate this rapidly growing field of research, the International Society for Extracellular Vesicles (ISEV) was formed in 2011. Through the rigorous activities of ISEV, MISEV guidelines for EV research [1, 2], position papers on the biology, analysis, and application of EVs as well as survey outputs for global EV research are published for the benefit of those in the field [3]. ISEV has and continues to play a major role in organizing EV research that has expanded vastly beyond its beginnings in coagulation studies to virtually every field of study involving living organisms. As a matter of course, different classes of EVs have been described.

#### 2.3.2. EV types and terminologies

Until the 1980s, a plethora of names were used to refer to the enigmatic 'vesicles' observed to be released from different mammalian and non-mammalian cells; these included, but are not limited to, platelet dust, microparticles, virus-like particles, bone-matrix vesicles, 'extracellular vesicles', 'exosomes', and 'microvesicles' [56]. Presently, 2 main types of EVs have been designated based on their biogenesis and subcellular origin [57] despite the obscurity of several precise details that remain [57, 58]. These are microvesicles and exosomes of cell membrane and endosomal origin, respectively. Today, a wide variety of secreted membrane-bound vesicles have been described and are often assigned names based on their cell of origin (e.g., oncosomes from tumor cells), specific functions (e.g., tolerosomes with immune tolerance properties), size (e.g., nanoparticles and microparticles) or with a reference to their extracellular location (e.g., ectosomes and exovesicles) [59, 60]. Many of these names are pseudonyms for EVs with the same or similar properties (Table 1).

Nomenclature has been a topic of debate overseen by ISEV. In 2018, ISEV endorsed 'extracellular vesicles - EVs' as the generic term for vesicles secreted from viable cells. This terminology encompasses "particles naturally released from the cell that are delimited by a lipid bilayer and cannot replicate, i.e., do not contain a functional nucleus" [1]. Despite the recommendation of the generic term, and the unambiguity of a biogenetic definition, EV nomenclature remains controversial. The term 'exosome' is still often used generically in lieu of

'EVs' [3, 56]. Furthermore, many investigators define exosomes and microvesicles on bases other than biogenesis such as (1) size, in which case microvesicles are regarded as being larger than exosomes, (2) cargo specificity, referring to exosomes as particles that carry specific biomolecules that are absent from microvesicles, (3) biological functions, with exosomes often suggested to have specific or exclusive functions, and (4) separation by DC, whereby microvesicles are believed to sediment exclusively at high speeds of  $\sim$ 10,000 x g and exosomes at very high ultracentrifugation speeds of  $\sim$ 100,000 x g [56, 60].

Table 1. Types and characteristics of EVs

	Exosomes	Microvesicles
Origin	Endosome	Plasma membrane
Size	30-150 nm	30-1000 nm
Other names	Exovesicle	Ectosome
	Nanovesicle	Microparticle
	Nanoparticle	Blebbing vesicle
	Exosome-like vesicles	Shedding vesicle
Composition	Cytoplasmic proteins	
	Nucleic acids	
	Membrane proteins	
	Lipids	

The 2 main EV types are exosomes and microvesicles, with endosomal and plasma membrane origins, respectively. Exosomes are typically smaller than microvesicles, though their sizes overlap. They are each known by many other names and the names listed here are based on the size and extracellular location of the EVs. Many other names have been designated according to the cell of origin and specific function. EVs both carry proteins, lipids, and nucleic acids. Exosomes and microvesicles share specific biomolecular components, but this may differ depending on the cell type.

These 'non-biogenetic' definitions are both conflicting and confusing, since exosomes and microvesicles overlap in their size and composition (Figure 6) and cannot be completely separated by current EV isolation techniques, such that EV preparations often comprise a heterogenous mix of exosomes and microvesicles [47, 61-63]. Nonetheless, in the absence of exosome- and microvesicle-specific markers and sophisticated techniques to separate or identify them, ISEV strongly suggests that the use of the generic term EVs be accompanied with clear information on the physical characteristics (e.g., size and density), cargo specificity (i.e., biochemical/biomolecular composition) and cell of origin of the EV preparation under investigation [1].

Indeed, EV nomenclature and biogenesis are coincident concepts, an understanding of which has direct implications for the design of EV studies and the development of technologies for isolating and studying EV subpopulations and subtypes.

#### 2.3.3. EV biogenesis

#### 2.3.3.1. The biogenesis of exosomes

Exosomes are formed as part of the endocytic pathway [57, 64, 65]. Their biogenesis begins with the inward budding of the membrane of early endosomes to form intraluminal vesicles (ILVs). With the accumulation of multiple ILVs, the early endosome matures into a late endosome otherwise known as a multivesicular body – MVB. MVBs then fuse with the cells plasma membrane to release exosomes into the extracellular space (Figure 6A). Exosomes are generally very small with a diameter of 30-150 nm.

ILVs bud off from endosomal membrane microdomains comprised of lipids and membrane-associated proteins that eventually enclose cytoplasmic proteins and nucleic acids. The main mechanisms of exosome biogenesis are (1) cargo clustering at the endosomal membrane and (2) cytoplasmic cargo sorting into the pre-formed membrane cargo clusters [57]. The complex molecular machineries involved in these mechanisms include the endosomal sorting complex required for transport (ESCRT)-dependent and ESCRT independent machineries (Figure 6B) [46, 66, 67]. The ESCRT machinery comprises dozens of proteins that are assembled into four complexes – ESCRT 0, I, II and III. These complexes, in conjunction with their associated proteins, coordinate the sequential clustering of transmembrane proteins to endosomal membrane microdomains, sorting of cytoplasmic cargo to the microdomains, membrane deformation at the site of the microdomain into invaginated buds with sequestered cytoplasmic cargo, and, finally, fission of this microdomain to form vesicles [57, 59, 68]. *Plasmodium* species lack the ESCRT 0, I, and II subcomplexes, as well as several ESCRT III components and associated proteins; in fact, the *P. falciparum* genome encodes only 6 of the 26 ESCRT machinery proteins [69].

ESCRT-independent machineries are not as well elucidated as the ESCRT-dependent machinery. These include ceramide-dependent generation of endosomal membrane microdomains [70-72], tetraspanin-dependent exosome biogenesis [57] and SIMPLE- (small integral membrane protein of lysosomes and late endosomes) regulated exosome biogenesis [73]. It has been

suggested that ESCRT-dependent and ESCRT-independent molecular machineries may act independently or simultaneously on an MVB [59].

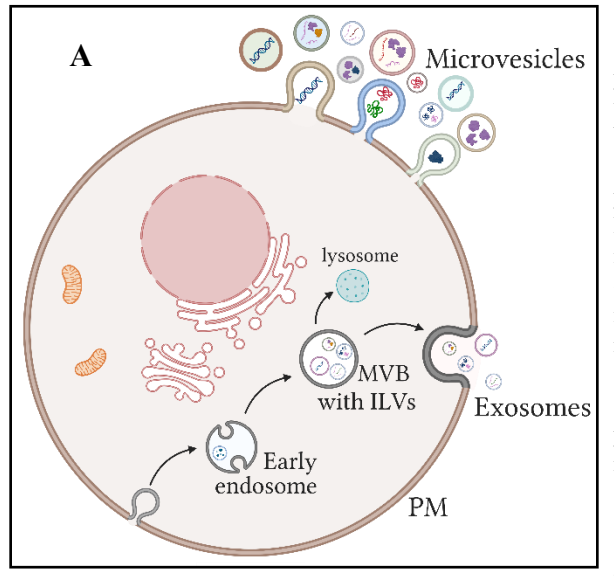
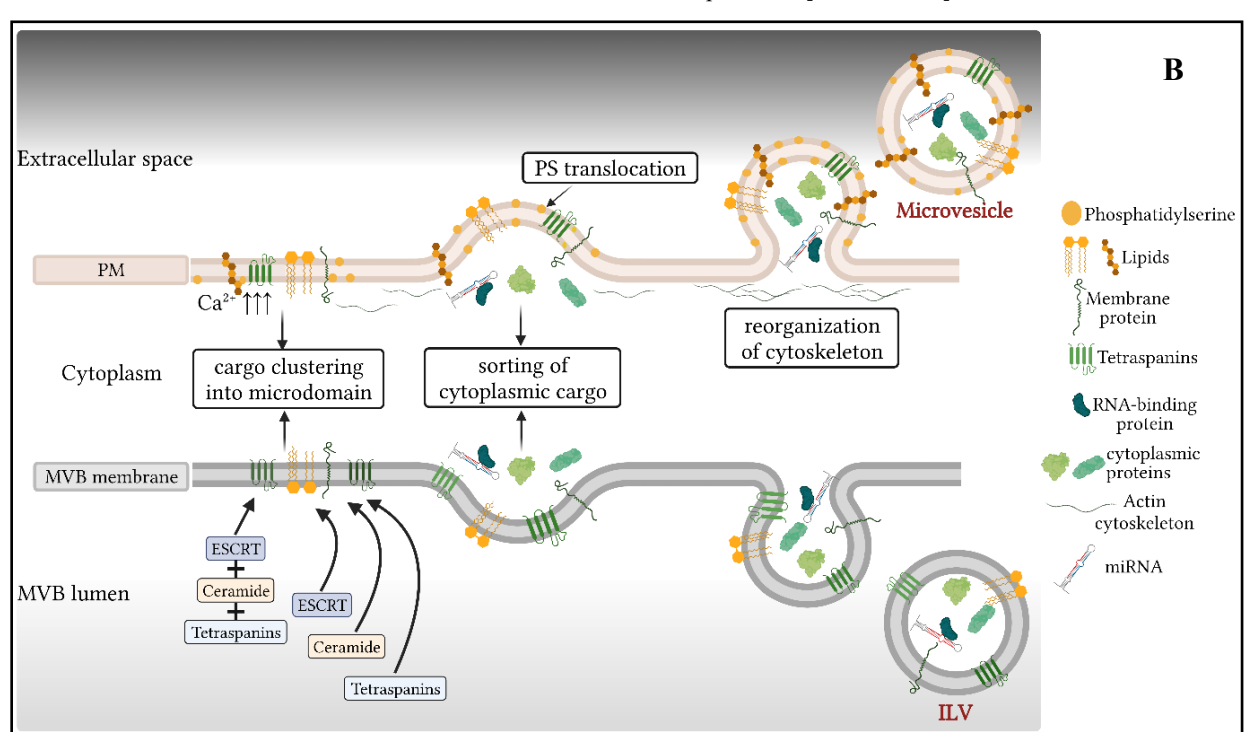


#### Figure 6. Biogenesis of EVs

(A) Microvesicles are formed by direct budding and fission of the plasma membrane (PM) and exosomes are formed as intraluminal vesicles (ILVs) within multivesicular bodies (MVBs) and released by fusion of the MVB with the PM. Cells may release exosomes and/ or microvesicles depending on their physiological or pathological state. EV populations released are vastly heterogenous in their size and specific composition. (B) Shared mechanisms of exosome and microvesicle biogenesis are clustering of cargo (lipids & transmembrane proteins) into microdomains on the MVB membrane & plasma membrane, respectively, and sorting of cytoplasmic cargo (proteins & nucleic acids) to the microdomains. Microvesicle biogenesis occurs by Ca<sup>2+</sup>-dependent enzymatic machineries that promote phosphatidylserine translocation (PS) & cytoskeleton reorganization at budding sites. ESCRT-dependent & ESCRTindependent (ceramide & tetraspanin dependent) machineries form ILVs which are future exosomes. Other mechanisms which are not yet well understood may be involved in the formation of EVs. Adapted from [57, 59, 77, 79]. Created with BioRender.com.



#### 2.3.3.2. The biogenesis of microvesicles

Microvesicles are formed by the direct outward budding and fission of the plasma membrane of the secreting cell (Figure 6A). They range broadly in size from 30 nm to 1 μm, although microvesicles outside this size range have been reported [46, 59]. The mechanisms of microvesicle formation and release from cells is less well understood, but much less complex than exosome biogenesis; similar to exosomes, however, are the mechanisms of membrane cargo clustering to form microdomains, which in the case of microvesicles, occurs at the cell's plasma membrane, and cytoplasmic cargo sorting to the membrane microdomains [57, 59]. Although the ESCRT-dependent machinery is unique to exosome biogenesis, certain ESCRT proteins are involved in the biogenesis of microvesicles [74, 75]. Also, ceramide, a molecular component of the ESCRT-independent biogenesis machinery for exosomes, has been shown to promote membrane deformation and microvesicle shedding [76].

Ca<sup>2+</sup>-dependent enzymatic machineries (flippases, floppases, scramblases, calpain) responsible for a loss of membrane asymmetry involved in microvesiculation are the most well described [77-79]. This is a mechanism that is unique to microvesicles (Figure 6B). When intracellular levels of Ca<sup>2+</sup> rise, phosphatidylserine is translocated from the plasma membranes inner leaflet to the outer leaflet; this leads to membrane deformation and reorganization of the cytoskeleton occurs, which promotes membrane budding and microvesicle formation [57]. Depending on the cell type, many other molecular machineries and mechanisms may be involved in the generation of microvesicles. These include cholesterol-dependent machinery, lipid-metabolism enzymes, and protein-dependent machinery (RAB proteins) [57, 59, 78, 79].

Whether a cell deploys one or more biogenetic pathways to release exosomes and/or microvesicles into the extracellular milieu is largely influenced by the cell type, growth conditions and physiological or pathological state of the cell [57, 59, 79]. In turn, the biogenesis mechanism(s) primarily determines the volume and nature of biomolecular cargo that is sorted into EVs, and this varies widely [57, 80, 81]. This results in the formation and release of EVs that are heterogenous in size and composition.

#### 2.3.4. The biomolecular composition of EVs

Since the discovery of EVs, numerous studies have been conducted to gain insight into their fundamental nature, identify EV markers, and predict their biological functions and applications

[59, 82]. From these studies, we now know that, whilst the biomolecular composition of an EV population often depends on the parent cell type [83, 84], cell culture conditions [85-87], and/or pathological and physiological state of the cell [88-91], it is generally similar across all EVs (Figure 7) [59, 61, 92]. The findings of the majority of EV omics investigations are curated in publicly accessible databases that are continuously updated, such as ExoCarta - <a href="http://www.exocarta.org/">http://www.exocarta.org/</a> [93] and vesiclepedia — <a href="http://www.microvesices.org/">http://www.microvesices.org/</a> [94]. These databases include information on EV protein, nucleic acid, and lipid composition.

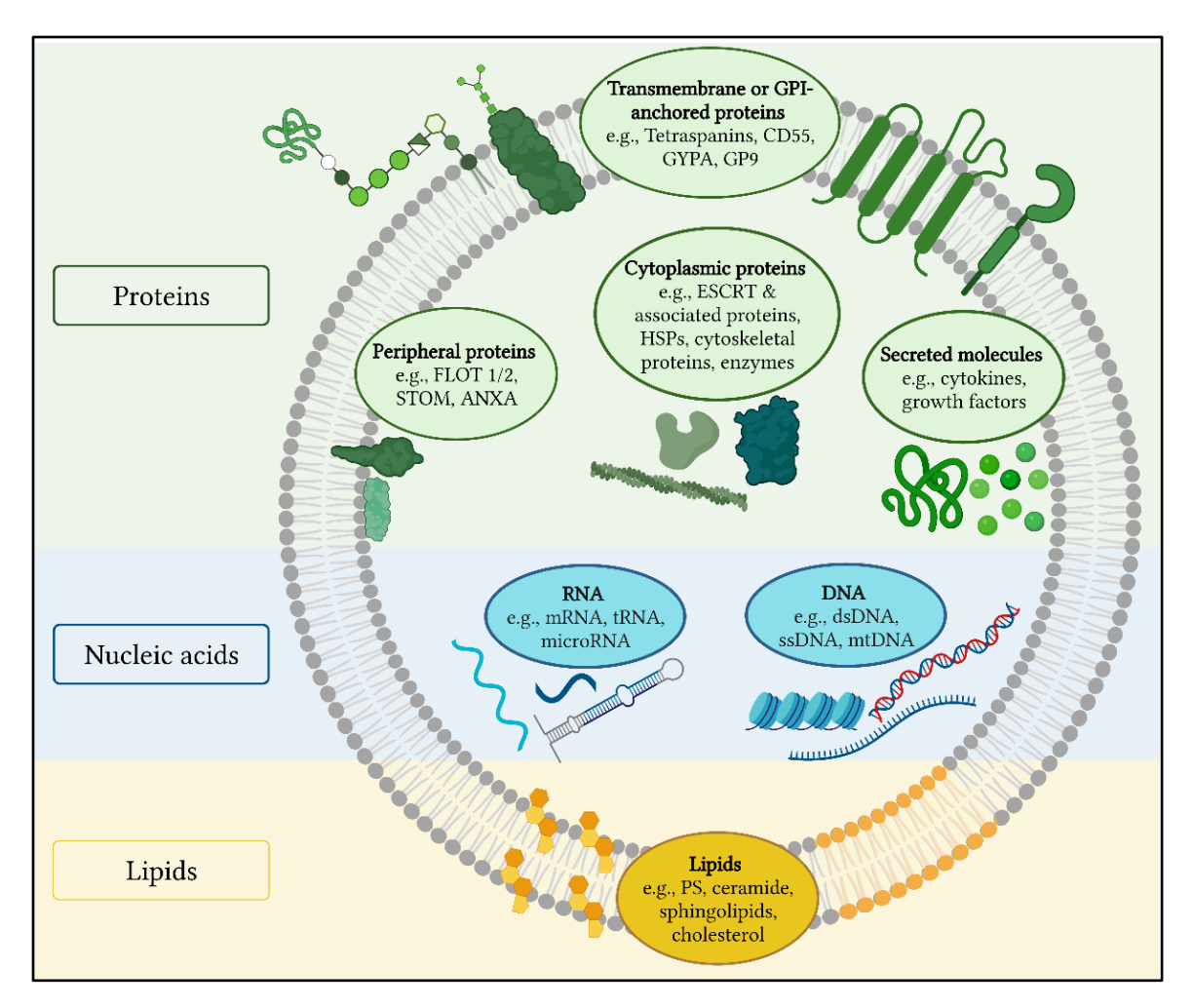


Figure 7. General biomolecular composition of EVs

All EVs contain protein, nucleic acids, and lipid cargo. Glycans and metabolites are also present. The specific biomolecular composition of EVs varies depending on the cell type, cell growth conditions, and disease state. Common proteins include tetraspanins – CD63, CD81, CD82, CD9; lipid raft proteins – flotillin 1/2, stomatin; ESCRT proteins – tumor susceptibility gene 101 (TSG101), ALG-2 interacting protein X (ALIX); ESCRT associated proteins – vacuolar protein sorting-associated protein (VPS4A/B); HSPs (heat shock proteins) – HSP70, HSPA8; cytoskeletal proteins – actin, tubulin, spectrin; enzymes – glyceraldehyde 3-phosphate dehydrogenase (GAPDH), enolase, pyruvate kinase. Adapted from [1, 57, 59]. Created with BioRender.com.

### **2.3.4.1. EV proteins**

Several research groups have characterized and compared the protein content of different types of EVs [59]. Proteins serve as the main markers for EVs and EV subpopulations/subtypes, since some proteins are present in all EVs, while others are found only in EVs from certain cell types [1, 61, 95]. Many classes of proteins are present on the membrane and within the lumen of EVs (Figure 7) that are derived from the parent cells plasma membrane, cytoplasm and/or endosome during biogenesis. [57, 92]. These proteins include transmembrane proteins, membrane-associated proteins, ESCRT components and ESCRT associated proteins [83, 88, 96, 97]. Also present are lipid raft proteins, such as flotillins and stomatin, that have been implicated in the cargo sorting into EVs [79, 98].

Other proteins not directly involved in their biogenesis, but often incorporated into EVs include heat shock proteins, cytoskeletal proteins, and enzymes. Some EVs, particularly larger sized at >200 nm, may contain proteins associated to non-endosomal compartments, such as the nucleus, mitochondria, endoplasmic reticulum, and Golgi apparatus [61]. Secreted molecules, such as cytokines and growth factors, have also been detected bound to or encapsulated in EVs [99, 100].

Functions of the many protein families found in EVs include EV biogenesis, membrane scaffolding, transport & adhesion, enzymatic activity, signal transduction, intracellular trafficking, chaperone activity, antigen presentation and complement binding [101].

#### 2.3.4.2. EV nucleic acids

Since the earliest studies that demonstrated EVs carry functional messenger RNA and microRNA [102-104], as well as ssDNA and mitochondrial DNA [105, 106], there has been intensive analyses of the nucleic acid composition of EVs, most notably RNA [107-109].

The loading of RNA into EVs is a highly specific process [110-112] and characterized EV-RNA species are diverse. They include non-coding RNA species, such as lncRNA, mitochondrial RNA, PIWI-interacting RNA, ribosomal RNA, small nuclear RNA, small nucleolar RNA, transfer RNA, vault RNA and Y RNA [107]. Circular RNAs are also present [113-115]. EVs are enriched with small RNAs, and EV-RNA is about 200 nucleotides long that may be intact or fragmented [92, 107]. The RNA cargo of EVs is now known to include both functional and non-functional RNA [107].

EV-DNA is not as well characterized as EV-RNA but the presence of dsDNA, as well as ssDNA and mtDNA, has been established [116], where EV-DNA is present in fragments of 100 bp up to 10 Kbp or more [109]. The functions of EV-DNA are still largely being elucidated [109].

Unlike free extracellular RNA and DNA, EV-RNA and EV-DNA are protected from enzymatic degradation; the benefit of this is being exploited to explore the application of EV genetic material in therapeutics [107-109].

## **2.3.4.3. EV lipids**

The successful delivery of EV proteins and nucleic acids to recipient cells largely relies on their encapsulation within the lipid bilayer of the EV membrane. In contrast to proteins and nucleic acids, however, EV lipids have received much less attention [8, 101]. Sphingomyelin, cholesterol, phosphatidylserine, and glycosphingolipids are the most enriched lipids in EVs [117]. While the overall lipid composition of EVs and their parent cell membrane are similar (plasma membrane or endocytic membrane), some lipids are specifically associated with different EV types [117]. There is evidence that the sorting of lipid cargo into membrane microdomains from which EVs originate is a highly regulated and selective process [118] thereby intensifying research efforts to validate the application of EV lipids as biomarkers and EVs in general as drug delivery systems [101, 117].

In addition to proteins, nucleic acids, and lipids, EVs also contain metabolites [119, 120] and glycans [121, 122], and research interest in these EV components is steadily increasing.

While the biomolecular composition of EVs is consequent of different biogenesis mechanisms and factors associated with the cell of origin, it has direct implications for the fate of a given EV population. The membrane lipids confer stability, and other membrane molecules (proteins, glycans, as well as lipids) are important for uptake by recipient cells, while the internal proteins, nucleic acids and metabolites exert phenotypic changes on the recipient cells [57, 123].

#### 2.3.5. Fate, biological functions, and applications of EVs

Upon secretion from their cell of origin, EVs traverse the extracellular space over long or short distances to reach recipient cells [124]. The biomolecular cargo of EVs are transferred to recipient cells following direct interaction with the EVs, internalization of the EVs, or membrane fusion (Figure 8); these are complex processes, none of which is fully understood [47, 57, 123]. When EVs dock at the plasma membrane, ligands on the EV bind to surface receptors on the recipient cell and the EVs act as signal transducers by triggering intracellular signaling pathways that

activate the cell. This mechanism of direct interaction may be behind target cell specificity [57] and there is evidence that EV interaction and uptake by cells is a highly specific process [125-127]. In view of this, EVs can be engineered with surface receptors to evade uptake by immune cells [128] or promote uptake by target cells [129, 130].

Non-specific uptake of EVs is probably directed by internalization and this mode of interaction may be shared by many cell types [123]. Internalization can occur by clathrin-mediated endocytosis [131, 132], caveola-dependent endocytosis [133, 134], lipid raft-dependent endocytosis [135, 136] and clathrin-independent endocytosis (macropinocytosis, micropinocytosis and phagocytosis) [137-139]. These methods of EV-cell interaction can occur concomitantly in the same cell [138, 140]. EVs can also interact non-specifically with recipient cells by direct fusion with the plasma membrane to release their contents [141]. This is mediated by membrane proteins and lipid raft-like domains on the EVs [123].

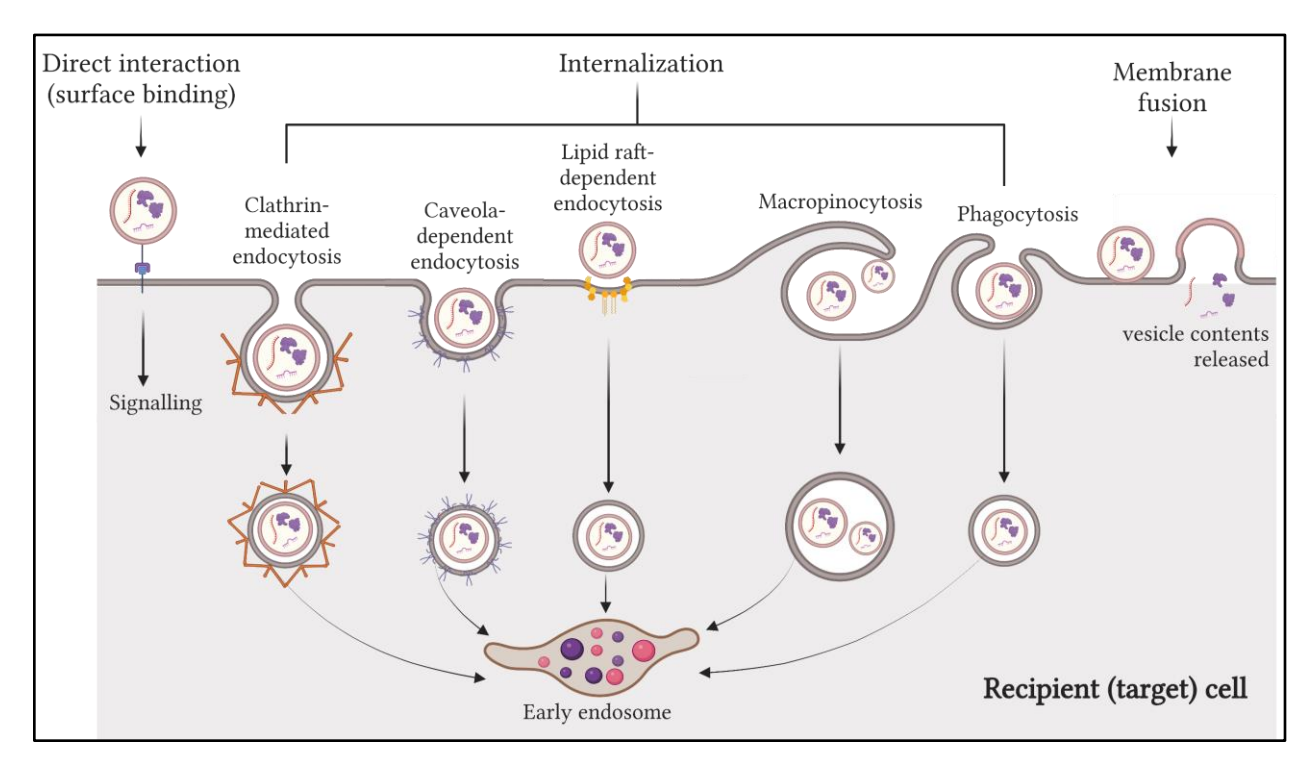


Figure 8. EV interaction with recipient cells

EVs can interact with recipient cells through direct interaction between ligands and receptors at the cell surface and trigger intracellular signaling pathways. Alternatively, EVs may be internalized by clathrin-dependent endocytosis, caveola-dependent endocytosis, lipid raft-dependent endocytosis, macropinocytosis and phagocytosis. Internalized EVs fuse with early endosomes. EV degradation in the endosomal pathway releases its cargo that is recycled by the cell. Membrane fusion between the EV and recipient cell may also occur, in which case the vesicle contents are released into the cytosol.

Adapted from [57, 123]. Created with BioRender.com.

The EV cargo released into recipient cells is the essence of the diverse and numerous functions that have been described for EVs in physiological and pathological processes. By virtue of the signaling function of EV cargo, EVs can activate recipient cells and/or regulate different cellular processes. In mammals, EVs function in virtually all organ systems, with physiological roles in liver homeostasis, bone calcification, cell maturation, coagulation, regulation of the nervous system, development of immunity and immune regulation [101, 107].

EVs mediate inflammation and immunosuppression and are directly involved in neurological disorders, inflammatory diseases, autoimmune diseases, and the progression of cancers [142]. The majority of what is known about the nature and functions of EVs is derived from studies in mammals and cancers. However, EVs are now known to play vital roles in lower organisms. Particularly, in parasitic organisms, EVs are important for parasite survival, disease pathogenesis, immune evasion, and immunomodulation [143-145]. Bacterial EVs are involved in molecular transport, host cell interactions as well as biofilm formation and stress responses to promote bacterial survival [101]. EVs also play key functions in the normal physiology of plants [101].

Typically, the amount, composition, and function of EVs is altered in diseased states. Coupled with the presence of EVs in virtually every body fluid, they have been designated suitable diagnostic, prognostic, and therapeutic biomarkers for a myriad of diseases [123, 146]. Other emerging applications include drug delivery, vaccines, gene therapy, immunotherapy, cancer therapy and tissue regeneration [146, 147]. The clinical application of EVs is, however, impeded by their intrinsic compositional heterogeneity that cannot be overemphasized. In-depth characterization of any EV population would address this issue. Be that as it may, reliable EV characterization is largely dependent on the successful isolation of a high quality, high yield, highly homogenous EV population of interest [148, 149]. An EV isolation technique or protocol that achieves all these criteria, is yet unavailable [148].

#### 2.3.6. EV isolation techniques and methodologies

EVs are isolated from biological fluids and tissues, as well as tissue or cell culture conditioned media (CM) for the purpose of discovery, diagnostic and preparative research to characterize EVs, validate disease biomarkers and apply EVs to clinical and mechanistic uses respectively [150]. Therefore, key factors that determine the choice of EV isolation technique are downstream analyses and application, as the co-isolation of impurities or use of certain reagents in an isolation

protocol may alter the cargo and/or functionality of EVs, rendering them unsuitable. Equally significant are the nature of the sample (e.g., viscosity and volume) and the cell source (an important consideration for heterogeneity since different cells release different EV subpopulations and some cells release multiple EV subtypes) [62, 149, 151, 152].

A variety of techniques are available which are based on diverse principles (Table 2) that allow the isolation of different EV populations based on their physical and biochemical properties including size, density, charge, and/or biomolecular composition [153-155]. Traditional techniques are differential centrifugation (DC), density gradient centrifugation (DGC), precipitation, immunoaffinity, ultrafiltration and size exclusion chromatography (SEC), while modern and emerging isolation techniques include commercial isolation kits, Flow Field-Flow Fractionation, Hydrostatic Filtration Dialysis, charge-based techniques (e.g., ion-exchange, ion concentration polarization) and microfluidics [153-156]. Each of these techniques has its own advantages and disadvantages [148], hence some are used in combination [154].

Available isolation techniques and methodologies yield EV preparations with diverse purity, composition, and function. [9, 10, 157-159]. In 2017, an international consortium revealed that "190 unique isolation methods and 1,083 unique protocols" were used to recover EVs from a total of 1,742 experiments. Indisputably, EV isolation methods are not standardized within specialized areas of research (including malaria EV research, discussed below, in section 2.4.5) or in the EV field in general. With a lack of standardized isolation methods, EVs will remain incompletely characterized and their functions inadequately validated, impeding progress in the field [148]. This is a major challenge as very few research groups focus on methodology and biology, with many studies being functional [3, 82]. In view of this, intensive collaborative efforts are being made by ISEV to improve standardization in EV isolation, characterization, functional studies, and data reporting with the goal of promoting the reproducibility of studies, interstudy comparison and reliable validation of functional EV studies [1, 12, 82]. Nevertheless, intriguing functions have been described for EVs released from a wide range of eukaryotic and prokaryotic cells, including *P. falciparum*.

Table 2. EV isolation techniques

Technique	Principle	Advantages	Disadvantages
Differential centrifugation	By sequentially increasing centrifugation speed, EVs are separated and isolated based on density, shape, and size	Affordable, accessible, accommodates large sample volumes, high EV yield	High initial equipment cost, low portability, user-dependent, time- consuming, labor intensive, unsuitable in clinical settings, EV aggregation, low throughput
Density gradient ultracentrifugation	Density-based separation through a density medium	High purity, affordable, accessible	High initial equipment cost, low portability, user-dependent, time- consuming, labor intensive, unsuitable in clinical settings, low EV yield, low throughput
Size exclusion chromatography	Size-based separation of EVs in suspension on a porous column	Separation of different sized EV populations, EV structure and function preserved, high purity, reproducible, clinical applicability	Low sample volume, low yield, expensive
Ultrafiltration	Size-based separation of EVs in suspension, trapped on a pore-containing membrane	Fast, easy operation, portability, affordable	Moderate purity, damage to EVs, low yield, membrane clogging, unsuitable in clinical settings
Immunocapture	Capturing by binding of antibodies to antigens on EVs	High purity, high specificity, isolation of EV subtypes, fast, easy operation, clinical applicability	Costly reagents, low sample volume, low EV yield, non- specific binding, loss of EV function
Precipitation	Water-excluding polymers to alter solubility and dispersibility of EVs. Separation based on size and density	High recovery, fast, easy operation, simple equipment, clinical applicability	Co-precipitation of contaminants, time-consuming, EV function altered
Microfluidics	Size-based, immunoaffinity- based, or dynamic. Isolates EVs through micrometer channels using capillary forces	High throughput, suitable for microvolume samples, fast, easy operation, clinical applicability, affordable	Low sensitivity, add-on expenses, clogging, low throughput of some applications

Traditional techniques for EV isolation are based on different principles that rely on the physical and chemical properties of EVs. Modern and emerging techniques (not listed in this table) are based on several principles including size exclusion, filtration, flow fractionation, ion-exchange, electrophoresis and immunoaffinity. Modern techniques include several commercially available kits. Adapted from [149, 153-156]

### 2.4. EVs in falciparum malaria

Clinical studies have found that compared to healthy individuals, plasma EVs are elevated in patients with falciparum malaria [160, 161], more so in cases of severe and cerebral malaria [160, 162-165]. In these studies, it was observed that the elevated EV titers detected during acute malaria significantly fell once patients had recovered from illness, and in many cases, returned to baseline levels. With this observation, EVs have been designated potential biomarkers for cerebral malaria to manage disease, monitor cure rates [162, 163] and to predict the risk of severe disease in vulnerable populations [161]. These plasma EVs include those derived from platelets, endothelial cell, white blood cells, and RBCs, and have been shown to carry parasite proteins associated with biology and virulence [166] as well as miRNAs that are important in malaria pathways and host-parasite interactions [167].

An in-depth analysis of EVs from patients with severe malaria, particularly cerebral malaria, would be helpful to investigate their role because much is unknown about the pathophysiology of severe malaria leading to death and these details are often restricted to terminal cases. However, investigating the severe forms of falciparum malaria, especially the immunopathology of cerebral malaria directly in humans, is limited by cultural and ethical constraints [168]. As such, experimental models of rodents and their malaria parasites are necessary to study the biology and pathology of severe falciparum malaria [168, 169]. These are extremely useful since many rodent malaria parasites, such as *P. berghei*, *P. yoelii* and *P. chabaudi*, induce pathologies and syndromes that are comparable to severe falciparum malaria [169]. Using these experimental models, a potential role for EVs in the pathogenesis of severe falciparum malaria has been established.

As in humans, plasma EVs have been detected in abundance in experimental models of cerebral malaria [170, 171] and contain proteins and miRNAs important for host-parasite interactions as well as disease pathogenesis [172-174]. Also, EVs from mice with cerebral and non-cerebral malaria have a very distinct lipid profile from healthy mice [175]. Plasma EVs from cerebral malaria mice have been shown to have a high procoagulant activity [170] and have a predilection for brain microvasculature [176]. More specifically, reticulocyte derived EVs from *P. yoelii* infected mice carry immunogenic parasite proteins [177] and studies have demonstrated the vaccine potential of EVs from experimental malaria models [172, 177, 178]. RBC-derived EVs

from cerebral malaria mice infected with *P. berghei* have been found to be highly pro-inflammatory and constitute a major proportion of the plasma EV population from different cells [171].

These findings have prompted investigations of the potential functions and applications of EVs derived from *P. falciparum* iRBCs. Unlike the other *Plasmodium* species that infect humans, *P. falciparum* can be continuously grown in RBCs in a robust *in vitro* culture system [179, 180]. *In vitro* cultures are an invaluable resource for the unmediated investigation of *P. falciparum* blood stages and their interaction with host RBCs [180], bearing in mind variations with the *in vivo* growth environment [181]. Several groups have utilized *in vitro* cultures of *P. falciparum* as a source of EVs to investigate their biogenesis, composition, functions, and applications. *In vitro* cultures of *P. falciparum* grown in RBCs conceivably constitute a heterogeneous population of vesicles that originate from the host RBC as well as the parasite. As these populations are inextricable, EVs from these cultures are purposefully referred to as *P. falciparum*-infected RBC derived EVs (*Pf*-iRBC-EVs) rather than *P. falciparum* EVs.

## 2.4.1. Biogenesis of Pf-iRBC-EVs

There are far more insights into the biogenesis of EVs from healthy RBCs than from *P. falciparum*-infected RBCs for which research is in its infancy. Immature RBCs known as reticulocytes, generate exosomes from endosomal compartments as an essential part of their maturation process [182, 183]. Mature RBCs lack the endosomal machinery for exosome biogenesis, nevertheless, they constitutively shed microvesicles from their plasma membrane as part of a homeostatic aging process [184, 185]. As for *P. falciparum*, there is preliminary evidence suggesting that it releases EVs via endocytic pathways and plasma membrane shedding (Figure 9).

As mentioned in sub-section 2.3.3, the four ESCRT complexes and their associated proteins are required for exosome biogenesis, while certain ESCRT proteins are recruited for the biogenesis of microvesicles; also, the ESCRT complexes 0, I and II are absent from *P. falciparum*, while some ESCRT III proteins and its associated components are preserved. A recent study has found that the ESCRT III machinery in *P. falciparum* is activated by a pathway different to what is obtainable in eukaryotes in which the upstream ESCRT complexes are conserved [186]. This involves the parasites ESCRT III protein, PfVps32 and the associated proteins, PfBro1 and PfVps60. Three mechanisms have been proposed:

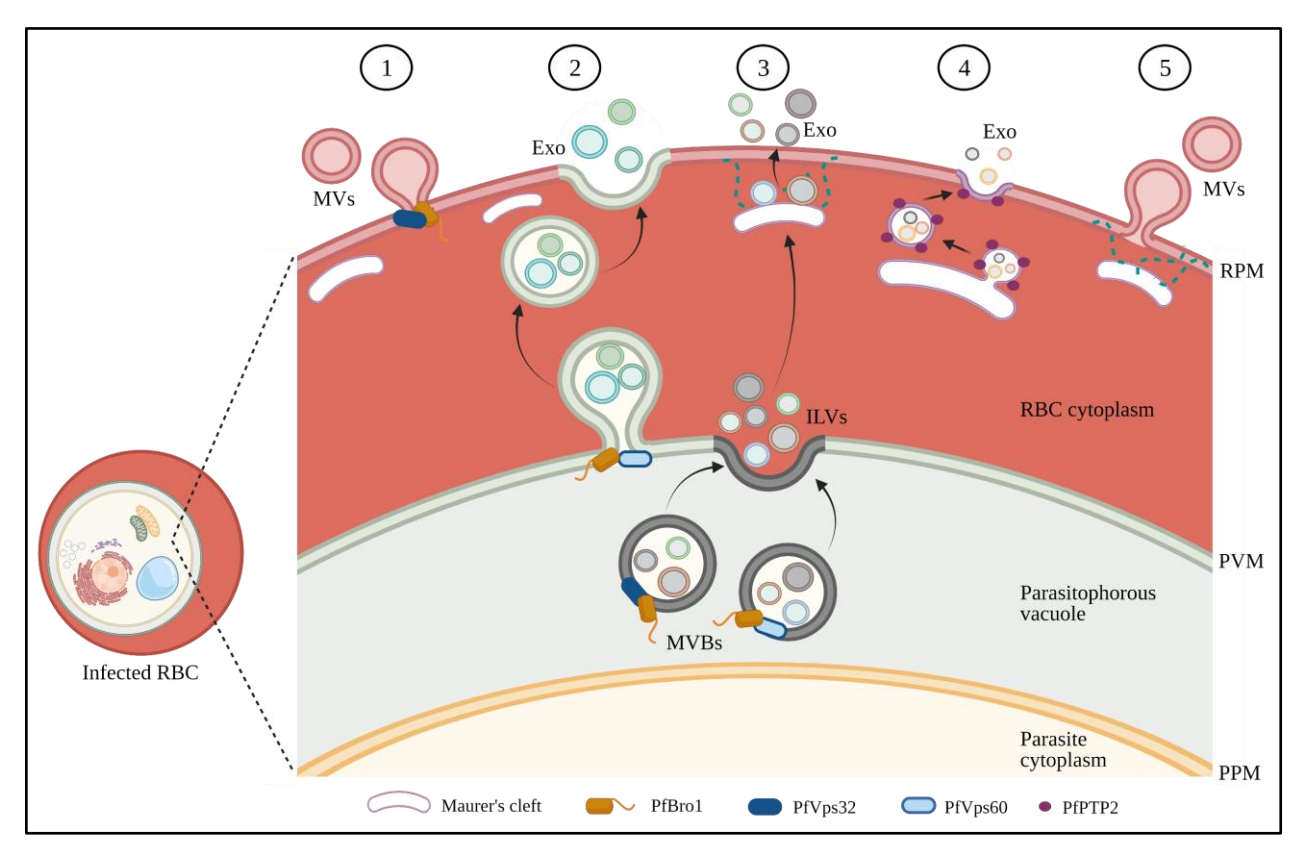


Figure 9. Proposed mechanisms of EV biogenesis in *Plasmodium falciparum*-infected RBCs (1), (2), (3) ESCRT-III-mediated EV biogenesis. (1) PfBro1 recruits PfVps32 at the RBC plasma membrane (RPM) generating microvesicles (MVs). (2) PfBro1 recruits PfVps60 at the parasitophorous vacuolar membrane (PVM) of the parasite generating multivesicular bodies (MVBs) that are released into the RBC cytoplasm, which subsequently fuse with the RPM to release exosomes (Exo). (3) Within the parasitophorous vacuole, PfBro1 recruits PfVps32 and PfVps60 to form MVBs which fuse with the PVM to release their intraluminal vesicles (ILVs) into the RBC cytoplasm. ILVs are then released from the RBC, possibly via activity of the Maurer's clefts. (4) PfPTP2-coated particles containing exosome-like vesicles bud off Maurer's clefts and fuse with the RPM to release the vesicles. (5) MVs directly bud off the RPM with involvement of the Maurer's clefts. RBC- red blood cell, PPM- parasite plasma membrane, PfPTP2- PfEMP1 trafficking protein 2. Culled from [186, 189, 190]. Created with BioRender.com.

(1) PfBro1 exported by the parasite into the RBC cytoplasm binds PfVps32 at the RBC membrane to trigger membrane budding and generate microvesicles, or, (2) binding of PfBro1 to PfVps60 at the PVM triggers MVB formation directly in the membrane, giving rise to MVBs that are released into the RBC cytoplasm and eventually fuse with the RBC plasma membrane releasing exosomes to the extracellular space and lastly, (3) binding of PfBro1 to PfVps60 and PfVps32 in the lumen of the parasitophorous vacuole triggers MVB formation and ILVs are released into the RBC cytoplasm when the MVB fuses with the PVM; exosomes are subsequently released to the extracellular space by an unknown mechanism, probably by budding off from Maurer's clefts [186].

Maurer's clefts are parasite-derived membrane-bound structures that are located at the periphery of the parasitized RBC and function as sorting compartments that receive cargo exported by the parasite and deliver it to the RBC membrane [187, 188]. Two independent earlier studies proposed that Maurer's clefts are a key component in the biogenesis of *Pf*-iRBC-EVs. First, Regev-Rudzki *et al* identified PfEMP1 trafficking protein 2- (PfPTP2) coated structures that bud off from the Maurer's clefts and suggested that exosome-like vesicles are released from these structures into the culture supernatant; their findings implicated PfPTP2 as a key protein in the biogenesis of *Pf*-iRBC-EVs and they likened the PfPTP2-coated particles to MVBs [189]. Second, Mantel *et al* demonstrated, by live imaging that *Pf*-iRBC-EVs were formed by direct "blebbing" off from the RBC membrane; however, by performing proteomic profiling and a series of enzyme protection assays in which they detected several Maurer's cleft proteins, they also suggested that malaria EVs originate from Maurer's cleft structures at the RBC membrane [190].

There is a lack of studies on the biogenesis and mechanisms of cargo packaging of *Pf*-iRBC-EVs, but in recent times, more research groups have investigated their composition. In general, knowledge of the biomolecular composition of EVs is crucial for unraveling their biogenesis mechanisms and determining unique markers that can identify different EV populations.

## 2.4.2. Composition of *Pf*-iRBC-EVs

Several omics studies have revealed that *Pf*-iRBC-EVs comprise human and parasite proteins as well as nucleic acid cargo (Table 3). While the EV cargo of the *P. falciparum* reference strain 3D7 is the most analyzed, EVs from other laboratory strains, and even short-term culture-adapted strains from malaria patients, have been investigated. Key biomolecules were shown to be conserved across *P. falciparum* strains.

Among the human proteins, hemoglobin and RBC membrane-associated proteins have been commonly identified [190-192]. These include band 3, stomatin, flotillins and cytoskeletal proteins. Many parasite proteins have been found to be enriched in *Pf*-iRBC-EVs and these include those important for invasion of RBCs, egress from RBCs, and generally, virulence [190-193].

Table 3. Biomolecular composition of Pf-iRBC-EVs

Biomolecular cargo	<i>P. falciparum</i> strain <sup>a</sup>	Summarized findings <sup>b</sup>	
Proteins	Isolate 9605	<ul> <li>■ RBC membrane-associated proteins &amp; hemoglobin</li> <li>■ 153 parasite proteins</li> <li>✓ Enrichment of Maurer's cleft &amp; rhoptry proteins</li> <li>✓ Enrichment of exported &amp; membrane-associated proteins</li> </ul>	
	3D7	<ul> <li>233 human proteins</li> <li>16 parasite proteins</li> <li>✓ Pf lactate dehydrogenase enriched in high parasitemia cultures</li> </ul>	[194]
	3D7	<ul> <li>178 human proteins</li> <li>101 parasite proteins</li> <li>✓ Enrichment of invasion and egress proteins</li> </ul>	[193]
	NF54	<ul> <li>■ 109 human proteins</li> <li>✓ Enzymes &amp; proteasome subunits</li> <li>■ 23 parasite proteins</li> <li>✓ Ribosomal &amp; transmembrane proteins, chaperones, enzymes</li> </ul>	[195]
	3D7, NF54, TM01, TM02	<ul> <li>► &gt;150 human proteins</li> <li>✓ Conserved content in <i>P. falciparum</i> strains</li> <li>✓ RBC proteins (Hemoglobin, Band 3, CD47 etc.)</li> <li>► &gt;150 parasite proteins</li> <li>✓ Conserved content in <i>P. falciparum</i> strains</li> <li>✓ Virulence proteins (e.g. erythrocyte binding antigen-175 etc.)</li> </ul>	[192]
	3D7 & CS2	<ul> <li>RBC lipid raft proteins (e.g., stomatin, band 3)</li> <li>&gt;80 parasite proteins</li> <li>✓ Maurer's cleft &amp; parasitophorous vacuole membrane proteins</li> <li>✓ Invasion proteins e.g., rhoptry proteins</li> <li>Conserved content in <i>P. falciparum</i> strains</li> </ul>	[190]
Nucleic acids	3D7	<ul> <li>Human miR-451a &amp; let-7b in abundance</li> <li>Human miR-451a is functional and complexed with human Ago-2</li> </ul>	[196]
	3D7	<ul> <li>&gt;90 % of small RNA content is human</li> <li>✓ miRNAs, tRNAs, Y-RNAs, vault RNAs (involved in drug resistance), snoRNAs and piRNAs present</li> <li>✓ miR-451a is the most abundant</li> <li>~120 P. falciparum RNA detected</li> <li>✓ Mostly rRNA, tRNA &amp; snoRNA</li> <li>✓ mRNAs coding exported proteins &amp; drug resistance proteins</li> </ul>	[197]
	3D7	<ul> <li>Human miR-451a, miR-486, miR-181a identified</li> <li>Human miRNAs are complexed with Ago-2</li> </ul>	[198]
	3D7, NF54, TM01, TM02	■ Human miR-451a is significantly elevated	[199]
	3D7	<ul> <li>Human miR-451a is the most abundant species</li> <li>Majority of detected miRNA regulate cell adhesion</li> <li>P. falciparum gDNA present &amp; triggers an innate immune response</li> </ul>	[200]
Linida	Dd2	<ul> <li>Enrichment of phosphatidylserine &amp; phosphatidylinositol</li> <li>Enrichment of sphingolipids with signaling functions</li> </ul>	[201]
Lipids	3D7	■ Enrichment of phosphatidylcholine	[202]
VOCs	НВ3	■ Enrichment of the insect attractant, hexanal	[203]

 <sup>&</sup>lt;sup>a</sup> 3D7 is the canonical reference strain of *P. falciparum*; CS2, NF54, Dd2 and HB3 are laboratory-adapted strains; isolate 9605 was culture-adapted from a Kenyan child with cerebral malaria; TM01 and TM02 were culture-adapted from Thai patients with uncomplicated and severe falciparum malaria, respectively.
 <sup>b</sup> Not an exhaustive summary

Conversely, most nucleic acids are human miRNA species, including miR-451a which has often been detected as the most abundant [196-200]. Interestingly, human and parasite small RNAs involved in drug resistance have been detected [197] and this may have implications for tackling the widespread drug resistance of *P. falciparum*. Plasmodial genomic DNA with immunogenic functions has also been found in *Pf*-iRBC-EVs [200]. Several specific biomolecules have been singled out for intensive investigations of their roles in *Pf*-iRBC-EVs. These are discussed in subsequent sections.

## 2.4.3. Pf-iRBC-EVs and P. falciparum biology: Parasite-parasite communication

For the propagation of its life cycle, the intraerythrocytic asexual blood stages of *P. falciparum* must differentiate into the sexual transmission stages that are picked up by feeding female Anopheles mosquitos (Figure 2). Sexual stages are a vital target for the development of transmission blocking antimalarials and vaccines. However, such research is currently hampered as gametocytes only occasionally appear in *in vitro* cultures and protocols for the large-scale production of gametocytes in continuous culture are often expensive, laborious, and unreliable [204, 205].

Two malaria EV research groups have demonstrated a potential role for *Pf*-iRBC-EVs in the induction of gametocytogenesis in culture systems. In the study by Mantel *et al*, when increasing concentrations of EVs isolated from the CM of parasite cultures were used to treat other ring-stage cultures of *P. falciparum*, high numbers of gametocytes were observed [190]. Using a different experimental design, similar observations were made by Regev-Rudzki *et al*. In a series of co-culture experiments with several laboratory strains of *P. falciparum*, it was observed that *Pf*-iRBC-EVs from ring-stage cultures, (which the authors termed "exosome-like vesicles") promoted differentiation of asexual stages to sexual stages [189]. The use of co-cultures in these experiments followed by successful isolation of EVs from the CM was significant as it emphasized communication between parasites mediated by EVs.

The parasite strains used by Regev-Rudzki *et al* expressed different drug resistance cassettes and different fluorescent proteins and were grown under drug pressure. Parasite strains died when cultured alone. However, surviving co-cultured parasite strains were positive for both drug resistance genes and the observed gametocytes showed both fluorescent proteins. Altogether, these findings were highly suggestive that EV-mediated active signaling occurred between parasite

strains that not only induced gametocytogenesis, but also promoted survival in the presence of drugs. Regev-Rudzki *et al* concluded that EVs functioned in the transfer of drug resistance between malaria parasites [189].

The Pf-iRBC-EVs in the experiments by Mantel et~al and Regev-Rudzki et~al were isolated from ring stage cultures that were maintained at low parasitemia, which is typically  $\leq 3\%$ . Proteomic analysis of Pf-iRBC-EVs isolated from high parasitemia cultures of 20-25% and low parasitemia cultures of 1-2% at the schizont stage revealed that the former was significantly enriched for P. falciparum lactate dehydrogenase (PfLDH) than the latter [194]. In separate bioassays, the growth of parasites in cultures was inhibited following treatment with Pf-iRBC-EVs from high parasitemia cultures, or their growth was rescued after the inhibition of PfLDH. This evidence suggested that Pf-iRBC-EVs can induce apoptosis in high parasitemia cultures through the suicide-signaling activity of their PfLDH cargo, thereby regulating parasite population in a 'quorum-sensing'-like manner [194].

## 2.4.4. Pf-iRBC-EVs in malaria immunopathogenesis: Parasite-host interaction I

Severe falciparum malaria is a disease characterized by "complex host-parasite immunopathological interactions", the landscape of which has not been fully elucidated [19]. The first evidence of an immunomodulatory role for *Pf*-iRBC-EVs came from experiments showing that *Pf*-iRBC-EVs mediate communication between *P. falciparum* and host cells of the innate immune system [190]. In this study, *Pf*-iRBC-EVs activated neutrophils and induced the expression of pro- and anti-inflammatory cytokines from macrophages after being actively taken up by these phagocytes. Furthermore, flow cytometry analysis of a panel of cell and activation markers for peripheral blood mononuclear cells indicated that monocytes are the main target cells [190].

Monocytes are vital in protective immune responses against malaria as well as immunopathogenesis [206], and these cells also actively take up *Pf*-iRBC-EVs [200, 207]. Sisquella *et al* described a mechanism by which ring stage *Pf*-iRBC-EVs carrying parasite genomic DNA activate monocytes and induce the secretion of type 1 interferons and other cytokines [200]. The mechanism, that involves STING (Stimulator of Interferon Genes)-dependent DNA sensing was verified using elaborate imaging studies of monocytes transfected with *P. falciparum* DNA [207]. The importance of *Pf*-iRBC-EVs and the associated parasite genomic DNA in STING-

dependent DNA sensing is unknown [200], however, the virulence protein, PfEMP1 in early-stage Pf-iRBC-EVs has been implicated in immune evasion. Pathway analysis of altered gene expression in human monocytes treated with PfEMP1-negative Pf-iRBC-EVs indicated a significant upregulation of pathways involving defense response, response to stress and cellular response to cytokine stimulus, none of which were upregulated in PfEMP1-positive Pf-iRBC-EVs [193]. In addition to the possibility of acting as a "decoy antigen" in immune evasion, the delivery of PfEMP1 in EVs to monocytes may assist in host manipulation [193].

RNA cargo in ring stage *Pf*-iRBC-EVs was recently suggested to play an indirect role in ensuring host survival and transmission to the mosquito by inhibiting synthesis of the chemokine CXCL10 [208]. Low levels of CXCL10 are present in uninfected individuals and uncomplicated cases of falciparum malaria [209], while elevated levels have been associated with fatal cases of cerebral malaria [210, 211]. Furthermore, *P. falciparum* uses CXCL10 in the culture environment as a cue for accelerated growth [208]. However, when parasite RNA in *Pf*-iRBC-EVs is released into monocytes, the RNA receptor, retinoic acid-inducible gene-I (RIG-I) is activated and, following a cascade of intracellular events, CXCL10 translation is repressed, and parasite growth is regulated [208].

With the existence of different *P. falciparum* strains and monocyte populations, it is possible that EVs from RBCs infected with *P. falciparum* strains that cause severe or uncomplicated malaria target different monocyte populations to be activated and/or modulated with different infection outcomes. Findings of a research group that set out to investigate the effect of EVs from cultures of different strains of *P. falciparum* on monocyte polarization would suggest this to be the case and it may be a virulence factor for certain *P. falciparum* strains [199]. *Pf*-iRBC-EVs also act on cells other than monocytes.

Endothelial cells lining the microvasculature of internal organs, including the brain, are a crucial component in the pathogenesis of severe and cerebral malaria because of the cytoadherence properties of *P. falciparum* that allows iRBCs to adhere to endothelial cells and sequester in multiple organs (Section 2.2). *Pf*-iRBC-EVs are internalized by endothelial cells and deliver functional host-derived RNA-induced silencing complexes that subsequently silence gene expression in recipient endothelial cells and disrupt endothelial barrier functions in blood vessels. Additionally, *Pf*-iRBC-EVs induce in endothelial cells, the release of pro-inflammatory cytokines

and expression of the surface receptor vascular cell adhesion protein 1 (VCAM-1), which may further contribute to vascular dysfunction [196]. Evidence shows that Pf-iRBC-EVs may be more directly involved in the immunopathogenesis of cerebral malaria by targeting microglia, which are the resident macrophages of the brain. *In vitro* studies using monocyte-derived microglia revealed that these cells also actively take up Pf-iRBC-EVs; internalized Pf-iRBC-EVs activate monocyte-derived microglia and stimulate an upregulation of the pro-inflammatory cytokine TNF- $\alpha$  and a concomitant downregulation of the anti-inflammatory cytokine IL-10 [212].

Lastly, trophozoite stage Pf-iRBC-EVs act on host RBCs prior to infection. Dekel et~al demonstrated that, following uptake of Pf-iRBC-EVs by uRBCs, intact 20S proteasomes released from the EVs disrupt and remodel the RBC cytoskeletal network by causing phosphorylation of cytoskeletal proteins, including  $\beta$ -adducin, ankyrin-1, dematin and Epb4.1. By so doing, P. falciparum primes the RBC for invasion by merozoites, ultimately promoting its own growth [213]. Dekel and colleagues have suggested that this process is a potential drug target to control parasitemia in clinical infection [213].

## 2.4.5. Pf-iRBC-EVs and their therapeutic application: Parasite-host interaction II

Many EVs cause or aggravate disease conditions and can, therefore, serve as drug targets; conversely, some EVs have natural medicinal properties and can be exploited as drugs and vaccines [214]. Furthermore, natural EVs and synthetic vesicles have been explored as drug carriers, targeting specific cells [58, 214].

In the early 2000s, Liu *et al* formulated a biodegradable microparticle containing the 19 kDa carboxyl-terminal fragment of the *P. falciparum* merozoite surface protein 1 (MSP1) and, following a series of assays, suggested the potential use of these synthetic microparticles as gene delivery systems to antigen-presenting cells that can prevent RBC invasion by parasites [215]. Compared to *P. vivax*, the application of synthetic nanoparticles and microparticles as vaccines has not been intensively researched or pursued [4].

Recently, however, *Pf*-iRBC-EVs were evaluated for their applicability as natural antimalarial drug delivery systems [216]. Atovaquone and tafenoquine, both lipophilic drugs, were loaded into EVs by co-incubation over 24 hours. When drug-loaded EVs, and free drugs were added to cultures of *P. falciparum*, the encapsulated drugs were found to inhibit parasite growth more efficiently. Furthermore, the drug-loaded *Pf*-iRBC-EVs were bound by iRBCs and uRBCs with high avidity

[216], suggesting that these EVs may be targeted to RBCs to prevent invasion. Indeed, *Pf*-iRBC-EVs can fuse efficiently to plasma membranes ensuring their successful uptake and cargo delivery [195].

Pf-iRBC-EVs also hold potential as natural killer cell-based antimalarial therapeutics [217]. In malaria infection, natural killer (NK) cells are the main source of IFN- $\gamma$ , which is required for controlling parasitemia [218], and non-responsive NK cells have been found to be the predominant phenotype in patients with severe malaria [217]. In a dose-dependent manner, Pf-iRBC-EVs, when used to treat NK cells in P. falciparum cultures, were found to alter their phenotype from non-responsive to responsive and concomitantly reduce parasitemia. In a series of knock-out experiments and RNA transcriptional analysis, the authors of this study implicated parasite RNA in this process and suggested that the RNA molecules in Pf-iRBC-EVs stimulated NK cells to mount an innate immune response by activating their cytosolic RNA sensors [217].

In summary, several studies have provided valuable insights into the biogenesis, composition, suggested functions, and potential applications of malaria derived EVs. However, a key challenge with these studies, particularly discovery studies to determine the physical and biochemical nature of *Pf*-iRBC-EVs, is the lack of standardization of isolation protocols and procedures (Table 4).

Many studies of the biology (and function) of malaria derived EVs have used different isolation protocols for DC, and have either not indicated the life stage of the cultures from which the EVs were isolated, or more commonly, isolated malaria EVs from cultures infected with only 1 stage of the parasite. This has hindered the reproducibility, comparability, and reliability of key studies. All things considered, the progress of malaria EV research hinges on standardization of EV isolation protocols and comprehensive analyses of malaria EV subpopulations and subtypes from all intraerythrocytic stages of *P. falciparum*.

Table 4. EV isolation techniques and Pf-iRBC EV populations characterized in omics studies.

Ref	iRBC EV	EV isolation				
	subpopulation <sup>a</sup>	Sample	Technique <sup>b</sup>	Rotor type <sup>c</sup>	Centrifugation	Centrifugation
		volume			speed <sup>d</sup>	time <sup>d</sup>
	-	1 L	DC	-	100,000 x g	1 hr
[190]						
	-	1 L	DC	-	100,000 x g	1 hr
[201]						
	-	1 L	DC	-	100,000 x g	1 hr
[196]						
404	Ring-to-trophozoite stage	300 mL	DC	70.1Ti	150,000 x g	2 hr
[191]	Trophozoite-to-ring stage					
-100-	Ring stage	15 mL	DC	-	20,000 x g	2 hr
[198]			<b>5</b> 6		1.50.000	
-200-	Ring stage	-	DC	-	150,000 x g	-
[200]		25. 1	D.C		110.000	<b>5</b> 0 ·
(202)	-	25 mL	DC	-	110,000 x g	70 min
[203]	D		OD Ca	CHIAOTE'	100.000	10.1
r1021	Ring stage	-	ODGe	SW40Ti	100,000 x g	18 hr
[193]		1.7	DC		100.000	1.1
r <b>107</b> 1	-	1 L	DC	-	100,000 x g	1 hr
[197]	Cabizant stage	25 mL	DC		110 000 ~	70 min
[194]	Schizont stage	23 IIIL	DC	-	110,000 x g	/O min
[174]	Mixed stages		SEC	NA		NA
[202]	Witxed stages	-	SEC	NA	-	NA
[202]	_	_	DC	_	150,000 x g	16 hr
[195]			БС		150,000 A g	10 III
[173]	Ring-to-trophozoite stage	400 mL	DC	Sorvall RC-6 plus	21,000 x g	70 min
[192]	Trophozoite-to-ring stage	700 1112	De	Sorvall WX80	110,000 x g	90 min
(-/ <b>-</b> )	Trophozoite-to-ring stage	400 mL	DC	Sorvall RC-6 plus	21,000 x g	70 min
[199]	rrophozone to ring stage	700 11112	DC	Sorvall WX80	110,000 x g	90 min
177]		.4.1(		T-1-1- 21)	, 0	

<sup>&</sup>lt;sup>a</sup> Different culture parameters are reported (e.g., parasite strain [see Table 3]), growth supplements etc.)

<sup>&</sup>lt;sup>b</sup> Additional techniques included in some protocols such as filtration, concentration, sucrose cushion, and density gradient

<sup>°70.1</sup>Ti & SW40Ti – Beckman Coulter; Sorvall RC-6 plus & WX80 – Thermofisher

<sup>&</sup>lt;sup>d</sup> Centrifugation speeds & times are indicative of that used to obtain the analyzed EV pellet(s)

<sup>&</sup>lt;sup>e</sup> This protocol did not isolate EVs by DC prior to ODG purification, which is typically the case

DC - differential (ultra)centrifugation, ODG -Optiprep density gradient, SEC - size exclusion chromatography

**Chapter 3: Methods** 

## 3.1. Cells: Red blood cells and parasite strain

Fresh human packed A+ RBCs anticoagulated with CPDA-1 (citric acid, sodium citrate, monobasic sodium phosphate, dextrose, and adenine) were obtained from anonymous donors at the Interstate Blood Bank, (Memphis, TN, USA) and the Canadian Blood Services (Vancouver, BC, Canada). The RBCs were non-leukoreduced and leukoreduced, respectively. After the EV isolation protocol was developed, only leukoreduced RBCs (from the Canadian Blood Services) were used. Upon receipt in the lab, RBCs were washed in incomplete<sup>a</sup> medium and diluted to a 50% hematocrit<sup>b</sup>, also with incomplete medium. Washed RBCs were stored at 4°C for a maximum of 14 days after collection from donors.

*P. falciparum* 3D7 reference strain freeze-stored in liquid nitrogen was thawed when needed according to standard protocols [219] using a combination of thawing solutions (12% NaCl and 1.67% NaCl).

#### 3.2. In vitro cell cultures: Parasite infected and uninfected cultures

P. falciparum was grown in A+ RBCs in complete cell culture medium comprised of RPMI 1640, 20 μg/mL gentamicin, 100 μM hypoxanthine, 25 mM HEPES and 200 mg/L sodium bicarbonate, supplemented with 0.5% AlbuMAX I. Cultures were kept stationary (i.e., not on a shaker). Culture conditions were kept at a temperature of 37°C and atmosphere of 5% CO<sub>2</sub>, 3% O<sub>2</sub>, and 95% N<sub>2</sub>. P. falciparum cultures were maintained in non-treated tissue culture flasks at high parasitemia<sup>c</sup> of ≥10% and low hematocrit of 1-2% to yield sufficient EVs for downstream analyses. To monitor parasite viability and parasitemia, thin smears of cultures were stained with 10% Giemsa and examined under a light microscope. Cultures were treated differently to achieve the different objectives of this thesis.

<sup>&</sup>lt;sup>a</sup> RPMI 1640 growth medium with 20 μg/ mL gentamicin only

<sup>&</sup>lt;sup>b</sup> Percentage of the volume of RBCs in a culture medium

<sup>&</sup>lt;sup>c</sup> Percentage of RBCs in a culture that are infected with *P. falciparum* 

For objective 1 (developing the malaria EV isolation protocol), to increase the proportion of a particular life stage within the cultures (i.e., majority ring, trophozoite, or schizont-stage iRBCs), parasites were synchronized by treatment with 5% D-sorbitol. At this stage of the research, synchrony was not of utmost importance and was performed mainly to ensure that parasites remained healthy. Cultures were often not highly synchronous and comprised 'mixed' parasite stages. For objectives 2 and 3 (malaria EV proteomics and transcriptomics respectively), parasites were kept tightly synchronized by alternating sorbitol and Percoll synchronization techniques.

Throughout this project, uninfected RBCs were also cultured in complete cell culture medium under the exact same conditions as iRBCs. uRBC cultures were checked for contamination by preparing thin smears, staining with 10% Giemsa, and examining under a light microscope.

## 3.2.1. Sorbitol synchronization

Sorbitol lyses trophozoite- and schizont-iRBCs, leaving ring-iRBCs and uRBCs (Figure 10A). Cultures of young rings at  $\sim$ 6 hours PI and  $\geq$ 10 % parasitemia were centrifuged to remove the culture media. 1 volume of packed iRBCs was resuspended in 10 volumes of 5% D-sorbitol, briefly vortexed and incubated at room temperature for 8 minutes. The suspension was centrifuged to remove the sorbitol and washed twice in incomplete medium to remove remaining sorbitol and residue of the lysed mature stage iRBCs. The cells were resuspended in the appropriate volume of fresh culture medium and re-incubated. Sorbitol synchronization was repeated after 48 hours.

## 3.2.2. Percoll synchronization

This density gradient technique recovers over 95% of mature stage iRBCs by separating them from ring-iRBCs and uRBCs. The technique used was adapted from [249]. Sorbitol synchronized cultures, with mature schizonts at ~40 hours PI and ≥10 % parasitemia, were centrifuged to remove the culture media. The packed cells were layered on a gradient with 65 % Percoll (at the bottom) and 35 % Percoll (on top) and centrifuged at 2500 rpm for 15 minutes with no brake (Figure 10B). The interface, which contains the mature stage iRBCs, settles below the top layer (culture medium), first interface (dead cells and debris) and 35 % Percoll layer. These mature stage iRBCs were collected and washed twice in incomplete medium. They were then diluted in fresh RBCs, resuspended in an appropriate volume of fresh complete culture medium and re-incubated.

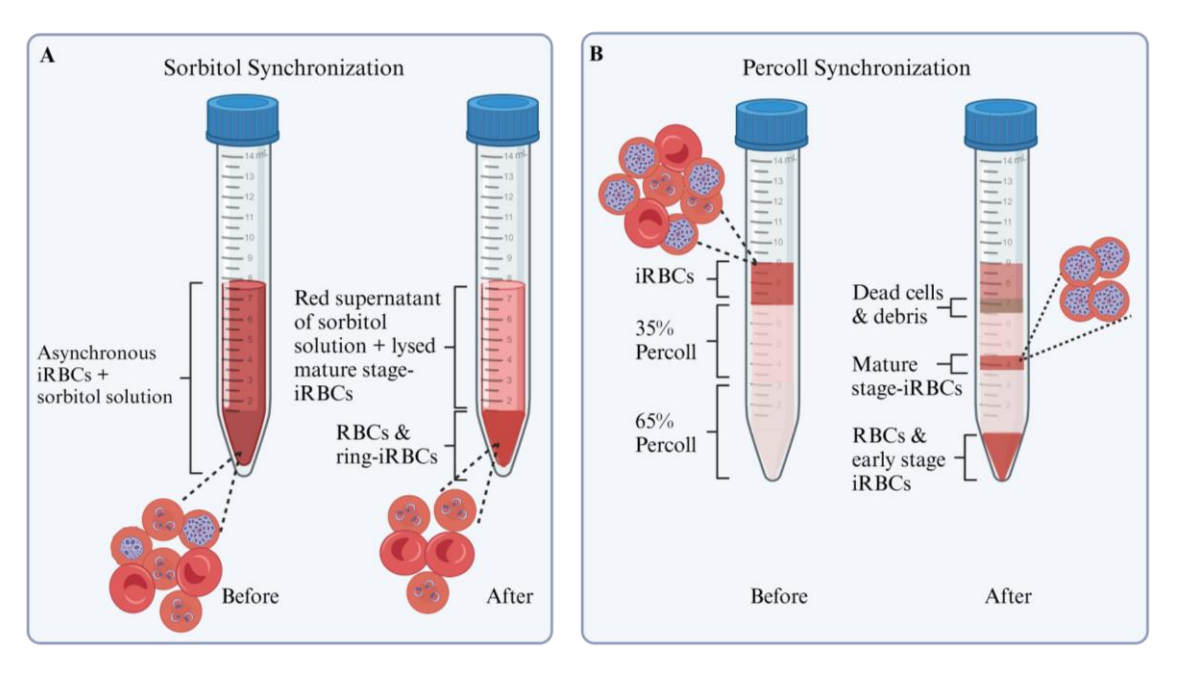


Figure 10. Synchronization techniques for *P. falciparum* cultures

Synchronization was essential for obtaining CM from high parasitemia, stage-specific cultures. The tubes on the left and right of images A & B represent before and after centrifugation, respectively. (A) Sorbitol recovers ring-iRBCs. (B) Percoll recovers mature stage iRBCs. Created with BioRender.com

## 3.3. Harvesting EV-containing CM

## 3.3.1. Mixed stage cultures (Objective 1)

After 12 hours of incubation for iRBC cultures (with mixed parasite stages) and 48 hours of incubation for uRBCs, CM was harvested by sequentially centrifuging the cell cultures at 300 x g and room temperature for 5 minutes to remove cells, 400 x g at 4°C for 15 minutes to remove dead cells, and 2000 x g at 4°C for 20 minutes to remove debris and large EVs. iRBCs and uRBCs from the first centrifugation step were returned to culture and re-incubated. For harvesting CM, TX 400 rotor was used in a Sorvall ST 16R centrifuge. CM was harvested only when iRBC cultures had a parasitemia of ≥10%. Harvested CM was stored at 4°C for up to 3 days or at -80°C for ≤2 months till needed for EV isolation.

## 3.3.2. Synchronized cultures (Objectives 2 and 3)

At synchronization, the time of invasion of RBCs was estimated based on the morphology of the parasite, so that the 48-hour asexual intraerythrocytic growth cycle could be accurately followed. This was crucial for the timely harvesting of CM from ring-, trophozoite-, or schizontiRBCs. Cultures were examined at 20-22 hours PI, 36-38 hours PI and 44-46 hours PI to verify

that the parasites were at the late ring, late trophozoite and mature schizont stages, respectively (Figure 11). At each post-invasion time point, CM was harvested by sequentially centrifuging the cell cultures as described above. As performed for objective 1, CM from uRBC cultures was harvested after 48 hours of incubation.

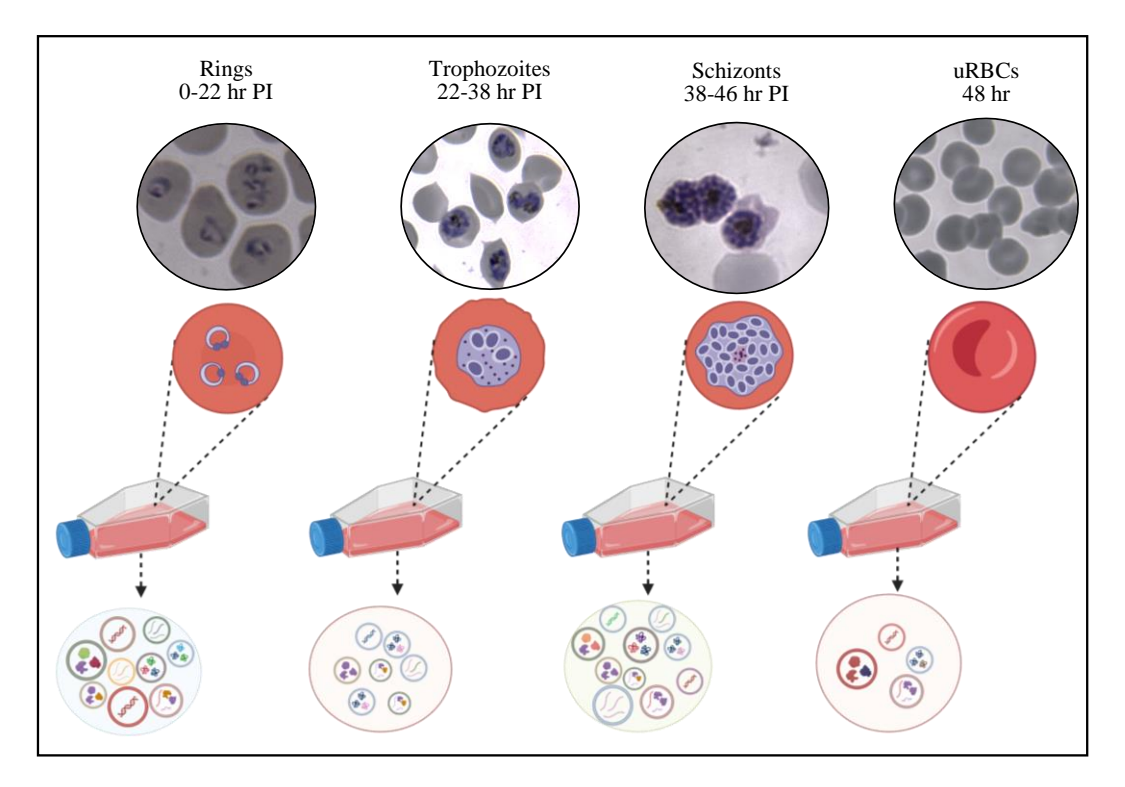


**Figure 11. CM harvest from synchronized cultures** CM was harvested at approximately 22-, 38-, and 46-hours post infection for ring, trophozoite and schizont iRBCs, respectively, and at 48 hours of incubation for uRBC control cultures. Created with BioRender.com

## 3.4. EV isolation by differential centrifugation

When harvested CM was frozen, it was thawed at 4°C during a 24- to 48-hour period, for EV isolation. Several combinations of CM volume (50 - 450 mL), PES membrane filters (0.2 μm, 0.45 μm and 0.8 μm), inclusion or exclusion of a concentration step, rotors (JLA-16.250 vs JA-25.50 and SW28 vs SW41 vs SW55), centrifugation speeds (10,000 x g to 110,000 x g) and centrifugation times (30 minutes – 3 hours), were used in multiple attempts to isolate the best EV preparation from *P. falciparum* iRBC cultures. In the final optimized protocol (Figure 12), harvested CM was passed through a 0.45 μm PES membrane bottle-top filter to remove any remaining debris, large EVs, and merozoites that may be present. The filtrate was then transferred to 50 mL tubes and centrifuged in a JA-25.50 fixed angle rotor at 10,000 x g and 4°C for 1 hour

with maximum acceleration and slow deceleration to obtain the first EV pellet, designated P1. The supernatant was stored at 4°C for no more than 24 hours to isolate the second EV pellet, designated P2. Using the same centrifugation settings to obtain P1, it was washed once in 35mL of 0.2  $\mu$ m filtered phosphate buffered saline (PBS). The pellet was often invisible at this step and was concentrated by resuspending in ~1mL of PBS and centrifuging in a TLA100.3 rotor at 10,000 g (14,000 RPM, k-factor 612) and 4°C for 1 hour (acceleration profile 9, deceleration profile 7). P1 was then resuspended in 20-50  $\mu$ L of PBS and aliquoted as necessary to avoid freeze-thaw cycles. P1 was either analyzed immediately or stored at -80°C until needed for analysis.

With larger volumes of CM, P1 EVs were isolated using the JLA-16.250 rotor by centrifugation at a higher speed of 30,000 x g and shorter run time of 40 minutes to obtain a qualitatively and quantitatively comparable P1 EV isolate. This modified version of the protocol was determined using the Intellifuge calculator for rotor protocol transfer by Beckman Coulter Life Sciences (https://www.beckman.com/centrifuges/rotors/calculator).

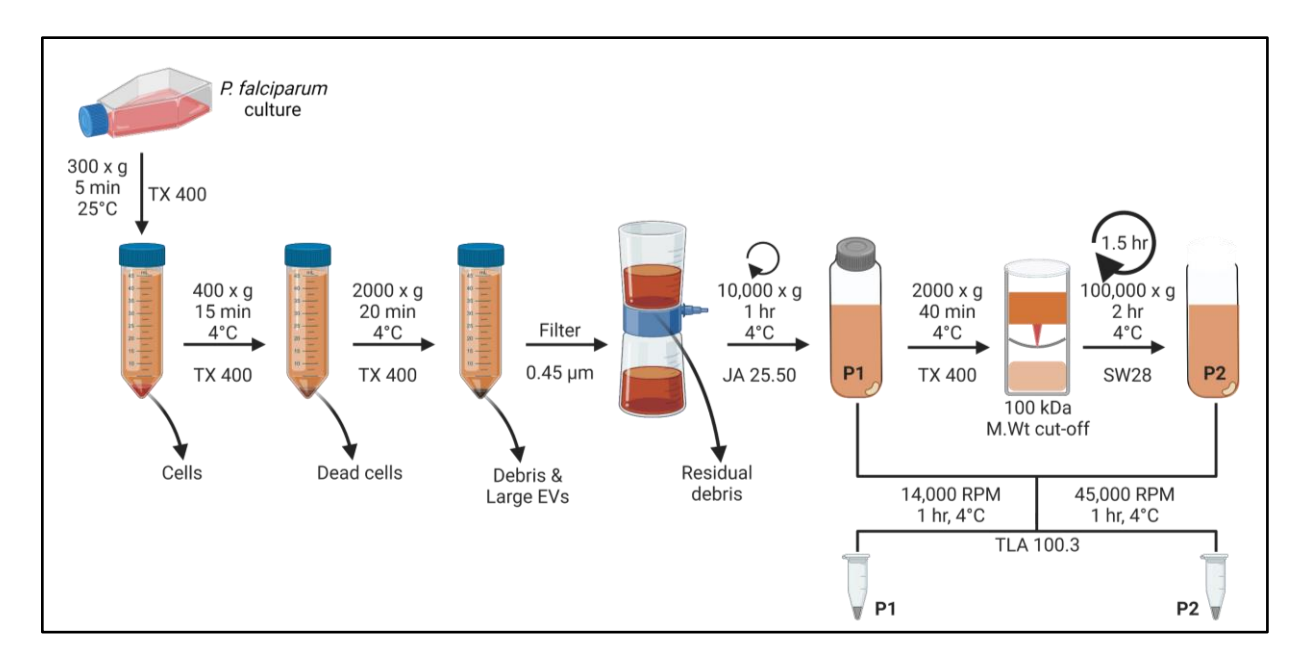


Figure 12. Optimized isolation protocol for *P. falciparum* infected RBC derived EVs

Two EV pellets are obtained, P1 and P2. The centrifugation settings for recovering P1 can be modified to accommodate larger volumes of CM (≥200 mL) and obtain a qualitatively and quantitatively comparable EV isolate. In this case, the filtrate is centrifuged in larger 250 mL tubes in a JLA-16.250 rotor at 30,000 x g and 4°C for 40 minutes. Created with BioRender.com.

The supernatant obtained from pelleting P1 was concentrated to reduce its volume for further processing. This was done by centrifugation in 100,000 MWCO PES Vivacell units in a Sorvall ST 16R centrifuge with a TX 400 rotor at 2000 x g and 4°C for 30-40 minutes. The concentrate was resuspended in up to 7 times its volume of PBS (~35mL) and centrifuged in an SW28 swing bucket rotor at 100,000 x g (exact RCF is 103,780 x g, 24,000 RPM, K-factor 336) and 4°C for 2 hours (acceleration profile 3, deceleration profile 6) to obtain the second EV pellet designated P2. As with P1, using the same centrifugation settings (except for the time that was reduced to 1.5 hours), P2 was washed once in 35mL of PBS. The pellet was concentrated by resuspending in ~1mL of PBS and centrifuging in a TLA100.3 rotor at 100,000 g (45,000 RPM, k-factor 59) and 4°C for 1 hour (acceleration profile 9, deceleration profile 7). P2 was finally resuspended in 20-50 μL of PBS and aliquoted as necessary to avoid freeze-thaw cycles. P2 was either analyzed immediately or stored at -80°C until needed for analysis. This protocol was also used to isolate EVs from uRBC control cultures.

### 3.5. Transmission electron microscopy (TEM)

To determine their physical properties (i.e., shape and size), EVs were visualized by TEM. Fresh EV preparations were fixed in 2.5% glutaraldehyde in 0.1M sodium-cacodylate buffer and stored for up to 1 week at 4°C. EV preparations were deposited on Formvar carbon-coated grids and negatively stained with 2% uranyl acetate solution. Stained grids were examined at 120kV on an FEI Tecnai G2 Spirit Twin electron microscope with a Gatan ultrascan 4000 4k X 4k CCD camera system model 895.

# 3.6. Nanoparticle tracking analysis (NTA)

NTA is a characterization technique that measures the size and concentration of nanoparticles in solution based on the principles of light scattering and Brownian motion [220]. NTA was performed on the Nanosight NS300 (Malvern Panalytical) located at the Centre for Applied Nanomedicine (CAN) platform at the Research Institute of the McGill University Health Center. The size detection range of the Nanosight NS300 is 10 to 1,000 nm while the detection range of concentration is  $10^6$  to  $10^9$  particles/mL.

Frozen EVs were thawed at 4°C and, depending on the nature of individual samples, were diluted with PBS up to 1 in 1000 to a final volume of 1 mL. EV samples were loaded into the sample chamber within which single particles were illuminated by a laser beam. The light scattered

by the particles was captured with an sCMOS camera in five 30-second videos at  $37^{\circ}$ C and a syringe pump speed of 25  $\mu$ L/s. NTA software 3.4 build 3.4.4 was used to analyze individual particles in the captured videos. Results were represented as the mean of all five captures for each EV preparation. Statistical analysis was performed using two-way ANOVA.

## 3.7. Flow cytometry (FC)

Single particle analysis of EV preparations was performed using the CytoFLEX (Beckman) located at the Centre for Applied Nanomedicine (CAN) platform at the Research Institute of the McGill University Health Center. The CytoFLEX is a flow cytometer equipped with 3 lasers (blue -488, red -640, and violet -405) and 11 avalanche photodiode detectors. Based on the EV concentrations determined by NTA, equivalent particle concentrations of samples were analyzed. In instances where particle concentrations were too low, total sample volumes were analyzed by FC and the particle concentrations normalized post analysis.

The expression of CD235a i.e., GYPA, was measured using anti-CD235a mouse monoclonal antibody, conjugated to phycoerythrin (BioLegend San Diego, US). EVs were diluted in 100 μL of PBS and stained with 10 μL of antibody (i.e., 1 in 10 dilution) at room temperature for 2 hours. The concentration of the antibody used was optimal, as determined by pre-titration. Excess antibodies and antibody aggregates were removed by running the samples through IZON columns (IZON Science, Massachusetts US). Experiments included a standard set of controls for EV FC: buffer only (0.1 μm filtered PBS), buffer with antibody, unstained EVs and isotype controls [221]. 10 μL of diluted samples were analyzed and acquired at low flow rate. Data analysis was performed with FlowJo version 10.8.1 (BD, Oregon, US).

## 3.8. Protein analysis: Gel electrophoresis and WBA

## 3.8.1. Preparation of controls

Controls for Western blot analysis (WBA) included free parasites (positive control for parasite proteins), RBC ghost membranes, RBC cytosol (positive controls for host proteins) and non-conditioned media (NCM – negative control for proteins). To prepare the parasites, 100 µL of packed iRBCs (from cultures for EV isolation) was washed in cold PBS and then lysed in 0.01% (w/v) saponin on ice for 3-5 minutes [222]. The lysed suspension was centrifuged to pellet the free

parasites from RBC cytosol and membranes. Parasites were washed in cold PBS, resuspended in 20 µL of PBS and stored at -80 °C.

RBC ghost membranes and cytosol were prepared as described by Steck & Kant [223]. 1 mL of packed RBCs (from the same unit as used in iRBC and uRBC cultures) was washed in PBS followed by lysis with 40 mL of 5 mM sodium phosphate buffer. The suspension was centrifuged at 20,000 x g and  $4^{\circ}\text{C}$  for 15 minutes.  $100 \,\mu\text{L}$  of the supernatant which contains RBC cytosol was stored at -80°C and the pellet of RBC ghost membranes was washed twice in the lysis buffer. RBC ghosts were stored at -80 °C.

## 3.8.2. Protein extraction and assay

EVs, free parasites, RBC ghosts, RBC cytosol and NCM were treated with radioimmunoprecipitation assay (RIPA) lysis buffer (Thermo fisher Scientific, Cat. No.: 89900) with added protease inhibitor (Thermo Fisher Scientific, Cat. no.: 78430) at a dilution of 1:100. Sample mixtures were incubated on ice for 20 minutes and briefly vortexed before and after incubation. The mixture was centrifuged at 14,000 x g and 4°C for 15 minutes to pellet the debris.

Protein quantification of the supernatant was performed using the Pierce<sup>TM</sup> BCA (bicinchoninic acid) protein assay according to the manufacturer's instructions (Thermo Fisher Scientific, Cat. no.: 23227). Using the microplate procedure, duplicates of standards of known concentrations and unknown samples were reacted with the kits working reagent for 30 minutes at 37°C. The absorbance was read at 562 nm on a Synergy H4 plate reader (BioTek Instruments). The protein concentration of each sample was extrapolated from a standard curve of the average blank-corrected 562 nm measurement for each known standard plotted against the respective protein concentrations.

#### 3.8.3. Gel electrophoresis and staining

Quantified proteins were separated by sodium dodecyl sulphate-polyacrylamide gel electrophoresis (SDS-PAGE). To predetermined volumes of lysed EV samples and controls (containing equivalent micrograms of protein), 6X Laemmli's buffer was added to a final concentration of 1X. Samples were heated at 95°C for 5 minutes and run on pre-cast 4-12% trisglycine gels at 225 V for 20-40 minutes. Separated proteins were visualized with Coomassie blue

(G-250 Stain, Bio-Rad, USA) or silver stain (Pierce<sup>TM</sup> silver stain kit, Thermo Scientific, USA) according to the manufacturer instructions.

# 3.8.4. Western blot analysis (WBA)

Characterization of the *Pf*-iRBC EVs was done by analyzing for different proteins using WBA. These were band 3, glycophorin A (GYPA), stomatin, spectrin (A and B), flotillin 1, flotillin 2, CD63 and, *P. falciparum* histoaspartic protease (*Pf*HAP). Depending on the nature of the protein to be detected, samples and controls were prepared with reducing buffer (with dithiothreitol - DTT) or nonreducing buffer (without DTT). Equivalent volumes or micrograms of protein from EV preparations and controls were loaded onto precast tris-glycine gradient gels (Thermo Fisher Scientific).

To allow for comparison of protein expression between samples, quantitative WBA was performed using total protein as an internal loading control [224]. Total sample proteins in PVDF membranes were visualized by staining with No-stain<sup>TM</sup> protein labelling reagent (Thermo Fisher Scientific, CA, USA). For Western blot normalization, the signal intensity of target proteins and total protein bands were analyzed and quantified with ImageJ (v1.53o) software.

Proteins were separated by SDS-PAGE, as described above, and transferred to PVDF membranes by semi-wet transfer at 20 V for 60 minutes. Membranes were blocked in 5% milk buffer for 1 hour and then incubated in primary antibody overnight. Dilutions of primary antibodies are listed in Table 5. This was followed by a one-hour incubation with horseradish-peroxidase-conjugated secondary antibody at a dilution of 1 in 5000. The primary antibodies were detected using enhanced chemiluminescence and visualized digitally on the BioRad Chemidoc MP imaging system.

#### 3.9. Protein analysis: Liquid chromatography-mass spectrometry analysis

Frozen EV samples were delivered to the Proteomics and Molecular Analysis Platform at the Research Institute of the McGill University Health Centre for liquid chromatography-mass spectrometry (LC-MS). Protein identification, characterization, and quantification was performed on the Thermo Scientific Ultimate 3000 HPLC and Orbitrap Fusion MS. 3-hour LC-MS was done to identify up to 2000 proteins.

Table 5. List of antibodies used in Western blot analysis.

Antibody	Supplier	Description	Host species	Molecular weight (kDa)	Dilution	Conditions
Glycophorin A	Abcam	Monoclonal	Rabbit	37	1:1000	Reducing
Band 3	Sigma	Monoclonal	Mouse	100	1:5000	Reducing
Spectrin	Sigma	Monoclonal	Mouse	220/ 240	1:5000	Reducing
Flotillin 1	ABclonal	Recombinant	Rabbit	47	1:1000	Reducing
Flotillin 2	Abcam	Monoclonal	Rabbit	49	1:1000	Reducing
Stomatin	ABclonal	Recombinant	Rabbit	36	1:500	Reducing
CD63	Abcam	Monoclonal	Mouse	40-50	1:500	Non-reducing
PfHAP	MR4	Monoclonal	Mouse	37	1:500	Reducing

Proteomics data was analyzed using the protein identification and comparison software, Scaffold 5 (version 5.1, Proteome Software Inc, Oregon, USA). In Scaffold, proteins were statistically displayed according to their exclusive unique peptide counts and identified by a minimum number of 3 peptides applying a 95% threshold for the probability of correctly identifying peptides and proteins.

STRING (<u>string-db.org</u>) was used to determine protein-protein interactions using a high confidence interaction score of 0.70 and MCL (Markov Cluster) algorithm. FunRich software, version 3.1.3 (functional enrichment analysis tool; <a href="http://www.funrich.org/">http://www.funrich.org/</a>) was used for analysis of human proteins, while PlasmoDB (<a href="plasmodb.org/plasmo/app">plasmodb.org/plasmo/app</a>) was used for the analysis of *P. falciparum* proteins. REVIGO (<a href="http://revigo.irb.hr/">http://revigo.irb.hr/</a>) was used for GO term summarization and visualization. The P-value cutoff for all statistical analyses was set to 0.05 using Bonferroni correction.

## 3.10. EV purification for RNA analysis

For the first few EV samples that were analyzed, RNA was extracted directly from EVs without pre-enzymatic treatment (with proteinase K and RNase A) of the EV preparations. This was to determine the baseline RNA profile of these preparations that may contain unencapsulated RNAs bound to ribonucleoproteins. Once this was determined, EV samples for RNA sequencing were pre-treated with proteinase K and RNase A so that RNA quantities could be compared before and after treatment to assess whether the RNAs detected were encapsulated in EVs [225]. These samples were subjected to the workflow in Figure 13, and described below.

Each EV sample was resuspended in 20 μl of PBS and split into 2. To one half, 90 μl of PBS was added, followed by 1 μl of 20 mg/mL proteinase K. Samples were then incubated at 37°C for 30 minutes. 1 μl of 20 mg/mL RNase A was added and the samples were incubated at room temperature for exactly 1 minute. 100 μl of TRIzol® was added to the treated samples, after which they were vortexed for 1 minute, incubated at room temperature for 5 minutes and immediately stored at -80°C until required for RNA extraction. 100 μl of TRIzol® was added to the untreated half. Samples were then vortexed for 1 minute, incubated at room temperature for 5 minutes and immediately stored at -80°C until required for RNA extraction.

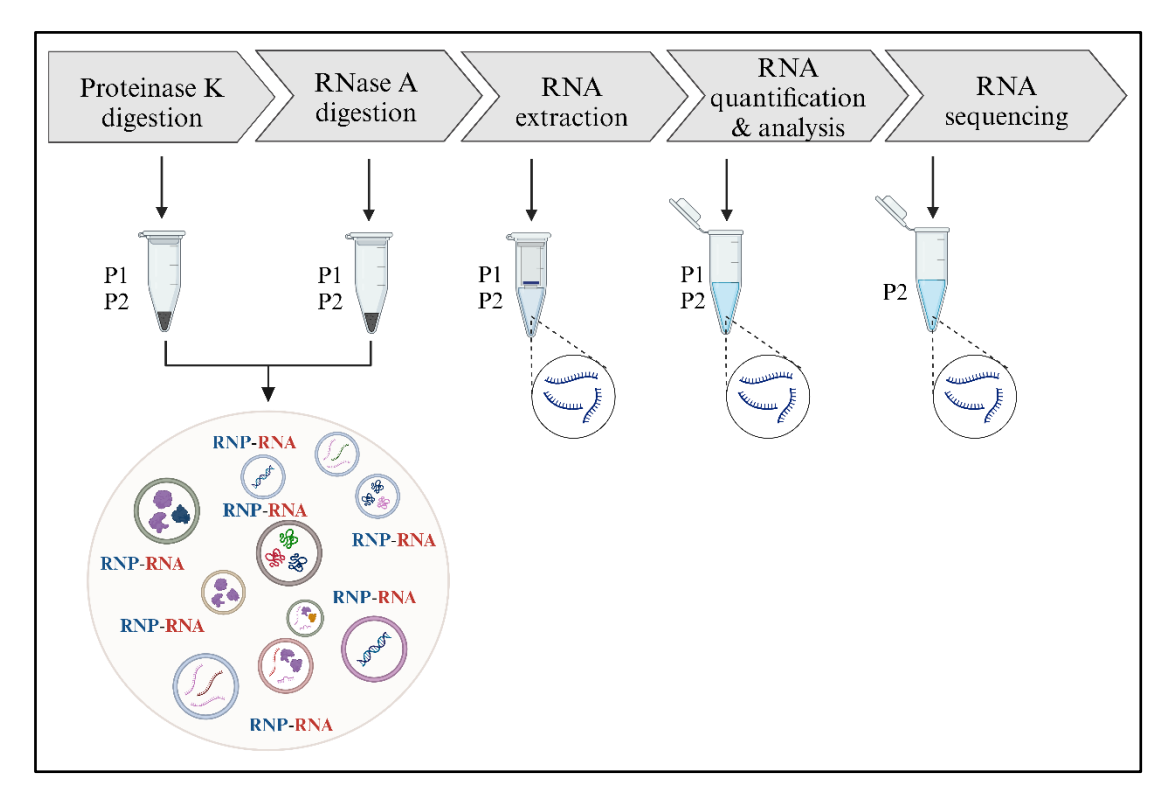


Figure 13. Workflow of EV-RNA extraction and analysis RNP-RNA: unencapsulated RNA bound to ribonucleoproteins (RNPs) that have been co-isolated with EVs. Proteinase K digestion degrades the RNPs to releases the RNA and expose them to degradation by RNase A treatment. Illustration created with Biorender.com

#### 3.11. RNA extraction

Total RNA was extracted using the Direct-zol<sup>TM</sup> RNA MiniPrep kit (Zymo Research, CA, USA) according to the manufacturer's instructions. This kit also effectively isolates small RNAs (17-200 nt). The kit worked best for malaria EV-RNA, as the procedure has few steps that minimizes the loss of any RNA that may be present in the EVs. The protocol excludes the need for phase separation, precipitation or post-purification and includes a DNase treatment step to remove unwanted DNA. RNA was also isolated from the EV-releasing cells in culture i.e., ring-iRBCs, trophozoite-iRBCs, schizont-iRBCs and uRBCs. Cells were not treated with proteinase K and RNase A.

#### 3.12. RNA detection and validation

RNA was detected and quantified by a NanoDrop™ spectrophotometer. Each EV and cell sample was analyzed in duplicates and the average concentrations and sample purity ratios (A260/A280 nm and A260/A230 nm) were recorded. Samples were then stored at -80°C until they could be further analyzed in a bioanalyzer. RNA was validated on an Agilent 2100 Bioanalyzer (Agilent Technologies) using an RNA Pico chip.

# 3.13. RNA sequencing

For small RNAs, libraries were prepared using QIAseq miRNA library kit (Qiagen). For poly-A RNA, transcriptome libraries were generated with the KAPA RNA HyperPrep (Roche) using a poly-A selection (Thermo Scientific). To characterize malaria EV-RNA, sequencing was performed on a Nextseq500 (Illumina).

Sequences were trimmed for sequencing adapters and low quality 3' bases using Trimmomatic version 0.35 [226] and aligned on a hybrid reference genome composed of the human genome version GRCh38 (gene annotation from Gencode version 37, based on Ensembl 103) and the *P. falciparum* genome version ASM276v2.56 using STAR (spliced transcripts alignment to a reference) version 2.7.1a [227]. During trimming of small RNA/microRNA sequences, reads that adhered to the expected read structure from the Qiagen sequencing kit were kept if the trimmed length was at least 16bp and if a unique molecular identifier of at least 10bp could be located between the two specified adapters.

Gene expressions were obtained as read counts directly from STAR, as well as computed using RNA-Seq by Expectation Maximization (RSEM) [228], in order to obtain normalized gene and transcript level expression, in transcripts per million values, for non-stranded RNA libraries. Reads with ambiguous mapping or multiple matches were ignored in the STAR quantifications. DESeq2 version 1.18.1 [229] was used to normalize gene read counts and produce sample clustering.

The results of the bioinformatics analyses were aggregated with MultiQC [230].

**Chapter 4: Results** 

## 4.1. Preface to developing a malaria EV isolation protocol (Objective 1)

Aptly put by Coumans *et al*, "Isolation is the key determinant of the outcome of any EV measurement" [149]. Successful EV isolation is determined by the preanalytical variables of sample collection and processing, while it determines the purity, concentration, nature, functional properties, and applicable downstream analyses of EVs [1, 149]. EV isolation itself is exceptionally challenging due to the heterogeneity of physical and biochemical properties of EVs coupled with the lack of standardization and robust reporting of EV isolation protocols; these ultimately deter the reproducibility of EV isolation and EV research in general [12].

DC, which is the most widely used technique for isolating EVs [7, 8] is particularly poorly standardized. An analysis of catalogued EV studies across diverse research fields (excluding malaria EVs) revealed that over 200 unique combinations of centrifugation steps and variable parameters were recorded for DC when used to isolate EVs from different and/or similar sample types; furthermore, in many instances, DC parameters were under-reported [82]. Similarly, with *in vitro* studies of malaria EVs, a wide variety of protocols are used to isolate *Pf*-iRBC-EVs, and DC parameters, especially rotor type, are often unreported (Table 4), hindering attempts to reproduce isolation protocols and recover similar EV preparations. Other variable parameters associated with DC include the sample volume, centrifugal force, centrifugation time, and k-factor. Different combinations of these parameters yield characteristically different EV populations even from the same starting sample [231-234]. Hence, the first objective of this research was to reproducibly isolate a reasonably consistent population of *Pf*-iRBC-EVs from CM by DC, using an optimized combination of DC parameters, with careful consideration of preanalytical variables associated with *in vitro P. falciparum* cultures.

DC separates EVs according to their size and density by subjecting a sample to sequentially increasing centrifugation speeds to pellet cells and debris at ~1500 x g (low speed), medium to large EVs (>200 nm) at ~10,000 x g (high speed) and small EVs (<200 nm) at ~100,000 x g (very high speed) [149, 235]. Different types of EVs can be pelleted at each centrifugation speed [61, 62]. However, the majority of malaria EV studies retain only the pellet from very high speed (ultra)centrifugation for analysis and discard the low and high-speed centrifugation pellets as debris (Table 4, [189, 236, 237]). This precludes the recovery of other EV subtypes possibly released by *P. falciparum* infected RBCs [238]. Clinical studies of malaria EVs [160, 163], as well

as studies in transfusion science [239, 240] have analyzed RBC-derived EVs isolated at low and high centrifugation speeds. More so, RBCs are the host cells of *P. falciparum* and are used in their *in vitro* cultivation. Therefore, it was important in this study to determine whether a DC protocol could be maximized to isolate different EV subtypes from *P. falciparum* infected RBCs at high speed and very high-speed centrifugation. Over the last decade, the long-standing fields of mammalian and cancer EV research have realized the importance of isolating and characterizing distinct EV subtypes released from the same cell type in a single study and urged a shift from focusing solely on EVs recovered from the final ultracentrifugation spin [63]. This was borne from the observation that, while 'core' biochemical components can be identified in all EV subtypes and subpopulations (from the same or different cell types respectively), some shared components are differentially abundant, while other biomolecules are exclusively present in specific EV subtypes or subpopulations [61, 241, 242]. Moreover, different biochemical compositions of EVs often translate to different downstream functions [62, 243-245].

Despite being time-consuming and associated with the risk of co-isolation of impurities, DC is the most suitable technique for isolating EVs from large volumes of samples [148] that are often required for malaria EVs. High speed centrifuges and ultracentrifuges required are often readily available to research labs, making the technique accessible and low-cost [60, 148]. Importantly, DC is argued to be the most efficient EV isolation technique and the gold-standard against which other techniques are compared [60, 148]. In addition, DC does not suffer low EV recovery or low specificity of recovered material that is common with other techniques [1]. With the optimized and reproducible protocol developed in this study, relatively consistent *Pf*-iRBC EV preparations were recovered and preliminarily characterized. This makes it possible to reliably compare the efficiency of modern and emerging techniques with DC with an understanding of the expected physical and biochemical properties of *Pf*-iRBC-EVs.

To achieve the objective of developing a malaria EV isolation protocol, *P. falciparum* was cultivated in RBCs and multiple attempts made to isolate EVs from the CM of the cultures using different combinations of the aforementioned parameters of DC. The presence of EVs in preparations was validated by analysis for EV markers and visualization of EVs. The results are detailed herein.

### 4.1.1. Optimizing *P. falciparum* culture parameters for EV isolation

When isolating EVs from CM by DC, the most important parameters that are considered are those associated with the technique itself, such as the rotor type, centrifugation speed, centrifugation time and k-factor [231, 233]. Considering these alone was insufficient for the successful isolation of *Pf*-iRBC-EVs, which were only recovered after optimizing the culture conditions. The *P. falciparum* culture-specific parameters that were found to be crucial are parasitemia, hematocrit, RBC age and RBC preparation. Table 6 summarizes the typical and modified conditions for these parameters.

Table 6: Modified P. falciparum culture conditions to increase EV yield.

P. falciparum culture parameter	Typical condition	Modified condition for EV isolation
Parasitemia	5%	≥10%
Hematocrit	4%	≤2%
Age of RBCs	Up to 28 days after collection	Up to 14 days after collection
RBC preparation	Not usually stated	Must be leukoreduced

During the early part of this study, *P. falciparum* cultures were maintained at 5-10% parasitemia and 4% hematocrit, and uRBC cultures were also kept at 4% hematocrit. However, at these conditions, P1 EVs were not isolated, P2 EVs had very heavy albumin contamination and any proteins present in P2 EVs were lost with attempts to remove the contamination by DGC (Appendix Figure 1). These findings remained after altering rotors, centrifugation speeds and centrifugation times and were indicative of two possibilities. Firstly, a poor EV isolation technique that demanded the need to ascertain the handling procedure and effectiveness of the technique. This was achieved by introducing HEK293 cells as a control in the further optimization of the protocol (Appendix Figure 2). Secondly, there was minimal EV yield.

To obtain high yields from any isolation protocol, purification of EVs is often from substantial volumes of CM collected from cultures of suspension cells at 60% or more of their maximum growth concentration [246]. A parasitemia of 5-10% meant that less than 10% of cells were releasing the EVs of interest i.e., *Pf*-iRBC-EVs. Hence, to increase the proportion of parasitized RBCs and maximize EV yields from iRBCs, the parasitemia was increased to over 10% and

reached more than 25% in some instances (Figure 14). Maintaining healthy *P. falciparum* cultures at high parasitemia, and especially in large volumes, is an arduous task. This was attainable by adopting a well-established protocol for maintaining very high parasitemia cultures [219] with slight modifications. To achieve high parasitemia, it is essential that the hematocrit is concomitantly reduced. By so doing, when schizonts burst, there are fewer RBCs available for the merozoites to invade and the proportion of iRBCs relative to all RBCs in the culture is higher.

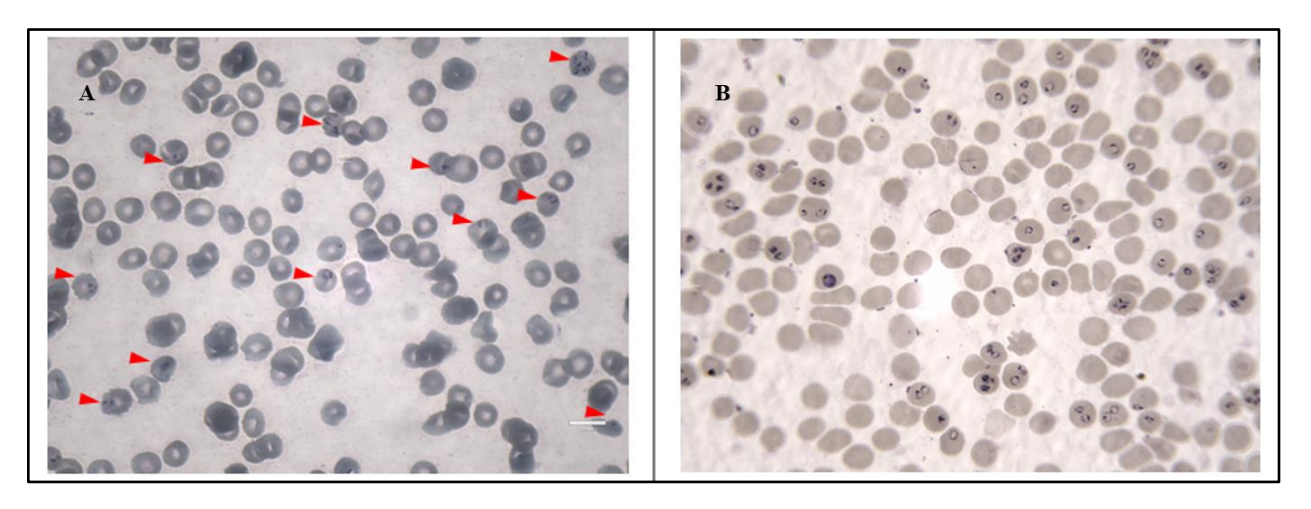


Figure 14. Optimizing malaria EV isolation protocol: Parasitemia *P. falciparum* is stained dark purple. (A) Cultures initially maintained at 5-10% parasitemia did not yield EVs for analysis. Parasites are indicated with red arrowheads. (B) high parasitemia cultures yielded sufficient EVs for characterization. Images A and B are taken from cultures of 6% and 25%, respectively at 1000 X magnification, scale bar 10µm.

It is uncertain whether reducing the hematocrit also reduced the amount of EVs released from uRBCs, but the age of RBCs is a known determinant of vesiculation. Homeostatically, and during storage, EVs carrying denatured hemoglobin increasingly bud off from the RBC membrane [184, 247] notably from 60 days in circulation [248] and 15 days of storage in blood banks [249]. This was verified for the purpose of this study. Analysis of the 2 major RBC EV markers, band 3 and GYPA [184], showed that both markers were more abundant in 28-day uRBC P1 and P2 EVs compared to 14-day uRBC P1 and P2 EVs, and all EV preparations contained hemoglobin that may be both non-EV and EV-associated (Figure 15). This suggested the release of a greater amount of EVs by aging RBCs than young RBCs, which is in line with the literature [184, 247, 249]. Altogether, these findings guided the strict use of only RBCs ≤14 days old in the iRBC test cultures and uRBC control cultures for EV isolation.

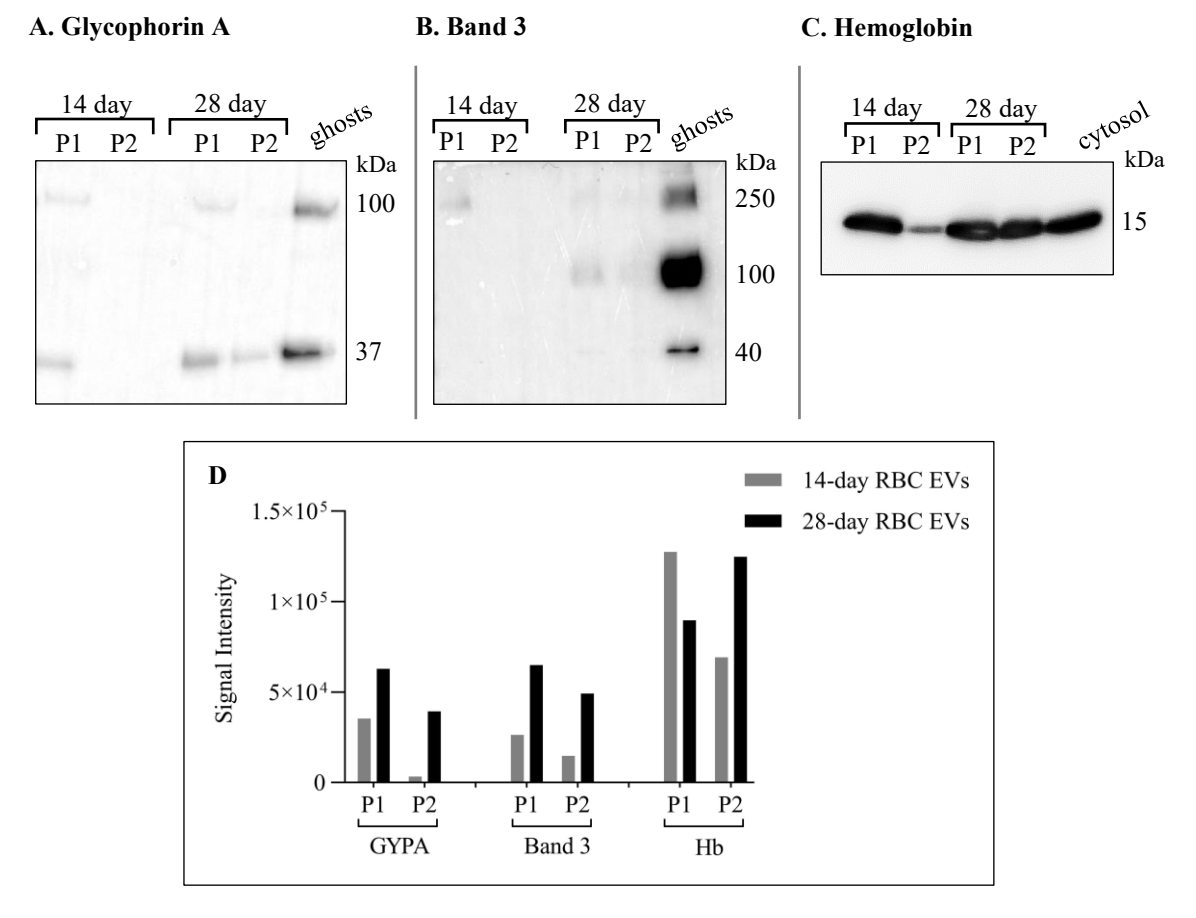


Figure 15. Optimizing malaria EV isolation protocol: Age of RBCs

(A) Glycophorin A and (B) Band 3 were more elevated in 28-day RBC EVs compared to 14-day RBC EVs, suggesting the release of more EVs. Although bands were only slightly detected, all were more intense in P2 subtypes than P1 subtypes. (C) All EVs contained hemoglobin, which is the main cytosolic protein that is eliminated from RBCs by vesiculation. (D) Densitometric analysis (performed using ImageJ) of glycophorin A (GYPA), band 3 and hemoglobin (Hb) in young (14-day) and aging (28-day) RBC derived EVs.

Another vital observation was the inconsistent detection of CD63. CD63 is a transmembrane protein that belongs to the tetraspanins family and is highly abundant in EVs, important in 'exosome' biogenesis (See subsection 2.3.3.1) and is a designated classical EV marker [250]. WBA of CD63 varied from one packed RBC unit to another, whereby it was completely undetected in EVs from cultures with some RBC units but detected in others (Figure 16A and Figure 16B respectively). This raised concerns during the development of the malaria-EV isolation protocol for multiple reasons. A phylogenetic analysis of *P. falciparum* did not detect any tetraspanins in their genome [251] and CD63 was not detected in WBA of the parasite in this study (Figure 16A). Therefore, it was unlikely that this protein was from *P. falciparum*. Also, considering that mature RBCs lack the endosomal machinery of which CD63 is an integral part, and its distinct absence

from RBC membranes (ghosts) in protein analyses in this study (Figure 16), the source of CD63 in the RBC EVs remained unclear. Adding to the perplexity was that CD63 has reportedly been detected in RBC derived EVs [84] and malaria derived EVs [203] and was indicated as a membrane component of RBC derived EVs [252] without being challenged by other authors.

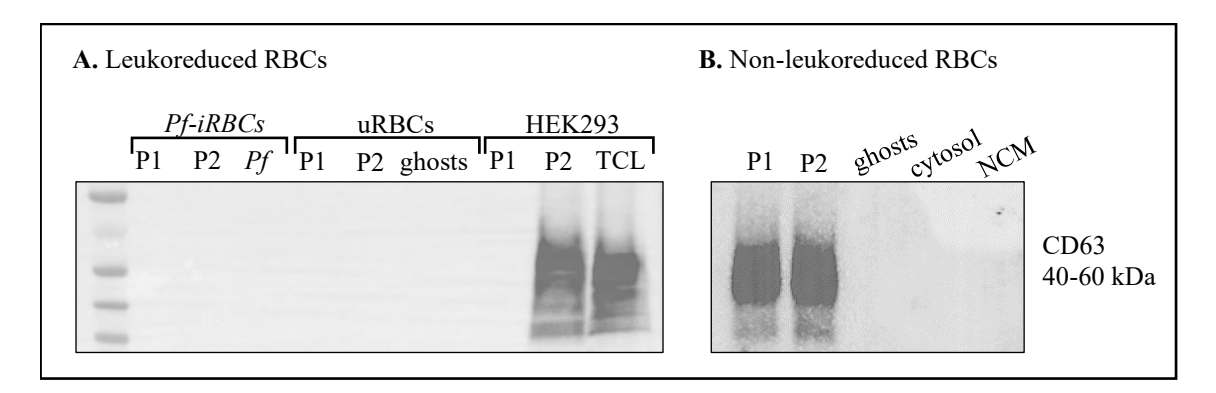


Figure 16. Optimizing malaria EV isolation protocol: RBC preparation

The method of preparing packed RBCs influences the composition of their EVs. (A) EVs isolated from leukoreduced RBCs do not contain CD63 and are unlikely to comprise other tetraspanins. HEK293, which is rich in CD63, was used as a positive control (B) uRBC EVs isolated from non-leukoreduced RBCs contained CD63. CD63 was not detected in RBC membrane ghosts or cytosol. Stage-specific iRBC EVs from cultures with non-leukoreduced RBCs were also positive for CD63 (Appendix Figure 3)

Non-conditioned media (NCM) was used as a negative control. TCL - total cell lysate

After the analyses of EVs from several packed RBC units, including an in-depth review of blood transfusion science literature, it was determined that the method of preparing packed RBC units before storage largely influences vesiculation in these blood products and the proteome of the vesicles produced [253, 254]. RBCs may be leukoreduced or non-leukoreduced. Leukoreduction is the removal of up to 99.995% of white blood cells from blood components by centrifugation or filtration to improve RBC quality; non-leukoreduced RBCs are processed by washing but retain white blood cells, platelets, and plasma [255]. Moving forward, the optimized protocol in this study strictly used leukoreduced RBCs that have also been plasma reduced and platelet reduced to ensure the quality of recovered *Pf*-iRBC-EVs.

## 4.1.2. Imaging mixed stage EVs

TEM of P1 and P2 *Pf*-iRBC-EVs revealed membrane-bound vesicles that were all small sized at ≤200 nm in diameter (Figure 17). However, while the P1 subtype appeared homogenous at approximately 200 nm, P2 EVs appeared smaller with a more heterogenous size distribution from 30-200 nm (Figure 17A and Figure 17B respectively). Both EV subtypes displayed a 'cup-shape'

morphology that is an artefactual feature caused by the chemical fixation and/or negative staining procedures of TEM, but nevertheless, a good indication of the presence of EVs [246, 256].

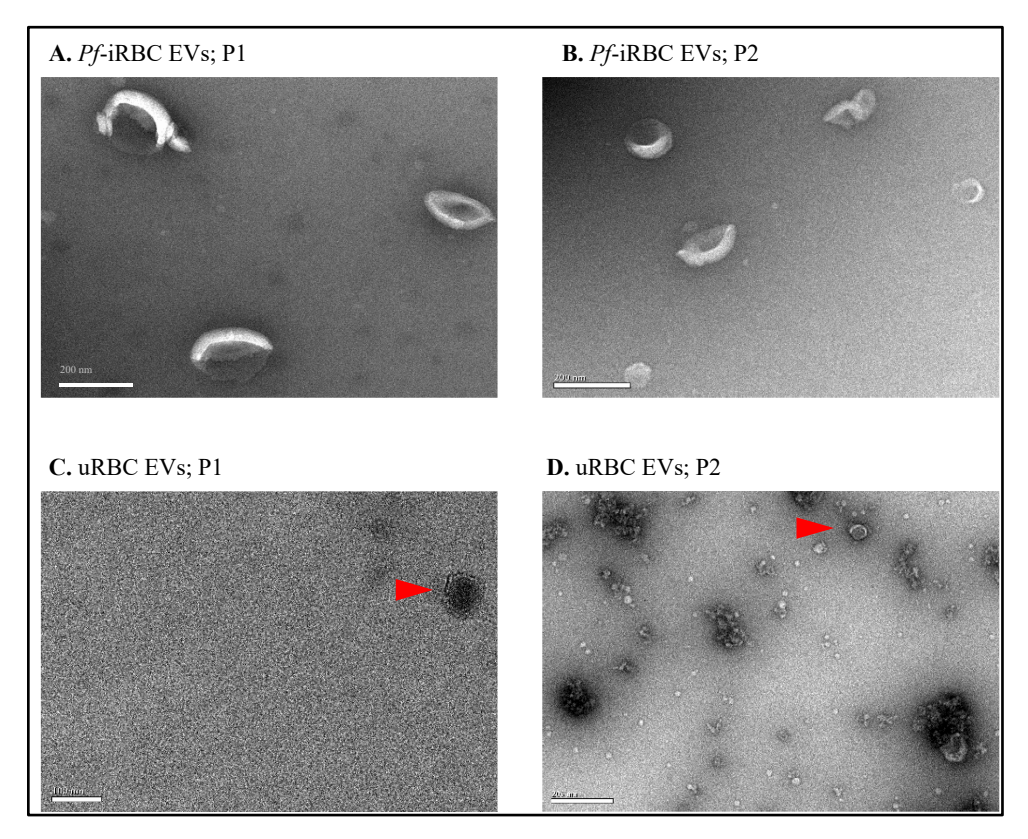


Figure 17. Visualizing EVs by TEM (A and B) Pf-iRBC EVs are small with a diameter of  $\leq$ 200 nm. (C and D) Very few uRBC EVs were observed (red arrowheads). (D) Numerous protein aggregates were observed in uRBC P2 EVs. Scale bar A, B, D = 200 nm Scale bar C = 100 nm

uRBC EVs were scantily present and more difficult to detect (Figures 17C and 17D). This may be due to the use of fresh RBCs for EV isolation and validates the majority of *Pf*-iRBC EVs analyzed are either parasite-induced or parasite-derived. Protein aggregates were observed in abundance in uRBC P2 EVs (Figure 17D).

## 4.1.3. Protein detection of mixed stage EVs

Several proteins in P1 and P2 *Pf*-iRBC-EV subtypes were revealed following SDS-PAGE and silver staining with a profile that was distinct from that of the host iRBC (total cell lysate) from which they were released (Figure 18). While this also held true for uRBC EVs and their host cells,

they appeared to have much fewer proteins compared to the *Pf*-iRBC EVs. Proteins were enriched, non-enriched or absent in P1 and P2 *Pf*-iRBC EVs compared to the host iRBCs.

There was albumin co-isolation from the culture medium observed as an ~60 kDa band (Figure 18), however, the other multiple protein bands observed provided evidence that the isolation protocol had successfully recovered two good EV preparations [246]. The separated proteins ranged broadly in size from ~10 kDa to ~200kDa and were expected to include both parasite and RBC proteins.

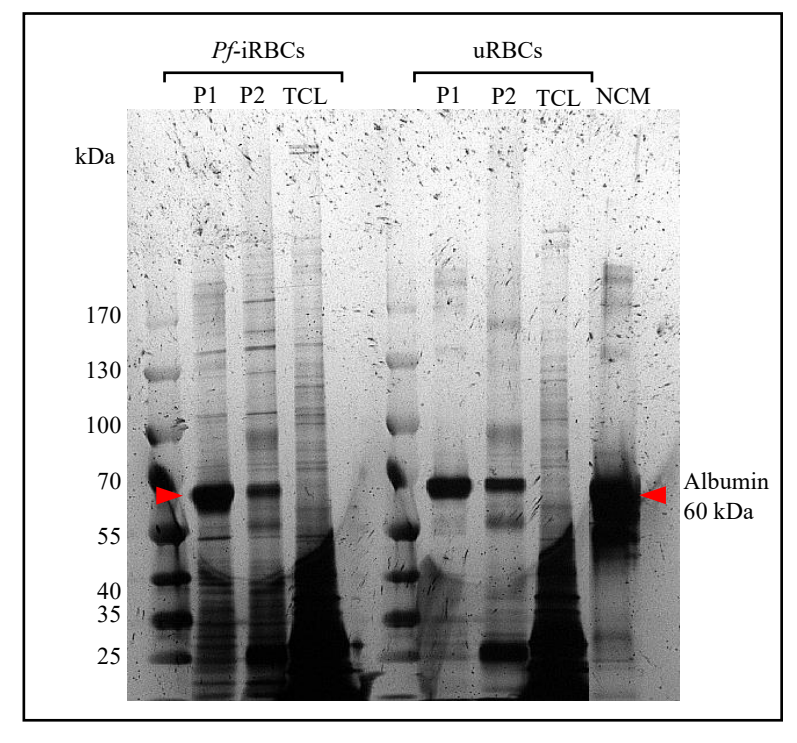


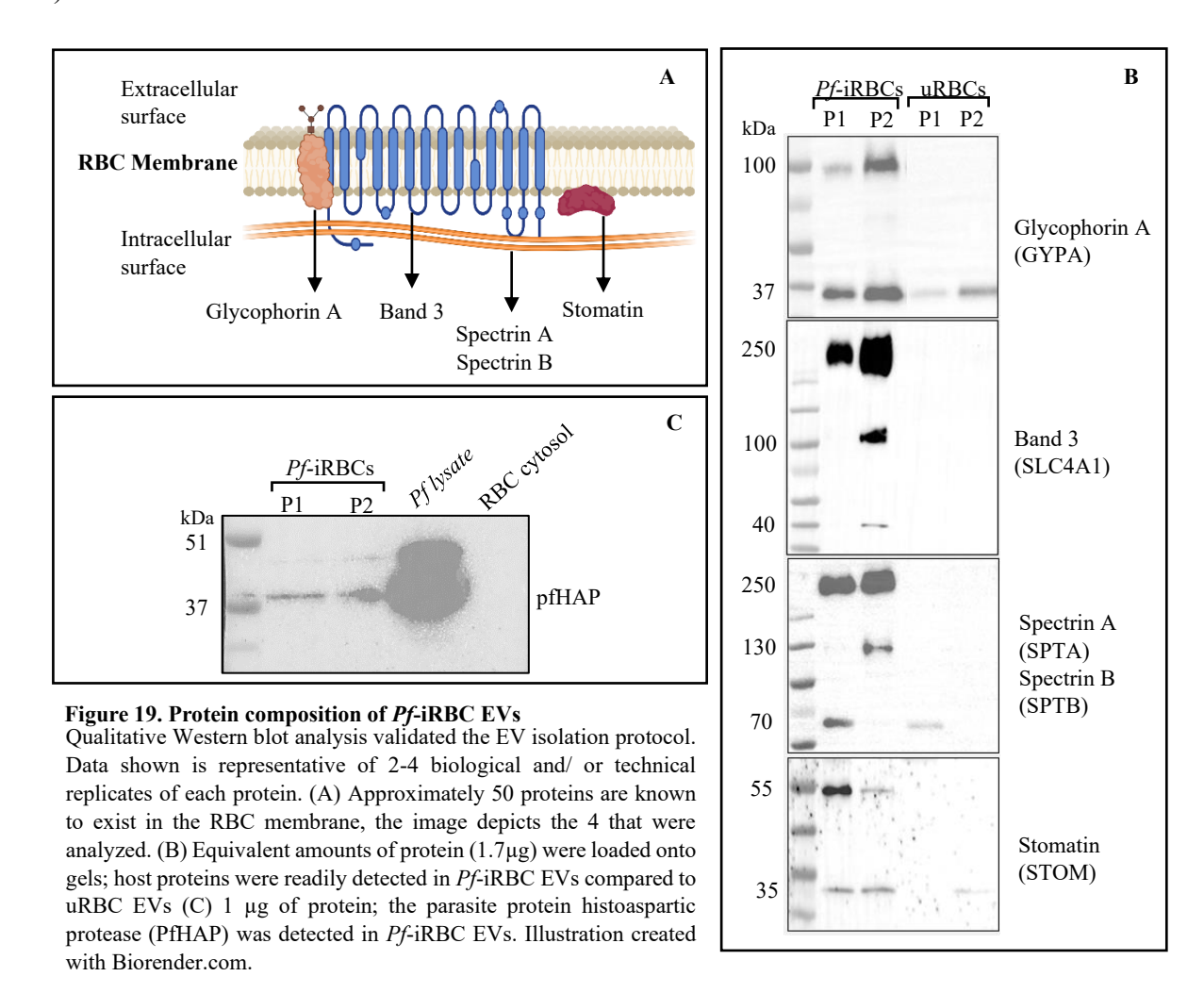
Figure 18. Protein separation and detection by SDS-PAGE and silver staining

2µg of each sample and control was loaded onto a pre-cast 4-12% tris glycine gel. Albumin co-isolation can be seen at 60 kDa (red arrowheads)

TCL – total cell lysate NCM – non-conditioned media

### 4.1.4. Protein composition of mixed stage EVs

To characterize and differentiate the *Pf*-iRBC-EV subtypes, immunoblotting of various proteins was performed. Because membrane proteins are important EV markers [61] and malariaderived EVs inevitably must exit from the host RBC membrane, four RBC membrane proteins were analyzed namely GYPA, band 3, spectrin (with 2 subunits A and B) and stomatin (Figure 19A).



As the designated RBC EV marker, GYPA (also known as CD235A) was expectedly detected in both *Pf*-iRBC and uRBC EV subpopulations and their respective P1 and P2 EV subtypes (Figure 19B). GYPA was observed as two separate dimers at 37 kDa and 90-100 kDa in *Pf*-iRBC-EVs and as a single 37 kDa dimer in uRBC EVs. Unlike GYPA however, band 3, which is the most abundant integral RBC membrane protein, was not detected in uRBC EVs and differentially present in *Pf*-iRBC-EV subtypes. A high molecular weight band 3 aggregate at 250 kDa was detected in P1 and

P2 malaria EVs. However, the band 3 protein at 100 kDa and a low molecular weight peptide at 40 kDa were also detected in the P2 malaria EVs. Similarly, the observed bands for spectrins A and B differed with the high molecular weight α and β bands observed at 240 kDa in *Pf*-iRBC-EVs and different polypeptides observed for *Pf*-iRBC P1 and P2 EVs at 65 kDa and 130 kDa, respectively. The lipid raft protein, stomatin, was detected in *Pf*-iRBC-EVs at the expected molecular weight of 32 kDa and as a dimer at 55 kDa. Stomatin was only detected in the uRBC P2 subtype and at 32 kDa. The vast difference observed between iRBC- and uRBC EVs prompted the need to examine the distribution of selected RBC membrane proteins in iRBCs and uRBCs by immunofluorescence microscopy (Appendix Figure 4), whereby, the RBC membrane proteins GYPA and flotillin 1 were found to aggregate significantly at the membrane of infected RBCs compared to uninfected RBCs. This may explain the greater abundance of GYPA in the Western blots of the *Pf*-RBC EVs compared to the uRBC EVs.

To determine that there were EVs originating from the parasite, *Pf*HAP was analyzed for. This protein is not exported by the parasite into the RBC cytosol (See Figure 3), but rather, is localized to the digestive vacuole. PfHAP was detected in both *Pf*-iRBC-EVs P1 and P2 (Figure 19C).

### 4.2. Preface to EV proteomics (Objective 2)

Proteins are an important component of many EVs, and crucial functions that have been described for EVs in both physiological and pathological states are attributed to their protein composition (See subsection 2.3.4.1). Early studies in the EV field focused on the biochemical nature of EVs, knowledge of which guided investigations of their functions and prompted their use as disease biomarkers [3]. However, with increasing interest in EVs, the research trend was reversed and there has been a disproportionate rise in functional EV studies, despite the tremendous knowledge gaps that remain regarding their biochemical composition. A global evaluation found that between 2010 and 2015, publications of EV functions increased six times more than omics studies and five times more than biomarker studies [82]. Similarly, there are appreciably more studies of the functions of malaria EVs [4].

Malaria EVs have been suggested to play vital roles in promoting parasite survival by inducing gametocytogenesis, transferring drug resistance genes between parasites, regulating parasite population, as well as contributing to the pathophysiology of the disease by immunomodulation and causing endothelial damage (See section 2.4). Important proteins that may be involved in several of these processes have not been fully identified. To deviate from the custom of putting EV 'function' before 'form', this research set out to conduct an extensive proteomic analysis and identify proteins that may be directly implicated in the various functions that have been proposed for malaria EVs.

Equally important was identifying proteins that can potentially be used to investigate the biogenesis of EVs in *P. falciparum*, since this is yet to be elucidated. In addition, there was the need to discover proteins that can be unequivocally designated as general or specific malaria EV markers. As has been established in this thesis, 'classical' EV markers, such as tetraspanins, are not conserved in *P. falciparum*. Furthermore, there is no EV protein database that malaria researchers can refer to as a resource for validation of malaria derived EVs, and *P. falciparum* is not listed in the available EV databases (i.e., <a href="http://www.exocarta.org/">http://www.exocarta.org/</a> and <a href="http://www.exocarta.org/">http://www.exocarta.org/</a>).

The preliminary protein characterization discussed in the previous section was performed to validate the malaria EV isolation protocol and used EVs isolated from asynchronous (mixed stage) cultures. Asynchronous cultures of *P. falciparum* contain all 3 life stages of the parasite at any

given point in time. To address the research question of this study, which aimed to characterize the physical and biomolecular properties of EVs released from RBCs infected with each asexual blood stage of *P. falciparum*, the second objective was to analyze the protein cargo in EVs released from RBCs infected with *P. falciparum* rings, trophozoites and schizonts. Many known publications of the protein composition of malaria EVs have focused on ring-iRBC EVs; some have analyzed EVs from ring to trophozoite stage iRBCs and trophozoite to ring stage iRBCs (which would contain mixed stage iRBC EVs), while in several cases, the life stage is not clearly indicated (Table 4). This has limited the reliable comparison of EVs from RBCs infected with specific stages of the parasite. However, the elaborate experimental design of this research allowed for a direct comparison of unique or shared proteins in EVs from the stage-specific *Pf*-iRBCs, as well as a comparison with published findings.

To achieve this objective, EVs had to be isolated from tightly synchronized cultures. In such cultures, at least 85% of the parasites are within a 6-hour window of the same life stage i.e., rings, trophozoites, or schizonts [219]. Parasites were synchronized using a combination of sorbitol and Percoll that was important to sustain large volume, high parasitemia cultures in a short synchronization window. Unlike the development of the EV isolation protocol, synchronous CM was crucial for the isolation and characterization of EVs from stage-specific *Pf*-iRBCs. For each experiment, 8 EV preparations were analyzed: ring-iRBC P1 and P2 EVs, trophozoite-iRBC P1 and P2 EVs, schizont-iRBC P1 and P2 EVs, and finally, the control uRBC P1 and P2 EVs.

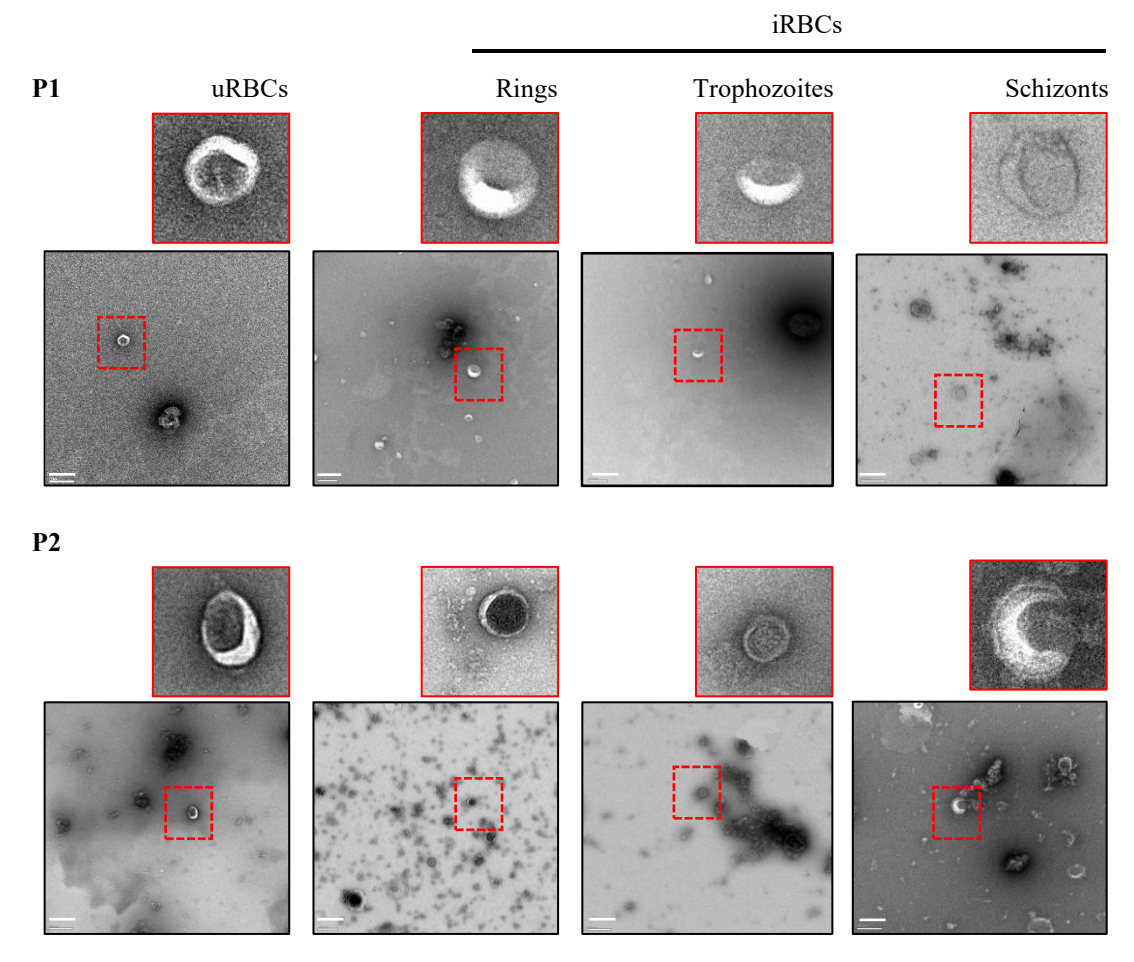
As recommended by ISEV, a combination of techniques was used to analyze single EVs in all preparations [1]. EVs were visualized by TEM to obtain information on their size and structure. EV size was also determined by Nanoparticle Tracking Analysis (NTA), which, in addition, was used for quantification. Lastly, single EVs were analyzed for their expression of the RBC EV marker, GYPA, using small particle flow cytometry (FC) [257]. GYPA and other proteins representing important categories present in EVs were analyzed in bulk EV preparations by WBA [1]. These comprised transmembrane proteins, cytosolic proteins with membrane binding ability, and cytoskeletal proteins. Detected proteins were validated by mass spectrometry, which provided a global picture of the protein composition of malaria EVs.

Compared to published proteomic studies of malaria EVs, this study detected a vast number of human and parasite proteins (>1000). Protein expression differed greatly between iRBC and uRBC

EVs, across subpopulations of ring-, trophozoite- and schizont-iRBC EVs, and between P1 and P2 subtypes of the stage-specific iRBC EVs.

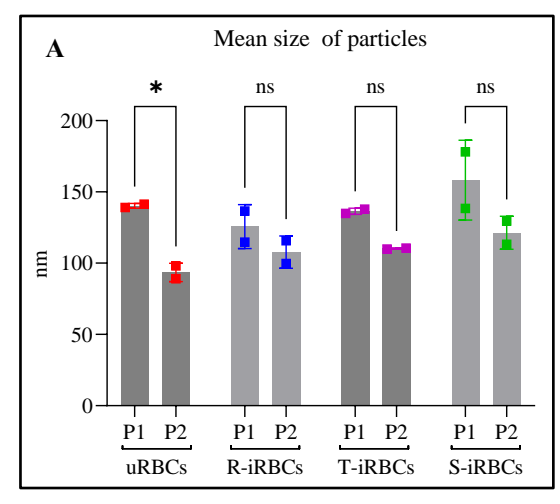
## 4.2.1. Physical characteristics of malaria EVs

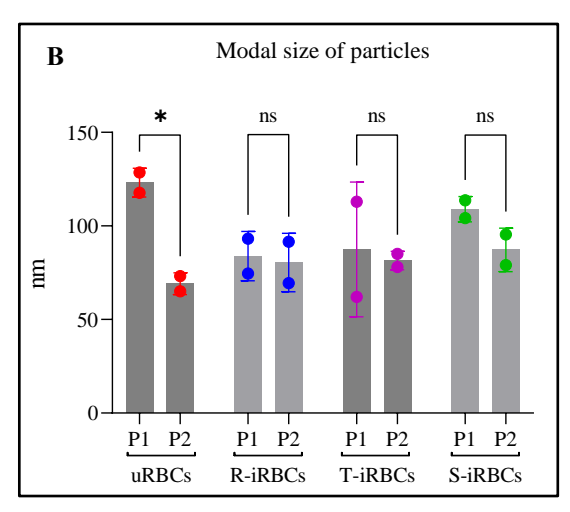
As observed for the EVs isolated from mixed stage cultures, electron microscopy of P1 and P2 stage-specific iRBC EVs revealed membrane-bound, cup-shaped vesicles that were small sized at ≤200 nm in diameter (Figure 20). The sizes of the EVs were also widely heterogenous. While EVs were difficult to detect in uRBC and trophozoite-iRBC EV samples, there were abundant EVs observed in the ring- and schizont iRBC preparations. P2 EV preparations had a lot more protein aggregates in the background than P1.



**Figure 20. TEM micrographs of uRBC EVs and** *P. falciparum* **stage specific iRBC EVs**Large images are wide-field representations of 4-6 captures of each EV sample and show heterogeneity of EV shape, size, and number as well as background quality. Insets show single EVs that have been zoomed in (small red boxes). Scale bar for all images is 200 μm. uRBC P1 & P2: 23,000x, ring-iRBC P1 & P2: 18,500x, trophozoite-iRBC P1 & P2: 18,500x & 23,000x respectively, schizont-iRBC P1 & P2: 23,000x.

NTA revealed the presence of EVs with a similar small size as seen with TEM, whereby the mean size of all EV populations was below 200 nm in diameter (Figure 21A). Although P1 iRBC EVs were generally larger than P2 iRBC EVs, the difference in their mean sizes was not statistically significant. In fact, the modal sizes of iRBC EVs were smaller than 100 nm, except for schizont-iRBC P1 EVs at 108.95 nm (Figure 21B). This indicated that high speed centrifugation and very high-speed ultracentrifugation both yield small malaria derived EVs. The mean and modal sizes of P1 and P2 uRBC EVs, although both small, were significantly different.





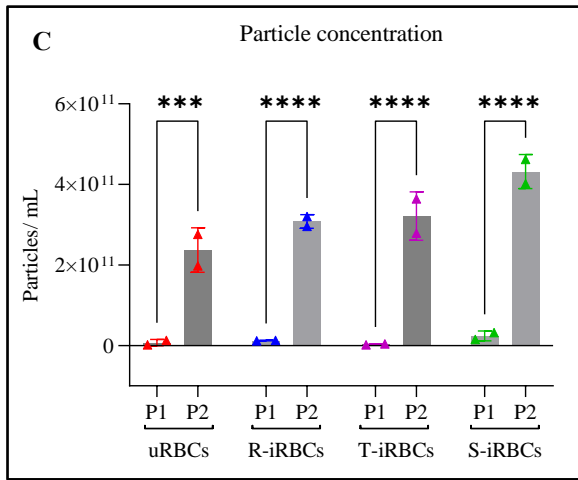


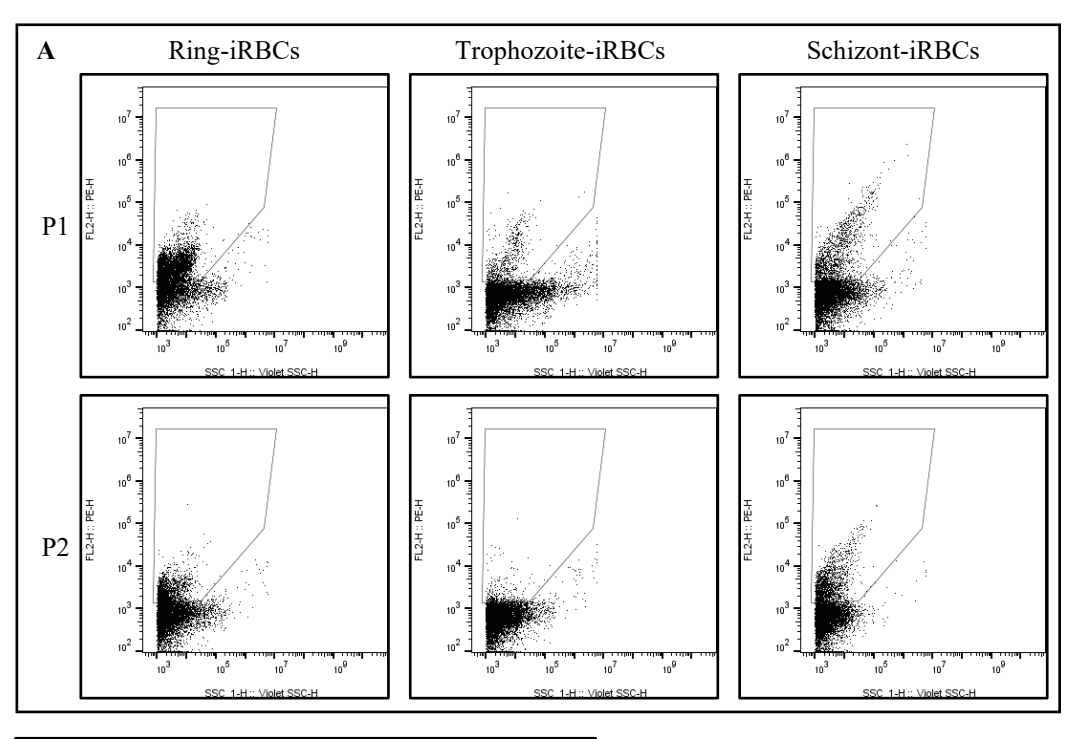
Figure 21. NTA of uRBC EVs and *P. falciparum* stage-specific iRBC EVs

(A) and (B) Malaria-derived EVs were observed to be mainly small sized EVs below 200 nm in diameter. (C) P1 EVs have significantly lower particle concentrations than P2 EVs. All data is a summary of 2 biological replicates. Statistical analysis was performed using two-way ANOVA. uRBCs – uninfected RBCs, R-iRBCs – ring infected RBCs, T-iRBCs – trophozoite infected RBCs, S-iRBCs – schizont infected RBCs. P1 EVs were isolated at 30,000 x g, P2 EVs were isolated at 100,000 x g.

Conversely, the particle concentrations of all P1 and P2 EV preparations were different. P2 EV concentrations were significantly higher than P1. The average particle concentrations of P1 EVs (2 biological replicates) were 1.24 x 10<sup>10</sup> for ring-iRBCs, 2.86 x 10<sup>9</sup> for trophozoite-iRBCs, and 2.38 x 10<sup>10</sup> for schizont iRBCs (Figure 21C). Respectively, this put P2 ring-, trophozoite-, and

schizont-iRBC EVs at 25, 112, and 18 times higher than their corresponding P1 iRBC EVs. There was no statistically significant difference across P1 or P2 iRBC EVs with regards to particle size and concentration.

Flow cytometric analysis of malaria EVs detected GYPA positive particles (Figure 22A). Although the particle concentrations of P1 iRBC EVs were drastically lower than those of P2 as determined by NTA, there were more GYPA positive particles in the P1 EV subtypes than P2 (Figure 22B). This was particularly evident for ring and schizont-iRBC EVs.



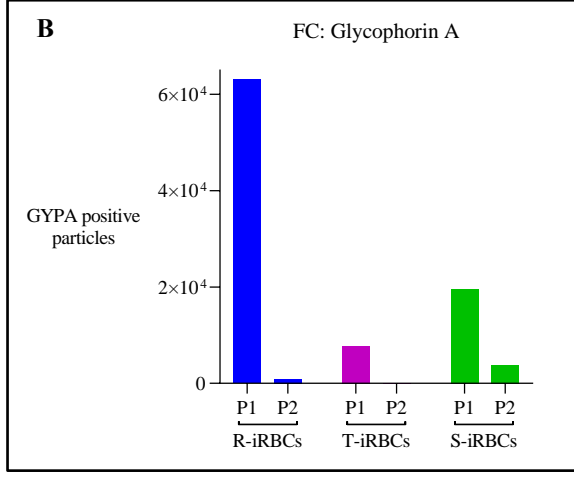
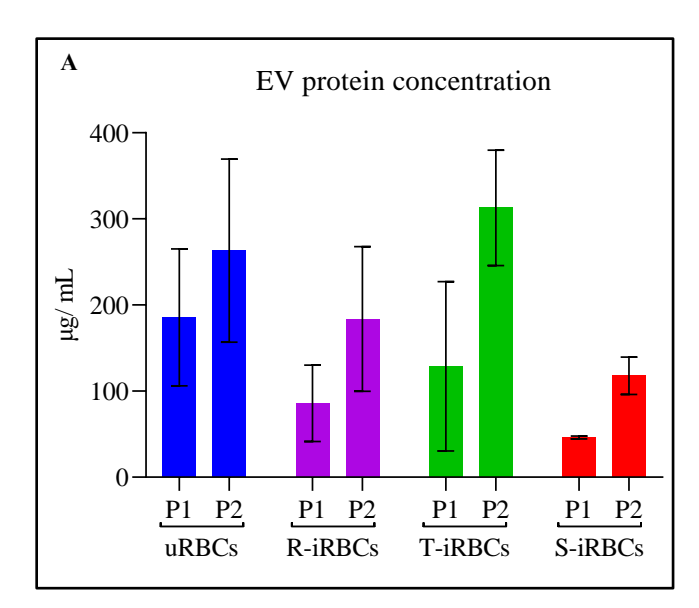


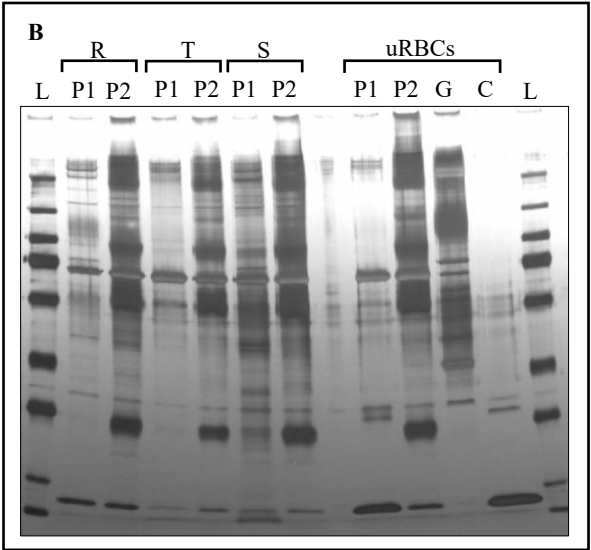
Figure 22. Flow cytometry of *P. falciparum* stage-specific RBC EVs with antiglycophorin A

- (A) GYPA positive particles were detected in all stage-specific iRBC EVs.
- (B) GYPA positive particles were more abundant in P1 EVs than in P2 EVs for ring-, trophozoite-, and schizont-iRBCs. Results are for a single biological replicate (R-iRBCs, T-iRBCs, S-iRBCs, respectively)

# 4.2.2. Total protein assay and in-gel protein detection of malaria EVs

BCA protein assay of multiple biological replicates of iRBC EVs consistently revealed higher protein concentrations for P2 than P1 EV subtypes (Figure 23A). The difference in protein concentrations was not statistically significant but was clearly reflected in the total protein staining of the SDS-PAGE (Figure 23B). Multiple proteins were observed for iRBC EVs and uRBC EVs, however, P2 EVs showed more protein bands with greater intensity than observed for P1. These were most noticeable at 250-, 100-, 55-, and 25 kDa.





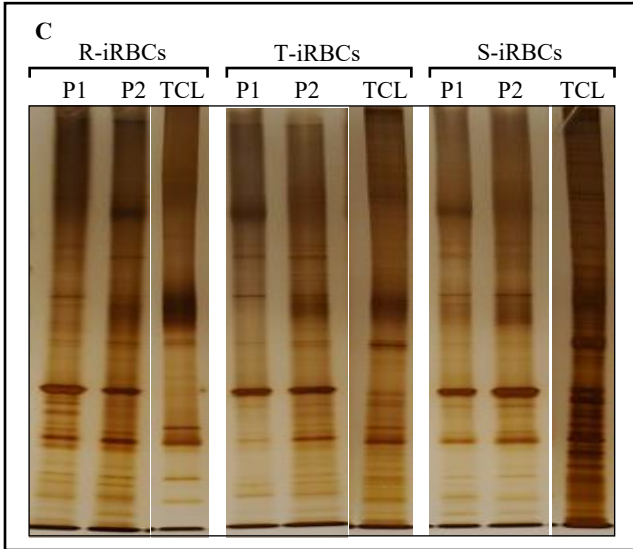


Figure 23. Protein assay and detection of *P. falciparum* stage-specific iRBC EVs

(A) Protein concentration of P2 EVs was consistently higher than P1 EVs. Data is shown for 2 biological replicates. (B) P1 and P2 had distinct global protein profiles with P2 EVs showing more bands with greater intensity than observed for P1. 0.5  $\mu g$  of protein loaded (C) Silver stain of EVs and their respective parasite stage lysates. Uncropped image is available in Appendix Figure 5. 0.5  $\mu g$  of protein loaded. L-ladder, R-rings, T-trophozoites, S-schizonts, i-infected, u-uninfected, RBCs-red blood cells, G-ghosts, C-cytosol, TCL-total cell lysate

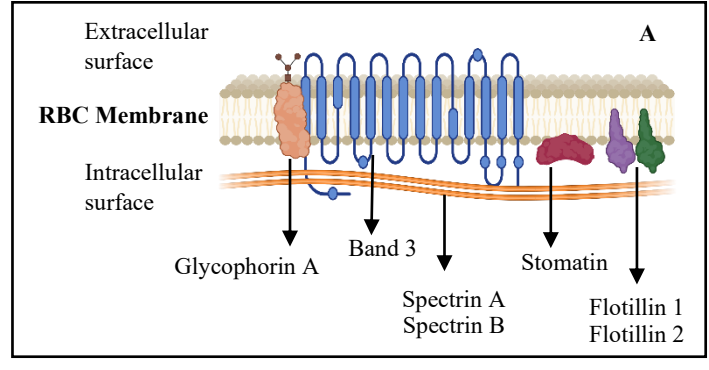
In Figure 23B, several unique global protein profiles were observed: (1) between P1 and P2 subtypes of each stage-specific iRBC EV population, (2) across the P1 subtypes of ring-, trophozoite-, and schizont iRBCs, (3) across the P2 subtypes of ring-, trophozoite-, and schizont iRBCs, (4) between iRBC EVs and uRBC EVs, and (5) between iRBC EVs and RBC ghost membranes and cytosol. In addition, a silver stain of SDS-PAGE that included parasite lysates revealed proteins in ring-, trophozoite- and schizont-iRBC EVs that were distinct from their respective ring, trophozoite and schizont cell lysates (Figure 23C). As with the mixed EV populations (Figure 18), proteins were enriched, non-enriched or absent in P1 and P2 *P. falciparum* stage specific-iRBC EVs compared to the host cells.

## 4.2.3. Protein composition of malaria EVs: Western blot analysis

Analyzed RBC membrane proteins were mainly enriched in P1 iRBC EVs (Figure 24A and Figure 24B). The expression profile for GYPA observed by FC was similarly observed with WBA where the marker was more abundant in P1 compared to P2 for the ring-, trophozoite-, and schizont-iRBCs. This trend was the same for band 3, flotillin 1, flotillin 2, spectrin (A and B) and stomatin for ring- and schizont-iRBC P1 and P2. The profiles differed for trophozoite-iRBC EVs. While GYPA and band 3 were clearly more abundant in trophozoite-iRBC P1 than P2, flotillin 1 was not detected in either trophozoite iRBC EV subtypes, flotillin 2 and spectrin were faintly detected in P2, and stomatin was faintly detected in P1 (Figure 24B). For all the biological replicates analyzed, the observations for ring-and schizont iRBC EVs were consistent, while that of trophozoite iRBC EVs was not. Flotillins were detected in uRBC P2 EVs, other analyzed proteins were not.

GYPA was detected as a 37 kDa dimer in all iRBC P1 and P2 EVs but also at 90-100 kDa in P1 EVs. Multiple bands were also seen in the immunoblots for band 3, spectrin and stomatin. In P1 iRBC EVs, band 3 was observed at the expected molecular weight of 100 kDa. The protein was faintly detected in schizont iRBC P2 EVs. Band 3 was also detected, although with much less intensity as a 250 kDa aggregate and 40 kDa peptide in P1 EVs for all stage-specific iRBCs. The 60 kDa band 3 peptide detected in the RBC ghost membranes was absent from EVs. In some experiments, this 60 kDa peptide was detected in P2 EVs but not in P1 EVs (Appendix Figure 6). Spectrin A and B were detected at their expected high molecular weights, 240 kDa and 220 kDa,

respectively. Polypeptides of spectrin were also observed at 130 kDa and 100 kDa for ring- and schizont iRBC P1 EVs.



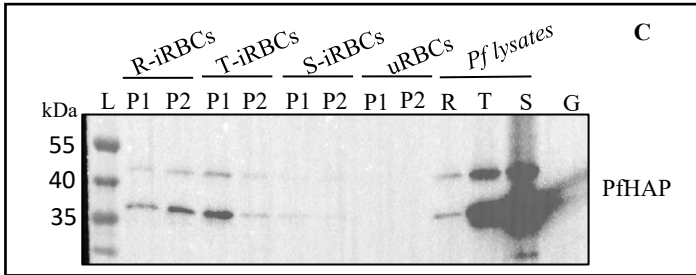
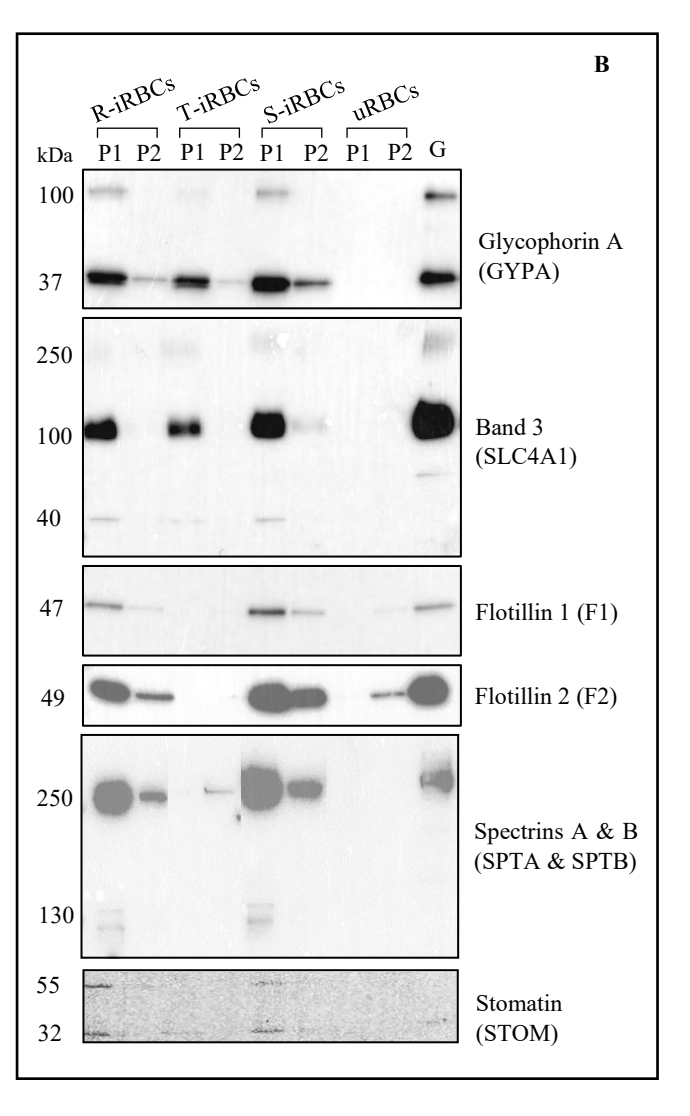


Figure 24. Protein composition of *P. falciparum* stage-specific iRBC EVs

Quantitative WBA to compare the enrichment of selected proteins in EV subpopulations and subtypes. Data shown is representative of 2-4 biological and/or technical replicates of each protein. (A) 6 RBC membrane proteins were analyzed. (B) 0.5 µg of protein was loaded for each sample. All proteins except flotillin 2 were detected only in iRBC EVs. All proteins were more abundant in P1 compared to P2. Stomatin was detected as very faint bands in EVs and RBC ghosts. Uncropped images for spectrin and stomatin blots are in Appendix Figure 5B. (C) 0.5 µg of protein; PfHAP was detected in Pf-iRBC EVs.

R-rings, T-trophozoites, S-schizonts, i-infected, u-uninfected, G-ghosts. Illustration created with Biorender.com.



Stomatin was only detected in ring- and schizont iRBC P1 EVs, albeit as faint bands at the predicted size of 32 kDa. Though present in the corresponding P2 EVs, it was mostly, faintly observed. The 55 kDa band (which was also observed in Figure 19) may in fact be Glut1 (glucose transporter type 1), which interacts specifically with stomatin, and reacts with antibodies directed against it [258]. Unlike stomatin, the other lipid raft proteins that were analyzed, flotillins 1 and 2 were visibly detected in ring- and schizont EVs. The abundance of flotillin 1, however, was much less than flotillin 2 in P1 and P2 EVs.

As observed with the mixed stage iRBC EVs (Figure 19C), PfHAP was detected in P1 and P2 EV subtypes of ring-, trophozoite-, and schizont-iRBCs (Figure 23C). However, it was observed only faintly in trophozoite iRBC P2 EVs and schizont iRBC P1 and P2 EVs. PfHAP was detected at 51 kDa, which is the predicted molecular weight of the proenzyme form. The parasite protein was also observed as a mature form at 37 kDa. As expected, PfHAP was detected in abundance in the trophozoite and schizont control cell lysates.

### 4.2.4. Protein composition of malaria EVs: Mass spectrometry

A total of 1,176 proteins were detected by MS. To properly analyze the proteomics data, all contaminants were excluded. These included *Bos taurus* proteins from the growth media, and human keratin proteins. 1,085 proteins remained, which comprised 275 human proteins and 810 *P. falciparum* proteins.

## 4.2.4.1. Quantitative analysis of proteins in P1 and P2 EVs

MS provided validation for the observed abundance profiles of human proteins analyzed by WBA (Figure 25). This was particularly true for ring-iRBC EVs, where GYPA, band 3, spectrin, stomatin, flotillin 1 and flotillin 2 were significantly more abundant in P1 EVs than in P2 EVs. Band 3, spectrin, and stomatin were more abundant in trophozoite-iRBC P1 than P2 while GYPA, band 3, spectrin and stomatin were more abundant in schizont-iRBC P1 than P2. These 5 proteins (considering spectrins A and B separately) were also revealed to be statistically more abundant in uRBC P1 than P2 despite their inconsistent detection by WBA. A notable observation was the significant abundance of the transferrin receptor (TFRC) in uRBC P2 EVs. This protein was completely absent from all iRBC EVs. TFRC is an important marker of 'exosomes' released by immature RBCS, i.e., reticulocytes [259].

Overall, P1 iRBC EVs and uRBC EVs had more host (human) proteins that were significantly abundant, compared to their corresponding P2 EVs. 43 human proteins were in abundance in ring-and schizont-iRBC P1 EVs compared to 14 and 9 proteins in P2 EVs, respectively. Trophozoite-iRBCs had the fewest number of significantly high proteins at 17 for P1 and 6 for P2. 49 proteins were enriched in uRBC P1 EVs and only 4 in the corresponding P2 EVs. For all EV populations, most human proteins present (over 200 each) were shared between subtypes, with identical averages or statistically insignificant changes across the subtypes.

Similarly, many *P. falciparum* proteins were shared between P1 and P2 iRBC EVs (Figure 26). These were 720 for ring-iRBC EVs, 777 for trophozoite-iRBC EVs, and 647 for schizont iRBC EVs. Also, P1 iRBC EVs had more parasite proteins that were significantly abundant, compared to their corresponding P2 EVs. Schizont-iRBC P1 had the most proteins at 162, followed by ring-iRBC P1 at 81, and trophozoite iRBC P1 at 33. There were 9 significantly abundant proteins in ring-iRBC P2, no significantly abundant proteins in trophozoite-iRBC P2, and a single protein abundant in schizont-iRBC P2.

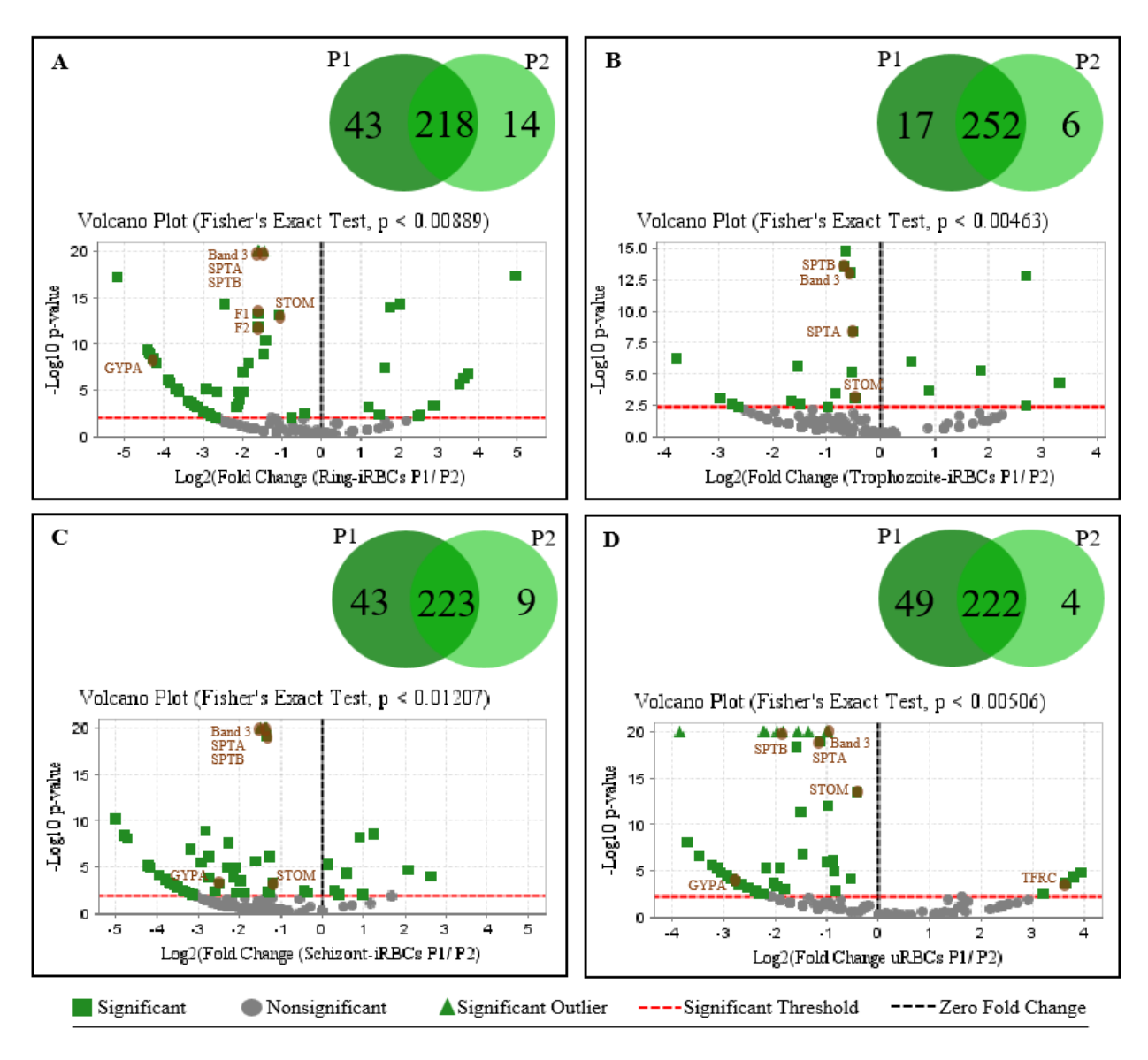
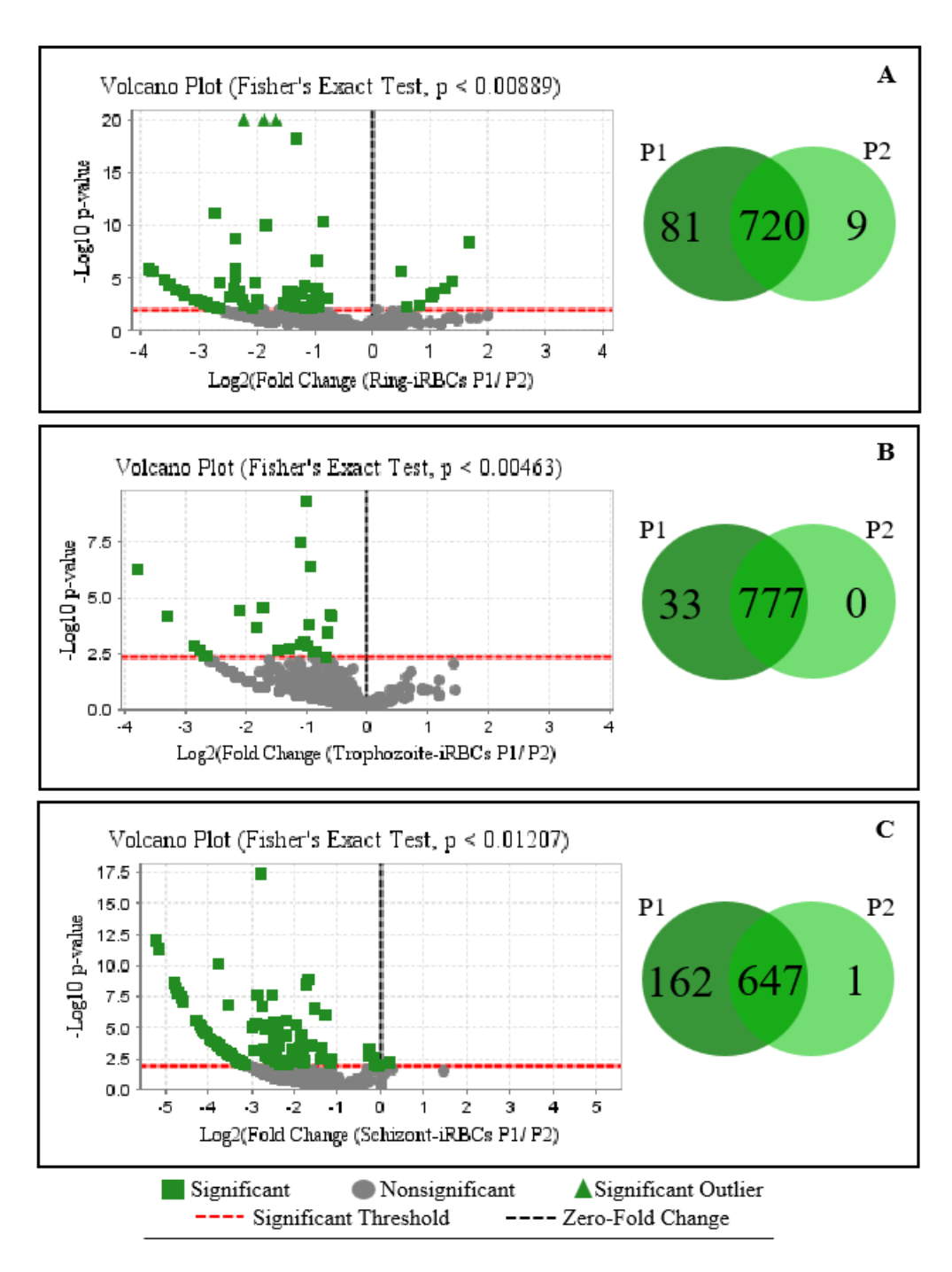


Figure 25. Relative abundance of human proteins in P1 and P2 EVs

Volcano plots show relative abundance of proteins in P1 and P2 EVs on the left and right of the zero-fold change line, respectively. Venn diagrams above volcano plots show the number of proteins that are significantly high in either EV subtype (P1 or P2, i.e., above the red horizontal significant threshold line) or present at similar levels in both EV subtypes (P1 and P2, i.e., below the significant threshold line). (A) All or (B, C, D) majority of the key EV markers analyzed by WBA (in brown) are significantly more abundant in P1 EVs. (D) The transferrin receptor (TFRC) was significantly abundant in uRBC P2 EVs but not in iRBC EVs. Data shown is of 2 independent biological replicates. SPTA-spectrin, STOM-stomatin, F1-flotillin 1, F2-flotillin 2, GYPA-glycophorin A



**Figure 26. Relative abundance of** *P. falciparum* **proteins in P1 and P2 EVs**Volcano plots show relative abundance of proteins in P1 and P2 EVs on the left and right of the zero-fold change line respectively. Venn diagrams on the right show the number of proteins that are significantly high in either EV subtype (P1 or P2, i.e., above the red horizontal significant threshold line) or present at similar levels in both EV subtypes (P1 and P2, i.e., below the significant threshold line). Data shown is of 2 independent biological replicates.

### 4.2.4.2. Known EV markers in P1 and P2 EVs

All proteins in iRBC- and uRBC EVs were checked against the online databases of the top 100 proteins often identified in EVs (<a href="http://www.exocarta.org/">http://www.exocarta.org/</a> and <a href="http://www.microvesicles.org/">http://www.microvesicles.org/</a>). 35 known markers were identified across all 8 EV samples, but many were in very low abundance; these included 26 human proteins and 9 *P. falciparum* proteins that are homologous to human proteins registered on the databases (Figure 27). Only proteins that were present in both biological replicates of each EV sample were included in the analysis.

Human proteins present in all iRBC EVs were GAPDH, PRDX2, HSPA8, ACTG1, CLTC, FLOT1, and STOM, while parasite proteins present in all iRBC EVs included CHC, PfPyrK, PfGAPDH, PfENO, PfFBPA, and PfPGK. Human TFRC, ENO and ALDOA, although present in uRBC EVs, were absent from all iRBC EVs. ANXA5, ANXA7, and CLTC absent from uRBC P1 EVs (ANXA5 was also absent from uRBC P2 EVs) were present in all iRBC EVs. CLTC was more enriched in all iRBC P2 EVs than the corresponding P1 EVs and even the parent cells. Interestingly, CLTC and CHC (the parasite homologue of CLTC) showed the highest protein ambiguity, sharing several peptides.

Ring- and schizont-iRBC P1 EVs shared several proteins that were absent from trophozoite-iRBC P1 EVs. These were all host proteins: GNAS, GNAI2, HSPA5, GNB1, ATP1A1, and VCP. On the other hand, ring- and trophozoite-iRBC P2 EVs shared several proteins that were absent from schizont-iRBC P2 EVs, including CCT2, LDHB, VCP and PfLDH. Very few markers were present in only 1 iRBC EV subtype; KPNB1 and SLC16A1 in schizont-iRBC P1 and EEF1A1 in trophozoite-iRBC P2. There was no marker present only in iRBC P1 or P2 EVs.

For an overall picture of the distribution of identified markers across all EVs, Figure 27 includes all proteins regardless of their abundance in EV subtypes. Table 7 shows significantly abundant known markers in each P1 and P2 EV sample. In this case, the parasite proteins PfFBPA and PfPGK, as well as human STOM were enriched in all iRBC P1 EVs, while the human protein CLTC was enriched in all iRBC P2 EVs. Ring-iRBC P1 and schizont-iRBC P1 were each enriched for most markers. Only ring-iRBC P1 EVs were enriched in BSG and FLOT1. Of the iRBC EVs, only trophozoite-iRBC P1 had abundant host GAPDH. Schizont-iRBC P1 had abundant ACTG1, PfLDH, PfRAB7 and VCP. For P2 subtypes, ring-iRBC EVs stood out as being enriched for LDHB and PfCHC.

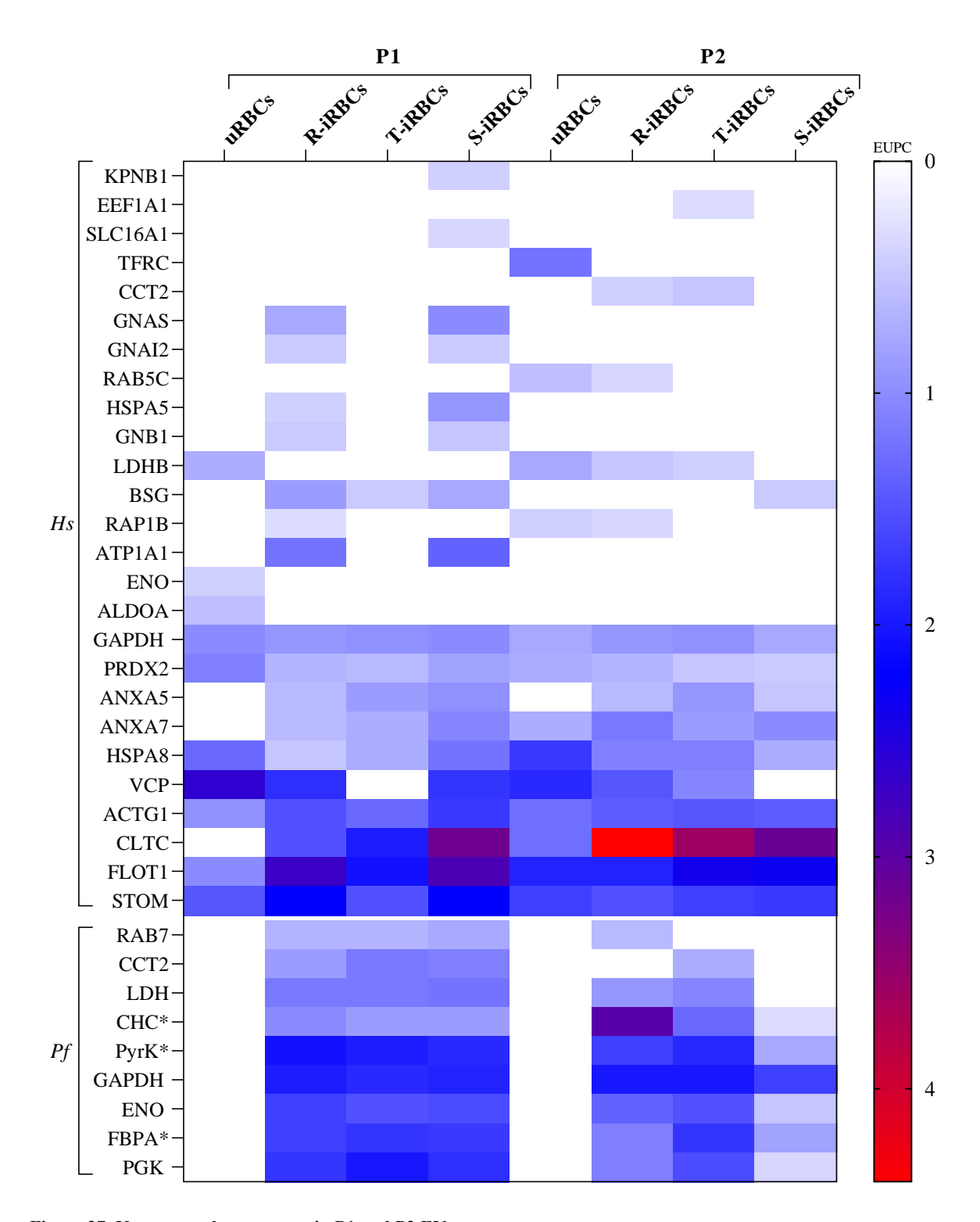


**Figure 27. Known markers present in P1 and P2 EVs**CHC\*, PyrK\* and FBPA\* are homologs of human CLTC, PKM and ALDOA with different gene names. *Hs- Homo sapiens, Pf- Plasmodium* falciparum, EUPC- exclusive unique peptide count

Table 7. Distribution of significantly abundant known EV markers in P1 and P2 EVs

		P1				P2			
	Name	uRBCs	R-	T-	S-	uRBCs	R-	T-	S-
EV			iRBCs	iRBCs	iRBCs		iRBCs	iRBCs	iRBCs
marker	A				,				
ACTG1	Actin				✓				
ANXA7	Annexin 7						✓		✓
ATP1A1	Sodium/potassium- transporting ATPase subunit alpha-1		✓						
BSG	Basigin		✓						
CCT2	T-complex protein 1 subunit beta		✓		✓				
CLTC	Clathrin heavy chain 1						✓	✓	✓
ENO1	Alpha enolase	✓							
FLOT1	Flotillin 1		✓						
GAPDH	Glyceraldhyde-3- phosphate dehydrogenase	✓		✓					
GNAS	Guanine nucleotide- binding protein G(s) subunit alpha isoforms short	✓	✓						
GNAI2	Guanine nucleotide- binding protein G(i) subunit alpha-2	<b>√</b>							
HSPA5	Endoplasmic reticulum chaperone		✓		✓				
LDHB	L-lactate dehydrogenase B chain						✓		
PfCHC	Clathrin heavy chain						✓		
PfENO	Enolase		✓		✓				
PfFBPA	Fructose-bisphosphate aldolase		✓	✓	<b>√</b>				
PfLDH	L-lactate dehydrogenase				✓				
PfPGK	Phosphoglycerate kinase		✓	✓	✓				
PfPyrK	Pyruvate kinase		✓		✓				
PfRAB7	Ras-related protein 7				✓				
PRDX2	Peroxiredoxin 2	✓							
STOM	Stomatin		✓	✓	✓				
TFRC	Transferrin receptor					✓			
VCP	Transitional endoplasmic reticulum ATPase				✓				

# 4.2.4.3. Comparison of iRBC EV proteomics dataset with published proteomes

Using the *Plasmodium* bioinformatics resource, PlasmoDB, the parasite proteomic dataset of iRBC EVs was compared against 2 published *P. falciparum* iRBC EV datasets [190, 191]. The EV proteome published by Mantel *et al* was from RBCs infected with parasite strains 3D7 or CS2 and included 86 parasite proteins; the proteome published by Abdi *et al* was from RBCs infected with a laboratory adapted clinical isolated referred to as 'isolate 9605' and included 153 parasite proteins.

More than 3 times the combined number of parasite proteins in the comparator studies was identified in this study and an important note was that for all the proteins analyzed, the minimum sequence coverage was 95% while in the other 2 studies, the maximum sequence coverage was less than 60%. When all 3 gene ID/accession number datasets were uploaded to PlasmoDB i.e., 810 proteins from this study, 153 proteins from Abdi *et al*, and 86 proteins from Mantel *et al*, 799, 153, and 82 proteins, respectively, were found. 84% of proteins from Abdi *et al* and 96% of proteins from Mantel *et al* overlapped with the gene output from this study (Figure 28A). A total of 827 *P. falciparum* proteins were identified when combining all 3 studies, 52 of which were shared. 24 of these proteins were in the top 50 *P. falciparum* proteins identified in this study but were differentially abundant across the different life-stage iRBC EV subpopulations and subtypes (Figure 28B). Many of these were invasion proteins (e.g., RhopH2 and RON3). Also noteworthy were the parasite homologues of the known EV markers PfGAPDH and PfFBPA. Among the 27 proteins shared with the dataset from Mantel *et al*, PyrK and PfENO (within the top 50 *P. falciparum* proteins identified here) were also identified.

Apart from the top 50 parasite proteins in this study, parasite homologues of EV markers were also detected by Abdi *et al*. These included PfCHC, PfRAB7, PfPGK and PfLDH, while Mantel *et al* detected PfPGK and PfLDH. Parasite proteins that were detected in at least 1 of the comparator studies, but not stably detected in all EV subpopulations or subtypes here were PfEMP3, KHARP, MAHRP, Pfmc-2TM, RIFIN and PTP. Although not detected by Mantel *et al* nor Abdi *et al*, PfEMP1 and STEVOR proteins were found in ring-iRBC P1 and P2, respectively. Plasmepsins, one of which was used in WBA to confirm the presence of EVs from parasite iRBCs (PfHAP AKA plasmepsin III; see Figure 19 and Figure 24), were also not stably detected across the EV subpopulations or subtypes and were not detected at all by Mantel *et al* nor Abdi *et al*.

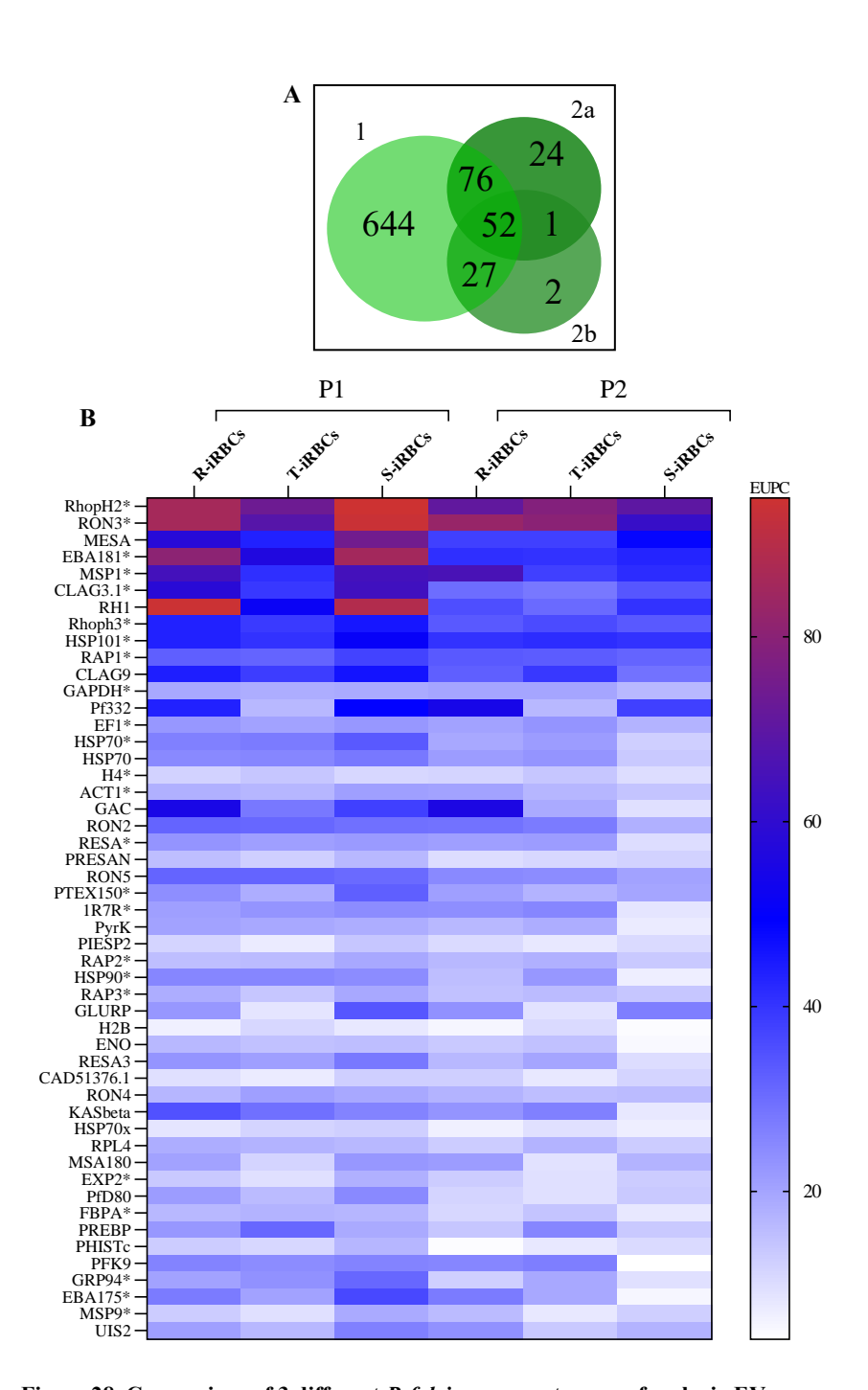


Figure 28. Comparison of 3 different *P. falciparum* proteomes of malaria EVs (A) Venn diagram of proteome from this study [1] and published proteome from Abdi *et al* [2a] and Mantel *et al* [2b]. (B) Top 50 parasite proteins identified in P1 and P2 EVs of ring-, trophozoite-, and schizont iRBCs, according to the exclusive unique peptide count (EUPC). \*24 proteins shared with datasets from 2a and 2b. EVs analyzed by Abdi *et al* were from ring to trophozoite and trophozoite to ring stage iRBCs, EVs analyzed by Mantel *et al* are likely from ring stage iRBCs; both studies isolated EVs by high-speed ultracentrifugation which is equivalent to the P2 EVs isolated in this study.

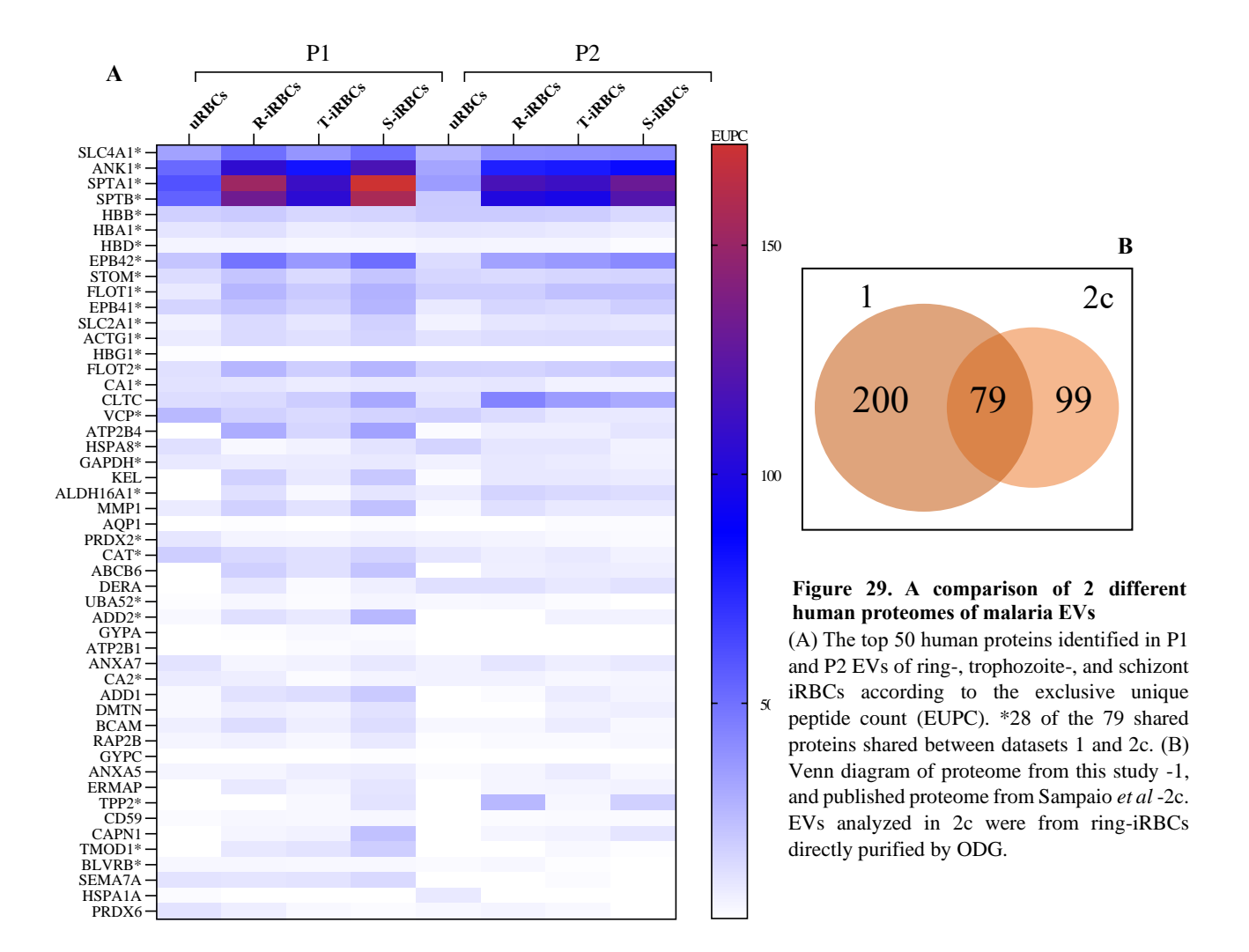
In the absence of access to the full human proteome datasets of Mantel *et al* and Abdi *et al*, the top human proteins identified in these studies were checked against the top 50 human proteins identified herein (Figure 29A). 18 of the top 20 human proteins identified by Mantel *et al* were differentially identified in all iRBC EV subtypes. These included hemoglobin, band 3 (SLC4A1), stomatin, spectrin and GYPA, all of which were also identified by Abdi *et al*. Also commonly identified by Mantel *et al* were the EV markers VCP, PRDX2, ANXA7, flotillin 1 and flotillin 2.

An accessible human proteome of malaria EVs [193] was compared using FunRich. Of the respective 275 and 178 proteins identified for the current and comparator study by Sampaio *et al*, 79 proteins were shared (Figure 29B), 28 of which were in the top 50 proteins in this study. As with Mantel *et al*, these also included hemoglobin, band 3 (SLC4A1), and spectrin, as well as EV markers stomatin, VCP, PRDX2, flotillin 1, flotillin 2, GAPDH, HSPA8, and ACTG1. Also detected by Sampaio *et al* was LDHB. As described with the volcano plots and heat maps, all these proteins displayed differential abundance across the different life-stage iRBC EV subpopulations and subtypes. As mentioned for the studies by Mantel *et al* and Abdi *et al*, unlike this study, the sequence coverage for human proteins analyzed by Sampaio *et al* was less than 60% (except for hemoglobin). Importantly, GYPA, ANXA7 and CLTC were not detected by Sampaio *et al*.

### 4.2.4.4. Secreted and non-secreted parasite proteins in malaria EVs

Selected parasite proteins were assessed on their localization in the infected RBCs (hence their potential use for investigating EV biogenesis in *P. falciparum*) i.e., whether they were secreted into the host cell cytoplasm, not secreted into the host cell cytoplasm and/or their membrane association. The secretory status of the 9 homologue EV markers (See Figure 27); 4 of which were in the top 50 parasite proteins – PfPyrK, PfGAPDH, PfENO, and PfFBPA) and the remaining top 50 proteins was predicted using a pseudo amino acid composition-based web server [260] available at <a href="http://www.imtech.res.in/raghava/pseapred/">http://www.imtech.res.in/raghava/pseapred/</a>.

Out of 55 proteins, 7 were predicted to be secretory, while 13 were predicted to be non-secretory, localized to various compartments, including the host cell cytoplasm and/or not associated with any membranes. The remaining 36 proteins were predicted to be non-secretory, localized to various compartments, excluding the host cell cytoplasm and/or associated with membranes. These 36 proteins are listed in Table 8.



PfPyrK, PfFBPA and PfRAB7 were all predicted to be secreted into the host cell cytoplasm. CHC was predicted to be non-secretory and is, as expected, localized to clathrin-coated vesicles. Most of the proteins are associated with membranes but may also be localized in other subcellular compartments of the parasite, such as the nucleus, nucleosome, mitochondrion, endoplasmic reticulum, digestive vacuole, and/or cytoplasm. Several of these proteins are located in the host cell surface knobs on the RBC membrane and Maurer's clefts. These include PfHSP101, RhopH3, MESA, PfPGK and RESA3. Proteins localized in the parasite membrane include PfENO and PfGAPDH, the invasion proteins EBA175 and EBA181, and RON3. PfEXP2, PfHSP101 and PfPTEX150 are all associated with the PTEX complex in the parasitophorous vacuolar membrane. Several proteins, particularly the rhoptry proteins, are located in the parasite DV. The cellular component of ontology of parasite proteins was sourced using PlasmoDB.

Table 8. Non-secretory *P. falciparum* iRBC EV proteins associated with membranes.

Protein name	<b>Protein ID</b>	Gene ID	Previous ID <sup>1</sup>	Cellular location <sup>2</sup>
Actin 1	ACT1	PF3D7_1246200	PFL2215w	N, C, AF, DV
Antigen 332, DBL-like protein	Pf332	PF3D7 1149000	PF11 0506	N, M, MC, HCM
Clathrin heavy chain, putative	CHC	PF3D7_1219100	PFL0930w	N, CCV
Cytoadherence linked asexual protein	CLAG9	PF3D7 0935800	PFI1730w	N, Rh, AP
9		_		
Elongation factor 1-alpha	-	PF3D7_1357000	PF13_0304	N, Mit, HCSK
Endoplasmin, putative	GRP94	PF3D7_1222300	PFL1070c	N, ER, CS, DV
Enolase	ENO	PF3D7_1015900	PF10_0155	N, C, Cy, M, DV
Erythrocyte binding antigen-175	EBA175	PF3D7_0731500	MAL7p1.176	M, Mic
Erythrocyte binding antigen-181	EBA181	PF3D7_0102500	PFA0125c	M, Mic
Exported protein 2	EXP2	PF3D7_1471100	PF14_0678	N, MDG, HCCV, PC, PVM
Glideosome-associated connector	GAC	PF3D7_1361800	MAL13P1.308	N, C, CS, AP
Glutamine-rich protein	GLURP	PF3D7_1035300	PF10_0344	CS
Glyceraldehyde-3-phosphate	GAPDH	PF3D7_1462800	PF14_0598	N, C, M, DV
dehydrogenase				
Heat shock protein 70	BIP	PF3D7_0917900	PFI0875w	N, C, ER, M, DV
Heat shock protein 70	HSP70	Pf3D7_0818900	PF08_0054	N, C, CS, DV
Heat shock protein 90	HSP90	PF3D7_0708400	PF07_0029	N, C, M, DV
Heat shock protein 101	HSP101	PF3D7_1116800	PF11_0175	N, C, ER, AC, MDG, MC, PC
High molecular weight rhoptry	RhopH3	PF3D7_0905400	PFI0265c	N, Rh, HCSK, PVM
protein 3				
L-lactate dehydrogenase	LDH	PF3D7_1324900	PF13_0141	N, C, CS, Mit, DV
Mature parasite-infected erythrocyte	MESA	PF3D7_0500800	PFE0040c	N, HCM, HCSK, MC
surface antigen				
Merozoite surface protein	MSA180	PF3D7_1014100	PF10_0138	C, CS
Merozoite surface protein 1	MSP1	PF3D7_0930300	PFI1475w	N, M, DV
Phosphoglycerate kinase	PGK	PF3D7_0922500	PFI1105w	N, C, DV, MC,
Plasmodium exported protein	-	PF3D7_0501000	PFE0050w	N, M, MC
Plasmodium exported protein	-	PF3D7_0424600	PFD1170c	N, HCM
(PHISTb)				
Translocon component	PTEX150	PF3D7_1436300	PF14_0344	N, AC, MDG, PC, PVM
Reticulocyte binding protein	RH1	PF3D7_0402300	PFD0110w	M, AC, Rh
homologue 1				
Rhoptry-associated protein 1	RAP1	PF3D7_1410400	PF14_0102	N, Rh, DV, PV
Rhoptry-associated protein 2	RAP2	PF3D7_0501600	PFE0080c	N, Rh, DV
Rhoptry-associated protein 3	RAP3	PF3D7_0501500	PFE0075c	N, Rh, DV
Rhoptry neck protein 2	RON2	PF3D7_1452000	PF14_0495	CS, M, RhN
Rhoptry neck protein 3	RON3	PF3D7_1252100	PFL2505c	N, M, Rh, CS, PV
Rhoptry neck protein 4	RON4	PF3D7_1116000	PF11_0168	N, Rh, RhN, DV
Rhoptry neck protein 5	RON5	PF3D7_0817700	MAL8P1.73	RhN
Ring-infected erythrocyte surface	RESA	PF3D7_0102200	PFA0110w	HCM, DV, MDG, PV
antigen				
Ring-infected erythrocyte surface	RESA3	PF3D7_1149200	PF11_0509	MC
antigen				

#### **Table 8 continued**

<sup>1</sup>ID used to search predicted secretory status. <sup>2</sup>Cellular location determined from references (publications or database records) cited on PlasmoDB.

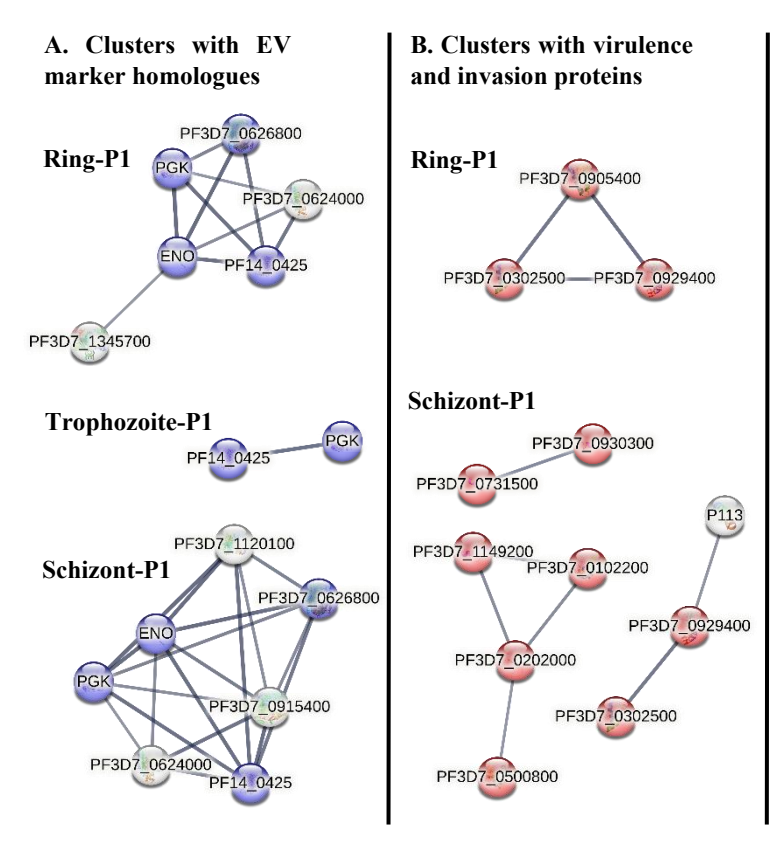
AC- apical complex, AF- actin filament, AP- apical part of cell, C- cytoplasm/ cytosol, CS- cell surface, Cy- cytoskeleton, CCV- clathrin coated vesicle, DV- digestive vacuole, ER- endoplasmic reticulum, HCCV- host cell cytoplasmic vesicle, HCM-host cell membrane, HCSK- host cell surface knobs, M- membrane, MC- Maurer's cleft, MDG- merozoite dense granules, Mic- microneme, Mit- mitochondrion, N- nucleus, Nu- nucleosome, PC- PTEX complex, PV- parasitophorous vacuole, PVM-parasitophorous vacuolar membrane, Rh- rhoptry, RhN- rhoptry neck, Ri- ribosome, V-vacuole

## 4.2.4.5. Gene ontology enrichment analysis of *P. falciparum* proteins

To determine if any of the recurring notable parasite proteins were involved in key pathological processes and pathways, the significantly abundant proteins identified in the iRBC P1 EV subtypes were analyzed with STRING. The protein networks yielded 7, 5, and 21 clusters for ring-, trophozoite-, and schizont-iRBC P1 EVs, respectively. Clusters with homologues of known human EV markers were identified in all 3 EV subtypes, however only ring- and schizont-iRBC P1 EVs had clusters of virulence and invasion proteins with strong networks. In addition, schizont-iRBC P1 EVs had a cluster of proteins that belong to the proteasome complex. Figure 30 shows these selected clusters relevant to this study. The protein interaction networks, however, appeared incomplete as several proteins with known interactions and belonging to protein families were disconnected in each network. Therefore, the proteins were further analyzed with the PlasmoDB resource for function prediction and metabolic pathway enrichment.

PlasmoDB did not recognize one ID, therefore of the 81 ring-iRBC P1 EVs and 162 schizont-iRBC P1 EVs uploaded to PlasmoDB, 80 and 161 proteins, respectively, were found. The 33 trophozoite-iRBC P1 EVs were all recognized. All 3 EV subtypes were compared (Figure 31A) and were found to share 18 significantly abundant proteins. Enriched KEGG metabolic pathways were purine metabolism, fructose and mannose metabolism, carbon fixation in photosynthetic organisms and carbapenem biosynthesis. An important biological process was the response to xenobiotic stimulus (GO:0009410) that is synonymous with drug resistance (Figure 31B). A notable protein identified in this process and in purine metabolism is heat shock protein 70 (BIP) that is listed in Table 8.

None of the 3 proteins that trophozoite-iRBC P1 EVs had in common with ring- or schizont iRBC P1 EVs were homologues of known EV markers, or in the top 50 identified parasite proteins, nor involved in virulence or invasion. Ring- and schizont iRBC P1 EVs shared 35 proteins. Enriched KEGG pathways in this subset were glycolysis/gluconeogenesis (with PfENO,



### C. Cluster with proteins of the proteasome complex in schizont-P1

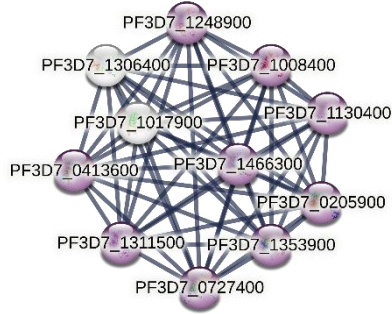


Figure 30. Protein interactions of significantly abundant proteins in P1 iRBC EVs

(A) iRBC P1 EVs contained clusters of PfFBPA (PF14\_0425), PfPyrK (PF3D7\_0626800) PfPGK, and PfENO (rings – top and schizont – bottom) or PfFBPA and PfPGK only (trophozoite – middle). The EV marker homologues colored in blue are involved in metabolic processes, including glycolysis. (B) Ring and schizont iRBC EVs contained clusters of virulence and invasion proteins in red (C) Schizont iRBC EVs also contained a cluster of proteasome complex proteins in purple.

PfPyrK and hexokinase), N-glycan biosynthesis, one carbon pool by folate and the biosynthesis of 12-, 14- and 16-membered macrolides. 4 important biological processes out of 125 listed were identified (Figure 31C). These were the most statistically significant enriched biological processes: adhesion of symbiont to microvasculature (GO:0020035) and adhesion of symbiont to host (GO:0044406), both of which are mediated by 6 members of the RIFIN protein family, cytoadherence linked asexual protein 8 (CLAG8), serine/threonine protein kinase (FIKK4.1) and *Plasmodium* exported protein (PHISTb - PF3D7\_0424600); antigenic variation (GO:0020033) involved the same 6 RIF proteins and lastly, activation of immune response (GO:0002253) mediated by PfENO. RNA binding (GO:0003723) was an important molecular function identified for the subset of ring- and schizont-iRBC P1 EV shared proteins (Figure 31D). The proteins involved in RNA binding were PfENO, PfHSP90, PfPyrK and RhopH2, among others.

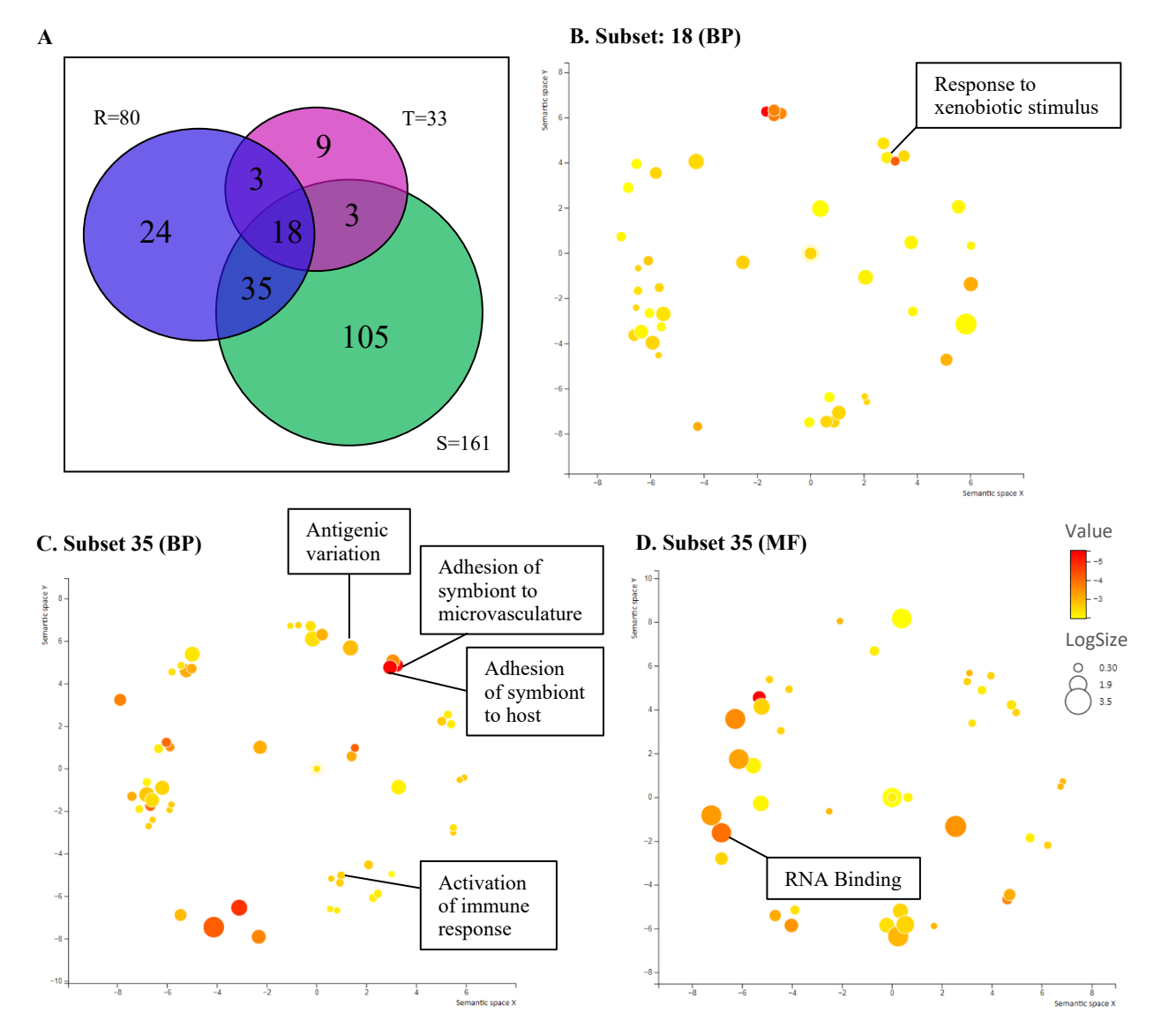


Figure 31. GO analysis of significantly enriched shared *P. falciparum* proteins in P1 iRBC EVs
(A) Venn diagram of proteins significantly high in ring-, trophozoite-, and schizont-iRBC P1 EVs. 18 proteins had similar abundance in the 3 EV subtypes. The greatest overlap was between ring- and schizont-iRBC EVs. (B) Response to xenobiotic stimulus (i.e., drug resistance) mediated by BIP, adenosine deaminase and M1-family alanyl aminopeptidase was enriched in the 3 EV subtypes. (C) Vital pathogenic processes were enriched in ring- and schizont-iRBC P1 EVs mediated by virulence proteins including RIF proteins, PfENO and CLAG8. (D). Relevant to this study was RNA binding, identified as a highly significant molecular function also mediated by important proteins including PfENO, PfHSP90, PfPYRK and RhopH2.

R- ring-iRBC P1, T- trophozoite-iRBC P1, S-schizont-iRBC P1, BP- biological process, MF- molecular function

Specifically enriched in ring-iRBC P1 EVs was inositol phosphate metabolism, and there were no metabolic pathways enriched for trophozoite-iRBC P1 EVs. Sphingolipid and methane metabolism were enriched for schizont-iRBC P1 EVs. PfRAB7 and 3 other plasmodial RAB proteins (RAB1b, RAB2, RAB6) were identified proteins involved in sphingolipid metabolism, while PfLDH was 1 of 4 proteins mediating methane metabolism.

Noteworthy were the distinct set of proteins enriched in the different iRBC P1 EVs that are involved in biological processes and molecular functions of interest (Figure 32). Ring- and schizont-iRBC P1 EVs were enriched for different proteins important in response to xenobiotic stimulus. For ring-iRBC P1 EVs, this included Kelch protein K13. MDR1, CDPK1, EBA175 and MSP1 were listed for schizont-iRBC P1 EVs. Additionally, schizont-iRBC P1 EVs were enriched for virulence proteins important for entry into host (GO:0044409; EBA175, CDPK1 etc.), regulation of immune response (GO:0050776; RESA and SERA5), and proteasome regulatory particle assembly (GO:0070682; RPT2, RPT3, etc.). None of these biological processes were enriched in trophozoite-iRBC P1 EVs. All the iRBC P1 EVs were enriched in proteins important in RNA binding. The full list of the proteins is provided in Appendix Table 1. Notably, response to xenobiotic stimulus and RNA binding were the most significant biological process and molecular function defined for the ring-iRBC P1 EVs, respectively. The most significant biological process for schizont-iRBC P1 EVs was proteasome regulatory particle assembly.

CDPK1 is crucial for sexual development, specifically gametogenesis in the mosquito. Because of the recurrence of this protein in various biological processes in the schizont-iRBC P1 EVs, the iRBC P1 EVs were specifically analyzed for other proteins that may be involved in sexual development. 8 proteins that may be important for gametocytogenesis in RBCs, due to their significant expression in mature asexual stages of *P. falciparum* and early-stage gametocytes [261], were significantly high in schizont iRBC P1 EVs compared to P2 but were also present in ring iRBC P1 EVs. These were two gametocyte exported proteins GEXP02 and GEXP12 (PF3D7\_1102500 and PF3D7\_1148700, respectively), three other exported proteins (PF3D7\_0424600, PF3D7\_0501000, PF3D7\_0936800), plasmepsin IV (PF3D7\_1407800), RESA (PF3D7\_0102200), and StAR-related lipid transfer protein (PF3D7\_0104200).

Ring- and schizont-iRBC P2 EVs were both enriched for MAHRP2. However, because of the very low number of significantly abundant proteins in these EV subtypes, as well as the absence of any significantly abundant proteins in the trophozoite-iRBC P2 EVs, these protein datasets were not analyzed further. Additionally, while the similarly abundant proteins of all 3 stage-specific iRBC P1 and P2 EVs had relevant enriched processes, the associated proteins were present at very low abundance with 4 or less exclusive unique peptide counts for identification. As such, these protein datasets were also not further analyzed.

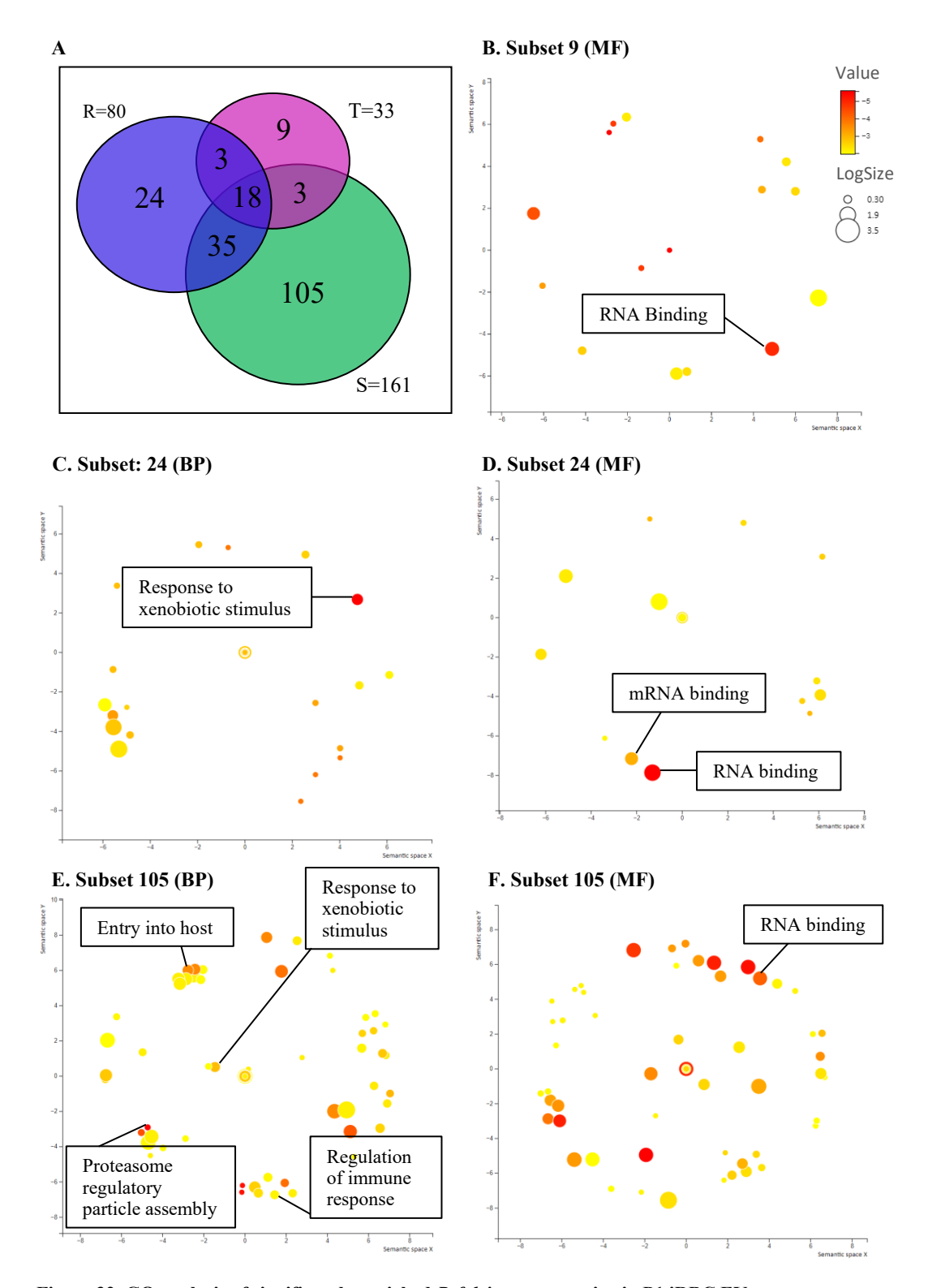


Figure 32. GO analysis of significantly enriched *P. falciparum* proteins in P1 iRBC EVs

(A) Venn diagram of proteins significantly high in ring-, trophozoite-, and schizont-iRBC P1 EVs. (B) Trophozoite-iRBC EVs (C & D) Ring-iRBC EVs. (E & F) Schizont iRBC EVs

R- ring-iRBC P1, T- trophozoite-iRBC P1, S-schizont-iRBC P1, BP- biological process, MF- molecular function

## 4.2.4.6. Gene ontology enrichment analysis of human proteins

More than 50% of the enriched human proteins across all iRBC P1 EVs and control uRBC EVs were associated with the plasma membrane and extracellular exosome (Figure 33A). Only the ring-iRBC P1 EVs were enriched for the membrane raft cellular component. This reflects the significant enrichment of the membrane raft proteins stomatin, flotillin 1 and flotillin 2 in this EV population shown in Figure 25A. All iRBC P1 EVs had proteins associated with cytoskeleton and none were enriched for the hemoglobin complex, unlike the uRBC P1 EVs.

iRBC P1 EVs and uRBC P1 EVs also differed largely in biological processes and molecular functions, as several were present only in the infected or uninfected EV subtypes (Figure 33B and Figure 33C). Unique to ring-iRBC P1 EVs were positive regulation of protein binding (GO:0032092), protein localization to plasma membrane (GO:0072659), and calmodulin binding (GO:0005516). Many GO terms were specific for schizont-iRBC P1 EVs, including toxin transport (GO:1901998), actin binding (GO:0003779), protein folding chaperone (GO:0044183), ATP-dependent protein folding chaperone (GO:0140662), and ATP-binding (GO:0005524). Calcium ion export (GO:1901660) was enriched only in trophozoite-iRBC P1 EVs.

For all the P2 EVs, there were no significantly enriched biological processes or molecular functions. While there were also no significantly enriched cellular components for trophozoite-and schizont iRBC P2 EVs, 78.57% of the enriched proteins in the ring-iRBC P2 EVs were associated with extracellular exosomes. These included CLTC, ANXA7 and LDHB that were also identified in this EV subtype in Table 7.

iRBC and uRBC P1 and P2 EVs had very similar enriched GO terms for the human proteins that were similarly abundant between the 2 EV subtypes (Figure 34). Over 60% of these proteins across all the EV subpopulations were associated with extracellular exosomes. There were also proteins associated with membrane rafts and proteasome complexes, although these were much less abundant. Overall, the enriched biological processes had very low percentages of proteins involved (<10%). Notable biological processes, however, were regulation of extracellular exosome assembly (GO:1903551), positive regulation of exosomal secretion (GO:1903543), glycolytic process (GO:0006096), and proteasome-mediated ubiquitine-dependent protein catabolic process (GO:0043161). Several of the shared human proteins between iRBC and uRBC P1 and P2 EVs were identified to be involved in energy dependent molecular functions. Each iRBC EV

subpopulation had over 15% of the shared human proteins annotated to RNA binding (GO:0003723).

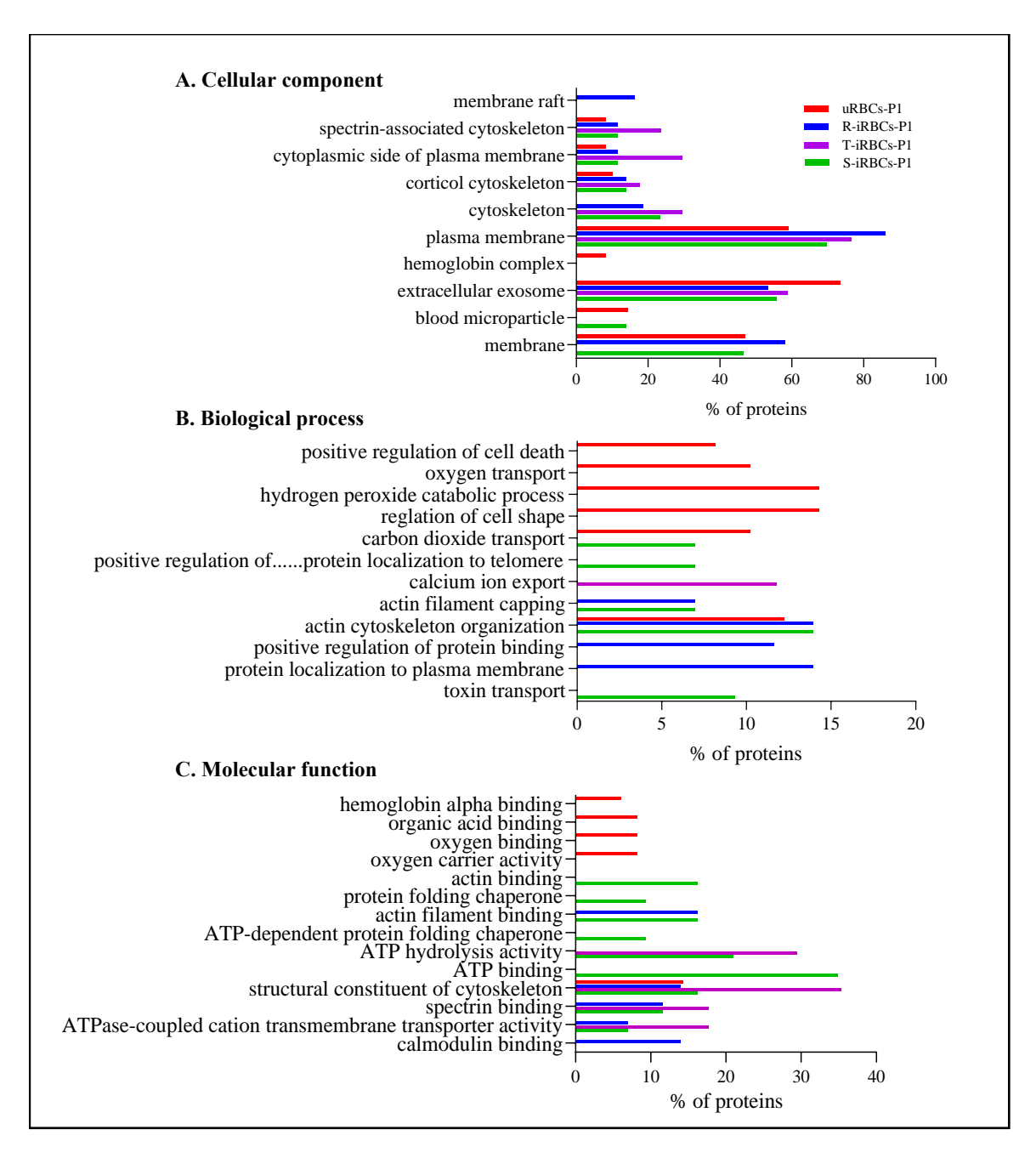


Figure 33. GO analysis of human proteins significantly enriched in P1 EVs

GO enrichment analysis was performed against the Uniprot human database. Data only shows enriched terms with (Bonferroni corrected) P-values of <0.05 to <0.001 for any given EV subtype (i.e., a numerical value of 0 was input for EVs with P-value >0.05). GO terms with no significant enrichment in any EV subtype were excluded from the summary.

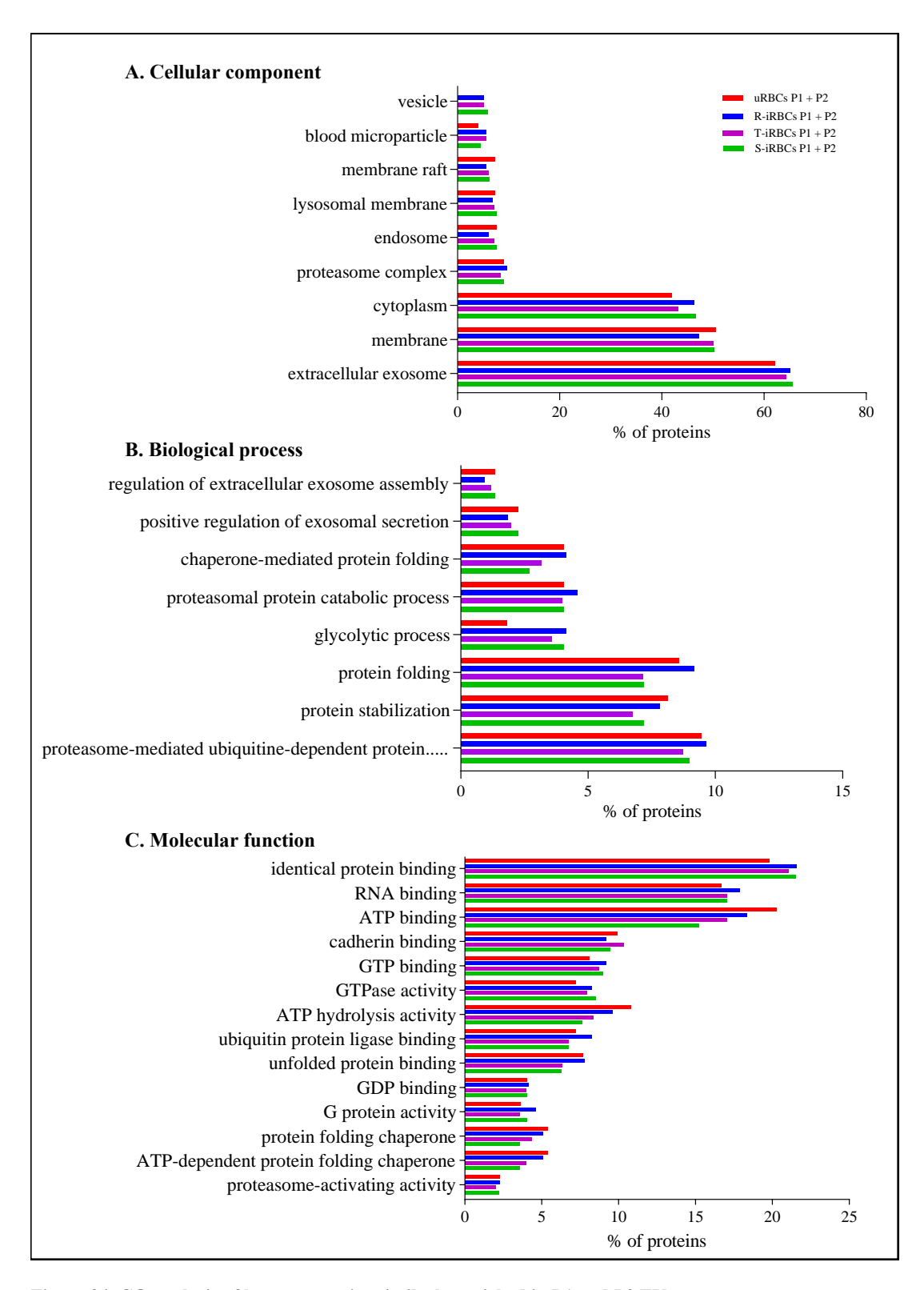


Figure 34. GO analysis of human proteins similarly enriched in P1 and P2 EVs

GO enrichment analysis was performed against the Uniprot human database. Data only shows enriched terms with (Bonferroni corrected) P-values of <0.05 to <0.001 for any given EV subtype (i.e., a numerical value of 0 was input for EVs with P-value >0.05). GO terms with no significant enrichment in any EV subtype were excluded from the summary.

### 4.3. Preface to EV transcriptomics (Objective 3)

RNA studies of EVs have become tremendously popular in recent times owing to the potential of RNA-containing EVs to deliver 'genetically encoded messages' to recipient cells [225] to regulate their function or be translated to proteins [262]. The amount and composition of RNA in EVs from different cells, as well as different EV subtypes from the same cell, is highly heterogenous [263], with some EVs containing very low quantities of RNA [264]. EVs containing appreciable amounts of RNA, however, hold potential as disease biomarkers and therapeutic agents [225]. Diverse types of RNA have been identified and characterized in EVs, including protein-coding RNA and several types of small noncoding RNAs. Malaria EV studies have focused on small RNAs, such as microRNAs, due to their regulatory function and importance in intercellular signaling (See Table 3).

As with many aspects of the EV field, EV-RNA research faces several challenges, particularly, the impact of poorly standardized EV isolation and purification methods on EV-RNA content, as well as the optimization of isolation and characterization methodologies for EV-RNA [225]. EV isolation protocols differ across known published malaria EV-RNA studies, and methods for analyzing EV-RNA, if optimized, have not been made known. Unlike cells, the RNA content of EVs is usually very small and co-isolated with unencapsulated RNA, which yields unreliable and misleading data analysis on the RNA composition of EV populations. Therefore, it was important to isolate and characterize RNA from isolated EVs with an optimized EV isolation protocol, such as that developed in the first objective of this study. This was also advantageous in allowing the direct comparison of RNA contents in EVs from different cells and EV subtypes from the same cell, since the presence, absence, or heterogeneity of the RNA content of malaria EV subpopulations or subtypes is unknown. To ensure the reliability of EV-RNA analysis, a protocol for removing unencapsulated RNA in EV preparations by pretreatment with proteinase K and RNAse A, as recommended by ISEV, was rigorously optimized [225].

The third objective of this thesis was to analyze and compare the RNA cargo in EVs released from RBCs infected with the ring, trophozoite, and schizont stages of *P. falciparum*. Therefore, EVs were isolated from tightly synchronized cultures. For the RNA cargo, 2 biological replicates were initially analyzed and quantified, and, contrary to the findings of the protein analysis, P1 EVs

had little to no RNA while P2 EVs were abundant in RNA. As such, the EV RNA of P2 EVs was sequenced and further analyzed, and the findings are detailed here.

Like with proteomics, RNA molecules important in EV biogenesis, specific functions, virulence, and potential as markers were specifically researched. Unlike published transcriptomic studies of malaria EVs however, the focus was not only on microRNAs.

### 4.3.1. RNA detection in untreated EVs

The amount of RNA in each EV sample varied widely between biological replicates. However, the overall trend remained the same, whereby P1 EVs had lower RNA concentrations compared to their corresponding P2 EVs. Concentrations as low as 2 ng/µl were sometimes recorded for P1 EVs. Bioanalysis of P1 and P2 EVs, as well as their parent cells, revealed differences in the RNA concentrations and sizes (Figure 35).

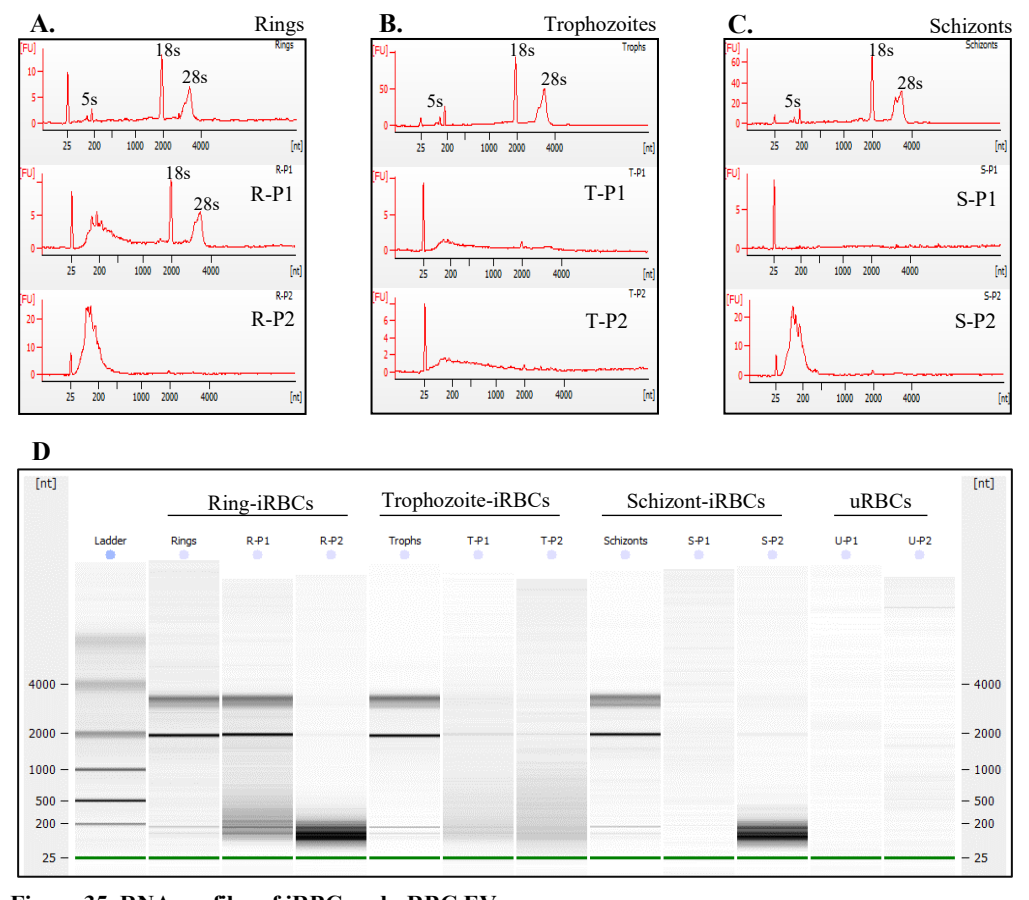


Figure 35. RNA profiles of iRBC and uRBC EVs

Electropherograms showing fluorescence intensity (FU) against size distribution in nucleotides (nt) for (A) ring-iRBCs and ring-iRBC EVs (B) trophozoite-iRBCs and trophozite-iRBC EVs (C) schizont-iRBCs and schizont-iRBC EVs (D) RNA bands of iRBCs, iRBC EVs and uRBC EVs. (A) and (D) 18S and 28S peaks and bands can be seen for ring-iRBC P1 EVs. The peak at 25 nt in the electropherograms is the internal standard.

Peaks that may correspond to the *P. falciparum* 5S, 18S and 28S rRNA were seen in all cellular RNA as well as presumably corresponding to 18S and 28S rRNA in the ring iRBC P1 but were absent from all other iRBC EVs. Ring iRBC EVs had more abundant small RNAs than the parent cells with higher amounts in the P2 than P1 EVs. There were very low peaks of small RNAs seen for trophozoite iRBC EVs and no peaks in the schizont P1 EVs. Schizont P2 EVs had very similar RNA amount and size distribution to ring iRBC P2 EVs. There were no peaks or bands detected in uRBC EVs.

# 4.3.2. RNA detection and analysis in treated EVs

The results of RNA quantification for the sequenced sample set are presented in Figure 36. The amount of RNA in iRBC EV samples was lower after treatment with proteinase K and RNase A. This reduction was more drastic in P2 EVs. Post treatment, the concentrations of RNA in iRBC P1 EVs in ng/µL were as follows: Rings: 3.80, trophozoites: 3.45, schizonts: 4.20, while the corresponding P2 concentrations were: Rings: 12.40, trophozoites: 12.40, schizonts: 8.05. Expectedly, there was little to no RNA detected in uRBCs and uRBC EVs. The treated EV samples were analyzed further.

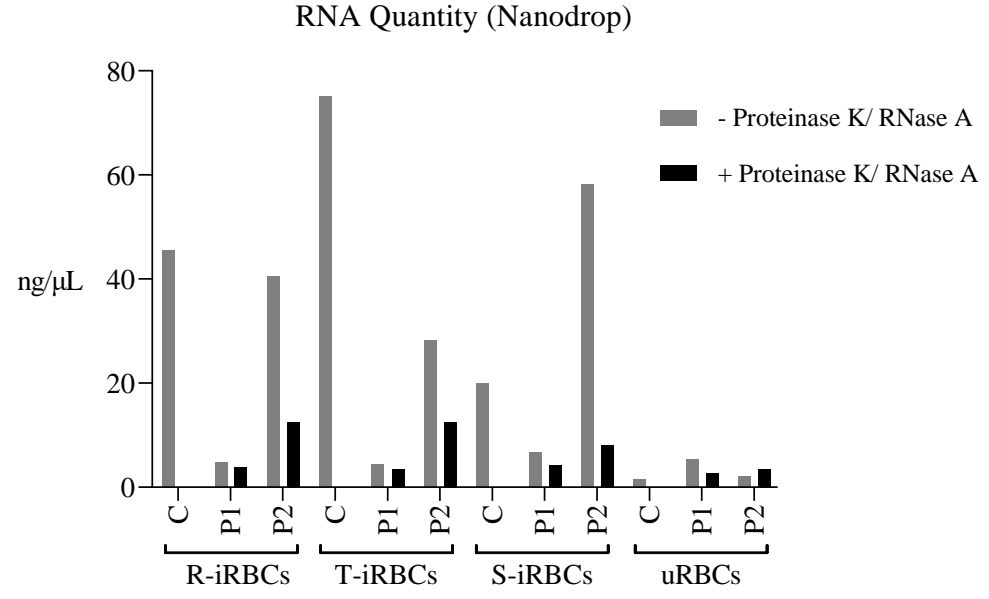


Figure 36. EV RNA detection with Nanodrop
Cells were not treated with proteinase K/RNase A.
C- parent cells (stage-specific iRBCs) from culture, R- rings, T- trophozoites, S- schizonts.

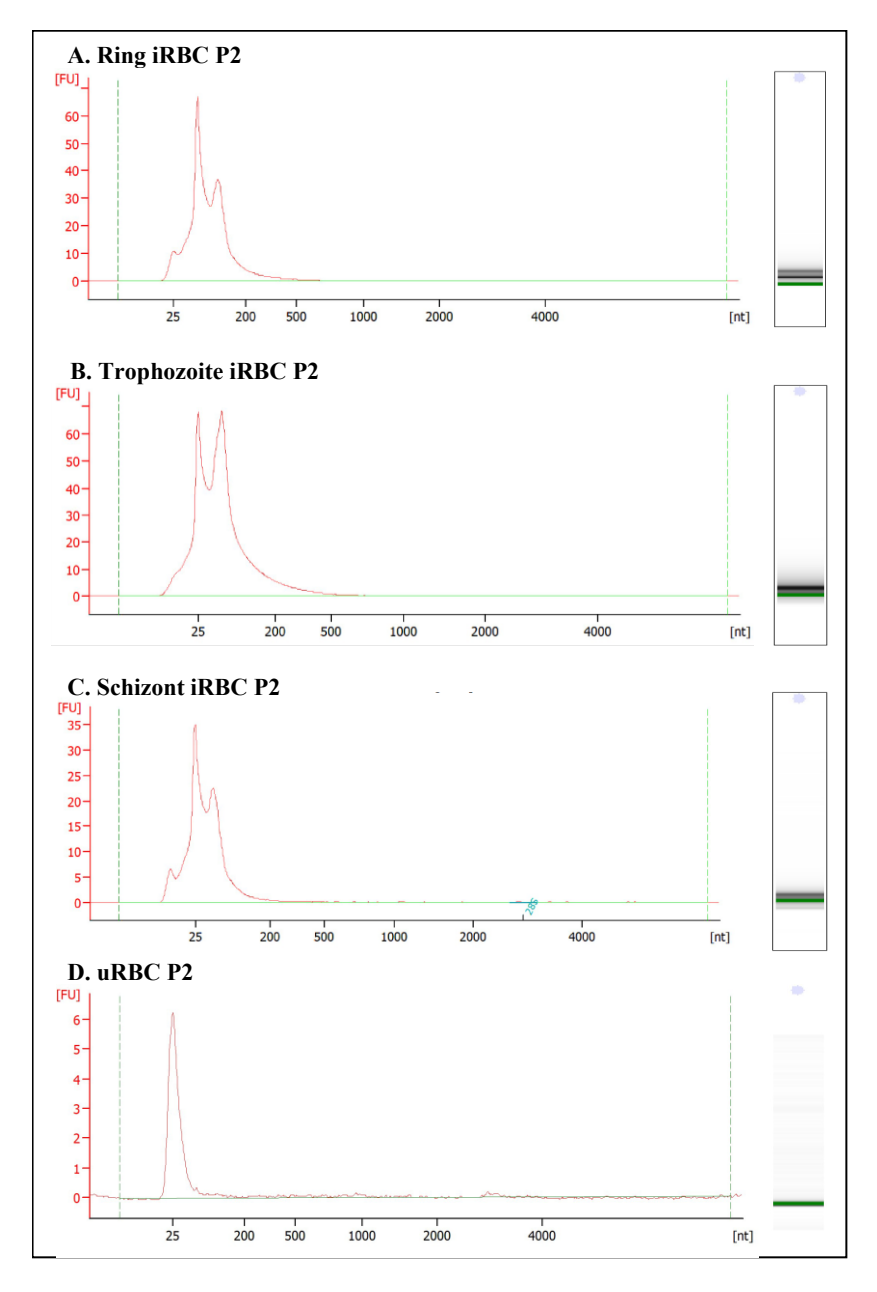
The quality of the RNA was assessed by the ratio of absorbance at 260 nm and 280 nm. A260/A280 is a measure of RNA purity and a ratio of ~2.0 is generally acceptable while A260/A230 is a measure for contamination and a range of 2.0-2.2 is generally acceptable. The 260/280 absorbance ratios for cellular RNA (except uRBCs) were all acceptable at ~2.0 while the 260/230 ratios deviated from the acceptable range of 2.0-2.2. These ratios are summarized in Table 9. At the extremely low values calculated for the treated P1 EVs, the RNA concentrations are not reliable, and this was reflected in the low purity ratios. The A260/A280 values for iRBC P2 EVs, although below ~2.0 were higher than those of P1 EVs. Low A260/A230 ratios however, indicated that these samples had some contamination, which is expected of EV-RNA [225]. Possible contamination includes phenol from RNA extraction reagents and laboratory derived contamination, which may potentially affect the validity of the RNA analysis data [225].

Table 9. Absorbance ratios to assess RNA purity.

		A260/A280	A260/A230
Ring-iRBCs	Cells	2.24	1.90
	P1 untreated	1.50	0.39
	P1 treated	1.24	0.36
	P2 untreated	2.15	1.76
	P2 treated	1.78	0.86
Trophozoite-iRBCs	Cells	2.28	2.53
	P1 untreated	1.54	0.52
	P1 treated	1.44	0.41
	P2 untreated	2.12	1.74
	P2 treated	1.81	1.01
Schizont-iRBCs	Cells	2.20	1.91
	P1 untreated	1.86	0.91
	P1 treated	1.72	0.52
	P2 untreated	2.20	2.19
	P2 treated	1.80	0.75
Uninfected RBCs	Cells	1.90	0.33
	P1 untreated	1.45	0.45
	P1 treated	1.43	0.30
	P2 untreated	1.05	0.23
	P2 treated	1.30	0.31

A260/A280 is a measure of RNA purity and a ratio of  $\sim$ 2.0 is generally acceptable. A260/A230 is a measure for contamination and a range of 2.0-2.2 is generally acceptable.

Because of the very low RNA concentrations detected in the P1 EVs, these samples were not validated in the Bioanalyzer and excluded from RNA sequencing. Figure 37 shows the Bioanalyzer profiles for the iRBC P2 EVs. The size distribution of the RNA from ring-, trophozoite-, and schizont iRBCs P2 EVs was similar (up to ~200 nucleotides) but there was a lower amount in schizont iRBC EVs than in ring- and trophozoite iRBC EVs. There was no evidence of intact 18S or 28S ribosomal RNA.



**Figure 37. RNA profiles of pre-treated iRBC P2 EVs** iRBC EVs were pre-treated with proteinase K and RNase A prior to assessment on a Bioanalyzer. Electropherograms showing fluorescence intensity (FU) against size distribution in nucleotides (nt) on the left and RNA bands on the right.

# 4.3.2.1. Small RNA, microRNA Sequencing

After adapter trimming, the number of reads remaining was very low, ranging from 15.9% of the total number of reads for trophozoite iRBC EVs to 46.6% for schizont iRBC EVs (Table 10). The remaining reads were aligned to the microRNA human and *P. falciparum* genome, and as expected, the obtained signal was very low. The percentage of reads that aligned were 10.5%, 6.8%, 4.4% and 0.3% for ring-iRBC P2, trophozoite-iRBC P2, schizont-iRBC P2 and uRBC P2, respectively (Figure 38). Less than 1% of the libraries mapped to the human database. Majority of the reads aligned to coding regions. However, most reads mapped to multiple locations on the genome and were not considered in the STAR quantification because of the uncertainty of their origin. Thus, this data was not further analyzed.

Table 10. Mapping results for small RNA/microRNA sequencing

Library	Reads	Filtered	% (After trimming)	Mapped	% Mapped
R-iRBC P2	1,163,505	421,981	36.3	389,370	92.3
T-iRBC P2	1,209,239	191,880	15.9	186,901	97.4
S-iRBC P2	1,303,105	606,838	46.6	571,030	94.1
uRBC P2	1,237,848	286,952	23.2	284,825	99.3

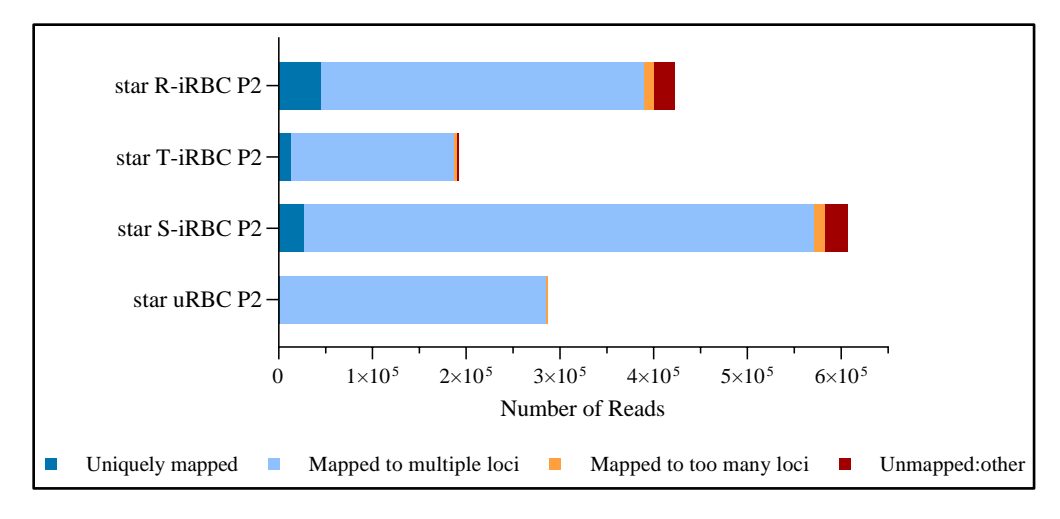


Figure 38. STAR alignment scores for small RNA sequencing R-rings, T-trophozoites, S- schizonts, u- uninfected. Recreated from MultiQC with GraphPad

## 4.3.2.2. RNA-Seq/ transcriptome

RNA sequencing yielded zero reads for uRBC P2 EVs, and this sample was not further analyzed. After adapter trimming of the RNA libraries prepared for each iRBC P2 EV sample, 100% of the reads remained for trophozite- and schizont iRBC EVs and 99.9% remained for ring iRBC EVs (Table 11). Similar with the small RNA libraries, the mapped reads aligned preferentially to the *P. falciparum* genome. The percentage of reads that were uniquely mapped are as follows: ring iRBC P2 - 60.5%, trophozoite-iRBC P2 - 83.9%, and schizont-iRBC P2 - 36.8% (Figure 39A). Most of the reads aligned to coding regions and over 96% of the reads were mRNA (Figure 39B).

Table 11. Mapping results for RNA sequencing

Library	Reads	Filtered	%	Mapped	% Mapped
			(After trimming)		
R-iRBC P2	31,287,956	31,263,185	99.9	26,799,565	85.7
T-iRBC P2	14,577,647	14,574,464	100	13,708,225	94.1
S-iRBC P2	25,253,966	25,246,724	100	19,378,529	76.8

### 4.3.2.3. Transcript analysis: Top 50 genes

For all the *H. sapiens* genes, there were no, or very low read counts recorded. The top 50 highest reads for *P. falciparum* were analyzed. Figure 40 shows a heat map of these genes and the normalized reads in each P2 EV subtype. Each gene appeared to have the lowest read counts in trophozoite iRBC P2 EVs compared to ring- and schizont iRBC EVs, however, statistical comparisons of enrichment were not made since a single biological replicate was analyzed. The similarity between ring- and schizont iRBC P2 EVs was in accordance with the sample clustering produced by DESeq (Figure 40B).

The most expressed genes for ring-, trophozoite- and schizont iRBC P2 EVs were merozoite surface protein 9 (MSP9; PF3D7\_1228600), conserved *Plasmodium* protein with unknown function (PF3D7\_1206300), and ring-infected erythrocyte surface antigen (RESA, PF3D7\_0102200), respectively. RESA, as well as 28S rRNA (PF3D7-1148640), also had a very high read count in ring-iRBC P2 EVs, while RESA3 (PF3D7\_1149200) was highly expressed in

schizont iRBC P2 EVs. Four of the top 50 genes coded for 4 of the most abundant proteins in the iRBC EVs (See Figure 28B). These were RESA, RESA3, MSP9, and MESA (mature parasite-infected erythrocyte surface antigen PF3D7\_0500800).

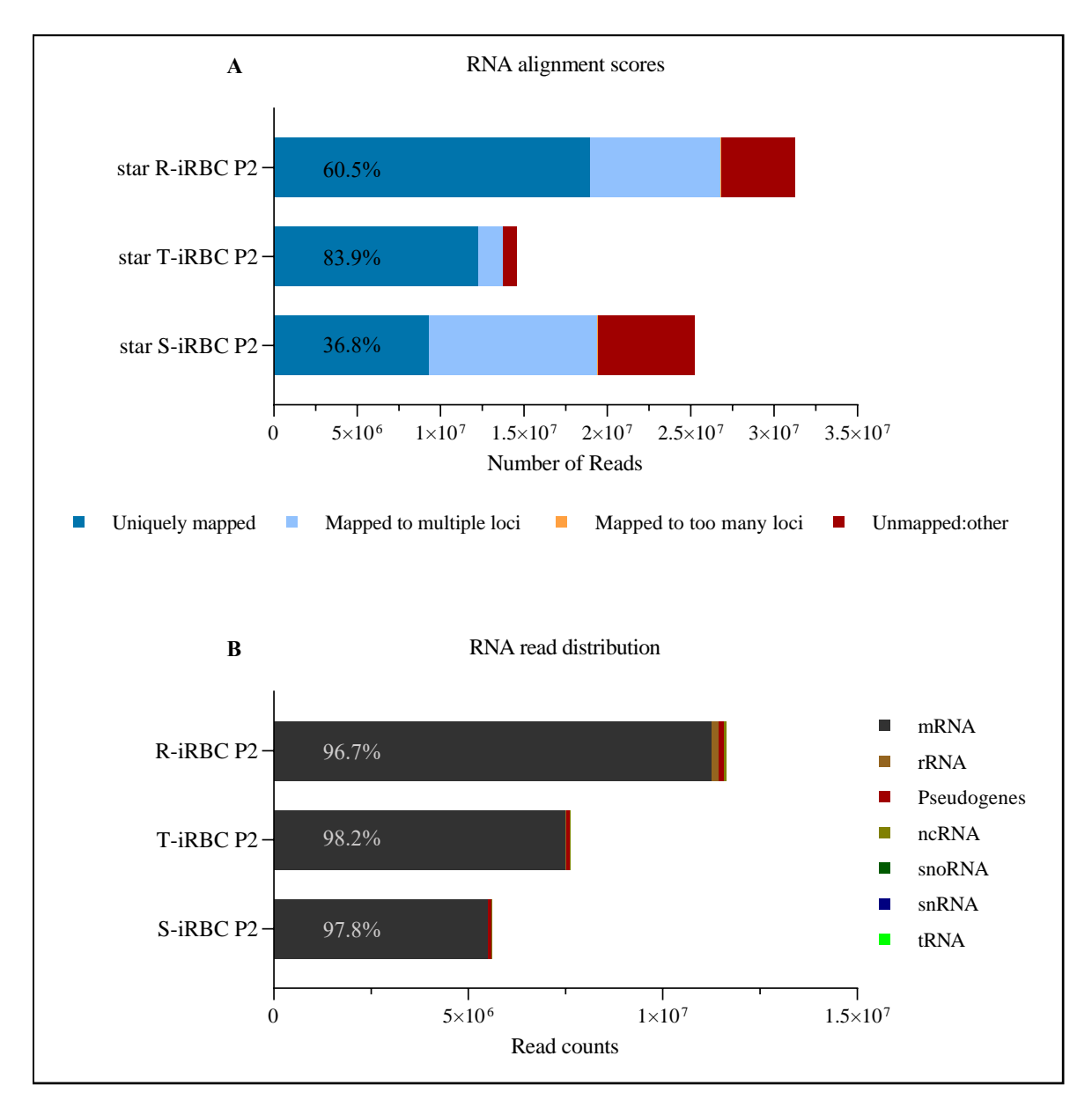
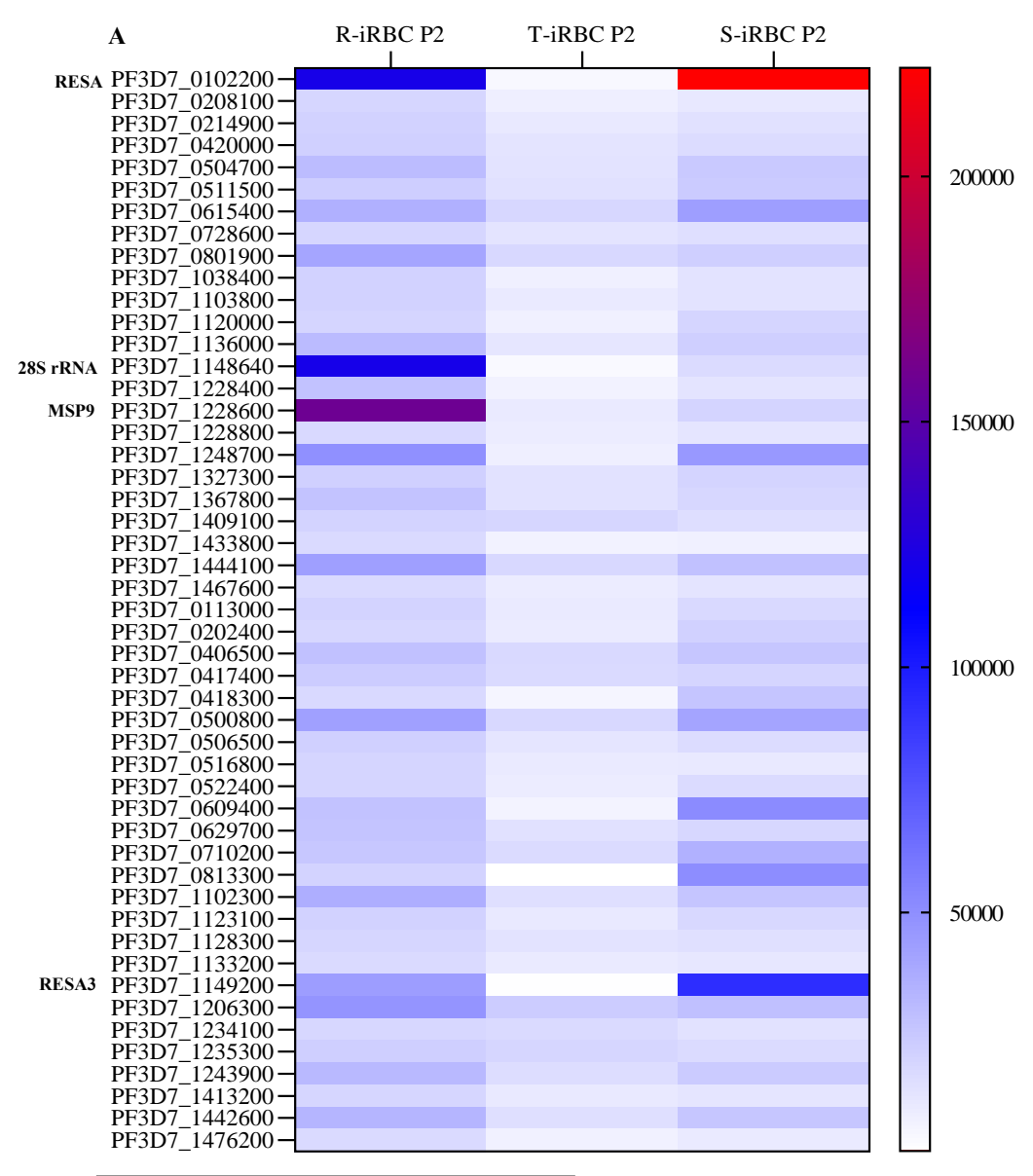


Figure 39. RNA sequencing analysis

(A) Normalized STAR RNA alignment scores: R-iRBCs 60.5%, T-iRBCs 83.9%, S-iRBCs 36.8% (B) RNA read distribution, using primary reads

R-rings, T-trophozoites, S- schizonts, u- uninfected. Recreated from MultiQC with GraphPad



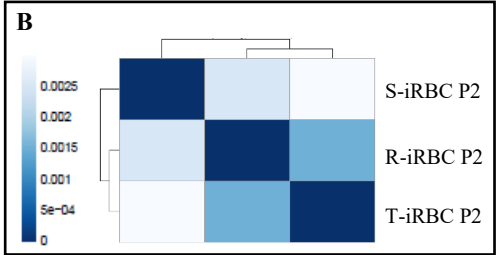


Figure 40. Transcript analysis
(A) Heatmap shows top 50 expressed genes out of 5739 *P. falciparum* in ring (R), trophozoite (T), and schizont (S) iRBC P2 EV RNA samples. The most expressed genes are indicated in bold (B) Sample clustering (Pearson correlation)

GO enrichment analysis retrieved several biological processes, including but not limited to sexual reproduction (GO:0019953), gamete generation (GO:0007276), modulation by symbiont of host immune response (GO:0052553), regulation of protein localization to membrane (GO:1905475), positive regulation of vesicle fusion (GO:0031340), and regulation of translation (GO:0006417) (Figure 41). Gamete generation and sexual reproduction are mediated by gametocyte-specific protein (Pf11-1; PF3D7\_1038400). Modulation by symbiont of host immune response is mediated by glutamic acid-rich protein (GARP; PF3D7\_0113000). Regulation of protein localization to membrane and positive regulation of vesicle fusion are both mediated by the putative C2 domain-containing protein (PF3D7\_0208100). Regulation of translation is mediated by translation-enhancing factor (PTEF; PF3D70202400) and the putative CCR4-NOT transcription complex subunit (NOT1-G; PF3D7\_1103800). These are all protein coding genes.

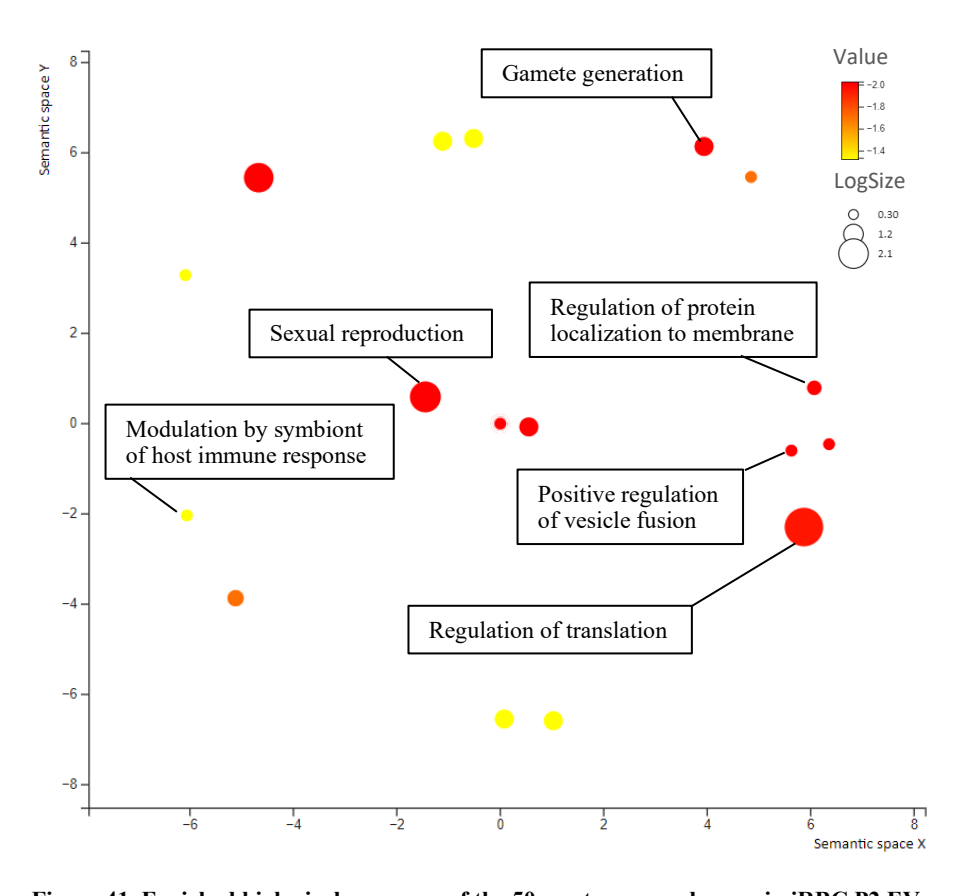


Figure 41. Enriched biological processes of the 50 most expressed genes in iRBC P2 EVs P value cutoff: 0.05

## 4.3.2.4. Transcript analysis: Specific gene searches

Genes encoding several proteins that were proposed as potential malaria EV markers (Table 7) or potentially useful in investigating malaria EV biogenesis (Table 8) were searched in the transcript analysis output to determine their read counts. These genes were grouped as those encoding virulence and invasion proteins, metabolic enzymes, rhoptry proteins 1 (read counts >400), rhoptry proteins 2 (read counts <400), chaperones, and other proteins. (Figure 42A-F). Several genes encoding proteins that were detected in all iRBC EVs (although more abundantly in P1 EVs) had very low read counts. Although comparisons were made across all 3 iRBC EVs, these were not based on statistical significance, since a single biological replicate was analyzed.

The virulence genes RH1, EBA181 and Pf332 had much higher expression in all EV populations compared to the other virulence and invasion genes (Figure 42A). The metabolic enzymes ENO, FBPA, PyrK, LDH, PGK and GAPDH had lower expression in all EVs (Figure 42B). There was a distinct difference in transcript levels of rhoptry neck proteins (Figure 42C) and rhoptry associated proteins (Figure 42D). The former (RON2, RON3, RON4, and RON5) were generally more expressed than the latter (RAP1, RAP2, and RAP3). The chaperones were also modestly expressed, except for HSP90 that had the highest expression, but this was limited to the ring- and schizont iRBC P2 EVs (Figure 42E). CHC had extremely low read counts (124, 96 and 78 in ring-, trophozoite-, and schizont iRBC P2 EVs respectively), while PTEX150 read counts were particularly high in ring- and schizont iRBC P2 EVs (Figure 42F).

EV biogenesis in *P. falciparum* remains poorly understood, but several homologous parasite ESCRT machinery proteins are known to be vital in the formation of MVBs, which are precursors of exosomes, while the involvement of others has been strongly inferred [186, 265]. These include PfVPs32, PfVps2, PfVps60, PfVPs4, PfVps46 and PfBro1. The genes encoding these proteins had similar levels of expression across the iRBC EVs except for PfVps32, and PfVps4 (Figure 43). PfVps32 was expressed the most in trophozoite iRBC P2 EVs, while PfVps4 was expressed the least in this EV subtype compared to ring- and schizont iRBC P2 EVs.

Another protein that was searched, which has also been suggested to play a role in malaria EV biogenesis, is PfPTP2 (*P. falciparum* PfEMP1 trafficking protein 2). The PfPTP2 gene had the highest expression in ring iRBC P2 EVs at 2221 read counts. This was followed by schizont iRBC P2 EVs at 1257 read counts, and trophozoite iRBC P2 EVs at 752 read counts. Another EMP1

trafficking protein, PfPTP5, was also expressed in iRBC EVs with high read counts ranging from 342 in trophozoite iRBC EVs to 2021 in schizont iRBC EVs.

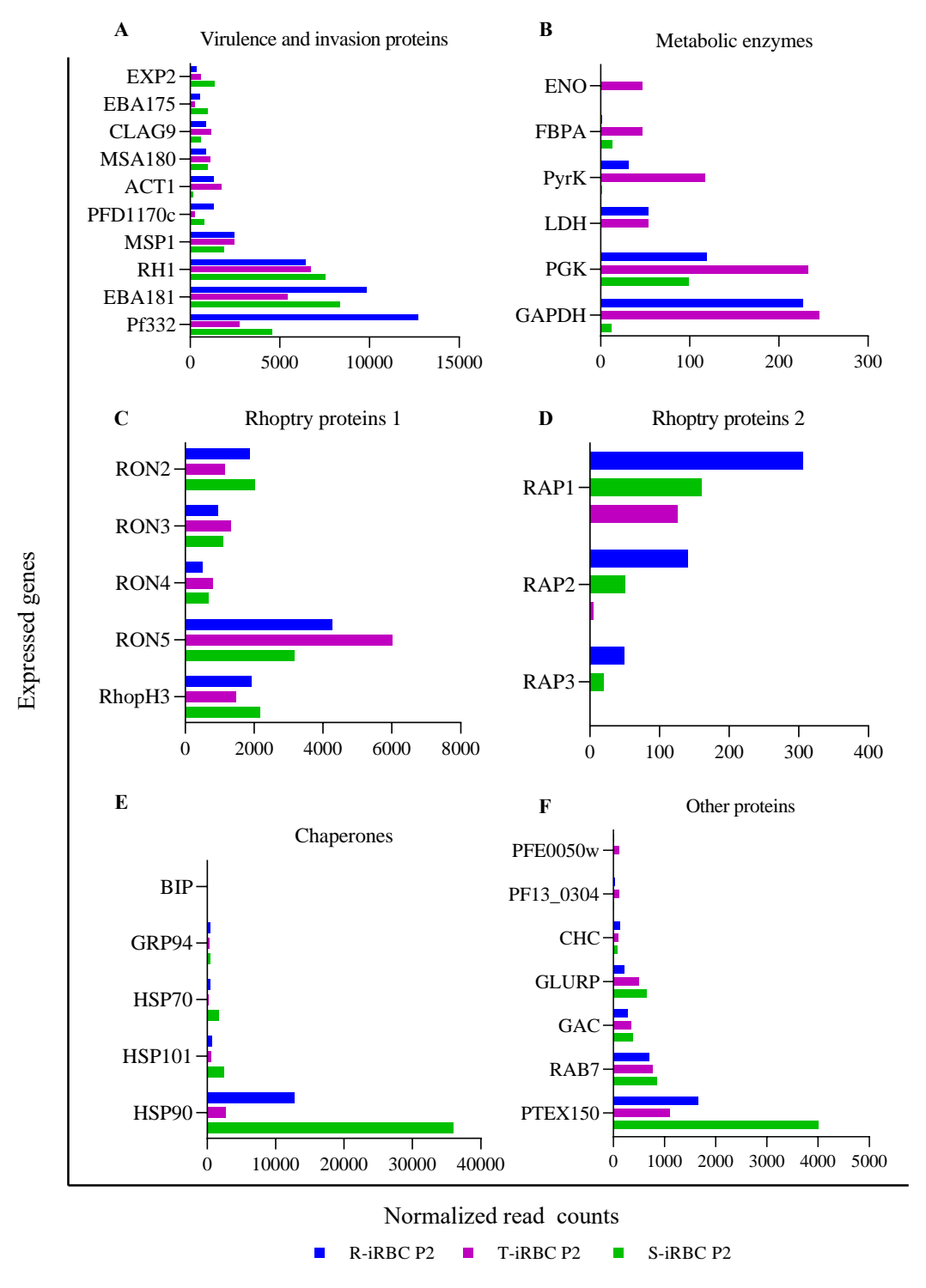


Figure 42. Normalized read counts of selected genes encoding potential malaria EV markers R-rings, T-trophozoites, S- schizonts

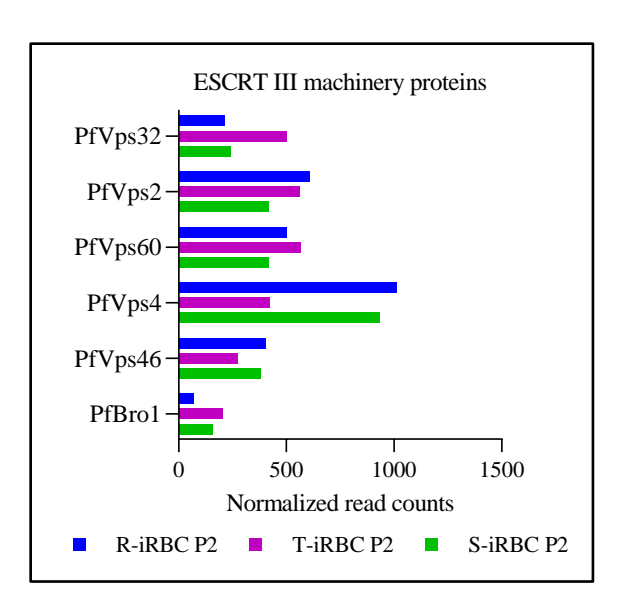


Figure 43. Normalized read counts for genes encoding parasite ESCRT III machinery proteins

**Chapter 5: Discussion** 

#### 5.1. Important considerations for malaria EV isolation

Compared to EV-containing body fluids, such as plasma, milk and cerebrospinal fluid, CM is considered a relatively simple sample from which to isolate EVs [1, 149]. With the addition of RBCs, *P. falciparum* cultures comprise 2 eukaryotic cells in a system that may contain remnant components of the most complex body fluid, blood (e.g., other cells and proteins), thereby creating a composite culture matrix. Furthermore, uninfected host RBCs, infected host RBCs, and intraerythrocytic parasites all release EVs into the CM that can neither be separated nor distinguished. While this research set out to develop a reproducible differential centrifugation protocol to isolate malaria EVs by optimizing several parameters associated with this EV isolation technique, awareness of the complex culture matrix made it pertinent to investigate and optimize parameters that are unique to malaria EV studies. These are: parasitemia, hematrocrit, age of RBCs used in culture, and the preparation of RBCs prior to use.

Although most published malaria EV studies have reported isolating EVs from cultures of low parasitemia and small volumes of CM, this could not be achieved here. Large CM volumes of 100-400 mL from healthy cultures of ≥10% parasitemia were essential to yield sufficient malaria EVs for downstream analyses. High parasitemia is achievable by reducing the hematocrit to below 2%. By lowering the hematocrit to simultaneously increase parasitemia, culture systems had fewer uRBCs releasing EVs and more Pf-iRBCs releasing the EV population of interest to this study. To further minimize the release of EVs from uRBCs and increase the quality and quantity of malaria EVs isolated, the RBC processing method and storage duration were found to be crucial because (1) non-leukoreduced RBCs resulted in the release of tetraspanin-positive uRBC EVs and malaria EVs, which is a false profile, as neither P. falciparum [251] nor mature RBCs [266] express tetraspanins, and (2) immunoblots of 14-day and 28-day old RBCs revealed a greater RBC EV marker expression in the latter, which provided evidence for increased vesiculation from 14 days of blood storage from the time of collection in accordance with the literature [240, 249, 267].

Careful consideration of these parameters afforded the reliable analysis of malaria EVs and interpretation of results, leading to the proposition that these be reportable parameters in malaria EV studies to promote inter-study comparison. These are summarized in Table 12. While all the parameters are vital, it is particularly important that studies report on whether leukoreduced or non-leukoreduced RBCs are used. This is not the current practice and is likely due to the lack of

awareness that residual leukocytes (and platelets) in non-leukoreduced RBC concentrates may release EVs and directly or indirectly induce vesiculation in stored RBCs [253, 268], thereby altering the proteome of *Pf*-iRBC EVs. The proteome can also be altered if RBCs older than 14 days are used due to increased vesiculation that accompanies aging. Furthermore, to achieve the required high parasitemia cultures for EV isolation, it is pertinent to grow the parasite in fresh RBCs as, after 2 weeks of storage, RBCs become increasingly resistant to merozoite invasion, thereby diminishing parasitemia [219].

Table 12. Reportable parameters in malaria EV studies

Parameter		Details	
RBCs for parasite	Blood group	A, B, AB, O	
culture	Processing method	Leukoreduced or non-leukoreduced	
	Storage duration from time of collection	1 to 14 days post collection	
<b>Culture conditions</b>	Nutrient source	AlbuMAX I, AlbuMAX II, or serum	
	Culture medium	Brand, supplements	
	Positioning	Stationary or shaking	
	Hematocrit	$\leq$ 2% or up to 4%	
	Parasitemia	Low or high, less than, or greater than 10%	
CM harvest	Intervals of harvest	E.g., 12- or 24-hours post invasion	
	Parasite life stage	Ring-, trophozoite-, schizont CM or mixed stages	
	Volume	Exact volume stated	
CM storage	Temperature	4°C, -80°C	
	Duration	Number of days, weeks, or months	
EV isolation	Concentration step	Vivacell units or other means used to concentrate CM	
	Rotor	Type of rotor & centrifuge	
	Centrifugation speeds	RPM, RCF, k factor	

Other relevant parameters that may influence parasite growth and, consequently, the nature and yield of malaria EVs include the blood group of donor RBCs (A, B, AB, or O), brand of growth medium, and growth supplement type (Albumax I, Albumax II, or serum). These were not investigated and can be looked at in future work.

The importance of the culture parameters in successfully isolating malaria EVs in this study cannot be overemphasized, however, this was not independent of optimizing the DC parameters that involved identifying a working combination of rotor types, filtration steps, concentration steps,

centrifugation speeds and centrifugation time. The findings of EV proteomics and transcriptomics validate the reproducibility and reliability of the malaria EV isolation protocol developed here. The EV populations and their subtypes analyzed in this study consistently had distinct characteristics across several biological replicates, indicating that the EV isolation protocol successfully separates 2 malaria EV subtypes: P1 EVs that are more enriched in proteins and P2 EVs that are more enriched in RNA. The identification of a protein-rich malaria EV subtype isolated at high-speed centrifugation validates the recommendation by the broader mammalian EV research community to not focus solely on EVs recovered from the final ultracentrifugation spin. This may be particularly important for malaria EVs.

In comparison with other published proteomics data that focused on EVs isolated by ultracentrifugation, EVs isolated in this study at high-speed centrifugation (and ultracentrifugation) and from high-parasitemia cultures not only had more parasite proteins than human proteins, but hundreds more parasite proteins, with over 95% probability of identity, than detected in other studies. This is despite not including a density gradient for purification. The importance of EVs isolated by ultracentrifugation is not disputed, as P2 EVs shared many proteins with P1 EVs but more importantly, were abundant in RNAs that may serve key functions in recipient cells.

It is important to note that the comparator studies included in the data analysis of this study purified malaria EVs by DGC, which may have minimized co-isolating impurities but also significantly diminished EV yield as evidence by the very low abundance of EV proteins. This was an issue in this study as well. While DGC is an excellent technique to purify EVs, it may not be the best option for malaria EVs that are not as abundant as EVs released from cancer cells and other mammalian cells. One solution may be to combine DC with specially designed SEC columns for EVs to remove co-isolating contaminants, such as those recently manufactured by IZON (www.izon.com). In addition, with the identification of specific malaria EV subtypes isolated by DC (that does not discriminate EV types), emerging techniques with shorter turnaround time and that accommodate large volumes of CM can be evaluated for their efficiency to isolate desired malaria EV subtypes. One such technique is a combination of Tangential Flow Filtration and SEC [269].

The EV isolation protocol developed in this study will be shared with the malaria EV community to further validate its reproducibility and encourage transparent reporting of EV isolation methodologies. This will mark a huge stride towards standardizing malaria EV research and promoting inter-study comparisons.

### 5.2. P. falciparum alters the nature of RBC-derived EVs

To gain insights into the effect of *P. falciparum* infection on the release and nature of EVs from the host RBCs, fresh uRBCs, stored for a maximum of 14 days were used as a control. Unlike other malaria EV studies that have compared EVs from *P. falciparum* iRBCs with those from calcium ionophore-treated uRBCs [190], uRBCs were not treated and kept under the same culture conditions as iRBCs. The core nature of EV subtypes from the young RBCs isolated at high-speed centrifugation and ultracentrifugation was found to closely resemble that of published data [270]. The mean diameter of P1 and P2 EVs was 140nm and 94nm respectively; major membrane proteins, cytoskeletal proteins, metabolic enzymes, and the lipid raft protein, stomatin were more abundant in P1 uRBC EVs compared to P2; both EV subtypes had much lower levels of flotillin 1 and flotillin 2 compared to stomatin, and lastly, both EV subtypes contained hemoglobin.

Comparing iRBC- and uRBC EVs, the differences in particle sizes and concentrations of the P1 or P2 subtypes were not statistically significant. However, fundamental differences between the protein composition of iRBC EVs (particularly from ring and schizont iRBCs) and uRBC EVs were noted. iRBC EVs were significantly more enriched in RBC membrane proteins (notably band 3, ankyrin 1 and protein 4.2), cytoskeletal proteins (spectrin A, spectrin B) and lipid raft proteins (stomatin, flotillin 1 and flotillin 2). The significantly greater abundance of membrane and membrane-associated proteins in *Pf*-iRBC-EVs suggests that *Pf*-iRBCs release biochemically distinct EVs that may determine their membrane mechanics and ultimately, promote uptake by target cells.

Nanomechanical studies have shown that the higher the protein content of EVs, the 'softer' they are [271] and may, therefore, be more readily taken up by recipient cells. Spectrin was especially more abundant in iRBC EVs than uRBC EVs. Spectrin and other cytoskeletal proteins have been detected in very low amounts in RBC EVs [97, 270] and these low levels are believed to be the result of dissociation of spectrin from band 3-ankyrin complexes, leading to buckling of the membrane bilayer, membrane budding and release of vesicles that are generally larger than

100nm in diameter [272, 273]. An alternative EV biogenesis pathway occurs when membrane proteins and associated cytoskeleton and raft proteins aggregate to form protein-rich membrane domains that eventually bud off as smaller EVs ~100nm [273]. The proteomic and NTA data of iRBC EVs suggests that this latter pathway may be what occurs in *Pf*-iRBCs.

A different EV biogenetic pathway in iRBCs is further supported by (1) the enrichment of several proteins involved in EV biogenesis in mammalian cells, such as annexin 7, (ANXA7), basigin (BSG), and clathrin (CLTC), in one or more iRBC EV subtypes but not in uRBC EVs; (2) the enrichment of host GAPDH and LDH in uRBC EVs compared to iRBC EVs and (3) the complete absence of host ENO from all iRBC EVs, but presence in uRBC EVs. Several metabolic enzymes are known to be enriched in EVs from fresh RBCs, as they bind tightly to band 3 complexes at the RBC membrane [270, 274, 275]. Evidently, host GAPDH, LDH and particularly ENO are selectively loaded into *P. falciparum* iRBC EVs.

Band 3 complexes also bind denatured hemoglobin, which is removed from RBCs in EVs physiologically and during storage [276, 277]. This vital function of RBC EVs was evident by the presence of band 3 and hemoglobin complexes in uRBC EVs. The absence of hemoglobin complexes and several other GO functions from iRBC EVs that were present in uRBC EVs suggests that the overall functions of these EV populations are inherently different. Furthermore, the transferrin receptor (TFRC), which is removed from immature RBCs (i.e., reticulocytes) in EVs during their maturation to RBCs, was detected only in uRBC EVs. The RBCs used in this study were mature, and detection of TFRC implies there may have been a few reticulocytes in the blood units. While *P. falciparum* can infect reticulocytes, the complete absence of this protein from all iRBC EV populations further suggests that *P. falciparum* infection alters the nature of EVs from RBCs, and the released iRBCs have different functions.

# 5.3. P. falciparum-iRBCs release multiple EV subtypes

In this study, the term 'EV subtype' refers to EVs pelleted at different centrifugation speeds but released from the same parent cells. The DC protocol developed here preserved and analyzed the pellets obtained from the penultimate high-speed centrifugation and final ultracentrifugation of CM from stage-specific *Pf*-iRBC cultures. TEM, NTA, FC, and WBA of both pellets found them to each contain EVs, designated as subtypes P1 and P2, respectively.

High-speed centrifugation (also referred to as intermediate speed) typically recovers denser medium sized EVs and/or aggregates of small EVs, while ultracentrifugation recovers small EVs [149]. However, both P1 and P2 were found to be primarily small sized with an average diameter of less than 200 nm but with different biochemical properties. P1 EVs of ring-, trophozoite-, and schizont-iRBCs were significantly and consistently more enriched for specific proteins analyzed by FC, WBA, and MS than their corresponding P2 EVs. This suggests that *P. falciparum*-iRBCs release small EVs that are biochemically distinct and can be successfully separated by DC based on their density, which is a measure of their cargo.

Although P1 EVs were found to contain more target proteins than P2, NTA revealed that P2 EVs had significantly greater particle concentration than P1. Furthermore, P2 had a greater total protein concentration than P1, as determined by BCA. This inverse relationship between particle concentration as well as total protein concentration and target protein enrichment suggests that P1 EVs, while fewer in particle number, load more protein cargo than P2 EVs and are therefore, denser and pellet earlier. Also, the higher total protein and particle concentrations of P2 was likely due to higher amounts of co-isolating non-EV proteins in P2 than P1. This was validated by MS, which showed that several Bos taurus contaminants were significantly more abundant in P2 compared to P1 (Appendix Figure 8). Ultracentrifugation is known to co-isolate EVs with non-EV material, such as contaminating proteins from growth media in CM. These contaminants obscure proteins of interest. Malaria EVs isolated by ultracentrifugation have been reported to have high abundance of contaminant proteins and low abundance of proteins of interest [193]. Impurities in P2 EVs, however, did not obscure their RNA cargo, which was revealed to comprise several messenger RNAs that can be investigated for their potential functions in recipient cells. Whether P1 EVs also contain important RNA will be determined by future experiments, although it is questionable, considering the very low amounts of RNA detected in these EV subtypes.

Indeed, P2 EVs were not significantly enriched in many host or parasite proteins compared to P1, and no biological processes, cellular components, or molecular functions were significant, other than annotation of a few human proteins to the extracellular exosome in ring-iRBC P2 EVs. Nevertheless, the majority of host and parasite proteins were similarly abundant in both EV subtypes for the ring-, trophozoite-, and schizont-iRBCs. The analysis of these shared proteins identified significant GO annotations, giving credence to the P2 preparations as important EV

subtypes. However, reliable, and successful downstream analyses of P2 EVs will only be achievable following purification to reduce the amount of co-isolated impurities. This is essential to compare their protein and RNA cargo to draw conclusions on the specific nature of these EV subtypes.

### 5.4. Specific markers can be defined for malaria EV subtypes

#### 5.4.1. Human proteins

To properly characterize EVs released from RBCs infected with the different intraerythrocytic life stages of *P. falciparum* and their respective subtypes, an in-depth analysis and comparison of the proteome of stage-specific iRBC EV subtypes was performed. A carefully selected panel of RBC membrane and membrane-associated proteins were analyzed by Western blotting to determine how their expression differs across the ring-, trophozoite-, and schizont iRBC EVs. These proteins included known EV markers specific to RBCs (band 3 and GYPA) and common to several cell types (spectrin, stomatin, flotillin 1, and flotillin 2).

Band 3 is the most abundant integral membrane protein of human RBCs. It is a multipass glycoprotein that is detected as a 90 to 100-kDa band. The high abundance of band 3 in iRBC P1 EVs (particularly ring- and schizont-iRBCs) and very low to no detection in P2 EVs suggests that it is a suitable marker for P1 subtypes of malaria EVs but not P2. Oxidative aggregation and degradation of band 3 begins in freshly collected RBCs and soon after storage [185, 270]. Band 3 aggregation is also induced by *P. falciparum* infection of RBCs [278]. Fragmentation of a 40-kDa peptide results from cleavage of band 3 on the cytoplasmic surface of RBCs, while cleavage of a 60-kDa peptide occurs on the extracellular surface [279, 280]. Aggregated band 3 was observed in RBC ghost membranes and iRBC P1 EVs. However, the differential expression of the 40-kDa peptide in P1 and 60-kDa peptide in P2 EVs (and RBC membranes) can be used to distinguish P1 EV subtypes and may be an indication of EVs with different biogenetic pathways.

Glycophorin A (GYPA, also known as CD235a) is also an integral membrane glycoprotein. Although GYPA was detected in very low amounts compared to band 3 and the other major RBC membrane proteins by MS, it was clearly detected in immunoblots of EVs at the expected molecular weight of 37-kDa, albeit in lower abundance in P2 than in P1 EVs. Therefore, GYPA may be a suitable marker for all subtypes of malaria EVs but should be analyzed in conjunction with at least 1 other marker when characterizing P2 malaria EVs. Like band 3, GYPA can be used

to distinguish the 2 malaria EV subtypes isolated by the DC protocol in this study. The expression of the 90 to 100-kDa homodimer in P1 EVs results from the highly specific dimerization of the GYPA transmembrane  $\alpha$ -helix [281, 282] and is apparently absent from all iRBC P2 EVs.

Spectrin accounts for 75% of the RBC cytoskeletal mass and is composed of 2 high molecular weight subunits: α spectrin (~240-kDa) and β spectrin (~220-kDa). Spectrin may be a marker for ring- and schizont iRBC P1 and P2 EVs considering the high abundance of the protein subunits detected in these subpopulations at approximately 250-kDa. Spectrin may also be used as a marker to distinguish the corresponding P1 and P2 EV subtypes, since the several bands observed around 130-kDa are specific to ring- and schizont iRBC P1 EVs. Spectrin is a substrate of the family of proteolytic enzymes, calpain [283], which are abundant in RBCs [284]. Unconstrained activation of calpains leads to the cleavage of spectrins into unique lower molecular weight breakdown products that have been used as disease biomarkers [285]. Also, calpain activity in RBCs is known to induce membrane blebbing [286] that is associated with EV formation. An intriguing observation of the MS data was that calpain-5 was enriched in ring- and schizont iRBC P1 EVs and was not detected in uRBC EVs (Appendix Figure 7). Calpain-5 is highly expressed in the brain [287] and was recently found to be localized to an RBC membrane microdomain that is important in susceptibility to malaria infection and disease [288]. Other proteins in this microdomain are ecto-ADP-ribosyltransferase 4 and aquaporin 1, both of which were identified only in ring- and schizont iRBC P1 EVs. It is, therefore, likely that the calpain-generated breakdown products of spectrin in malaria EVs not only serve to characterize these EVs but may potentially be useful as biomarkers of cerebral malaria.

Stomatin, flotillin 1, and flotillin 2 are highly abundant integral proteins of RBC membrane lipid rafts. Stomatin and flotillin 1 were detected in ring- and schizont iRBC EVs, serving as suitable markers. However, since the abundance of these proteins differed between biological replicates, they may not be efficient stand-alone markers and should be used in conjunction with flotillin 2, which was consistently detected in high abundance in these EV subpopulations. Furthermore, it was observed, from multiple biological replicates, that, unlike ring- and schizont iRBC EVs, the expression of band 3 and flotillin 2 in both trophozoite-iRBC EV subtypes is inconsistent. As such, in future characterizations of this EV subpopulation, it is important that GYPA be analyzed alongside band 3 and/or flotillin 2 in WBA.

The presence and enrichment of these selected proteins in the malaria EV subpopulations was validated by MS. Several known markers for EVs released by other cells, and therefore potential malaria EV markers, were detected by MS. Many of these markers were present in 2 or more EV subtypes (Figure 27) but were narrowed down to those that were significantly more abundant in one stage-specific iRBC EV subtype relative to its corresponding EV subtype (for example, ring iRBC P1 versus P2) (See Table 7). These include host and parasite proteins.

The overall MS data suggests that the host proteins GAPDH, PRDX2 (peroxiredoxin 2), annexins 5 and 7 (ANXA5 and ANXA7), HSPA8 (heat shock cognate 71-kDa protein), ACTG1 (actin) and CLTC (clathrin heavy chain 1) can be used to demonstrate the biochemical nature of malaria EVs. The markers present only in 1 EV subtype (e.g., KPNB1 and EEF1A1 in S-iRBC P1 and T-iRBC P2) or EV subpopulation (e.g., R-iRBC EVs) were in very low abundance and may, therefore, not be suitable subtype- or subpopulation-specific markers. Nevertheless, some of the high abundance markers may be used to further characterize EV subtypes of stage-specific iRBCs. For example, ATP1A1, BSG and GNAS may be suitable markers for ring iRBC P1 EVs; GAPDH may be suitable for characterizing trophozoite iRBC P1 EVs, while ACTG1 and VCP may be suitable markers of schizont iRBC P1 EVs. For P2 EVs, CLTC appears to be a very suitable marker for all stage-specific iRBC EVs, ANXA7 may be a good ring- and schizont iRBC EV marker, and LDHB a good marker for ring-iRBC EVs. In mammalian EV studies, clathrin (CLTC) and annexins have been established as markers of EVs isolated at ultracentrifugation speed [61, 289].

### **5.4.2.** Parasite proteins

Parasite proteins that are homologues of known mammalian cell EV markers were identified as potential malaria EV markers. PfCHC was very abundant in ring iRBC P2 EVs and is likely to be a good marker of this EV subtype. All other parasite proteins identified are more likely to be suitable markers of P1 subtypes: PfFBPA and PfPGK for all P1 EVs; PfENO and PfPyrK for ringand schizont iRBC EVs and PfLDH and PfRAB7 for schizont iRBC EVs. A study of EVs isolated from malaria positive plasma samples by high-speed centrifugation (at 19,000 x g) found high levels of PfENO, PfLDH and PfPGK [166]. Therefore, these proteins may serve as EV markers and disease biomarkers.

To validate the applicability of ATP1A1, BSG, GNAS, ACTG1, GAPDH, ANXA7, CLTC, VCP, LDHB, PfPyrK, PfGAPDH, PfENO, PfFBPA, PfPGK, and PfCHC in characterizing specific

malaria EV subtypes, it will be important to analyze these proteins by WBA, as was done for the RBC membrane and membrane-associated proteins. This is because proteins are often used to characterize EVs by WBA, and validated markers can then be applied in single EV analysis techniques such as immunoelectron microscopy, FC, and fluorescence NTA.

#### 5.4.3. Parasite RNA

The emphasis for detection markers in the general field of EV research has been on proteins. Whether RNA (and/or DNA) can also serve this purpose will only be determined with more research into the subcellular localization of different RNA species. For example, RNAs that are strictly associated with cytoplasmic complexes may be loaded into EVs and serve as general or subtype-specific EV markers [1]. Several parasite RNAs that encode virulence genes were found to be highly expressed in 1 or more iRBC P2 EVs. These included RESA, RESA3, MESA, Pf332, EBA181, and MSP9. The proteins encoded by many of these genes have been proposed in this study as being useful for investigating the biogenesis of malaria EVs. Considering the very high expression levels detected, it is worth investigating further the potential of these RNAs as stage-specific or subtype-specific EV markers. These genes could be used in conjunction with their translated proteins to further understand the biology and applications of malaria EVs.

As disease biomarkers, EV RNAs continue to gain popularity because, compared to other EV biomolecules, RNAs can be detected at very low levels using a wide range of methods [262]. The sheer amount of coding RNA present in the malaria EVs (over 5,700 messenger RNAs) suggests that selected RNA molecules may serve as biomarkers for malaria. Plasma levels of EVs have been found to be elevated in patients with cerebral malaria [162, 163], as well as in vulnerable age groups with uncomplicated malaria [161]. Identifying *P. falciparum* RNA transcripts in EVs from clinical malaria cases would validate the applicability of these EVs as predictive, diagnostic, or prognostic biomarkers of severe malaria [4].

This study has provided evidence of the presence of gene transcripts of proteins currently applied to rapid diagnostic tests for malaria such as PfMAHRP2 (which is specific for *P. falciparum*) and LDH (common to all *Plasmodium* species) [290]. 'Ultrasensitive' rapid diagnostic tests are a current focus of malaria control strategies to detect asymptomatic cases that drive transmission [290, 291]. Malaria EV-RNA may be explored for such diagnostic purposes.

The most suitable RNA candidates as EV detection markers or malaria biomarkers would be those that are either only expressed in malaria EVs or more abundant in malaria EVs relative to their parent cells. This cannot yet be determined as the RNA from malaria infected RBCs was not sequenced simultaneously with the *Pf*-iRBC-EVs.

#### 5.5. Correlating malaria EV composition and function

A goal of this study was to determine whether malaria EVs contain biomolecules that may be directly involved in any of the functions that have been suggested for them i.e., immunomodulation, gametocytogenesis and drug resistance.

Enolase, RESA, and SERA 5 are proteins involved in immune response in malaria that were found in *Pf*-iRBC-EVs. Although a glycolytic enzyme, enolase is known to induce a strong immune response in malaria and has been explored in vaccine studies [292]. Parasite and human enolase are highly species specific, and this was also observed in the MS data. There was no human enolase detected in malaria EVs. RESA and SERA 5 are involved in the regulation of immune responses in malaria [293, 294]. All 3 proteins are crucial for parasite survival and induce protective antibodies in malaria infected individuals. GARP was detected as one of the most expressed genes in all the iRBC P2 EVs. Like enolase, RESA, and SERA 5, GARP is involved in malaria immune responses [295].

Several proteins that may be important for gametocytogenesis were found in malaria EVs, including RESA [261]. The processes and biomolecules directly involved in gametocytogenesis in *Plasmodium* species are not clearly understood and investigating the gametocytogenesis-associated proteins in EVs may provide further insight into this process that is crucial for parasite propagation. These proteins were found mainly in ring- and schizont iRBC EVs. Future studies will involve strategic testing of the effect of EVs from these stage-specific cultures, as well as RESA on the differentiation of asexual stages to sexual stages. This would be necessary to validate or refute the suggested involvement of EVs in gametocytogenesis [189, 190]. Interestingly, biomolecules involved in gametogenesis were also found to be present in malaria EVs. These were the protein CDPK1 and gene transcript Pf11-1. It would be compelling to investigate whether *P. falciparum* releases EVs containing these biomolecules, particularly Pf11-1 to be picked up by mosquitos and facilitate gametogenesis in the mosquito.

Many proteins were identified that are involved in drug resistance. Noteworthy are Kelch13 and MDR1 (multidrug resistance protein 1) that were detected in different iRBC EV subtypes. The gene transcripts were also expressed in the sequenced EVs. Mutations in Kelch 13 have been associated with the resistance to artemisinin both *in vivo* and *in vitro* [296] Artemisinin and its derivatives are currently the most important antimalarial drugs to which drug resistance is being increasingly reported. Mutations in MDR1, on the other hand, are directly associated with resistance to several antimalarial drugs, including chloroquine, halofantrine and mefloquine [297].

Several virulence proteins and genes were found in abundance in the malaria EVs, such as Pf332, EBA181, EBA175, and CLAG9, which are involved in invasion, cell-cell adhesion and/or cytoadherence. *Pf*-iRBCs may release EVs containing virulence and invasion biomolecules targeted to RBCs to prime them for parasite invasion or targeted to immune cells as a decoy mechanism. In addition, resident virulence proteins may confer increased virulence properties on less virulent parasite strains in recipient iRBCs, thereby contributing to the cytoadherence-associated phenomena. Future studies need to be done to determine the contributions of specific virulence proteins in malaria EVs using techniques that have been employed in cancer research to investigate the protein/RNA-specific function of EVs in recipient cells [104].

26S protease regulatory subunits were found mainly in the schizont iRBC EVs. These subunits are part of the 26S proteasome that performs vital regulatory functions in cells and have been found in EVs from various cells, including RBCs [298]. EVs have gained popularity as delivery vehicles of a different type of regulatory molecule – microRNAs. In contrast to published findings (Table 3), a reliable mapping of human or *P. falciparum* microRNA could not be obtained for the RNA in the malaria EVs in this study. Human microRNA may not have been found due to modifications of the RBC by the parasite and a reasonable explanation for the absence of parasite microRNA would be the extremely low proportion of small RNAs in its genome, precisely 1.3% [299]. Future work will involve deciphering the regulatory functions of proteasome complexes in malaria EVs.

#### 5.6. Investigating EV biogenesis in *P. falciparum*

EVs released from RBCs infected with *P. falciparum* will likely comprise 3 populations of EVs: host EVs from uninfected RBCs, host EVs from infected RBCs (which may contain parasite proteins that have been secreted into the RBC cytoplasm or exported to the RBC membrane) and EVs released by the parasite (first into the RBC cytoplasm and then to the extracellular space). As

these populations cannot be separated, it was important to identify parasite proteins that are not secreted into the RBC (i.e., localized to the parasite). These proteins are believed to be crucial for investigating the biogenesis of EVs in *P. falciparum*. Also researched were RNA molecules that code for these and other proteins that may also be involved in EV biogenesis.

PfCHC is localized to the parasite, specifically the nucleus and clathrin-coated vesicles within the parasite. Parasite and human clathrin (CHC and CLTC, respectively) share several peptides resulting in ambiguous identification of the homologues in the species. As such, it is highly likely that PfCHC is more abundant in malaria EVs than determined by the MS analysis. In addition, CLTC was more enriched in P1 and P2 EVs than the RBC membrane of parent cells. Proteins involved in EV biogenesis are often more abundant in EVs than in their parent cells, which makes PfCHC a potential candidate for studies of malaria EV biogenesis. Clathrin is recruited to endosomal membranes and is required for the formation of clathrin-coated vesicles within which cargo is delivered to endosomes in the process of MVB formation, leading to exosome formation and release [300]. The localization of clathrin to endosomal membranes and formation of MVBs involves several ESCRT proteins and accessory proteins, including Vps4 (vacuolar protein sorting-associated protein 4) [301]. RNA coding the *P. falciparum* Vps4 homolog was detected in all 3 iRBC P2 EVs, and PfVps4 has been found to mediate the formation of MVBs in the parasite, although not in the context of EV biogenesis [265]. Be that as it may, studies of PfCHC and Vps4 will provide insights into the biogenesis of specific types of EVs in *P. falciparum*.

The data so far strongly supports recent findings that *P. falciparum* possesses an ESCRT-dependent EV biogenesis pathway [186]. Two homologous ESCRT-III proteins of *P. falciparum*, PfVps32 and PfVps60, as well as the Bro1-containing homologue, PfBro1, are suggested to be involved in the formation of malaria EVs and are expressed in all 3 asexual intraerythrocytic life stages of the parasite [186]. These proteins were not identified by MS in any iRBC EVs, however, RNA encoding all 3 proteins were detected in the P2 EVs from ring-, trophozoite-, and schizont iRBCs. It is important that further experiments be performed to determine the presence or absence of these RNA molecules in the corresponding P1 EVs. It is unclear why no parasite ESCRT proteins were identified in the malaria EVs by MS. Since several proteins that were found to be enriched in the malaria EVs were also predicted to be localized to the same subcellular locations and membranes as PfVps32, PfVps60, PfVps4 and PfBro1 [186], co-localization studies of these

enriched EV proteins and the ESCRT proteins, including immunoblotting experiments, may provide some clarity.

PfVps32 and PfBro1 are also present in RBC cytoplasm and may directly induce budding of microvesicles at the host cell membrane [186]. It has also been suggested that microvesicles bud directly from the RBC membrane following the involvement of specialized parasite-derived structures in infected RBCs, called Maurer's clefts [190]. Another proposed EV biogenesis pathway at the RBC membrane involves the budding of PfPTP2-coated vesicles off Maurer's clefts followed by membrane fusion and release of exosomes [189]. Any of these 3 suggested EV biogenesis pathways at the RBC membrane, as well as the EV biogenesis that begins in the parasite, would incorporate RBC membrane and membrane-associated proteins, probably in various modified forms. This may explain the distinct profiles observed for band 3, GYPA, spectrin and stomatin for all iRBC P1 and P2 EV subtypes and suggests that these RBC proteins can also serve in understanding malaria EV biogenesis, by investigating specific modifications present in different EVs. Parasite proteins that localize to the Maurer's clefts can also be researched for their potential involvement. The most enriched Maurer's cleft proteins in the malaria EVs were Pf332 (antigen 332, DBL-like protein), HSP101, MESA, PGK, *Plasmodium* exported protein (PF3D7 0501000), and RESA3.

Like the Vps proteins, PfPTP2 protein was not detected by MS, but RNA encoding the protein was detected in abundance. It is uncertain why these proteins were not detected in the current study but may be attributed to the different culture conditions and EV isolation techniques used in the different studies. PfPTP5 is also localized to the Maurer's clefts and no biological functions have been assigned to this protein. PfPTP5 was detected by MS in all iRBC EVs except trophozoite-iRBC P1 EVs and the gene was expressed in all iRBC P2 EVs. No studies are known to have investigated the involvement of PfPTP5 in malaria EV biogenesis, which may provide new insights or support current findings.

An important aspect of EV biogenesis is cargo loading, which is believed to be a very specific process. The data from this study is in accordance with this theory. More proteins were detected in P1 EVs and RNA in P2 EVs. There also appeared to be a trend that was observed for certain groups of proteins. Rhoptry associated proteins (RAP) were generally expressed lower than rhoptry neck proteins (RON) in all iRBC P2 EVs. Chaperones also had an overall low transcript abundance,

except for HSP90. Furthermore, while it is difficult to directly compare the abundance of a gene transcript and its translated protein in an EV, genes of certain proteins that were in abundance in P2 EVs were absent in those EVs. For example, enolase, which was detected by MS in ring- and schizont iRBC P1 and P2 EVs, had no read counts for either of these EV subpopulations. Assessing the downstream function of RNAs or proteins was outside the scope of this study. However, future studies can simultaneously investigate the function of a malaria EV protein against its corresponding gene transcript in recipient cells.

**Chapter 6: Conclusion and summary** 

This thesis set out to achieve 3 objectives that were to develop an optimized and reproducible DC protocol for the isolation of malaria EVs, as well as to compare and characterize the protein and RNA cargo of EVs isolated from *in vitro* cultures of RBCs infected with the ring, trophozoite and schizont stages of *P. falciparum*, using this optimized protocol.

In the development of the malaria EV isolation protocol, different combinations of modifications to the parameters of DC were attempted while simultaneously optimizing parameters that are specific to *P. falciparum* cultures. The DC parameters were centrifugal force, centrifugation time, rotor type, K-factor, and sample volume. The *P. falciparum* culture parameters were parasitemia, hematocrit, age of RBCs used to grow the parasites and the method of preparation of these RBCs. Parasitemia and hematocrit were optimized to increase the proportion of *P. falciparum* infected RBCs in the culture releasing the EVs of interest to this study. To minimize the confounding effect of non-RBCs, non-RBC EVs and RBC-derived EVs on the analysis of malaria-derived EVs and interpretation of results, RBCs used in the parasite culture were leukoreduced and not older than 14 days of storage. The final protocol was validated by performing a preliminary protein analysis of selected RBC EV markers.

Altogether, these parameters were crucial for the successful and reproducible isolation of malaria EVs. With malaria EV isolation protocols by DC not being standardized, and the lack of awareness of the importance of RBC age and preparation, this study provides an optimized and easy to follow protocol that can be used to promote standardized research. Furthermore, the observations of this study point out the need for transparent reporting on several *P. falciparum* culture parameters.

Using the developed protocol, two malaria EV subtypes, designated P1 and P2, were isolated from cultures of RBCs infected with each intraerythrocytic asexual life stage. Parasites in culture were tightly synchronized, and EV-containing conditioned media was harvested from the cultures at 22-, 38-, and 46-hours post infection for *P. falciparum* ring, trophozoite, and schizont infected RBCs, respectively. Parasite stage-specific iRBC EVs were characterized using a combination of NTA, TEM and FC for single EV analysis. To compare and characterize their protein cargo, WBA and LC-MS were performed. To compare and characterize their RNA cargo, EVs were pre-treated with RNAse A, and the EV RNA was extracted, quantified by Nanodrop, validated on a Bioanalyzer, and sequenced on a Nextseq500. The P1 and P2 EVs isolated in this study were found

to be small EVs that represent biochemically distinct subtypes – P1 EVs contain more proteins and P2 EVs more RNA. The protein and RNA profiles differed across ring-, trophozoite-, and schizont infected RBC EVs.

Select host and parasite proteins were identified as suitable markers to characterize malaria-derived EV subpopulations and subtypes. Several parasite proteins that are localized to the parasite in the infected RBC were identified. Also identified were parasite proteins that are important for immunomodulation, gametocytogenesis, gametogenesis, drug resistance, virulence, and cellular regulation. These proteins can be further investigated to understand the biogenesis and biology of EVs in *P. falciparum*, as well as their downstream functions and potential biomedical applications.

Malaria derived EVs did not contain substantial amounts of microRNA but were abundant in messenger RNAs. However, this does not preclude their presence in the malaria EVs but could be due to technical issues in the library preparation, which is subject to validation. Like the proteomics analysis, several virulence and invasion genes, metabolic enzymes, and chaperones were found to have different levels of expression across the stage-specific iRBC EVs. Also expressed in malaria EVs were parasite homologues of the ESCRT III machinery important for EV biogenesis. Further investigations of these genes are important to understanding malaria EVs and specific cargo loading in these EVs.

This study provides a reproducible protocol for isolating 2 malaria EV subtypes; the study also provides an extensive protein and RNA profile for malaria EVs from which select biomolecules can be studied to determine their functions in recipient cells and their overall importance to the biology of the parasite and pathogenesis of the disease.

#### References

- 1. Théry, C., et al., Minimal information for studies of extracellular vesicles 2018 (MISEV2018): a position statement of the International Society for Extracellular Vesicles and update of the MISEV2014 guidelines. Journal of Extracellular Vesicles, 2018. 7(1): p. 1535750.
- 2. Lötvall, J., et al., Minimal experimental requirements for definition of extracellular vesicles and their functions: a position statement from the International Society for Extracellular Vesicles. Journal of Extracellular Vesicles, 2014. 3: p. 26913.
- 3. Couch, Y., et al., *A brief history of nearly EV-erything The rise and rise of extracellular vesicles*. Journal of Extracellular Vesicles, 2021. **10**(14).
- 4. Opadokun, T. and P. Rohrbach, *Extracellular vesicles in malaria: an agglomeration of two decades of research.* Malaria Journal, 2021. **20**(1): p. 442.
- 5. Bannister, L.H., et al., A Brief Illustrated Guide to the Ultrastructure of Plasmodium falciparum Asexual Blood Stages. Parasitology Today, 2000. **16**(10): p. 427-433.
- 6. Pease, B.N., et al., Global Analysis of Protein Expression and Phosphorylation of Three Stages of Plasmodium falciparum Intraerythrocytic Development. Journal of Proteome Research, 2013. 12(9): p. 4028-4045.
- 7. Gardiner, C., et al., *Techniques used for the isolation and characterization of extracellular vesicles: results of a worldwide survey.* Journal of Extracellular Vesicles, 2016. **5**(1): p. 32945.
- 8. Royo, F., et al., Methods for Separation and Characterization of Extracellular Vesicles: Results of a Worldwide Survey Performed by the ISEV Rigor and Standardization Subcommittee. Cells, 2020. **9**(9): p. 1955.
- 9. Andreu, Z., et al., *Comparative analysis of EV isolation procedures for miRNAs detection in serum samples.* Journal of Extracellular Vesicles, 2016. **5**: p. 31655.
- 10. Brennan, K., et al., A comparison of methods for the isolation and separation of extracellular vesicles from protein and lipid particles in human serum. Scientific Reports, 2020. **10**(1): p. 1039.
- 11. Tauro, B.J., et al., Comparison of ultracentrifugation, density gradient separation, and immunoaffinity capture methods for isolating human colon cancer cell line LIM1863-derived exosomes. Methods, 2012. **56**(2): p. 293-304.
- 12. Nieuwland, R., et al., *Reproducibility of extracellular vesicle research*. European Journal of Cell Biology, 2022. **101**(3).
- 13. CDC. *Malaria's Impact Worldwide*. 2021 December 16, 2021 [cited 2023 May 25]; Available from: https://www.cdc.gov/malaria/malaria worldwide/impact.html.
- 14. WHO, World malaria report 2022, W.H. Organization, Editor. 2022: Geneva.
- 15. Bannister, L.H., et al., *Three-Dimensional Ultrastructure of the Ring Stage ofPlasmodium falciparum: Evidence for Export Pathways*. Microscopy and Microanalysis, 2004. **10**(5): p. 551-562.
- 16. Hanssen, E., K.N. Goldie, and L. Tilley, *Ultrastructure of the Asexual Blood Stages of Plasmodium falciparum*, in *Electron Microscopy of Model Systems*, T. MullerReichert, Editor. 2010. p. 93-116.
- 17. Wunderlich, J., P. Rohrbach, and J.P. Dalton, *The malaria digestive vacuole*. Frontiers in Bioscience-Scholar, 2012. **4**(4): p. 1424-1448.

- 18. Amit-Avraham, I., et al., *Antisense long noncoding RNAs regulate var gene activation in the malaria parasite Plasmodium falciparum*. Proceedings of the National Academy of Sciences, 2015. **112**(9): p. E982-E991.
- 19. Lee, W.-C., B. Russell, and L. Rénia, *Sticking for a Cause: The Falciparum Malaria Parasites Cytoadherence Paradigm.* Frontiers in Immunology, 2019. **10**.
- 20. Foley, M. and L. Tilley, *Home improvements: Malaria and the red blood cell.* Parasitology Today, 1995. **11**(11): p. 436-439.
- 21. Lew, V.L., T. Tiffert, and H. Ginsburg, Excess hemoglobin digestion and the osmotic stability of Plasmodium falciparum—infected red blood cells. Blood, 2003. **101**(10): p. 4189-4194.
- 22. Cowman, A.F., et al., *Malaria: Biology and Disease*. Cell, 2016. **167**(3): p. 610-624.
- 23. Rudlaff, R.M., et al., *Three-dimensional ultrastructure of Plasmodium falciparum throughout cytokinesis.* PLoS Pathogens, 2020. **16**(6): p. e1008587.
- 24. Oehring, S.C., et al., *Organellar proteomics reveals hundreds of novel nuclear proteins in the malaria parasite Plasmodium falciparum*. Genome Biology, 2012. **13**(11): p. R108.
- 25. Broadbent, K.M., et al., Strand-specific RNA sequencing in Plasmodium falciparum malaria identifies developmentally regulated long non-coding RNA and circular RNA. BMC Genomics, 2015. **16**(1).
- 26. Coban, C., M.S.J. Lee, and K.J. Ishii, *Tissue-specific immunopathology during malaria infection*. Nature Reviews Immunology, 2018. **18**(4): p. 266-278.
- 27. Deroost, K., et al., *The immunological balance between host and parasite in malaria.* FEMS Microbiology Reviews, 2016. **40**(2): p. 208-257.
- 28. Wassmer, S.C., et al., *Investigating the Pathogenesis of Severe Malaria: A Multidisciplinary and Cross-Geographical Approach.* The American Journal of Tropical Medicine and Hygiene, 2015. **93**(3 Suppl): p. 42-56.
- 29. WHO, Severe Malaria. Tropical Medicine & International Health, 2014. 19: p. 7-131.
- 30. Moxon, C.A., et al., *New Insights into Malaria Pathogenesis*. Annual Review of Pathology: Mechanisms of Disease, 2020. **15**(1): p. 315-343.
- 31. Walker, I.S. and S.J. Rogerson, *Pathogenicity and virulence of malaria: Sticky problems and tricky solutions.* Virulence, 2023. **14**(1): p. 34.
- 32. Udeinya, I.J., et al., An in Vitro Assay for Sequestration: Binding of Plasmodium falciparum Infected Erythrocytes to Formalin-Fixed Endothelial Cells and Amelanotic Melanoma Cells. The Journal of Protozoology, 1985. **32**(1): p. 88-90.
- 33. Cooke, B.M., et al., *Mechanisms of cytoadhesion of flowing, parasitized red blood cells from Gambian children with falciparum malaria*. Am J Trop Med Hyg, 1995. **53**(1): p. 29-35.
- 34. Carlson, J., et al., *Human cerebral malaria: association with erythrocyte rosetting and lack of anti-rosetting antibodies.* The Lancet, 1990. **336**(8729): p. 1457-1460.
- 35. Lee, W.-C., B. Russell, and L. Rénia, *Evolving perspectives on rosetting in malaria*. Trends in Parasitology, 2022. **38**(10): p. 882-889.
- 36. Handunnetti, S.M., et al., *Uninfected erythrocytes form "rosettes" around Plasmodium falciparum infected erythrocytes*. American Journal of Tropical Medicine and Hygiene, 1989. **40**(2): p. 115-8.
- 37. Roberts, D.J., et al., *Autoagglutination of malaria-infected red blood cells and malaria severity.* The Lancet, 2000. **355**(9213): p. 1427-1428.

- 38. Chotivanich, K., et al., *Platelet-Induced Autoagglutination of Plasmodium falciparum-Infected Red Blood Cells and Disease Severity in Thailand*. The Journal of Infectious Diseases, 2004. **189**(6): p. 1052-1055.
- 39. Biswas, A.K., et al., *Plasmodium falciparum Uses gC1qR/HABP1/p32 as a Receptor to Bind to Vascular Endothelium and for Platelet-Mediated Clumping.* PLoS Pathogens, 2007. **3**(9): p. e130.
- 40. Pain, A., et al., Platelet-mediated clumping of <i>Plasmodium falciparum</i> -infected erythrocytes is a common adhesive phenotype and is associated with severe malaria. Proceedings of the National Academy of Sciences, 2001. 98(4): p. 1805-1810.
- 41. Josefine Dunst, F.K.a.K.M., *Cytokines and Chemokines in Cerebral Malaria Pathogenesis*. Frontiers in Cellular and Infection Microbiology, 2017. 7: p. 324.
- 42. Acharya, P., et al., *Host-Parasite Interactions in Human Malaria: Clinical Implications of Basic Research.* Frontiers in Microbiology, 2017. **8**.
- 43. Wassmer, S.C. and G.E.R. Grau, *Severe malaria: what's new on the pathogenesis front?* International Journal for Parasitology, 2017. **47**(2-3): p. 145-152.
- 44. Babatunde, K.A., et al., *Role of Extracellular Vesicles in Cellular Cross Talk in Malaria*. Frontiers in Immunology, 2020. **11**.
- 45. Armingol, E., et al., *Deciphering cell–cell interactions and communication from gene expression*. Nature Reviews Genetics, 2021. **22**(2): p. 71-88.
- 46. Raposo, G. and W. Stoorvogel, *Extracellular vesicles: Exosomes, microvesicles, and friends*. The Journal of Cell Biology, 2013. **200**(4): p. 373-383.
- 47. Cocucci, E. and J. Meldolesi, *Ectosomes and exosomes: shedding the confusion between extracellular vesicles*. Trends in Cell Biology, 2015. **25**(6): p. 364-372.
- 48. Chargaff, E. and R. West, *The biological significance of the thromboplastic protein of blood.* Journal of Biological Chemistry, 1946. **166**(1): p. 189-97.
- 49. Wolf, P., *The Nature and Significance of Platelet Products in Human Plasma*. British Journal of Haematology, 1967. **13**(3): p. 269-288.
- 50. Crawford, N., The Presence of Contractile Proteins in Platelet Microparticles Isolated from Human and Animal Platelet-free Plasma. British Journal of Haematology, 1971. **21**(1): p. 53-69.
- 51. Hargett, L.A. and N.N. Bauer, *On the Origin of Microparticles: From "Platelet Dust" to Mediators of Intercellular Communication*. Pulmonary Circulation, 2013. **3**(2): p. 329-340.
- 52. Pan, B.-T. and R.M. Johnstone, *Fate of the transferrin receptor during maturation of sheep reticulocytes in vitro: Selective externalization of the receptor.* Cell, 1983. **33**(3): p. 967-978.
- 53. Harding, C., J. Heuser, and P. Stahl, *Receptor-mediated endocytosis of transferrin and recycling of the transferrin receptor in rat reticulocytes*. Journal of Cell Biology, 1983. **97**(2): p. 329-339.
- 54. Johnstone, R.M., et al., Vesicle formation during reticulocyte maturation. Association of plasma membrane activities with released vesicles (exosomes). Journal of Biological Chemistry, 1987. **262**(19): p. 9412-9420.
- 55. Raposo, G., et al., *B lymphocytes secrete antigen-presenting vesicles*. Journal of Experimental Medicine, 1996. **183**(3): p. 1161-1172.
- 56. Witwer, K.W. and C. Théry, Extracellular vesicles or exosomes? On primacy, precision, and popularity influencing a choice of nomenclature. Journal of Extracellular Vesicles, 2019. **8**(1): p. 1648167.

- 57. Van Niel, G., G. D'Angelo, and G. Raposo, *Shedding light on the cell biology of extracellular vesicles*. Nature Reviews Molecular Cell Biology, 2018. **19**(4): p. 213-228.
- 58. Xie, S., Q. Zhang, and L. Jiang, *Current Knowledge on Exosome Biogenesis, Cargo-Sorting Mechanism and Therapeutic Implications*. Membranes, 2022. **12**(5): p. 498.
- 59. Colombo, M., G. Raposo, and C. Théry, *Biogenesis, Secretion, and Intercellular Interactions of Exosomes and Other Extracellular Vesicles*. Annual Review of Cell and Developmental Biology, 2014. **30**(1): p. 255-289.
- 60. Gould, S.J. and G. Raposo, *As we wait: coping with an imperfect nomenclature for extracellular vesicles*. Journal of Extracellular Vesicles, 2013. **2**(1): p. 20389.
- 61. Kowal, J., et al., *Proteomic comparison defines novel markers to characterize heterogeneous populations of extracellular vesicle subtypes.* Proceedings of the National Academy of Sciences, 2016. **113**(8): p. E968-E977.
- 62. Tkach, M., et al., *Qualitative differences in T-cell activation by dendritic cell-derived extracellular vesicle subtypes.* The EMBO Journal, 2017. **36**(20): p. 3012-3028.
- 63. Tkach, M., J. Kowal, and C. Théry, Why the need and how to approach the functional diversity of extracellular vesicles. Philosophical Transactions of the Royal Society B: Biological Sciences, 2018. **373**(1737): p. 20160479.
- 64. Huotari, J. and A. Helenius, *Endosome maturation*. The EMBO Journal, 2011. **30**(17): p. 3481-3500.
- 65. Hessvik, N.P. and A. Llorente, *Current knowledge on exosome biogenesis and release*. Cellular and Molecular Life Sciences, 2018. **75**(2): p. 193-208.
- 66. Colombo, M., et al., Analysis of ESCRT functions in exosome biogenesis, composition and secretion highlights the heterogeneity of extracellular vesicles. Journal of Cell Science, 2013. **126**(24): p. 5553-5565.
- 67. Stuffers, S., et al., *Multivesicular Endosome Biogenesis in the Absence of ESCRTs.* Traffic, 2009. **10**(7): p. 925-937.
- 68. Hurley, J.H., *ESCRT complexes and the biogenesis of multivesicular bodies*. Current Opinion in Cell Biology, 2008. **20**(1): p. 4-11.
- 69. Leung, K.F., J.B. Dacks, and M.C. Field, *Evolution of the Multivesicular Body ESCRT Machinery; Retention Across the Eukaryotic Lineage*. Traffic, 2008. **9**(10): p. 1698-1716.
- 70. Trajkovic, K., et al., Ceramide Triggers Budding of Exosome Vesicles into Multivesicular Endosomes. Science, 2008. **319**(5867): p. 1244-1247.
- 71. Goñi, F.M. and A. Alonso, *Effects of ceramide and other simple sphingolipids on membrane lateral structure*. Biochimica et Biophysica Acta (BBA) Biomembranes, 2009. **1788**(1): p. 169-177.
- 72. Kajimoto, T., et al., Ongoing activation of sphingosine 1-phosphate receptors mediates maturation of exosomal multivesicular endosomes. Nature Communications, 2013. 4: p. 2712.
- 73. Zhu, H., et al., *Mutation of SIMPLE in Charcot–Marie–Tooth 1C alters production of exosomes*. Molecular Biology of the Cell, 2013. **24**(11): p. 1619-1637.
- 74. Booth, A.M., et al., *Exosomes and HIV Gag bud from endosome-like domains of the T cell plasma membrane.* Journal of Cell Biology, 2006. **172**(6): p. 923-35.
- 75. Nabhan, J.F., et al., Formation and release of arrestin domain-containing protein 1-mediated microvesicles (ARMMs) at plasma membrane by recruitment of TSG101 protein. Proceedings of the National Academy of Sciences of the United States of America, 2012. 109(11): p. 4146-51.

- 76. Bianco, F., et al., *Acid sphingomyelinase activity triggers microparticle release from glial cells*. The EMBO Journal, 2009. **28**(8): p. 1043-1054.
- 77. Hugel, B., et al., *Membrane Microparticles: Two Sides of the Coin.* Physiology, 2005. **20**(1): p. 22-27.
- 78. Piccin, A., W.G. Murphy, and O.P. Smith, *Circulating microparticles: pathophysiology and clinical implications*. Blood Reviews, 2007. **21**(3): p. 157-171.
- 79. Pollet, H., et al., *Plasma Membrane Lipid Domains as Platforms for Vesicle Biogenesis and Shedding?* Biomolecules, 2018. **8**(3): p. 94.
- 80. Colombo, M., et al., Analysis of ESCRT functions in exosome biogenesis, composition and secretion highlights the heterogeneity of extracellular vesicles. Journal of Cell Science, 2013. **126**(24): p. 5553-5565.
- 81. Bobrie, A., et al., Diverse subpopulations of vesicles secreted by different intracellular mechanisms are present in exosome preparations obtained by differential ultracentrifugation. Journal of Extracellular Vesicles, 2012. **1**(1): p. 18397.
- 82. Van Deun, J., et al., *EV-TRACK: transparent reporting and centralizing knowledge in extracellular vesicle research.* Nature Methods, 2017. **14**(3): p. 228-232.
- 83. Soloveva, N., et al., *Proteomic Signature of Extracellular Vesicles Associated with Colorectal Cancer.* Molecules, 2023. **28**(10).
- 84. Tripisciano, C., et al., Extracellular Vesicles Derived From Platelets, Red Blood Cells, and Monocyte-Like Cells Differ Regarding Their Ability to Induce Factor XII-Dependent Thrombin Generation. Frontiers in Cell and Developmental Biology, 2020. 8.
- 85. Palviainen, M., et al., *Metabolic signature of extracellular vesicles depends on the cell culture conditions*. Journal of Extracellular Vesicles, 2019. **8**(1): p. 1596669.
- 86. Hong, J., et al., *Analysis of the Escherichia coli extracellular vesicle proteome identifies markers of purity and culture conditions.* Journal of Extracellular Vesicles, 2019. **8**(1): p. 1632099.
- 87. Almeria, C., et al., Heterogeneity of mesenchymal stem cell-derived extracellular vesicles is highly impacted by the tissue/cell source and culture conditions. Cell & Bioscience, 2022. 12(1): p. 51.
- 88. Contursi, A., et al., *Tumor-Educated Platelet Extracellular Vesicles: Proteomic Profiling and Crosstalk with Colorectal Cancer Cells.* Cancers, 2023. **15**(2): p. 350.
- 89. O'Grady, T., et al., Sorting and packaging of RNA into extracellular vesicles shape intracellular transcript levels. BMC Biology, 2022. **20**(1): p. 72.
- 90. Martin-Jaular, L., et al., *Unbiased proteomic profiling of host cell extracellular vesicle composition and dynamics upon HIV-1 infection.* The EMBO journal, 2021. **40**(8): p. e105492-e105492.
- 91. Misawa, T., et al., *Identification of Novel Senescent Markers in Small Extracellular Vesicles*. International Journal of Molecular Sciences, 2023. **24**(3).
- 92. Abels, E.R. and X.O. Breakefield, *Introduction to extracellular vesicles: biogenesis, RNA cargo selection, content, release, and uptake.* 2016, Springer.
- 93. Mathivanan, S., et al., *ExoCarta 2012: database of exosomal proteins, RNA and lipids.* Nucleic Acids Research, 2012. **40**(Database issue): p. D1241-4.
- 94. Kalra, H., et al., *Vesiclepedia: a compendium for extracellular vesicles with continuous community annotation.* PLoS Biology, 2012. **10**(12): p. e1001450.
- 95. Jeppesen, D.K., et al., *Reassessment of Exosome Composition*. Cell, 2019. **177**(2): p. 428-445.e18.

- 96. Cheng, L., et al., *Proteomic and lipidomic analysis of exosomes derived from ovarian cancer cells and ovarian surface epithelial cells.* Journal of Ovarian Research, 2020. **13**(1): p. 13.
- 97. Prudent, M., et al., *Proteomics of Stored Red Blood Cell Membrane and Storage-Induced Microvesicles Reveals the Association of Flotillin-2 With Band 3 Complexes.* Frontiers in Physiology, 2018. **9**.
- 98. de Gassart, A., et al., *Lipid raft-associated protein sorting in exosomes*. Blood, 2003. **102**(13): p. 4336-44.
- 99. Fitzgerald, W., et al., A System of Cytokines Encapsulated in ExtraCellular Vesicles. Scientific Reports, 2018. **8**(1).
- 100. Lima, L.G., et al., *Tumor microenvironmental cytokines bound to cancer exosomes determine uptake by cytokine receptor-expressing cells and biodistribution.* Nature Communications, 2021. **12**(1).
- 101. Yáñez-Mó, M., et al., *Biological properties of extracellular vesicles and their physiological functions*. Journal of Extracellular Vesicles, 2015. **4**(1): p. 27066.
- 102. Ratajczak, J., et al., Membrane-derived microvesicles: important and underappreciated mediators of cell-to-cell communication. Leukemia, 2006. **20**(9): p. 1487-1495.
- 103. Valadi, H., et al., Exosome-mediated transfer of mRNAs and microRNAs is a novel mechanism of genetic exchange between cells. Nature Cell Biology, 2007. **9**(6): p. 654-659.
- 104. Skog, J., et al., Glioblastoma microvesicles transport RNA and proteins that promote tumour growth and provide diagnostic biomarkers. Nature Cell Biology, 2008. **10**(12): p. 1470-1476.
- 105. Balaj, L., et al., *Tumour microvesicles contain retrotransposon elements and amplified oncogene sequences*. Nature Communications, 2011. **2**(1): p. 180.
- 106. Guescini, M., et al., *Astrocytes and Glioblastoma cells release exosomes carrying mtDNA*. Journal of Neural Transmission (Vienna), 2010. **117**(1): p. 1-4.
- 107. O'Brien, K., et al., RNA delivery by extracellular vesicles in mammalian cells and its applications. Nature Reviews Molecular Cell Biology, 2020. **21**(10): p. 585-606.
- 108. Zhang, Y., et al., *Recent advances in exosome-mediated nucleic acid delivery for cancer therapy.* Journal of Nanobiotechnology, 2022. **20**(1).
- 109. Ghanam, J., et al., *DNA in extracellular vesicles: from evolution to its current application in health and disease.* Cell & Bioscience, 2022. **12**(1).
- 110. Pigati, L., et al., Selective Release of MicroRNA Species from Normal and Malignant Mammary Epithelial Cells. PLoS ONE, 2010. 5(10): p. e13515.
- 111. Nolte-'t Hoen, E.N.M., et al., Deep sequencing of RNA from immune cell-derived vesicles uncovers the selective incorporation of small non-coding RNA biotypes with potential regulatory functions. Nucleic Acids Research, 2012. **40**(18): p. 9272-9285.
- 112. Chiou, N.-T., R. Kageyama, and K.M. Ansel, *Selective Export into Extracellular Vesicles and Function of tRNA Fragments during T Cell Activation*. Cell Reports, 2018. **25**(12): p. 3356-3370.e4.
- 113. Fanale, D., et al., Circular RNA in Exosomes. 2018, Springer Singapore. p. 109-117.
- 114. Zhang, H., et al., Exosome circRNA secreted from adipocytes promotes the growth of hepatocellular carcinoma by targeting deubiquitination-related USP7. Oncogene, 2019. **38**(15): p. 2844-2859.

- 115. Wang, J., et al., Circular RNA expression in exosomes derived from breast cancer cells and patients. Epigenomics, 2019. 11(4): p. 411-421.
- 116. Thakur, B.K., et al., *Double-stranded DNA in exosomes: a novel biomarker in cancer detection*. Cell Research, 2014. **24**(6): p. 766-769.
- 117. Skotland, T., et al., *An emerging focus on lipids in extracellular vesicles*. Advanced Drug Delivery Reviews, 2020. **159**: p. 308-321.
- 118. Nishida-Aoki, N., et al., *Lipidomic Analysis of Cells and Extracellular Vesicles from High-and Low-Metastatic Triple-Negative Breast Cancer.* Metabolites, 2020. **10**(2): p. 17.
- 119. Zhang, Y., et al., Metabolites as extracellular vesicle cargo in health, cancer, pleural effusion, and cardiovascular diseases: An emerging field of study to diagnostic and therapeutic purposes. Biomedicine & Pharmacotherapy, 2023. 157.
- 120. Wu, Y., et al., *Metabolomics of Extracellular Vesicles: A Future Promise of Multiple Clinical Applications*. International Journal of Nanomedicine, 2022. **17**: p. 6113-6129.
- 121. Surman, M., et al., *Human melanoma-derived ectosomes are enriched with specific glycan epitopes*. Life Sciences, 2018. **207**: p. 395-411.
- 122. Williams, C., et al., *Glycosylation of extracellular vesicles: current knowledge, tools and clinical perspectives.* Journal of Extracellular Vesicles, 2018. 7(1): p. 1442985.
- 123. Gurung, S., et al., *The exosome journey: from biogenesis to uptake and intracellular signalling.* Cell Communication and Signaling, 2021. **19**(1).
- 124. Stahl, P.D. and G. Raposo, *Exosomes and extracellular vesicles: the path forward*. Essays in biochemistry, 2018. **62**(2): p. 119-124.
- Hazan-Halevy, I., et al., *Cell-specific uptake of mantle cell lymphoma-derived exosomes by malignant and non-malignant B-lymphocytes*. Cancer Letters, 2015. **364**(1): p. 59-69.
- 126. Laulagnier, K., et al., Amyloid precursor protein products concentrate in a subset of exosomes specifically endocytosed by neurons. Cellular and Molecular Life Sciences, 2018. **75**(4): p. 757-773.
- 127. Zhao, L., et al., *Exosome-mediated siRNA delivery to suppress postoperative breast cancer metastasis*. Journal of Controlled Release, 2020. **318**: p. 1-15.
- 128. Belhadj, Z., et al., A combined "eat me/don't eat me" strategy based on extracellular vesicles for anticancer nanomedicine. Journal of Extracellular Vesicles, 2020. **9**(1): p. 1806444.
- 129. Richter, M., P. Vader, and G. Fuhrmann, *Approaches to surface engineering of extracellular vesicles*. Advanced drug delivery reviews, 2021. **173**: p. 416-426.
- 130. Dumontel, B., et al., *Nanotechnological engineering of extracellular vesicles for the development of actively targeted hybrid nanodevices*. Cell & Bioscience, 2022. **12**(1).
- 131. Horibe, S., et al., *Mechanism of recipient cell-dependent differences in exosome uptake*. BMC Cancer, 2018. **18**(1).
- 132. Yoon, J.H., et al., *Uptake and tumor-suppressive pathways of exosome-associated GKN1 protein in gastric epithelial cells.* Gastric Cancer, 2020. **23**(5): p. 848-862.
- 133. Kiss, A.L. and E. Botos, *Endocytosis via caveolae: alternative pathway with distinct cellular compartments to avoid lysosomal degradation?* Journal of Cellular and Molecular Medicine, 2009. **13**(7): p. 1228-1237.
- 134. Nanbo, A., et al., Exosomes derived from Epstein-Barr virus-infected cells are internalized via caveola-dependent endocytosis and promote phenotypic modulation in target cells. Journal of Virology, 2013. **87**(18): p. 10334-47.

- 135. Koumangoye, R.B., et al., Detachment of Breast Tumor Cells Induces Rapid Secretion of Exosomes Which Subsequently Mediate Cellular Adhesion and Spreading. PLoS ONE, 2011. **6**(9): p. e24234.
- 136. He, L., et al., Ovarian cancer cell-secreted exosomal miR-205 promotes metastasis by inducing angiogenesis. Theranostics, 2019. **9**(26): p. 8206-8220.
- 137. Feng, D., et al., *Cellular internalization of exosomes occurs through phagocytosis*. Traffic, 2010. **11**(5): p. 675-87.
- 138. Tian, T., et al., Exosome Uptake through Clathrin-mediated Endocytosis and Macropinocytosis and Mediating miR-21 Delivery\*. Journal of Biological Chemistry, 2014. 289(32): p. 22258-22267.
- 139. Nakase, I., et al., Active macropinocytosis induction by stimulation of epidermal growth factor receptor and oncogenic Ras expression potentiates cellular uptake efficacy of exosomes. Sci Rep, 2015. 5: p. 10300.
- 140. Emam, S.E., et al., Liposome co-incubation with cancer cells secreted exosomes (extracellular vesicles) with different proteins expressions and different uptake pathways. Scientific Reports, 2018. **8**(1): p. 14493.
- 141. Prada, I. and J. Meldolesi, *Binding and Fusion of Extracellular Vesicles to the Plasma Membrane of Their Cell Targets*. International Journal of Molecular Sciences, 2016. **17**(8).
- 142. Yates, A.G., et al., *In sickness and in health: The functional role of extracellular vesicles in physiology and pathology in vivo.* Journal of Extracellular Vesicles, 2022. **11**(1).
- 143. Marcilla, A., et al., *Extracellular vesicles in parasitic diseases*. Journal of Extracellular Vesicles, 2014. **3**: p. 25040.
- 144. Montaner, S., et al., *The Role of Extracellular Vesicles in Modulating the Host Immune Response during Parasitic Infections.* Frontiers in Immunology, 2014. **5**.
- 145. Schorey, J.S., et al., *Exosomes and other extracellular vesicles in host-pathogen interactions*. EMBO Reports, 2015. **16**(1): p. 24-43.
- 146. Zhang, Y., et al., *Exosomes: biogenesis, biologic function and clinical potential.* Cell & Bioscience, 2019. **9**(1).
- 147. Jafari, D., et al., Designer Exosomes: A New Platform for Biotechnology Therapeutics. BioDrugs, 2020. **34**(5): p. 567-586.
- 148. Ramirez, M.I., et al., *Technical challenges of working with extracellular vesicles*. Nanoscale, 2018. **10**(3): p. 881-906.
- 149. Coumans, F.A.W., et al., *Methodological Guidelines to Study Extracellular Vesicles*. Circulation Research, 2017. **120**(10): p. 1632-1648.
- 150. Witwer, K.W., et al., Standardization of sample collection, isolation and analysis methods in extracellular vesicle research. Journal of Extracellular Vesicles, 2013. **2**(1): p. 20360.
- 151. Tauro, B.J., et al., *Two Distinct Populations of Exosomes Are Released from LIM1863 Colon Carcinoma Cell-derived Organoids*. Molecular & Cellular Proteomics, 2013. **12**(3): p. 587-598.
- 152. Iwai, K., et al., *Isolation of human salivary extracellular vesicles by iodixanol density gradient ultracentrifugation and their characterizations.* Journal of extracellular vesicles, 2016. 5(1): p. 30829.
- 153. Kurian, T.K., et al., *Elucidating Methods for Isolation and Quantification of Exosomes: A Review.* Molecular Biotechnology, 2021. **63**(4): p. 249-266.

- 154. Shirejini, S.Z. and F. Inci, *The Yin and Yang of exosome isolation methods: conventional practice, microfluidics, and commercial kits.* Biotechnology Advances, 2022. **54**: p. 107814.
- 155. De Sousa, K.P., et al., *Isolation and characterization of extracellular vesicles and future directions in diagnosis and therapy.* WIREs Nanomedicine and Nanobiotechnology, 2022.
- 156. Liangsupree, T., E. Multia, and M.-L. Riekkola, *Modern isolation and separation techniques for extracellular vesicles*. Journal of Chromatography A, 2021. **1636**: p. 461773.
- 157. Van Deun, J., et al., *The impact of disparate isolation methods for extracellular vesicles on downstream RNA profiling.* Journal of Extracellular Vesicles, 2014. **3**(1): p. 24858.
- 158. Paolini, L., et al., Residual matrix from different separation techniques impacts exosome biological activity. Scientific Reports, 2016. 6(1): p. 23550.
- 159. Gutiérrez García, G., et al., Analysis of RNA yield in extracellular vesicles isolated by membrane affinity column and differential ultracentrifugation. PLOS ONE, 2020. **15**(11): p. e0238545.
- 160. Nantakomol, D., et al., *Circulating Red Cell-derived Microparticles in Human Malaria*. Journal of Infectious Diseases, 2011. **203**(5): p. 700-706.
- 161. Antwi-Baffour, S., et al., Plasma mEV levels in Ghanain malaria patients with low parasitaemia are higher than those of healthy controls, raising the potential for parasite markers in mEVs as diagnostic targets. Journal of Extracellular Vesicles, 2020. **9**(1): p. 1697124.
- 162. Combes, V., et al., Circulating Endothelial Microparticles in Malawian Children With Severe Falciparum Malaria Complicated With Coma. JAMA, 2004. **291**(21): p. 2542-2544.
- 163. Mfonkeu, J.B.P., et al., *Elevated Cell-Specific Microparticles Are a Biological Marker for Cerebral Dysfunctions in Human Severe Malaria*. Plos One, 2010. **5**(10).
- 164. Sahu, U., et al., Promoter Polymorphisms in the ATP Binding Cassette Transporter Gene Influence Production of Cell-Derived Microparticles and Are Highly Associated with Susceptibility to Severe Malaria in Humans. Infection and Immunity, 2013a. 81(4): p. 1287-1294.
- 165. Sahu, U., et al., Association of TNF level with production of circulating cellular microparticles during clinical manifestation of human cerebral malaria. Human Immunology, 2013b. 74(6): p. 713-721.
- 166. Antwi-Baffour, S., et al., *Proteomic analysis of microparticles isolated from malaria positive blood samples.* Proteome Science, 2017. **15**.
- 167. Ketprasit, N., et al., *The characterization of extracellular vesicles-derived microRNAs in Thai malaria patients*. Malaria Journal, 2020. **19**(1).
- 168. Brian De Souza, J. and E.M. Riley, *Cerebral malaria: the contribution of studies in animal models to our understanding of immunopathogenesis.* Microbes and Infection, 2002. **4**(3): p. 291-300.
- 169. De Niz, M. and V.T. Heussler, *Rodent malaria models: insights into human disease and parasite biology.* Current Opinion in Microbiology, 2018. **46**: p. 93-101.
- 170. Combes, V., et al., ABCA1 Gene Deletion Protects against Cerebral Malaria. The American Journal of Pathology, 2005. **166**(1): p. 295-302.

- 171. Couper, K.N., et al., Parasite-Derived Plasma Microparticles Contribute Significantly to Malaria Infection-Induced Inflammation through Potent Macrophage Stimulation. PLoS Pathogens, 2010. **6**(1): p. e1000744.
- 172. Martin-Jaular, L., et al., Exosomes from Plasmodium yoelii-Infected Reticulocytes Protect Mice from Lethal Infections. PLoS ONE, 2011. **6**(10): p. e26588.
- 173. Tiberti, N., et al., Exploring experimental cerebral malaria pathogenesis through the characterisation of host-derived plasma microparticle protein content. Scientific Reports, 2016. **6**(1): p. 37871.
- 174. Cohen, A., et al., Differential plasma microvesicle and brain profiles of microRNA in experimental cerebral malaria. Malaria Journal, 2018. 17.
- 175. Batarseh, A.M., et al., *Investigation of Plasma-Derived Lipidome Profiles in Experimental Cerebral Malaria in a Mouse Model Study*. International Journal of Molecular Sciences, 2023. **24**(1).
- 176. El-Assaad, F., et al., *Production, Fate and Pathogenicity of Plasma Microparticles in Murine Cerebral Malaria*. Plos Pathogens, 2014. **10**(3).
- 177. Martín-Jaular, L., et al., Spleen-Dependent Immune Protection Elicited by CpG Adjuvanted Reticulocyte-Derived Exosomes from Malaria Infection Is Associated with Changes in T cell Subsets' Distribution. Frontiers in Cell and Developmental Biology, 2016. 16;4:131.
- 178. Demarta-Gatsi, C., et al., *Histamine releasing factor and elongation factor 1 alpha secreted via malaria parasites extracellular vesicles promote immune evasion by inhibiting specific T cell responses*. Cellular Microbiology, 2019. **21**(7): p. e13021.
- 179. Trager, W. and J.B. Jensen, *Human Malaria Parasites in Continuous Culture*. Science, 1976. **193**(4254): p. 673-675.
- 180. Trager, W. and J.B. Jensen, *Continuous culture of Plasmodium falciparum: its impact on malaria research*. International Journal for Parasitology, 1997. **27**(9): p. 989-1006.
- 181. LeRoux, M., V. Lakshmanan, and J.P. Daily, *Plasmodium falciparum biology: analysis of in vitro versus in vivo growth conditions.* Trends in Parasitology, 2009. **25**(10): p. 474-481.
- 182. Johnstone, R.M., et al., Exosome formation during maturation of mammalian and avian reticulocytes: evidence that exosome release is a major route for externalization of obsolete membrane proteins. Journal of Cellular Physiology, 1991. **147**(1): p. 27-36.
- 183. Blanc, L. and M. Vidal, *Reticulocyte membrane remodeling: contribution of the exosome pathway.* Current Opinion in Hematology, 2010. **17**(3): p. 177-183.
- 184. Willekens, F., et al., *Erythrocyte vesiculation: A self-protective mechanism?* British journal of haematology, 2008. **141**: p. 549-56.
- 185. Bosman, G.J.C.G.M., et al., *The proteome of erythrocyte-derived microparticles from plasma: new clues for erythrocyte aging and vesiculation.* Journal of Proteomics, 2012. **76**: p. 203-210.
- 186. Avalos-Padilla, Y., et al., *The ESCRT-III machinery participates in the production of extracellular vesicles and protein export during Plasmodium falciparum infection.* Plos Pathogens, 2021. **17**(4).
- 187. Spycher, C., et al., Genesis of and trafficking to the Maurer's clefts of Plasmodium falciparum-infected erythrocytes. Molecular and Cellular Biology, 2006. **26**(11): p. 4074-85.
- 188. De Koning-Ward, T.F., et al., *Plasmodium species: master renovators of their host cells.* Nature Reviews Microbiology, 2016. **14**(8): p. 494-507.

- 189. Regev-Rudzki, N., et al., Cell-Cell Communication between Malaria-Infected Red Blood Cells via Exosome-like Vesicles. Cell, 2013. **153**(5): p. 1120-1133.
- 190. Mantel, P.-Y., et al., Malaria-Infected Erythrocyte-Derived Microvesicles Mediate Cellular Communication within the Parasite Population and with the Host Immune System. Cell Host & Microbe, 2013. 13(5): p. 521-534.
- 191. Abdi, A., et al., Proteomic analysis of extracellular vesicles from a Plasmodium falciparum Kenyan clinical isolate defines a core parasite secretome [version 1; peer review: 1 approved, 2 approved with reservations]. Wellcome Open Research, 2017. **2**(50).
- 192. Vimonpatranon, S., et al., Extracellular Vesicles Derived from Early and Late Stage Plasmodium falciparum-Infected Red Blood Cells Contain Invasion-Associated Proteins. Journal of Clinical Medicine, 2022. 11(14): p. 4250.
- 193. Sampaio, N.G., et al., Extracellular vesicles from early stage Plasmodium falciparum-infected red blood cells contain PfEMP1 and induce transcriptional changes in human monocytes. Cellular Microbiology, 2018. **20**(5).
- 194. Correa, R., et al., Extracellular vesicles carrying lactate dehydrogenase induce suicide in increased population density of Plasmodium falciparum in vitro. Scientific Reports, 2019.

  9.
- 195. Abou Karam, P., et al., *Malaria parasites release vesicle subpopulations with signatures of different destinations*. EMBO reports, 2022. **23**(7).
- 196. Mantel, P.Y., et al., *Infected erythrocyte-derived extracellular vesicles alter vascular function via regulatory Ago2-miRNA complexes in malaria.* Nature Communications, 2016. 7.
- 197. Babatunde, K.A., et al., *Malaria infected red blood cells release small regulatory RNAs through extracellular vesicles.* Scientific Reports, 2018. **8**(1).
- 198. Wang, Z.S., et al., Red blood cells release microparticles containing human argonaute 2 and miRNAs to target genes of Plasmodium falciparum. Emerging Microbes & Infections, 2017. 6.
- 199. Khowawisetsut, L., et al., Differential Effect of Extracellular Vesicles Derived from Plasmodium falciparum-Infected Red Blood Cells on Monocyte Polarization. International Journal of Molecular Sciences, 2023. 24(3).
- 200. Sisquella, X., et al., *Malaria parasite DNA-harbouring vesicles activate cytosolic immune sensors*. Nature Communications, 2017. **8**.
- 201. Gulati, S., et al., *Profiling the Essential Nature of Lipid Metabolism in Asexual Blood and Gametocyte Stages of Plasmodium falciparum*. Cell Host & Microbe, 2015. **18**(3): p. 371-381.
- 202. Borgheti-Cardoso, L.N., et al., Extracellular vesicles derived from Plasmodium-infected and non-infected red blood cells as targeted drug delivery vehicles. International Journal of Pharmaceutics, 2020. **587**.
- 203. Correa, R., et al., *Volatile organic compounds associated with Plasmodium falciparum infection in vitro*. Parasites & Vectors, 2017. **10**.
- 204. Delves, M.J., et al., *Routine in vitro culture of P. falciparum gametocytes to evaluate novel transmission-blocking interventions.* Nature Protocols, 2016. **11**(9): p. 1668-1680.
- 205. Omorou, R., et al., *Protocols for Plasmodium gametocyte production in vitro: an integrative review and analysis.* Parasites & Vectors, 2022. **15**(1).
- 206. Ortega-Pajares, A. and S.J. Rogerson, *The Rough Guide to Monocytes in Malaria Infection*. Frontiers in Immunology, 2018. **9**: p. 2888.

- 207. Ofir-Birin, Y., et al., *Monitoring extracellular Vesicle Cargo Active Uptake by Imaging Flow Cytometry*. Frontiers in Immunology, 2018. **9**.
- 208. Ofir-Birin, Y., et al., *Malaria parasites both repress host CXCL10 and use it as a cue for growth acceleration*. Nature Communications, 2021. **12**(1).
- 209. Aguilar, R., et al., Changing plasma cytokine, chemokine and growth factor profiles upon differing malaria transmission intensities. Malaria Journal, 2019. **18**(1).
- 210. Wilson, N.O., et al., *CXCL4 and CXCL10 predict risk of fatal cerebral malaria*. Disease Markers, 2011. **30**(1): p. 39-49.
- 211. Herbert, F., et al., Evidence of IL-17, IP-10, and IL-10 involvement in multiple-organ dysfunction and IL-17 pathway in acute renal failure associated to Plasmodium falciparum malaria. Journal of Translational Medicine, 2015. 13(1).
- 212. Mbagwu, S.I., et al., *Human Microglia Respond to Malaria-Induced Extracellular Vesicles*. Pathogens, 2020. **9**(1).
- 213. Dekel, E., et al., 20S proteasomes secreted by the malaria parasite promote its growth. Nature Communications, 2021. **12**(1).
- 214. Moloudizargari, M., M.H. Asghari, and A. Goel, *The therapeutic triad of extracellular vesicles: As drug targets, as drugs, and as drug carriers.* Biochemical Pharmacology, 2021. **192**: p. 114714.
- 215. Liu, S., et al., Microparticle-mediated gene delivery for the enhanced expression of a 19-kDa fragment of merozoite surface protein 1 of Plasmodium falciparum. Biotechnology Progress, 2010 Jan-Feb;26(1):257-62.
- 216. Borgheti-Cardoso, L.N., et al., Extracellular vesicles derived from Plasmodium-infected and non-infected red blood cells as targeted drug delivery vehicles. International Journal of Pharmaceutics, 2020. **587**: p. 119627.
- 217. Ye, W.J., et al., *Microvesicles from malaria-infected red blood cells activate natural killer cells via MDA5 pathway.* Plos Pathogens, 2018. **14**(10).
- 218. Burrack, K.S., G.T. Hart, and S.E. Hamilton, *Contributions of natural killer cells to the immune response against Plasmodium*. Malaria Journal, 2019. **18**(1).
- 219. Radfar, A., et al., *Synchronous culture of Plasmodium falciparum at high parasitemia levels*. Nature Protocols, 2009. **4**(12): p. 1899-1915.
- 220. Bachurski, D., et al., Extracellular vesicle measurements with nanoparticle tracking analysis An accuracy and repeatability comparison between NanoSight NS300 and ZetaView. Journal of Extracellular Vesicles, 2019. **8**(1): p. 1596016.
- Welsh, J.A., et al., *MIFlowCyt-EV: a framework for standardized reporting of extracellular vesicle flow cytometry experiments.* Journal of Extracellular Vesicles, 2020. **9**(1).
- 222. Cooper, R.A., *SDS-PAGE and Western Blotting of Plasmodium falciparum Proteins*. Malaria Methods and Protocols, ed. D.L. Doolan. 2002, Totowa, NJ, USA: Humana Press. 1.
- 223. Steck, T.L. and J.A. Kant, [16] Preparation of impermeable ghosts and inside-out vesicles from human erythrocyte membranes, in Methods in Enzymology. 1974, Academic Press. p. 172-180.
- 224. Pillai-Kastoori, L., A.R. Schutz-Geschwender, and J.A. Harford, *A systematic approach to quantitative Western blot analysis*. Analytical Biochemistry, 2020. **593**: p. 113608.
- 225. Mateescu, B., et al., *Obstacles and opportunities in the functional analysis of extracellular vesicle RNA an ISEV position paper.* Journal of Extracellular Vesicles, 2017. **6**(1): p. 1286095.

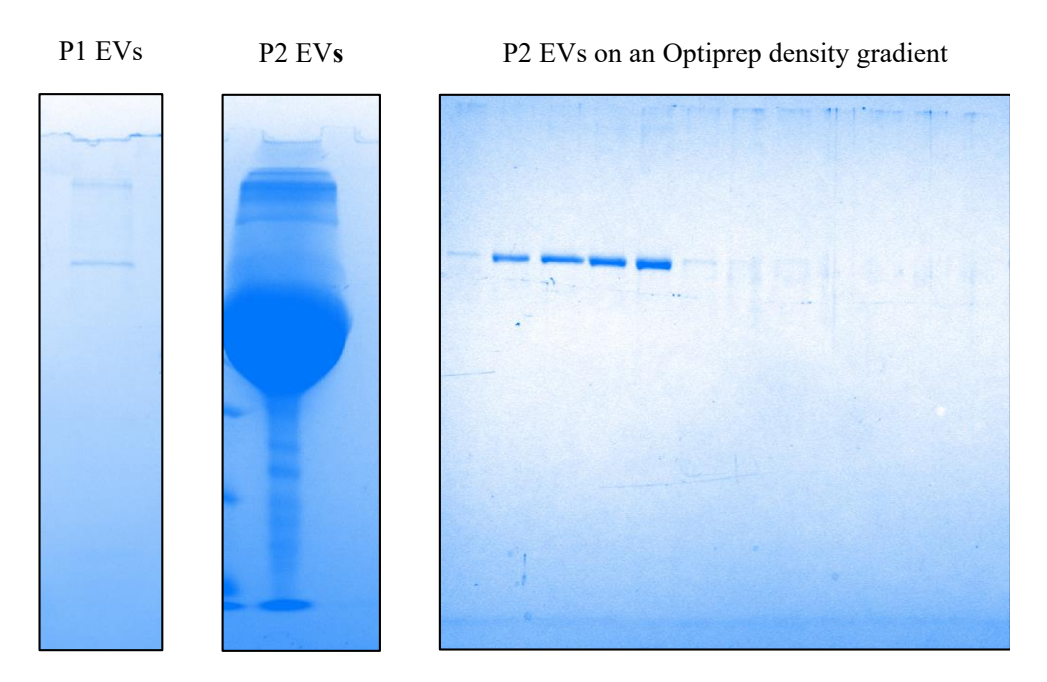
- 226. Bolger, A.M., M. Lohse, and B. Usadel, *Trimmomatic: a flexible trimmer for Illumina sequence data*. Bioinformatics, 2014. **30**(15): p. 2114-2120.
- 227. Dobin, A., et al., *STAR: ultrafast universal RNA-seq aligner*. Bioinformatics, 2013. **29**(1): p. 15-21.
- 228. Li, B. and C.N. Dewey, *RSEM: accurate transcript quantification from RNA-Seq data with or without a reference genome.* BMC Bioinformatics, 2011. **12**(1): p. 323.
- 229. Love, M.I., W. Huber, and S. Anders, *Moderated estimation of fold change and dispersion for RNA-seq data with DESeq2*. Genome Biology, 2014. **15**(12): p. 550.
- 230. Ewels, P., et al., *MultiQC*: summarize analysis results for multiple tools and samples in a single report. Bioinformatics, 2016. **32**(19): p. 3047-3048.
- 231. Cvjetkovic, A., J. Lötvall, and C. Lässer, *The influence of rotor type and centrifugation time on the yield and purity of extracellular vesicles*. Journal of Extracellular Vesicles, 2014. **3**.
- 232. Jeppesen, D.K., et al., Comparative analysis of discrete exosome fractions obtained by differential centrifugation. Journal of Extracellular Vesicles, 2014. **3**(1): p. 25011.
- 233. Livshits, M.A., et al., Isolation of exosomes by differential centrifugation: Theoretical analysis of a commonly used protocol. Scientific Reports, 2015. **5**(1): p. 17319.
- 234. Torres Crigna A, et al., *Inter-Laboratory Comparison of Extracellular Vesicle Isolation Based on Ultracentrifugation*. Transfusion Medicine and Hemotherapy, 2020: p. 1-12.
- 235. Zaborowski, M.P., et al., Extracellular Vesicles: Composition, Biological Relevance, and Methods of Study. Bioscience, 2015. 65(8): p. 783-797.
- 236. Mbagwu, S., et al., *Production and Characterization of Extracellular Vesicles in Malaria*, in *Extracellular Vesicles: Methods and Protocols*, W.P. Kuo and S. Jia, Editors. 2017. p. 377-388.
- 237. Dekel, E., et al., *Antibody-Free Labeling of Malaria-Derived Extracellular Vesicles Using Flow Cytometry*. Biomedicines, 2020. **8**(5).
- 238. Opadokun, T., J. Agyapong, and P. Rohrbach, *Protein Profiling of Malaria-Derived Extracellular Vesicles Reveals Distinct Subtypes*. Membranes, 2022. **12**(4): p. 397.
- Wannez, A., et al., *Extracellular Vesicles in Red Blood Cell Concentrates: An Overview.* Transfusion Medicine Reviews, 2019. **33**(2): p. 125-130.
- 240. Gamonet, C., et al., *Processing methods and storage duration impact extracellular vesicle counts in red blood cell units.* Blood Advances, 2020. **4**(21): p. 5527-5539.
- 241. Haraszti, R.A., et al., *High-resolution proteomic and lipidomic analysis of exosomes and microvesicles from different cell sources*. Journal of Extracellular Vesicles, 2016. **5**(1): p. 32570.
- 242. Palma, J., et al., *MicroRNAs are exported from malignant cells in customized particles*. Nucleic Acids Research, 2012. **40**(18): p. 9125-9138.
- 243. Keerthikumar, S., et al., *Proteogenomic analysis reveals exosomes are more oncogenic than ectosomes.* Oncotarget, 2015. **6**(17): p. 15375-15396.
- 244. Minciacchi, V.R., et al., *Large oncosomes contain distinct protein cargo and represent a separate functional class of tumor-derived extracellular vesicles*. Oncotarget, 2015. **6**(13): p. 11327-11341.
- 245. Xu, R., et al., *Highly-purified exosomes and shed microvesicles isolated from the human colon cancer cell line LIM1863 by sequential centrifugal ultrafiltration are biochemically and functionally distinct.* Methods, 2015. **87**: p. 11-25.

- 246. Théry, C., et al., *Isolation and characterization of exosomes from cell culture supernatants and biological fluids.* Current Protocols in Cell Biology, 2006. **Chapter 3**: p. Unit 3.22.
- 247. Kriebardis, A.G., et al., *RBC-derived vesicles during storage: ultrastructure, protein composition, oxidation, and signaling components.* Transfusion, 2008. **48**(9): p. 1943-1953.
- 248. Willekens, F.L.A., et al., *Hemoglobin loss from erythrocytes in vivo results from spleen-facilitated vesiculation.* Blood, 2003. **101**(2): p. 747-751.
- 249. Laurén, E., et al., *Phospholipid composition of packed red blood cells and that of extracellular vesicles show a high resemblance and stability during storage*. Molecular and Cell Biology of Lipids, 2018. **1863**(1): p. 1-8.
- 250. Andreu, Z. and M. Yanez-Mo, *Tetraspanins in extracellular vesicle formation and function*. Frontiers in Immunology, 2014. **5**.
- 251. Huang, S., et al., The phylogenetic analysis of tetraspanins projects the evolution of cell-cell interactions from unicellular to multicellular organisms. Genomics, 2005. **86**(6): p. 674-684.
- 252. Thangaraju, K., et al., Extracellular Vesicles from Red Blood Cells and Their Evolving Roles in Health, Coagulopathy and Therapy. International Journal of Molecular Sciences, 2020. 22(1): p. 153.
- 253. Antonelou, M.H., et al., Effects of pre-storage leukoreduction on stored red blood cells signaling: A time-course evaluation from shape to proteome. Journal of Proteomics, 2012. **76**: p. 220-238.
- 254. Tzounakas, V.L., et al., Leukoreduction makes a difference: A pair proteomics study of extracellular vesicles in red blood cell units. Transfusion and Apheresis Science, 2021. **60**(3).
- 255. Shapiro, M.J. To filter blood or universal leukoreduction: what is the answer? Critical Care, 2004. 8 (Suppl 2): p. S27.
- 256. Rikkert, L.G., et al., Quality of extracellular vesicle images by transmission electron microscopy is operator and protocol dependent. Journal of Extracellular Vesicles, 2019. **8**(1): p. 1555419.
- 257. Welsh, J.A., et al., *Extracellular Vesicle Flow Cytometry Analysis and Standardization*. Frontiers in Cell and Developmental Biology, 2017. **5**.
- 258. Zhang, J.-Z., et al., Association of Stomatin (Band 7.2b) with Glut1 Glucose Transporter. Archives of Biochemistry and Biophysics, 1999. **372**(1): p. 173-178.
- 259. Vidal, M., *Exosomes in erythropoiesis*. Transfusion Clinique et Biologique, 2010. **17**(3): p. 131-137.
- Verma, R., et al., *Identification of Proteins Secreted by Malaria Parasite into Erythrocyte using SVM and PSSM profiles.* BMC Bioinformatics, 2008. **9**(1): p. 201.
- 261. Silvestrini, F., et al., Protein Export Marks the Early Phase of Gametocytogenesis of the Human Malaria Parasite Plasmodium falciparum. Molecular and Cellular Proteomics, 2010. 9(7): p. 1437-1448.
- 262. Kim, K.M., et al., RNA in extracellular vesicles. WIREs RNA, 2017. 8(4): p. e1413.
- 263. Crescitelli, R., et al., Distinct RNA profiles in subpopulations of extracellular vesicles: apoptotic bodies, microvesicles and exosomes. Journal of Extracellular Vesicles, 2013. 2(1): p. 20677.
- Wang, K., et al., Export of microRNAs and microRNA-protective protein by mammalian cells. Nucleic Acids Research, 2010. **38**(20): p. 7248-59.

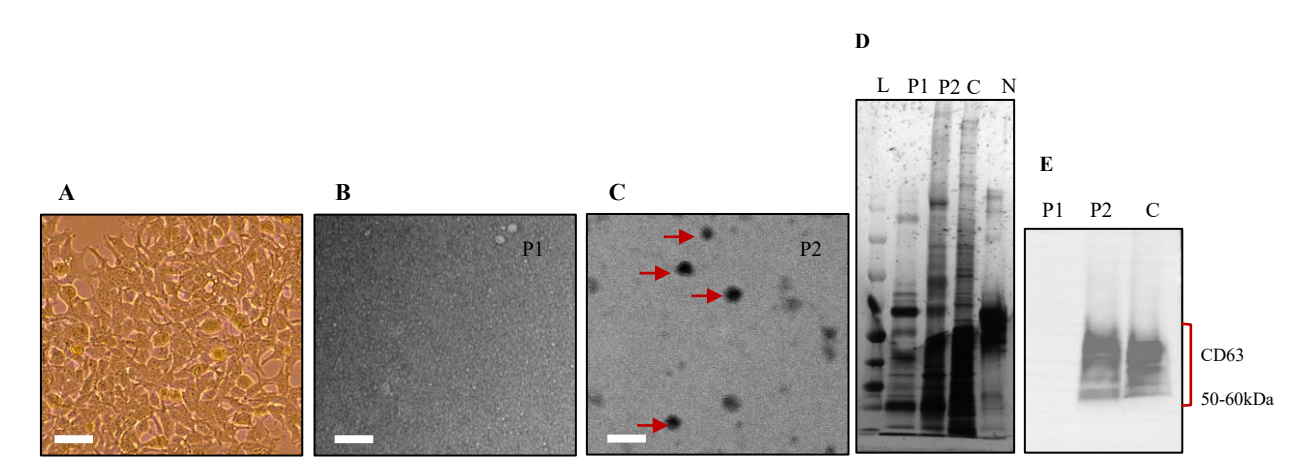
- 265. Yang, M., et al., *The Plasmodium falciparum Vps4 homolog mediates multivesicular body formation.* Journal of Cell Science, 2004. **117**(17): p. 3831-3838.
- 266. Boucheix, C. and E. Rubinstein, *Tetraspanins*. Cellular and Molecular Life Sciences, 2001. **58**(9): p. 1189-1205.
- 267. Bebesi, T., et al., *Storage conditions determine the characteristics of red blood cell derived extracellular vesicles.* Scientific Reports, 2022. **12**(1).
- 268. Greenwalt, T.J., C.Z. Sostok, and U.J. Dumaswala, *studies in red-blood-cell preservation* .1. Effect of the other formed elements. Vox Sanguinis, 1990. **58**(2): p. 85-89.
- 269. Visan, K.S., et al., Comparative analysis of tangential flow filtration and ultracentrifugation, both combined with subsequent size exclusion chromatography, for the isolation of small extracellular vesicles. Journal of Extracellular Vesicles, 2022. 11(9): p. 12266.
- 270. Bosman, G.J.C.G.M., et al., *The proteome of red cell membranes and vesicles during storage in blood bank conditions*. Transfusion, 2008. **48**(5): p. 827-835.
- 271. Sorkin, R., et al., *Nanomechanics of Extracellular Vesicles Reveals Vesiculation Pathways*. Small, 2018. **14**(39): p. 1801650.
- 272. Gov, N.S., Less is more: removing membrane attachments stiffens the RBC cytoskeleton. New Journal of Physics, 2007. **9**(11): p. 429.
- 273. Gov, N., et al., Chapter 4 Cytoskeletal Control of Red Blood Cell Shape: Theory and Practice of Vesicle Formation, in Advances in Planar Lipid Bilayers and Liposomes. 2009, Academic Press. p. 95-119.
- 274. Campanella, M.E., H. Chu, and P.S. Low, *Assembly and regulation of a glycolytic enzyme complex on the human erythrocyte membrane*. Proceedings of the National Academy of Sciences, 2005. **102**(7): p. 2402-2407.
- 275. Freitas Leal, J.K., et al., Vesiculation of Red Blood Cells in the Blood Bank: A Multi-Omics Approach towards Identification of Causes and Consequences. Proteomes, 2020. **8**(2): p. 6.
- 276. Willekens, F.L.A., et al., *Erythrocyte vesiculation: a self-protective mechanism?* British Journal of Haematology, 2008. **141**(4): p. 549-556.
- 277. Bosman, G.J.C.G.M., et al., *Erythrocyte ageingin vivoandin vitro: structural aspects and implications for transfusion*. Transfusion Medicine, 2008. **18**(6): p. 335-347.
- 278. Giribaldi, G., et al., Growth of Plasmodium falciparuminduces stage-dependent haemichrome formation, oxidative aggregation of band 3, membrane deposition of complement and antibodies, and phagocytosis of parasitized erythrocytes. British Journal of Haematology, 2001. 113(2): p. 492-499.
- 279. Wagner, S., et al., *Immunochemical characterization of a band 3-like anion exchanger in collecting duct of human kidney*. American Journal of Physiology-Renal Physiology, 1987. **253**(2): p. F213-F221.
- 280. Czerwinski, M., et al., Degradation of the human erythrocyte membrane band 3 studied with the monoclonal antibody directed against an epitope on the cytoplasmic fragment of band 3. European Journal of Biochemistry, 1988. 174(4): p. 647-654.
- 281. Challou, N., et al., Sequence and Structure of the Membrane-Associated Peptide of Glycophorin A. Biochemistry, 1994. **33**(22): p. 6902-6910.
- 282. Lemmon, M.A., et al., Glycophorin A dimerization is driven by specific interactions between transmembrane alpha-helices. Journal of Biological Chemistry, 1992. **267**(11): p. 7683-9.

- 283. GOLL, D.E., et al., *The Calpain System*. Physiological Reviews, 2003. **83**(3): p. 731-801.
- 284. Inomata, M., et al., *A variety of calpain/calpastatin systems in mammalian erythrocytes*. Biochimica et Biophysica Acta (BBA) Molecular Cell Research, 1993. **1178**(2): p. 207-214.
- 285. Abou-El-Hassan, H., et al., *Protein Degradome of Spinal Cord Injury: Biomarkers and Potential Therapeutic Targets.* Molecular Neurobiology, 2020. **57**(6): p. 2702-2726.
- 286. Föller, M., S.M. Huber, and F. Lang, *Erythrocyte programmed cell death*. IUBMB Life, 2008. **60**(10): p. 661-668.
- 287. Waghray, A., et al., *Molecular cloning and characterization of rat and human calpain-5*. Biochemical and Biophysical Research Communications, 2004. **324**(1): p. 46-51.
- 288. Olivieri, A., et al., *Structural organization of erythrocyte membrane microdomains and their relation with malaria susceptibility.* Communications Biology, 2021. **4**(1): p. 1375.
- 289. Kilinc, S., et al., *Oncogene Regulated Release of Extracellular Vesicles*. 2020, Cold Spring Harbor Laboratory.
- 290. Poti, K.E., et al., *HRP2: Transforming Malaria Diagnosis, but with Caveats.* Trends in Parasitology, 2020. **36**(2): p. 112-126.
- 291. Das, S., et al., Performance of an ultra-sensitive Plasmodium falciparum HRP2-based rapid diagnostic test with recombinant HRP2, culture parasites, and archived whole blood samples. Malaria Journal, 2018. 17(1): p. 118.
- 292. Pal-Bhowmick, I., et al., *Protective Properties and Surface Localization of Plasmodium falciparum Enolase*. Infection and Immunity, 2007. **75**(11): p. 5500-5508.
- 293. Moyano, E.M., et al., *Molecular cloning and characterisation of the RESA gene, a marker of genetic diversity of Plasmodium falciparum*. Molecular Biology Reports, 2010. **37**(6): p. 2893-902.
- 294. Miller, S.K., et al., A subset of Plasmodium falciparum SERA genes are expressed and appear to play an important role in the erythrocytic cycle. Journal of Biological Chemistry, 2002. 277(49): p. 47524-32.
- 295. Raj, D.K., et al., *Anti-PfGARP activates programmed cell death of parasites and reduces severe malaria.* Nature, 2020. **582**(7810): p. 104-108.
- 296. Ariey, F., et al., A molecular marker of artemisinin-resistant Plasmodium falciparum malaria. Nature, 2014. **505**(7481): p. 50-5.
- 297. Reed, M.B., et al., *Pgh1 modulates sensitivity and resistance to multiple antimalarials in Plasmodium falciparum*. Nature, 2000. **403**(6772): p. 906-909.
- 298. Tzounakas, V.L., et al., *Red cell proteasome modulation by storage, redox metabolism and transfusion.* Blood Transfusion, 2022. **20**(1): p. 27-39.
- 299. information, N.c.f.b. *Plasmodium falciparum*. 2023 [cited 2023 September 16]; Available from: https://www.ncbi.nlm.nih.gov/datasets/taxonomy/5833/.
- 300. Elsner, C., S. Ergün, and N. Wagner, *Biogenesis and release of endothelial extracellular vesicles: Morphological aspects*. Annals of Anatomy Anatomischer Anzeiger, 2023. **245**: p. 152006.
- 301. Bache, K.G., et al., STAM and Hrs Are Subunits of a Multivalent Ubiquitin-binding Complex on Early Endosomes. Journal of Biological Chemistry, 2003. **278**(14): p. 12513-12521.

## Appendix

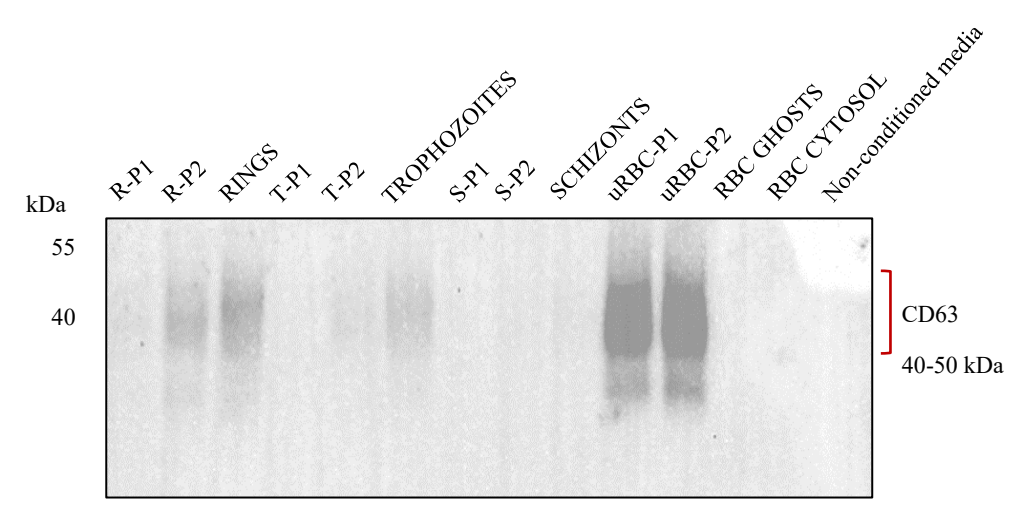


Appendix Figure 1. EV isolation at low parasitemia
Related to section 4.1.1. Low parasitemia cultures yielded no P1 EVs (left) and P2 EVs with heavy albumin contamination (middle). Proteins present in P2 EVs were lost when separated on a density gradient (right)



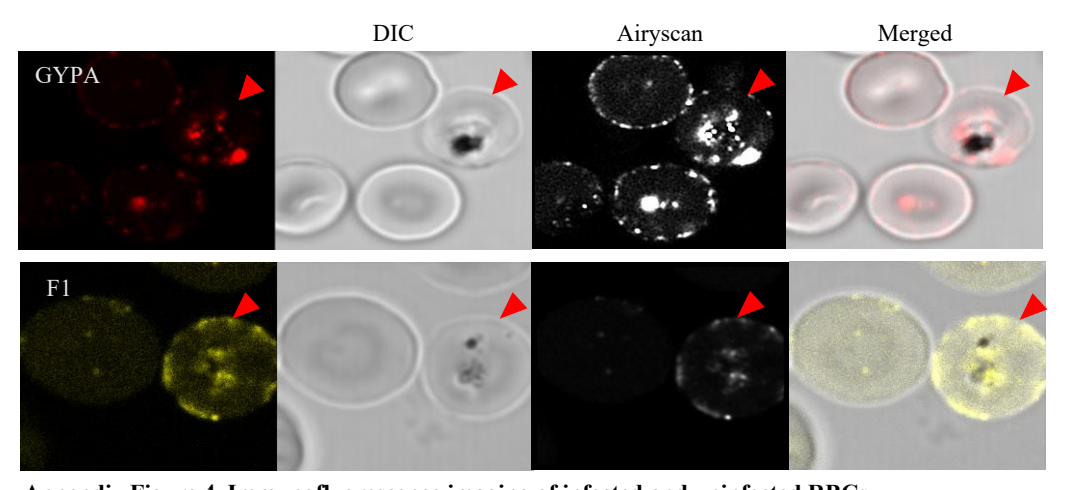
Appendix Figure 2. Optimizing EV isolation with HEK293 cells

Related to section 4.1.1. (A) Cells at >80% confluence, scale bar 10  $\mu$ m. (B) and (C) Electron microscopy images. Only EVs pelleted at 100,000 x g could be visualized by TEM i.e., P2. EVs are shown by red arrows. Scale bar is 200 nm (D) Silver stained SDS-PAGE showing distinct banding of P1, P2, total cell lysate -C. Non-conditioned media -N used as a control. L-ladder. (E) CD63 positive HEK293 P2 EVs and cells. CD63 is 50-60 kDa

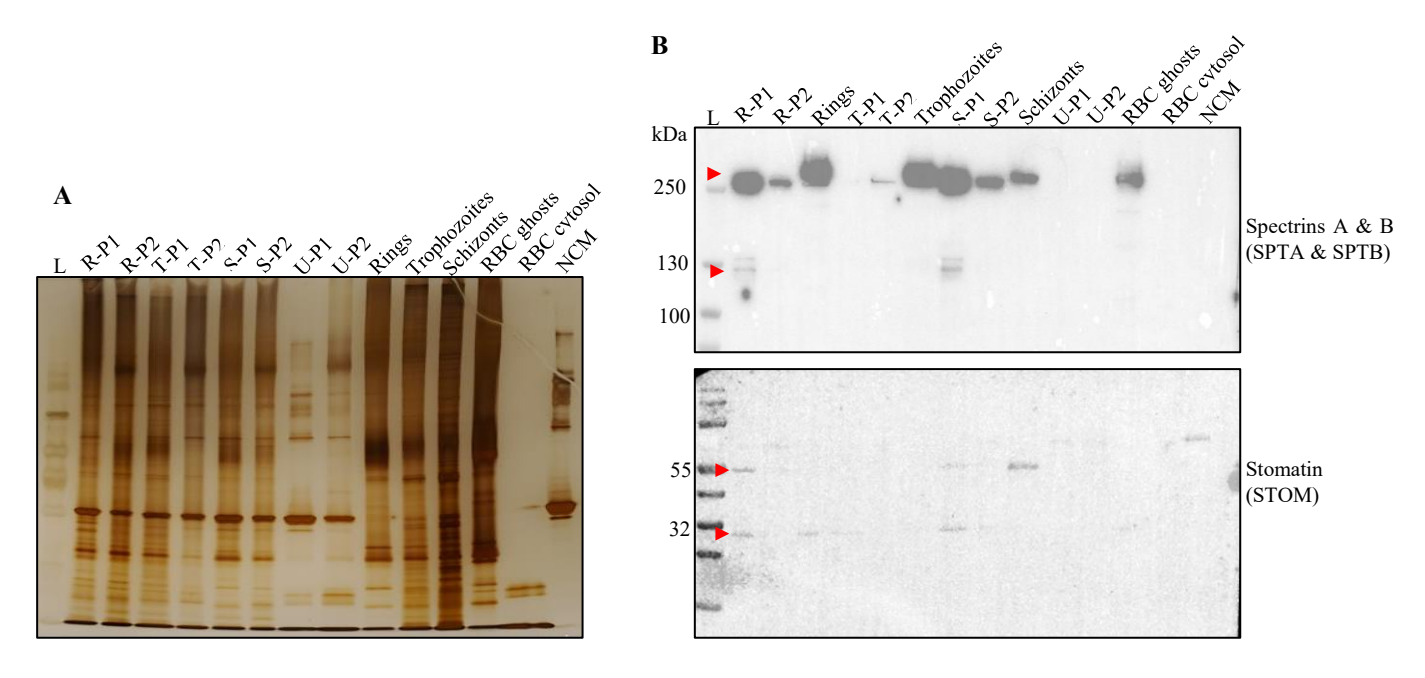


Appendix Figure 3. False C63+ malaria EVs isolated from cultures using non-leukoreduced RBCs.

Related to Figure 16. uRBC EVs are strongly CD63 positive. The intensity of CD63 in iRBC EVs reduces with maturation of the parasite.



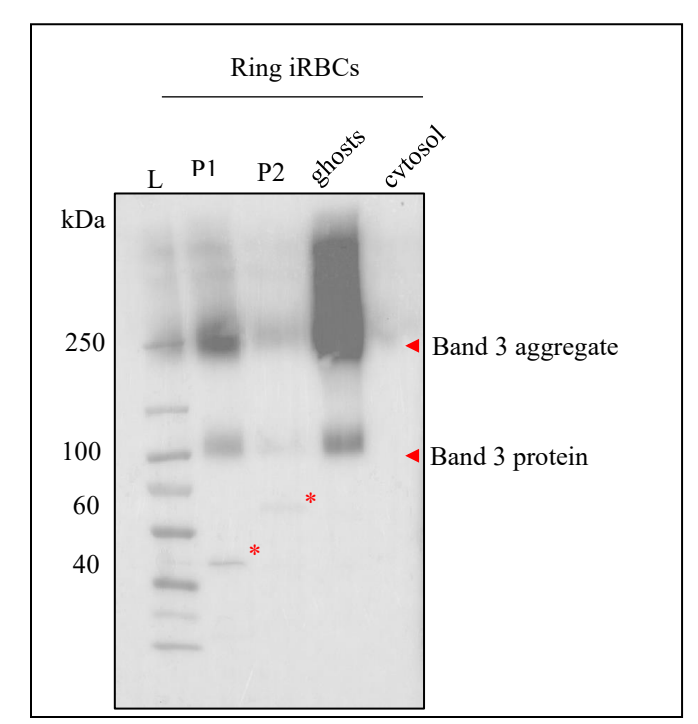
Appendix Figure 4. Immunofluorescence imaging of infected and uninfected RBCs Related to Figure 19 and Figure 24. Imaging of the RBC membrane proteins glycophorin A (GYPA), and flotillin 1 (F1) showed the proteins to aggregate significantly at the membrane of infected RBCs. Infected RBCs are marked with red arrowheads.



## Appendix Figure 5. Uncropped images

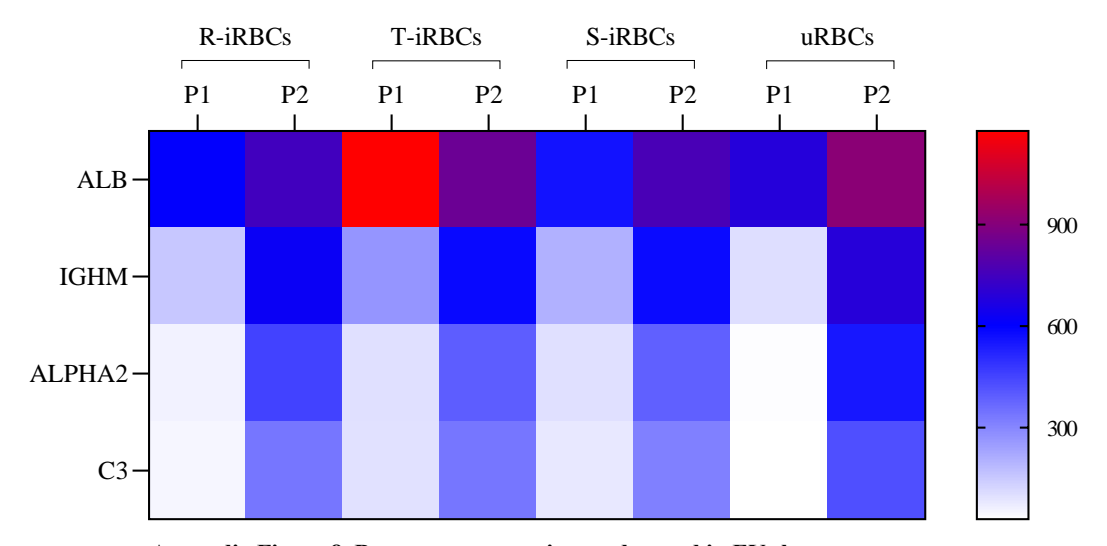
(A) Silver stain of EVs and their respective parasite stage lysates. Related to Figure 23. (B) WBA of spectrin top, and stomatin -bottom in stage-specific iRBC EVs and uRBC EVs. Red arrowheads mark protein bands at their respective molecular weights. Related to Figure 24.

L--ladder, R-rings, T-trophozoites, S-schizonts, i-infected, u-uninfected, RBCs-red blood cells, G-ghosts, C-cytosol, NCM-non conditioned media.

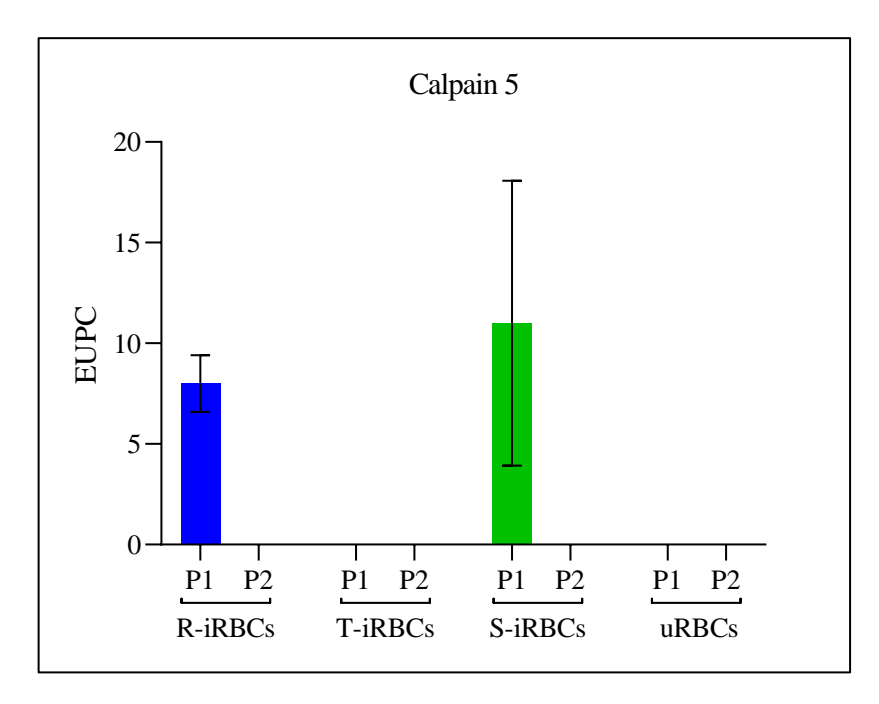


## Appendix Figure 6. WBA of band 3

Ring iRBC EVs showing a 40 kDa band in P1 and a 60 kDa band in P2, both marked with a red asterisk. Related to Figure 24.



Appendix Figure 8. Bos taurus contaminants detected in EVs by mass spectrometry Heavy contamination from co-isolating proteins in the growth medium is seen in all P2 EVs. Co-isolation of contaminants is much lower in P1 EVs R-rings, T-trophozoites, S-schizonts, u-uninfected RBCs, i-infected RBCs



Appendix Figure 7. Expression of Calpain 5 in iRBC EVs

Host calpain 5 was present only P1 EVs of ring- and schizont iRBCs. Calpain-5 is involved in microvesiculation and cleaves spectrin. Cleavage products of spectrin were observed only in P1 EVs of ring- and schizont iRBCs. R-rings, T-trophozoites, S-schizonts, u-uninfected RBCs, i-infected RBCs, EUPC-exclusive unique peptide count.

Appendix Table 1. Full list of proteins from GO analysis of iRBC EVs

	Ring-P1	Trophozoite-P1	Schizont-P1
Response to	PF3D7_1357800 (CCT4)		PF3D7_0525100 (ACS10)
xenobiotic stimulus	PF3D7_1343700 (Kelch13)		PF3D7_1344800 (ATCase)
	PF3D7_1350100 (KRS1)		PF3D7_0106300 (ATP6)
	PF3D7_1126000 (ThrRS)		PF3D7_0217500 (CDPK1)
	PF3D7_1225800 (UBA1)		PF3D7_1012400 (HGPRT)
			PF3D7_0523000 (MDR1)
			PF3D7_0915400 (PFK9)
			PF3D7_1408000 (PMII)
			PF3D7_1008700 (N/A)
			PF3D7_1251200 (N/A)
Entry into host			PF3D7_0217500 (CDPK1)
			PF3D7_0731500 (EBA175)
			PF3D7_0423500 (GAPM2)
			PF3D7_0930300 (MSP1)
			PF3D7_1342600 (MyoA)
			PF3D7_0722200 (RALP1)
			PF3D7_1335400 (RH2a)
			PF3D7_0424200 (RH4)
			PF3D7_1104400 (Trx-mero)
			PF3D7_1459400 (N/A)
Regulation of			PF3D7_0102200 (RESA)
immune response			PF3D7_0207600 (SERA5)
Proteasome			PF3D7_1008400 (RPT2)
regulatory particle			PF3D7_0413600 (RPT3)
assembly			PF3D7_1306400 (RPT4)
			PF3D7_1130400 (RPT5)
			PF3D7_1248900 (RPT6)
RNA binding	PF3D7_1006200 (ALBA3)	PF3D7_1368200 (ABCE1)	PF3D7_0525100 (ACS10)
	PF3D7_0108300 (ARP)	PF3D7_1010600 (eIF2beta)	PF3D7_1347500 (ALBA4)
	PF3D7_0935800 (CLAG9)	PF3D7_0617900 (H3.3)	PF3D7_0106300 (ATP6)
	PF3D7_1105100 (H2B)	PF3D7_0519400 (RPS24)	PF3D7_1108400 (CK2alpha)
	PF3D7_1350100 (KRS1)	PF3D7_0814000 (N/A)	PF3D7_1145400 (DYN1)
	PF3D7_1107300 (PAIP1)		PF3D7_1007900 (EIF3D)
	PF3D7_1011800 (PREBP)		PF3D7_0815600 (EIF3G)
	PF3D7_0501500 (RAP3)		PF3D7_1419700 (EIF3H)
	PF3D7_0905400 (RhopH3)		PF3D7_1361800 (GAC)
	PF3D7_1323400 (RPL23)		PF3D7_0423500 (GAPM2)
	PF3D7_1129000 (SPDS)		PF3D7_1222300 (GRP94)
	PF3D7_1309100 (N/A)		PF3D7_0320900 (H2A.Z) PF3D7_1012400 (HGPRT)
			_ ` ` ′
			PF3D7_0202000 (KAHRP)
			PF3D7_1324900 (LDH)
			PF3D7_0930300 (MSP1)

		PF3D7_1224300 (PABP1)
		PF3D7_0915400 (PFK9)
		PF3D7_1223100 (PKAr)
		PF3D7_1343000 (PMT)
		PF3D7_1105600 (PTEX88)
		PF3D7_1410400 (RAP1)
		PF3D7_1318800 (SEC63)
		PF3D7_1438900 (Trx-Px1)
		PF3D7_0209800 (UAP56)
		PF3D7_0402000 (N/A)
		PF3D7_0517000 (N/A)
		PF3D7_0619400 (N/A)
		PF3D7_0823800 (N/A)
		PF3D7_1357000 (N/A)
		PF3D7_1357100 (N/A)
		PF3D7_1459400 (N/A)
		PF3D7_1462300 (N/A)
PF3D7_1006200 (ALBA3)		
PF3D7_0108300 (ARP)		
PF3D7_1107300 (PAIP1)		
PF3D7_1011800 (PREBP)		
	PF3D7_0108300 (ARP) PF3D7_1107300 (PAIP1)	PF3D7_0108300 (ARP) PF3D7_1107300 (PAIP1)